UNIVERSITY OF CALIFORNIA
RIVERSIDE

Carborane Anions: As Weakly Coordinating Counterions and Coordinating Ligands for Catalyst Design

A Dissertation submitted in partial satisfaction
of the requirements for the degree of

Doctorate of Philosophy

in

Chemistry

by

James Henry Wright

August 2013

Dissertation Committee:
Dr. Vincent Lavallo, Chairperson
Dr. Christopher Reed
Dr. Pingyun Fen

The Dissertation of James Henry Wright is approved:

Committee Chairperson

University of California, Riverside

Acknowledgements

I would like to acknowledge all the great chemists that I have been privileged to work with. While too many to list my best attempt will be made to include the members Chris Reed's and Vince Lavallo's research groups. It was my work with Christos Douvris, Kee-Chan Kim, Evgenii Stoyanov, Irina Stoyanov, Yun Zhang, Paul Richardson, Amy Avelar,Matt Nava, and Fook Tham in which I was taught the basics of research. Gabe Mueck deserves a special thanks for his work in our collaborative work resulting in the publication used in this dissertation. It was also with great pleasure I got to learn from and mentor some terrific chemists. They include Carlos Hernandez, Uday Chauhan, Javier Farjado, David Woen, Kin Li, Dong Nguyen, Ernesto Delgado, Jess Estrada, Christopher Lugo, Allen Chan, Sean Quinlivan, Ahmad Hellany, Steven Cummings, David Weinberger, and Matt Asay. Computational work was done by Christos Kefalidis and Laurent Maron.Of course I would not have been able to meet and work with these people if it were not for Chris Reed and Vince Lavallo. To them I am especially grateful and hope that I have expressed my gratitude in words and hard work.

I would also like to thank Cindy Larive and Joseph Childers. The Dean's Fellowship that I was awarded for the last two quarters allowed me to continue my research while also developing my career. My focus could be on chemistry and made it possible for me to finish.

Personally, I would also like to acknowledge my wrestling coaches as well. Coach Balash always said, "the harder I work the luckier I get", and Coach Don's

“find a way” have motivated and to continue to inspire me. I will always be indebted to my wonderful parents who have put up with my “science” experiments and other mischief. To my wife, Serena, I want to say thank you. Your love has gotten me through some very difficult times, and I owe you an amazing vacation now that I’m done.

The text, figures, and schemes for the following chapters have been reproduced, in part or in their entirety, from the following published or submitted manuscripts.

Chapter 2:"R_3E^+ Carborane Salts of the Heavier Group 14 Elements: E = Ge, Sn and Pb. " J. H. Wright II, G. W. Meuck, F. S. Tham, C. A. Reed *Organometallics* **2010**, 29, 4066-4070.

Chapter 3: “Perhalogenated Carba-*closo*-dodecaborate Anions as Ligand Substituents: Applications in Gold Catalysis.” V. Lavallo, J. H. Wright, F. S. Tham, S. Quinlivan. *Angewandte Chemie Int. Ed.* **2013**, 52, 3172- 3176.

Chapter 4: “Observation of Room Temperature B-Cl Activation of the $HCB_{11}Cl_{11}^-$ Anion and Isolation of a Stable Anionic CarboranylPhosphazide.” J. Farardo Jr., A. L. Chan, J. Wright, V. Lavallo. **2013** Submitted.

Chapter 5: “Click-Like Reactions with the Inert $HCB_{11}Cl_{11}^-$ Anion Leads to Heterocycles with Unusual Aromatic Character." J. H. Wright, C. Kefalidis, F. S. Tham, L. Maron, V. Lavallo. *Inorg. Chem.* **2013**, 52, 6223-6229.

Chapter 6: “Isolation of a 12-Vertex Deltahedral Carborane Radical Anion with anEven Number of Skeletal Electrons.” M. Asay, C. E. Kefalidis, J. Estrada, D. S. Weinberger, J. Wright, C. Moore, A. L. Rheingold, L. Maron, V. Lavallo. **2013** Submitted.

ABSTRACT OF THE DISSERTATION

Carborane Anions: As Weakly Coordinating Counterions and Coordinating Ligands for Catalyst Design

by

James Henry Wright

Doctor of Philosophy, Graduate Program in Chemistry
University of California, Riverside, August 2013
Dr. Vincent Lavallo, Chairperson

1-carba-*closo*-dodecaborates, more commonly referred to as carborane anions, are icosahedral CB_{11} cages with substituents at each vertex. These substituents are highly variable allowing for a large range of properties. Such properties include being weakly basic, chemically inert, non-nucleophilic, and resistant to reduction or oxidation. Due to these properties, carborane anions have been given the term “weakly coordinating” to describe their interactions with cations. The isolation of numerous reactive species, superacids, and coordinatively unsaturated cations are testaments to the weak coordinating ability of carboranes.

Recently carborane anions have begun being transition from being used for fundamental chemistry to applied chemistry with their utility in Lewis acid catalysis being explored by a number of research groups. This dissertation follows this transition as the exploration and discovery of new cations is explored in Chapter 2. Next by careful substitution at the C-vertex the synthesis of carborane anions that can coordinate to transition metals was attempted. By limiting the coordination of the transition metal to the substituent off the C-vertex

the carborane ligand can stabilize traditional transition metal catalysts. The two specific substituents targeted in this research are phosphines and azides.

Phosphines are an obvious choice as their use in transition metal catalysis is ubiquitous. Chapter 3 reports the synthesis and coordination to a gold (I) center of the diisopropyl undecachlorocarborane phosphine anion, $i\text{Pr}_2\text{P}(\text{CB}_{11}\text{Cl}_{11})^-$ .Upon coordination to the gold, zwitterionic and anionic complexes were isolated. These compounds success in hydroamination of alkynes with amines serve as a proof of principle in the use of carboranes in ligand design.

Azides arethe next target for the synthesis of new carborane anion ligands, since the azide can be a versitile synthon. Chapter 4 discusses the attempted synthesis of the undecachlroinated carboranyl azide, $\text{N}_3\text{CB}_{11}\text{Cl}_{11}^-$, and the competing side reaction discovery. This cycloaddition results it the cleavage of a typically inert B-Cl bond.

The discovery of a new reaction involving both a carbon and a boron vertex being substituted resulted in the expansion of possible carborane fused triazole anions. Before these can be used as ligands their fundamental chemistry is studied in Chapters 5 and 6. The study of the carborane fused heterocycle resulted in the synthesis of a triazolium carborane zwitterion and a triazolium carborane radical anion.

Table of Contents

List of Schemes

Lists of Figures

Lists of Tables

Chapter One: Introduction

1.1 Background:

1-carba-*closo*-dodecaborate anions, more commonly referred to as carborane anions, are icosahedral clusters with the generic formula of $CB_{11}X_{12}^-$ (Figure 1.1). The dodecahydrido, $CHB_{11}H_{11}^-$, molecule was discovered in 1967 at DuPont from decaborane.[1] In 1984, a Czech research group published its improved synthesis also starting from decaborane.[2] Decaborane's toxicity and high cost motivated an alternative synthesis from sodium borohydride and boron trifluoride etherate.[3] Despite the lower cost of the starting materials, the low yield, small scale, and lack of reproducibility has plagued this alternate route.

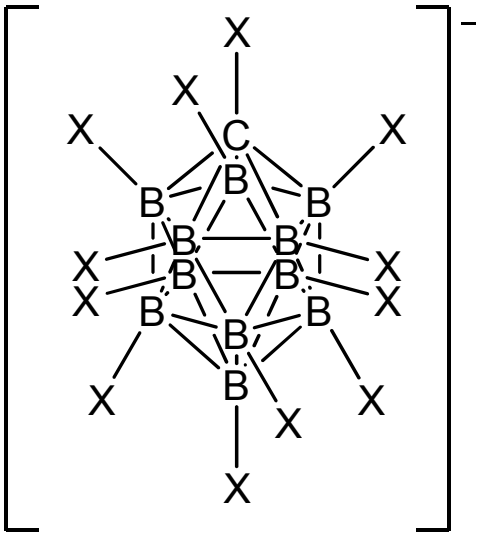

Figure 1.1: The carborane anion with the formula $CB_{11}X_{12}^-$

1.2 Weakly Coordinating Anions

The term weakly coordinating anion (WCA) entered the chemical lexicon in 1973 when the use of non-coordinating anions was taken to task.[4] In this Journal of Chemical Education paper, it looks at the common weakly coordinating anions of the day. This included perchlorate (ClO_4^-), tetrafluoroborate (BF_4^-), nitrate (NO_3^-), hexafluorophosphate (PF_6^-), perrhenate (ReO_4^-), hexafluoroantimonate (SbF_6^-), hexafluoroarsenate (AsF_6^-), and hexafluorosilicate (SiF_6^-). Since this paper's publication the discovery and use of more weakly coordinating anions have grown and now include triflate ($CF_3SO_3^-$), perfluorotetraphenylborate (F_{20}-BPh_4), fluorinated alkoxyaluminates ($Al(OR^F)_4^-$), dodecaborates ($B_{12}X_{12}^{2-}$), and carboranes ($CB_{11}X_{12}^-$).

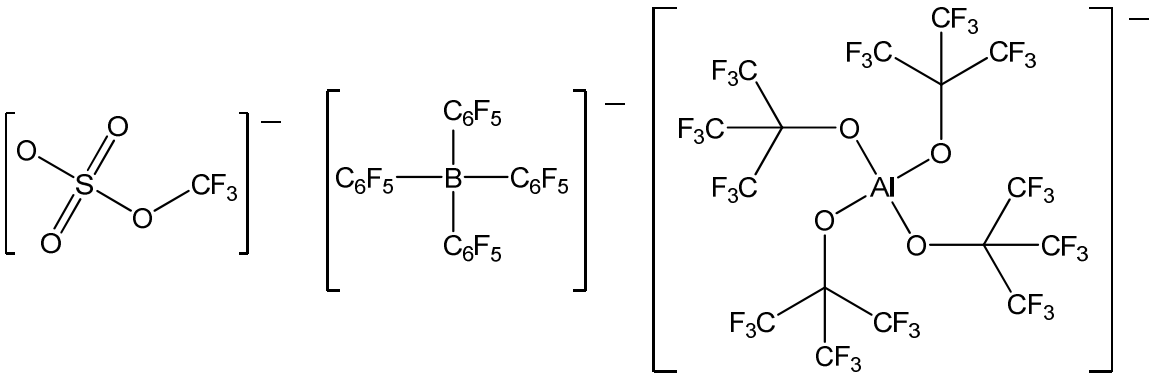

Figure 1.2: Example of weakly coordinating anions that have been recently synthesized and used. **A:** triflate **B**: perfluorotetraphenylborate **C**: fluorinated alkoxyaluminate

1.3 Carboranes as WCA

Caboranes have been utilized by a number of groups as weakly coordinating anions. The single anionic charge of $CHB_{11}H_{11}^-$ stems from the replacement of a BH^- vertex in $B_{12}H_{12}^{2-}$ with the isoelectronic CH (Figure 1.3). The charge is then delocalized throughout the cage by complex bonding. The lines forming the icosahedron in Figure 1.2 do not represent the normal two electron bond, but instead represent the complex connectivity of 3 center 2 electron bonds. There are 26 electrons that make up the sigma bonding for the 12 vertices. This phenomenon is referred to as σaromaticity. In contrast to the complex 3 center two electron bonding of the cage, the bonds from the vertex to the outer substituents are classical two electron sigma bonds.[5]

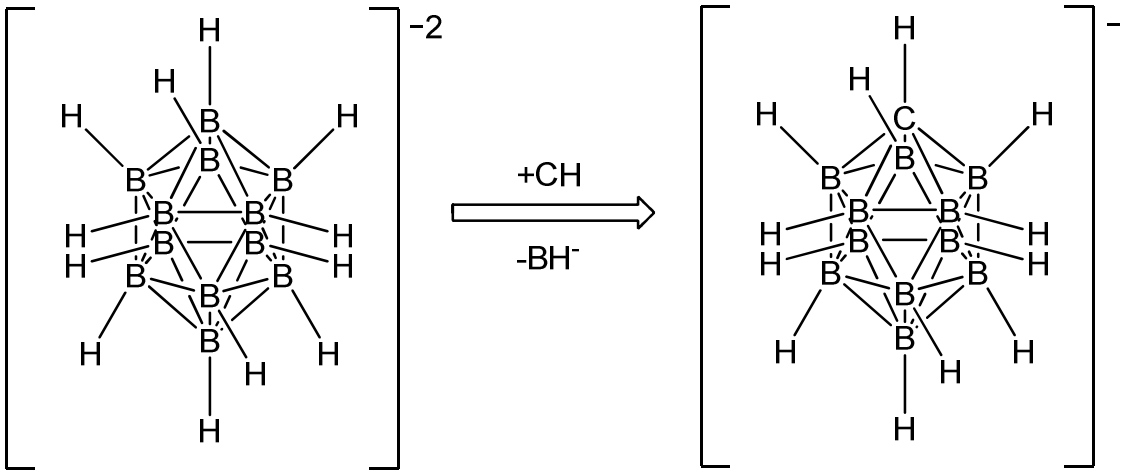

Figure 1.3: $B_{12}H_{12}^{2-}$ is isoelectronic with $CHB_{11}H_{11}^-$

1.4 Carborane C-X Derivatives

The C-H vertex of the parent carborane, $CHB_{11}H_{11}^-$, is weakly acidic and can be deprotonated with n-butyl lithium. The lithio-carborane is then reacted with and electrophile to synthesis a C-substituted carborane (Scheme 1.1). Direct substitution from the $CHB_{11}H_{11}^-$ anion can result in quick modification of the carborane's physical and chemical properties, however low yields and regeneration of the starting material is common.[6] The lithio-carborane is both a nucleophile and a strong base. This basicity can result in undesired reaction that results in regeneration of the starting carborane. As an improved approach by using B-X substituted carboranes (Chapter 1.5) the deprotonated carborane remains sufficiently nucleophilic with a decrease in basicity.[7]

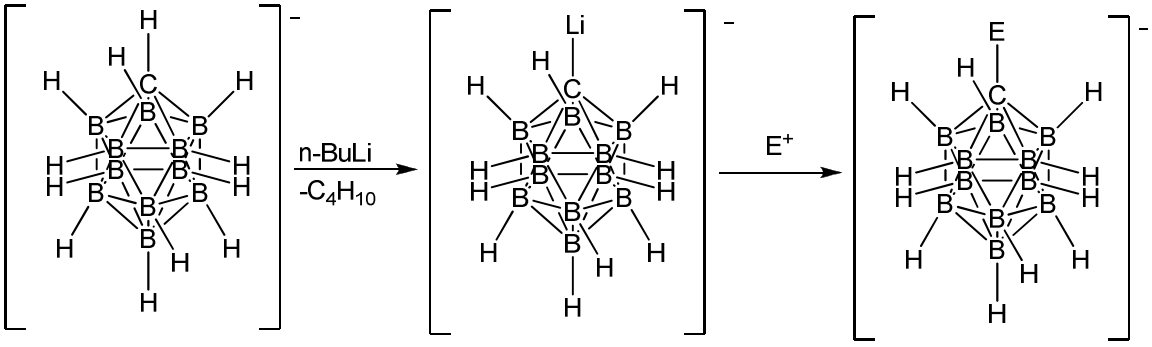

Scheme 1.1: The deprotonation of the C-vertex followed by electrophilic substitution

This new approach has been used to synthesis a number of C-substituted carboranes. A good example of the decrease in basicity while the nucleophilicity is maintained is Ozerov's use of sodium hydride to deprotonate $CHB_{11}Cl_{11}^-$.[8]

1.5 Carborane B-X Derivatives

In addition to substitution at the CH vertex, carborane anions have the ability to be substituted at B-H vertices to allow for unique physical, chemical, and electrical properties. The B-H vertex can be modified through reactions similar to electrophilic aromatic substitution (Scheme 1.2). Substitution occurs at the 12 position (antipodal to the carbon) first as it is the most basic. Subsequent electrophilic substitution occurs on the lower pentagonal belt. The remaining 5 borons of the top pentagonal belt are substituted if the electrophile is sufficiently strong.[5]

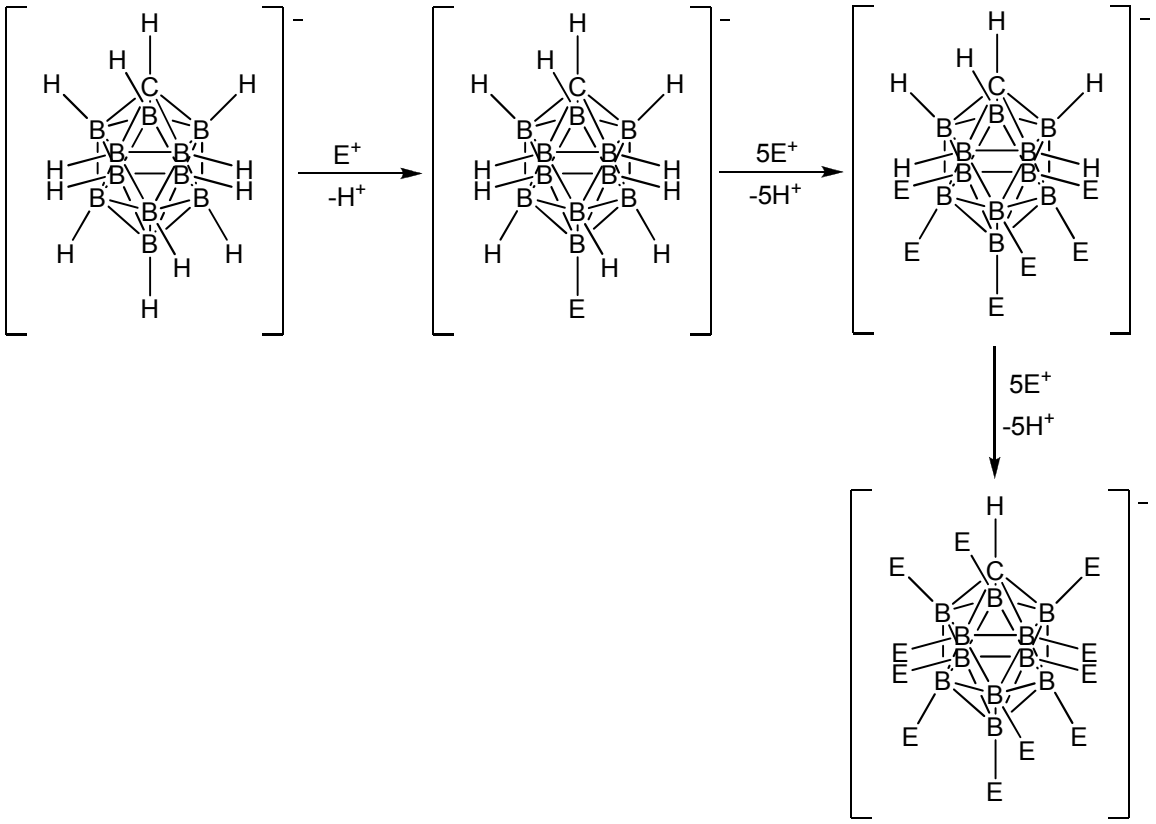

Scheme 1.2: Electrophilic substitution reactions of the B-H vertices on the carborane anion

Some of the most basic and inert carborane anions are when the substituents are halogen atoms. The stability and weakly coordinative ability of these anions stem from the σ aromaticity of the CB_{11}^- cluster and is enhanced when the negative charge is further shielded by halogens.[9] The B-substituted carboranes discussed in this dissertation are the hexabromocarborane ($CHB_{11}H_5Br_6^-$), undecachlorocarborane ($CHB_{11}Cl_{11}^-$), and the undecabromocarborane ($CHB_{11}Br_{11}^-$).

1.5 Carborane Uses

The ability to synthesize many different carborane anions by boron vertex and carbon vertex substitution increases their utility as weakly coordinating anions[5]. There are multiple examples of how inert and weakly coordinating these carborane anions are. Perhaps most indicative of the weakly coordinating nature is the isolation of the strongest Brønsted acid without the addition of Lewis acids.[10] By using the definition of Brønsted acidity, the strongest acid would have the weakest conjugate base. Research in quantifying this effect is being investigated by other groups.[9a, 9b, 11]

Additional examples of carboranes being used as weakly coordination anions are the isolation of reactive carbocations. This includes the isolation of Wheland intermediates,[12] HC_{60}^{+} ,[13] and the isopropylium ion.[14] It can be said that the carborane anion is more inert than hydrocarbons. After much dispute carboranes were used in the isolation of a free silylium ion.[15]

The reactive cations isolated with carborane anions can also be used as strong Lewis acids. A few groups have been able to make these Lewis acids behave catalytically in certain reactions. The trialkylsilylium carborane has been used as catalysts in the ring opening polymerization of the cyclic chlorophoshazene trimer[16] and hydrodefluorination of perfluoroalkyls.[17] An alumenium carborane was the catalyst in the carbon-carbon coupling of C(sp^3)-F bonds.[18]

Carboranes have also been used to weakly coordinate to transition metals. The isolation of cationic species from Vaska's complex was achieved with of triethylsilylium hexabromocarborane ($CHBH_5Br_6^-$).[19] The synthesis of phosphonium carboranes and subsequent reaction with rhodium under a hydrogen atmosphere resulted in a carborane-based rhodium complex.[20] Other carborane-based transition metal complexes are ever increasing and their utility in catalysis is being explored.

1.6 Conclusion

Carboranes have been showed to be one of the best weakly coordinating anions to form reactive cations. This is the focus of the initial research discussed in Chapter 2. The focus then shifted to incorporate the carborane anion into ligands to stabilize reactive transition metal catalysts. The development of the phosphine C-substituted carborane allowed for easy entrance into transition metal catalysis with the hydromination of a gold (I) complex in Chapter 3. In Chapter 4, the attempts to synthesis the perchlorinated carborane azide results in an interesting side reaction. This side reaction and resulting triazole fused carborane is explored in Chapter 5. The final chapter discusses the methylation and the study of a triazolium fused carborane zwitterion's redox properties to direct the synthesis of a radical anion.

1.7 Physical Hazards of Chemicals

On December 29, 2008, I had just finished my fourth quarter of graduate school at University of California Riverside. That day my perspective on chemistry, research, and life had changed significantly.At University of California Los Angeles, a staff researcher just a few months younger than me had a terrible accident. While scaling up a reaction that she had done previous a few months prior the syringe came apart exposing her to tertiary-butyl lithium. *t*-butyl lithium is a pyrophoric compound, meaning that it will ignite upon exposure to air. The ensuing fire and the response by her coworkers left her with third degree burns on over 40% of her body. She would succumb to these injuries eighteen days later at Ronald Reagan UCLA Medical Center.[21]

While my research at that time did not involve *t*-butyl lithium other pyrophorics and chemicals with a high degree of physical hazards was being used. In the ensuing days, weeks, months, and even years I have been following not only all the details involving this accident and the legal court case being carried out but any analysis of better laboratory practices that could come from it. I was made more cognizant of the actions undertaken by my colleagues and myself. Basic first aid and additional training and had been pursued vigorously by me in areas of safety, even areas where my research has not been exposed to yet.

In case people were getting complacent with safety, a year later, January 7, 2010, a senior graduate student at Texas Tech University was involved in an

accident involving a derivative of nickel hydrazine perchlorate.[22] According to the United States Chemical Safety and Hazard Investigation Board (CSB) who investigated the accident, the researcher was training a first year graduate student on how to make and test this explosive compound. Based on earlier work he felt it was safe to scale up the reaction and make 10 grams of material. The senior graduate student had three fingers amputated, a perforation to his eye, and other cuts and burns as a result of a violent explosion. Two other near misses were also discovered in this laboratory during the course of the investigation. The CSB's report indicates that laboratory workers were not aware of a verbally established rule limiting synthesis on energetic material to no more than 100 milligrams.

A very important lesson highlighted in the accident investigation is that the physical hazards are often overshadowed by the health hazards. A 2006 report also by the CSB examined combustible dust hazard and its inclusion in manufacture's Safety Data Sheets (SDS).[23] Analysis of 140 SDSs of known combustible dusts resulted in only 59% including language referring to the explosive nature of the dust, and none list the physical properties of the combustible dust.

1.9 Purpose for Safety's Inclusion

The American Chemical Society (ACS) President, Bassum Z. Shakhashiri commissioned a special committee to promote excellence in post-secondary chemical education as a means to fulfilling the ACS mission "to advance the broader chemistry enterprise and its practitioners for the benefit of Earth and its people."[24] The commission was charged to address two main questions:

1. What are the purposes of graduate education in the chemical sciences?
2. What steps should be taken to ensure they address important societal issues as well as the needs and aspirations of graduate students?

The commission was comprised of faculty and administrators from many prestigious universities as well as representatives from industry. In their full report, they reached five major conclusions ranging from career preparation to understanding the job market. One of the five major conclusions of the report deals directly with safety. Number 3 reads: "Academic chemical laboratories must adopt best practices. Such practices have led to a remarkably good record of safety in the chemical industry and should be leveraged."

It is my opinion that safety cannot be implemented by a university through policy or the government through additional regulations. Safety and safe laboratory practices must be established by the campus community through positive interactions of undergraduate students, graduate students, postdoctoral fellow,

principal investigators, staff, and campus administration. Only when communication and safety practices flow freely from top-down and bottom-up will progress be made. It is my intention of including safety considerations to begin this communication and to highlight important lessons that I have learned.

Inclusion of safety information is not typically included for a majority of publications and very rarely included in dissertations. I feel that chemical safety is as much of a part of my graduate education that its inclusion alongside the research and theory is more than warranted. This also serves as a ways to prevent institutional loss of safety lessons.

1.10 Safety Considerations

In my graduate experience, I notice the underestimation or inability of risk involving a wide variety of operations. While risk may not ever be completely eliminated for a given procedure or action, it is possible to greatly reduce or mitigate the risk to an acceptable level. At the beginning of graduate school formal analysis of my understanding in four subdisciplines of chemistry was tested. These subdisciplines include inorganic, organic, analytical, and physical chemistry. Any deficiencies in these are remedied by additional coursework or testing. Not tested is a student's knowledge of chemical hazards and adherence to best practices to control the risk. These topics are covered in about an hour during the first week during a whirlwind of different trainings and orientations.

After the accidents at UCLA and Texas Tech, I reevaluated some of my own work practices and found areas of improvement. I definitely had fallen under the trap of becoming complacent of the hazards after repeat work with a compound. Instead of recognizing the fact that a reaction or procedure was successful because of all the controls were in place, the underestimation of the hazard begins to take effect.

I have also noticed in the course of writing this dissertation that the hazards of organic azides and triazoles were not fully appreciated. It wasn't until I began reading the explosive testing of different triazolium carboranes when I began recognizing the full risk associated with these compounds.[25] Without extensive testing I cannot say whether my successful work with these compounds stem from luck, working on small scales, or from properties of these compounds.

UCR encourages the use of the Integrated Safety and Environmental Management system and its five step process which I have found very helpful.[26]The five steps are define work, analyze hazards, develop controls, perform work, and ensure performance. I feel that Step 2, analyze hazards, is something that most people can improve on, and that universities can help influence through education. I know that my graduate career has made me much more proficient at analyzing hazards. Step 5, ensure performance, can be important in preventing complacency and is mostly dependent of the laboratory's safety culture.

Figure 1.4 : Integrated Safety and Environmental Management's five step process

Chemicals and chemical research is inherently hazardous and full of risks. With the primary goal of universities being to educate, this provides an opportunity for the university to engage with researcher on these risks and best practices to reduce these risks. A successful education must contain a component of safety to ensure the individual is prepared to conduct research safely and to enter the workforce prepared.

1.11 References

1. Knoth, W. H., *J. Am. Chem. Soc.* **1967,** 89, 1274.

2. (a) Jelinek, T.; Plesek, J.; Hermanek, S.; Stibr, B., *Collect. Czech. Chem. Commun.* **1986,** 51, 819; (b) Tse, J. S.; Lee, F. L.; Gabe, E. J., *Acta Crystallogr., Sect. C: Cryst. Struct. Commun.* **1986,** C42, 1876.

3. Franken, A.; King, B. T.; Rudolph, J.; Rao, P.; Noll, B. C.; Michl, J., *Collect. Czech. Chem. Commun.* **2001,** 66, 1238.

4. Rosenthal, M. R., *J. Chem. Ed.* **1973,** 50, 331.

5. Koerbe, S.; Schreiber, P. J.; Michl, J., *Chem. Rev.* **2006,** 106, 5208.

6. Jelinek, T.; Baldwin, P.; Scheidt, W. R.; Reed, C. A., *Inorg. Chem.* **1993,** 32, 1982.

7. Nava, M. J.; Reed, C. A., *Inorg. Chem.* **2010,** 49, 4726.

8. Ramirez-Contreras, R.; Ozerov, O. V., *Dalton Trans.* **2012,** 41, 7842.

9. (a) Koppel, I. A.; Burk, P.; Koppel, I.; Leito, I.; Sonoda, T.; Mishima, M., *J. Am. Chem. Soc.* **2000,** 122, 5114;(b) Stoyanov, E. S.; Kim, K.-C.; Reed, C. A., *J. Am. Chem. Soc.* **2006,** 128, 8500; (c) Reed, C. A., H+, CH3+, and *Acc. Chem. Res.* **2010,** 43, 121.

10. Juhasz, M.; Hoffmann, S.; Stoyanov, E.; Kim, K.-C.; Reed, C. A., *Angew. Chem., Int. Ed.* **2004,** 43, 5352.

11. (a) Strauss, S. H., *Chem. Rev.* **1993,** 93, 927;(b) Tsang, C. W.; Yang, Q. C.; Sze, E. T. P.; Mak, T. C. W.; Chan, D. T. W.; Xie, Z. W., *Inorg. Chem.* **2000,** 39, 5851;(c) Krossing, I.; Raabe, I., *Angew. Chem., Int. Ed.* **2004,** 43, 2066;(d) Meyer, M. M.; Wang, X. B.; Reed, C. A.; Wang, L. S.; Kass, S. R., *J. Am. Chem. Soc.* **2009,** 131, 18050.

12. Reed, C. A.; Fackler, N. L. P.; Kim, K. C.; Stasko, D.; Evans, D. R.; Boyd, P. D. W.; Rickard, C. E. F., *J. Am. Chem. Soc.* **1999,** 121, 6314.

13. Reed, C. A.; Kim, K.-C.; Bolskar, R. D.; Mueller, L. J., *Science* **2000,** 289, 101.

14. Kato, T.; Stoyanov, E.; Geier, J.; Gruetzmacher, H.; Reed, C. A., *J. Am. Chem. Soc.* **2004,** 126, 12451.

15. Kim, K.-C.; Reed, C. A.; Elliott, D. W.; Mueller, L. J.; Tham, F.; Lin, L.; Lambert, J. B., *Science* **2002,** 297, 825.

16. Zhang, Y.; Huynh, K.; Manners, I.; Reed, C. A., *Chem. Commun.* **2008**, 494.

17. Douvris, C.; Ozerov, O. V., *Science* **2008,** 321, 1188.

18. Gu, W. X.; Haneline, M. R.; Douvris, C.; Ozerov, O. V., *J. Am. Chem. Soc.* **2009,** 131, 11203.

19. Douvris, C.; Reed, C. A., *Organometallics* **2008,** 27, 807.

20. Douglas, T. M.; Molinos, E.; Brayshaw, S. K.; Weller, A. S., *Organometallics* **2007,** 26, 463.

21. State of California Department of Industrial Relations , University of California Los Angeles, Investigation Report. **2009**.

22. United States Chemical Safety and Hazard Investigation Board, Texas Tech University laboratory explosion **2010**. http://www.csb.gov/assets/document/CSB_Study_TTU_.pdf.

23. United States Chemical Safety and Hazard Investigation Board, Investigation report combustible dust hazard study. **2006**.http://www.csb.gov/assets/1/19/Dust_Final_Report_Website_11-17-06.pdf

24. American Chemical Society Presidential Commission, Advancing Graduate Education in the Chemical Sciences. **2012**.http://portal.acs.org/portal/PublicWebSite/about/governance/CNBP_031603

25. (a) Belletire, J. L.; Schneider, S.; Wight, B. A.; Strauss, S. L.; Shackelford, S. A.,*Synthetic Commun.* **2012,** 42, 155; (b) Shackelford, S. A.; Belletire, J. L.; Boatz, J. A.; Schneider, S.; Wheaton, A. K.; Wight, B. A.; Hudgens, L. M.; Ammon, H. L.; Strauss, S. H., *Org. Lett.* **2009,** 11, 2623.

26. Univeristy of California Riverside Department of Chemistry, UCR Chemistry Departement Chemical Hygiene Plan. **2012**. http://www.ehs.ucr.edu/laboratory/CHP/ChemistryCHP.2012.09.10.pdf.

Chapter Two: R_3E+ Carborane Salts of the Heavier Group 14 Elements: E=Ge, Sn, and Pb

2.1 Abstract:

The synthetic and structural chemistry of catalytically useful trialkylsilylium salts with weakly coordinating carborane anions, $R_3Si(CHB_{11}X_{11})$, has been extended to the heavier group 14 elements. $Et_3Ge(CHB_{11}H_5Br_6)$ was prepared from Et_3GeH and trityl $CHB_{11}H_5Br_6^-$. Its X-ray crystal structureshows ion-like character very similar to its Si congener. The heavier element analogues, $Et_3E(CHB_{11}H_5Br_6)$ (E = Sn, Pb), were prepared by chloride ion abstraction from Et_3SnCl and Et_3PbCl, respectively, using $Et_3Si(CHB_{11}H_5Br_6)$. Their crystal structures differ from those of the four-coordinate lighter elements by adopting five-coordinate trigonal-bipyramidal stereochemistries, reflecting the periodic table transition of these elements from semi-metals to metals. The carborane anions are weak, bridging, axial ligands connecting trigonal Et_3E^+ cation-like moieties in polymeric chain structures. When the less coordinating $CHB_{11}Cl_{11}^-$ anion is used, excess germane competes with the carborane anion for coordination to Ge and a salt of the new hydride-bridged cation $[Et_3Ge\text{-}H\text{-}GeEt_3]^+$ can be isolated. It has a distinctive vGeHGe IR band at ca. 1740 cm^{-1} analogous to the 1875 cm^{-1} band of the $[Et_3Si\text{-}H\text{-}Si\text{-}Et_3]^+$ cation. Comparable chemistry is not observed for the Sn and Pb congeners.

2.2 Introduction:

Of all group-related elements in the periodic table, those of group 14 have perhaps the greatest opportunity to show diverse behavior. C is a nonmetal, Si and Ge are semi-metals,and Sn and Pb are metals. Trigonal-planar trialkyl R_3E^+ cations are stabilized in R_3C^+ carbocations by hyperconjugationand can be put in a bottle and characterized by X-ray crystallography when weakly coordinating carboranes, $CHB_{11}R_5X_6^-$ (Figure 2.1), are used as counterions.[1] On the other hand, three-coordinate trialkylsilylium ions, R_3Si^+ are unknown in condensed phases because hyperconjugative stabilization is weaker and silicon is both larger and more electropositive than carbon.[2] It is difficult to prevent coordination of a solvent molecule to Si, and there is no anion sufficiently weakly coordinating to yield a truly free R_3Si^+ ion, unless of course the R group is switched to a bulky aryl substituent.[3] Nevertheless, “ion-like” trialkylsilyl species $R_3Si^{\delta+}Y^{\delta-}$ are well known with weakly coordinatinganions,[2,4,5] and the closest approach to date uses a fluorinated carborane anion in $Me_3Si(EtCB_{11}F_{11})$.[6] The sum of the C-Si-C angles in the Me_3Si moiety is 354.4^o, only ca. 6^o short of trigonal planarity. Some might call this ionic. While not quite free silylium ions, these ion-like species behave like silylium ions. They are electrophiles par excellence, and research emphasis on silylium ions has now shifted from debate over their existence to exploitation of their reactivity.[7]

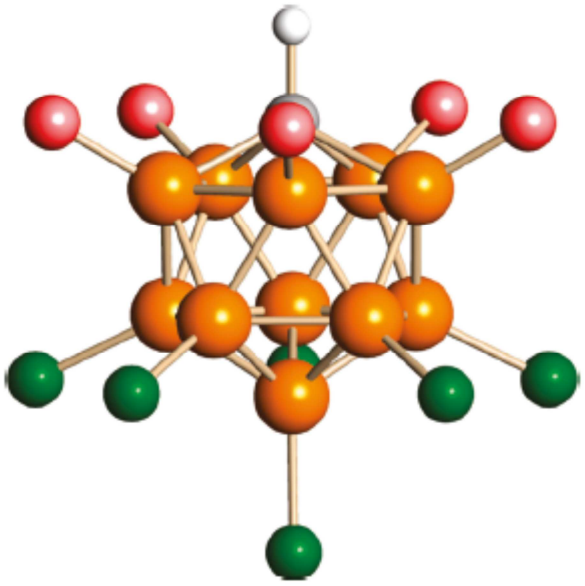

Figure 2.1. Schematic representation of the icosahedral CB_{11}-based carborane anions used in this work: $CHB_{11}H_5Br_6^-$ (red=H,green=Br) and $CHB_{11}Cl_{11}^-$(red, green=Cl).

For reasons of increasing size and metallic character, it is expected that R_3E^+ ions will become progressively less “free” when descending group 14. The closest approach to trialkyl R_3E^+ cations (E = Ge, Sn, Pb) has been made with tri n-butyl and trimethyl cationic moieties coupled with perfluorinatedtetraphenylborate[8] or permethylated carborane $CB_{11}Me_{12}^-$ anions.[9,10] The solid-state structures with permethylated carborane anions have been deduced from X-ray, EXAFS, and DFT calculations to favor five-coordination via significant coordination of methyl groups from the alkane-like anion. The tendency of these heavier R_3E^+ cations to behave as metals and expand their coordination number overrides any vestige of nonmetallic

sp^2behavior. It is hard to imagine the existence of a three-coordinate trialkyl cation with Ge, Sn, or Pb in a condensed phase, although free, or nearly free, cations have been well established with trialkylsilyl[11] and bulky aryl[12] substituents. However, these substituents are less useful than simple alkyls for reactivity and catalytic studies.

We have become interested in developing the systematic chemistry of trialkylgermyl, -stannyl, and -plumbyl cationlike species with halogenated carborane anions in order to make comparisons to their silicon congeners. R_3Si(carborane) species are effective new catalysts for the room-temperature polymerization of cyclo-hexachlorotriphosphazene in solution[13] and the hydrodefluorination of fluorocarbons.[14] In the latter case, carborane anions are the only anions sufficiently inert to survive the extremely electrophilic conditions.

Herein, we report the synthesis, isolation, and X-ray crystal structures of the heavier group 14 element Et_3E(carborane) compounds (E=Ge, Sn, and Pb) using halogenated carborane anions (Figure 1). Ethyl substituents on the central element E and the hexabrominated carborane anion $CHB_{11}H_5Br_6^-$ were initially chosen for these studies so that direct structural comparisons could made to the previously X-ray characterized silyl analogue $Et_3Si(CHB_{11}H_5Br_6)$.[15] When coupled with the less basic[16] undecachlorinated carborane anion, $CHB_{11}Cl_{11}^-$, the Ge species is vulnerable to formation of the dimeric hydride-bridged $[R_3Ge\text{-}H\text{-}GeR_3]^+$ cation in the presence of excessR_3GeH. This unusual μ-hydride is analogous to

the $[R_3Si\text{-}H\text{-}SiR_3]^+$ $[CHB_{11}Cl_{11}]^-$ salts that were discovered when silyl cation formation is performed in the presence of excess silane and the very weakest coordinating anions.[17] Attempts to prepare the corresponding hydride bridged cations with Sn failed.

2.3 Results and Discussion:

Synthesis of $R_3E(CHB_{11}H_5Br_6)$ for E=Ge, Sn, and Pb. Of the routes available to synthesize ion-like R_3E^+ species for the heavier group 14 elements, electrophilic removal of hydride from R_3EH using an analogous lighter element cation (eq 1) is one of the most reliable. This method exploits the generally decreasing E-H bond strength going down the group. Thus, as it does with Et_3SiH, trityl ion readily abstracts hydride from Et_3GeH at room temperature (eq 2.1) to yield triphenylmethane and the Et_3Ge^+ moiety. A nondonor, weakly basic solvent such as o-dichlorobenzene must be used to prevent solvent coordination to the Ge center.

$$Et_3GeH + [Ph_3C^+][CHB_{11}H_5Br_6^-] \rightarrow Ph_3CH + Et_3Ge(CHB_{11}H_5Br_6) \quad (2.1)$$

The analogous reactions with Et_3SnH and Et_3PbH are experimentally problematic. Color changes with Et_3SnH suggest complex redox chemistry is occurring rather than hydride abstraction, and the low thermal stability of lead hydrides[18] makes room-temperature reactions impossible. Instead, the preferred

method is to use a silyl carborane as a chloride rather than hydride acceptor (eqs 2.2 and 2.3):

$$Et_3SnCl + Et_3Si(CHB_{11}H_5Br_6) \rightarrow Et_3SiCl + Et_3Sn(CHB_{11}H_5Br_6) \quad (2.2)$$

$$Et_3PbCl + Et_3Si(CHB_{11}H_5Br_6) \rightarrow Et_3SiCl + Et_3Pb(CHB_{11}H_5Br_6) \quad (2.3)$$

All three $Et_3E(CHB_{11}H_5Br_6)$ compounds (E=Ge, Sn, Pb) were isolated as colorless solids in reasonable unoptimized yield (45-80%). As shown in the Supporting Information Figure S7, IR spectroscopy identifies the vE-C peak of the Et_3E+ moiety at 531, 510, and 451 cm^{-1} for E=Ge, Sn, and Pb, respectively. The corresponding peak for vSiC is 570 cm^{-1}. Only the germyl carborane had sufficient solubility in nondonor solvents for characterization by NMR spectroscopy, and the ^1H results in o-dichlorobenzene are as expected. Ge does not have a suitable NMR nucleus to explore the relationship between downfield chemical shift and the degree of germylium ion character that was so useful in Si chemistry. Thus, crystals for X-ray analysis were sought in each case and were typically grown directly from reaction mixtures by layering o-dichlorobenzene solutions with hexanes. Also included is a fourth structure: that of the Et_3Sn^+ cation coupled with the somewhat less coordinating undecachlorocarborane anion. This compound was prepared in the same manner as eq 3 using $Et_3Si(CHB_{11}Cl_{11})$ as the halide-abstracting agent.

X-ray Structures of $Et_3E(CHB_{11}H_5Br_6)$ for E = Ge, Sn, and Pb. True to the trend in the periodic table that makes the covalent radius of Ge relatively close to Si

(filling of the 3d orbitals) and the radius of Sn relatively close to that of Pb (filling of the 4f orbitals, i.e., the lanthanide contraction), the structure of $Et_3Ge(CHB_{11}H_5Br_6)$ is very similar to its Si congener, while that of Sn is very similar to Pb. As shown in Figure 2.2, $Et_3Ge(CHB_{11}H_5Br_6)$ has a flattened tetrahedral, four-coordinate geometry and is molecularly discrete.

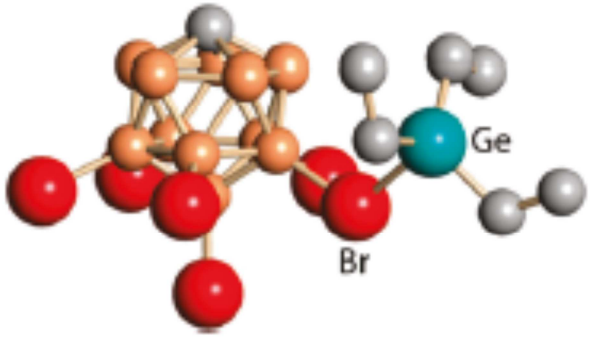

Figure 2.2. X-ray structure of $Et_3Ge(CHB_{11}H_5Br_6)$ (H atoms omitted for clarity).

On the other hand, the Sn (Figure 2.3) and Pb (Figure 2.4) analogues have five-coordinate trigonal-bipyramidal structures with bridging carborane anions, giving rise to polymeric structures.

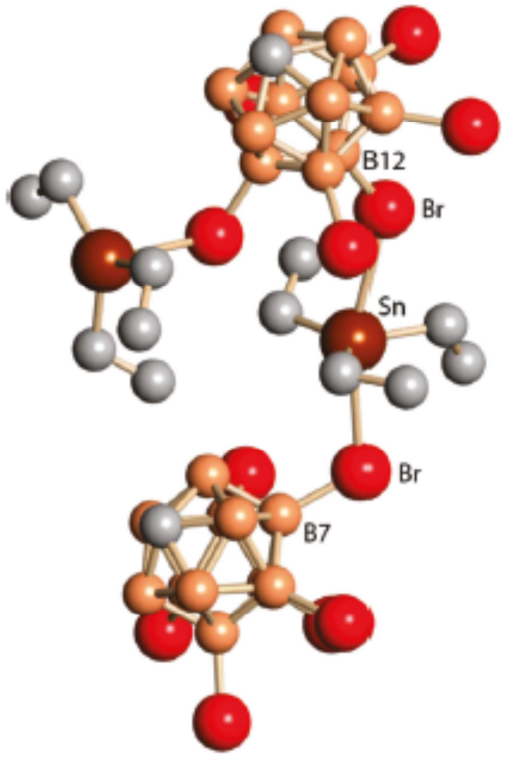

Figure 2.3. X-ray structure of $Et_3Sn(CHB_{11}H_5Br_6)$ (H atoms omitted for clarity).

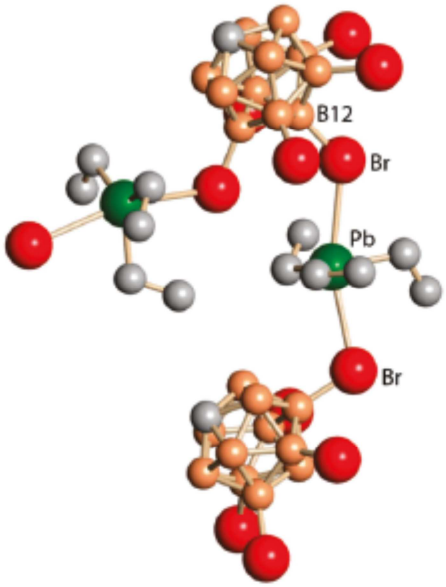

Figure 2.4. X-ray structure of $Et_3Pb(CHB_{11}H_5Br_6)$ (H atoms omitted for clarity).

This explains their relative solubilities. Only the molecularly discrete Si and Ge derivatives have significant solubility in chlorocarbon solvents. The five-coordinate structures of the heavier elements have stereochemistries that are related to bis-alkene complexes of trialkyl Sn and Ge cations[19] and base-stabilized triaryl tin cations.[20,21]

Like the Si analogue, the Ge structure is not fully ionic. Nevertheless, the Et_3Ge^+ moiety is clearly only weakly coordinated to the carborane anion and shows a close approach toward trigonal planarity. The coordinated B-Br bond (1.994 Å) of the anion is detectably elongated relative to the range of uncoordinated B-Br bonds (1.937-1.955 Å). The sum of the C-Ge-C angles is351.9^o, ca.8^o shy of planarity. The Ge-Br distance of 2.535(2) Å is ca. 0.21 Å longer than the covalent Ge-Br bond in Ph_3GeBr (2.317Å)[22] but very much shorter than the sum of the van der Waals radii (3.85 Å). The average Ge-C bond length is 1.943 Å. In the corresponding Si compound,[23] the sum of the C-Si-C angles is 349.0^o and the Si-Br bond lengthening is ca. 0.23 Å. The close parallel between Si and Ge is striking.

There is also a close parallel between Sn and Pb in their polymeric $Et_3E(CHB_{11}H_5Br_6)$ structures (Figures 3,4). Indeed, they are isomorphous and crystallize in the same space group. The sum of the C-E-C angles is very close to 360^o in both cases, but this should not be taken as an indication of Et_3E^+ ionicity because it reflects nearly equivalent axial interactions from Br atoms of

the $CHB_{11}H_5Br_6^-$ anion, giving rise to trigonal-bipyramidal coordination. The axial interactions to the carborane anions are relatively weak and suggest distinctly ion-like structures: $[Et_3E^{\delta+}][CHB_{11}H_5Br_6^{\delta-}]$. The two axial Sn-Br distances of 2.965 and 3.074 Å are ca. 0.5 Å longer than that in Ph_3SnBr (2.491Å),[24] and the Pb-Br distances of 3.117 and 3.158Å in $Et_3Pb(CHB_{11}H_5Br_6)$ are ca. 0.3Å longer than in a typical covalent Pb-Br bond such as that in Ph_3PbBr (2.852Å).[25] As expected, these long bonds are nevertheless considerably shorter than the sum of the van der Waals radii (4.02 and 3.87Å for Sn and Pb, respectively). The Pb-coordinated B-Br bonds of the carborane anion (1.973 and 1.963Å) are marginally elongated compared to the noncoordinated B-Br bonds (1.943-1.954Å). This distortion of the anion is not significantly different from that in the Sn structure, where the coordinated B-Br distances are 1.975 and 1.966Å and the noncoordinated ones are 1.940-1.947Å.

One additional X-ray structure has been determined in connection to this work, that of $Et_3Sn(CHB_{11}Cl_{11})$. As expected, when the central atom is a metal, it also forms a carborane anion-bridged polymeric structure with trigonalbipyramidal coordination at Sn, but there is one difference. The anion bridges through the 7, 9 positions rather than the more common 7, 12 positions. The reason probably lies in the predominance of crystal-packing forces over site basicity, as seen in the X-ray structure of the carborane acid $H(CHB_{11}Cl_{11})$.[26] Although the 12 position is calculated to be more basic than the 7-11 positions, the difference is

small and the solid-state structure of the acid shows protonation via Cl atoms in the 7-11 positions.

The undecachloro carborane anion is less basic[16] and less coordinating[17] than the hexabromo analogue, so a somewhat more ionic complex might be expected. The average Sn-C bond length of 2.136(2)Å in the undecachloro compound is nominally shorter than that in the hexabromo complex (2.140(2)Å), but this is barely statistically significant. The average axial Sn-Cl distance of 2.991Å is 0.45Å longer than that in Me_3SnCl[27] and 0.50Å longer than in Ph_3SnCl,[28] but on a percentage basis, these extensions are not particularly different from those in the hexabromo structure. Overall, these data indicate that in this particular structural motif it is difficult to use X-ray structural data to measure relative binding tendencies of carborane anions to R_3E^+ cations. This contrasts with the data on discrete molecular structures like Et_3Si(carborane), where the degree of pyramidalization at Si is an excellent guide to silylium ion character.[2] Nevertheless, the following reactivity studies confirm that the undecachloro anion is less coordinating than the hexabromo analogue.

Formation of the $[Et_3Ge\text{-}H\text{-}GeEt_3]^+$ Cation. When the synthesis of $Et_3Ge(CHB_{11}Cl_{11})$ is carried out according to eq 1 in the presence of excess Et_3GeH, the germane competes with the carborane anion for coordination to Ge and forms the $[Et_3Ge\text{-}H\text{-}GeEt_3]^+$ cation (eq 4):

$$Et_3Ge(CHB11Cl11) + Et_3GeH \rightarrow [Et_3Ge\text{-}H\text{-}GeEt_3^+][CHB_{11}Cl_{11}^-] \qquad (2.4)$$

The reaction is reversible. Indeed, the easiest way to prepare $Et_3Ge(CHB_{11}Cl_{11})$ is to remove Et_3GeH from the "dimer" product by heating under vacuum. The formation reaction only proceeds with the undecachloro carborane anion; the hexabromo anion is too strongly coordinated. This chemistry exactly parallels that of Si.[17]

The μ-hydrido product is readily characterized by IR spectroscopy, where a broad, distinctively shaped peak assigned to vGeHGe is observed at ca. 1740 cm^{-1}. This absorption is similar to that observed in the corresponding $[Et_3Si\text{-}H\text{-}SiEt_3]^+$ cation at 1875 cm^{-1} (Figure 2.5) and at generally higher frequencies in related hydride-bridged carbocations.[29]

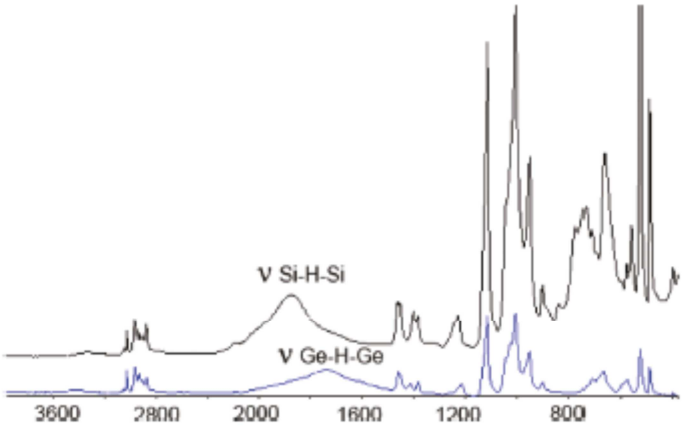

Figure 2.5. IR spectra of $[Et_3SiHSiEt_3][CHB_{11}Cl_{11}]$ (black) and $[Et_3GeHGeEt_3][CHB_{11}Cl_{11}]$ (blue).

The analogous Sn hydride-bridged species does not form when $[Ph_3C^+][CHB_{11}Cl_{11}^-]$ is treated with excess Et_3SnH (or $n\text{-}Bu_3SnH$) in o-dichlorobenzene. There was no evidence in the IR spectrum for a SnHSn peak

expected at ca. 1650 cm^{-1}. The lack of stannane adduct formation may be related to intrinsic Lewis basicity differences or to the higher lattice energy of the low-solubility polymeric $Et_3Sn(CHB_{11}Cl_{11})$. The low thermal stability of lead hydrides[18] prevented our exploration of the corresponding reaction with Et_3PbH.

2.4 Conclusion

The successful synthesis and isolation of Et_3E(carborane) species for E=Ge, Sn, and Pb adds to the available repertory of cation-like R_3E^+ Lewis acids of group 14 elements that are coupled with extremely inert carborane counterions. As illustrated by the example of the reaction of $Et_3Ge(CHB_{11}Cl_{11})$ with Et_3GeH to form the $[Et_3Ge\text{-}H\text{-}GeEt_3]^+$ cation, this opens the way to an exploration of their reactivity with weak bases L to form higher coordinate cations of the type $[R_3EL]^+$. Of further interest is the possibility that these cation-like Lewis acids will allow systematic studies of R_3E^+ cations in important catalytic roles such as the polymerization of phosphazenes[13] and the activation of C-F bonds.[14]

2.5 Experimental:

Reactions were carried out in an inert atmosphere glovebox (O_2, H_2O < 1 ppm). Solvents were dried following literature procedures,[30] distilled under Ar, and stored over 4Å molecular sieves in the glovebox. $[Ph_3C][CHB_{11}H_5Br_6]$,

$[Ph_3C][CHB_{11}Cl_{11}]$, $Et_3Si(CHB_{11}H_5Br_6)$, and $Et_3Si(CHB_{11}Cl_{11})$ were prepared by literature methods.[31] Triethyltin chloride (98%) was purchased from Strem, triethylgermane (98%) from Aldrich, and triethyllead chloride from Pfaltz and Bauer and used as received. Caution: Trialkyl derivatives of group 14 elements are highly toxic and should be handled with great care. X-ray data can be found in the Appendix.

$Et_3Ge(CHB_{11}H_5Br_6)$.

In a 12mL vial equipped with a magnetic stir bar, $[Ph_3C][CHB_{11}H_5Br_6]$ (122 mg, 0.142 mmol) was dissolved in dry o-dichlorobenzene (1 mL). To this orange solution was added Et_3GeH (0.1 mL, 0.6 mmol) with stirring. The solution turned clear within seconds. Within 10 min, a white precipitate had formed and hexane was added to facilitate additional crystallization. The product was filtered off and collected on a medium frit (89 mg, 81%). Single crystals were grown by careful layering of the reaction mixture with n-hexane. ^{1}H NMR(ODCB-d4, 300 MHz, 25^{o}C): 2.71 (s, CH carborane), 1.75-1.67 (q, CH2), 1.16-1.10 ppm (t, CH3). Anal. Calcd for $C_7H_{21}B_{11}Br_6Ge$: C, 15.80; H, 3.63. Found: C, 13.69; H, 2.48. FT-IR [ATR]: Figure 2.6.

$[(Et_3Ge)_2H][CHB_{11}Cl_{11}]$.

Et_3GeH (0.5 mL, 3.09 mmol) was added to a stirring suspension of $[Ph_3C][CHB_{11}Cl_{11}]$ (308.5 mg, 0.403 mmol) in o-dichlorobenzene (1 mL). The mixture became clear after a few seconds and was allowed to stir for an

additional 10 min. n-Hexane was added while stirring to give a white precipitate, which was filtered off (0.23 g, 68%). FT-IR [ATR] spectrum: see Figure 5. Upon heating at 130^{o}C under vacuum for 3 h, the diagnostic vGeHGe band at 1740 cm^{-1} disappeared, giving $Et_3Ge(CHB_{11}Cl_{11})$; see Figure 2.5. Anal. Calcd for $C_{13}H_{32}B_{11}Cl_{11}Ge_2$: C, 18.53; H, 3.83. Found: C, 18.71; H, 3.40.

$Et_3Sn(CHB_{11}H_5Br_6)$.

$Et_3Si(CHB_{11}H_5Br_6)$ was prepared from $[Ph_3C][CHB_{11}H_5Br_6]$ (135 mg, 0.157 mmol) and excess Et_3SiH in o-dichlorobenzene (3 mL). Hexanes (0.5 mL) was added to ensure complete product precipitation. The product was filtered off and resuspended in o-dichlorobenzene, and Et_3SnCl (52 mg, 0.21 mmol) was added dropwise. n-Hexane (0.5 mL) was carefully layered onto the reaction mixture, and small, colorless X-ray quality crystals of $Et_3Sn(CHB_{11}H_5Br_6)$ grew over a week (58 mg, 45%). FT-IR [ATR]: Figure 2.8. Anal. Calcd for $C_7H_{21}B_{11}Br_6Sn$: C, 10.19; H, 2.57. Found: C, 10.16; H, 2.37.

$Et_3Pb(CHB_{11}H_5Br_6)$.

This was prepared in the same manner as $Et_3Sn(CHB_{11}H_5Br_6)$ using Et_3PbCl (40.6 mg, 0.123 mmol) and $Et_3Si(CHB11H5Br6)$ (91.0 mg, 0.124 mmol) in o-dichlorobenzene (3 mL) and stirring for 24 h. X-ray quality crystals were grown by careful layering of n-hexane (78.2 mg, 70%). FT-IR [ATR]: Figure 2.9. Anal. Calcd for $[Et_3Pb][CHB_{11}H_5Br_6]$: C, 9.20; H, 2.32. Found: C, 9.52; H, 2.56.

$Et_3Sn(CHB_{11}Cl_{11})$ •$C_6H_4Cl_2$.

$Et_3Si(CHB_{11}Cl_{11})$ was prepared from $[Ph_3C][CHB_{11}Cl_{11}]$ (53.4 mg, 0.07 mmol) and Et_3SiH in o-dichlorobenzene (3 mL), adding n-hexane (0.5 mL) after 10 min to precipitate the product. Longer stirring times sometimes led to the formation of waxy solids. $Et_3Si(CHB_{11}Cl_{11})$ was filtered off (11.7 mg, 0.018 mmol) and resuspended in o-dichlorobenzene. Three drops of Et_3SnCl was added and the reaction mixture stirred for 24 h. Crystals of an o-dichlorobenzene solvate suitable for X-ray analysis were grown by careful layering of the reaction mixture with n-hexane (5.3 mg, 40%). FT-IR [ATR]: Figure 2.10.Anal. Calcd for $Et_3Sn(CB_{11}Cl_{11})$: C, 11.51; H, 2.21. Found: C, 10.98; H, 2.10.

2.8 Supplemental Information:

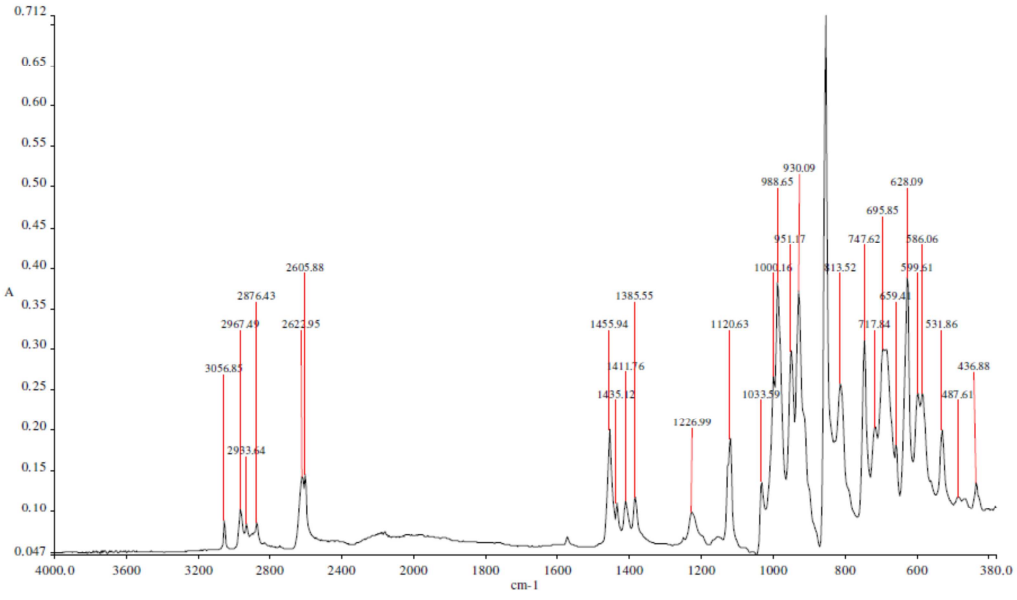

Figure 2.6. ATR IR spectrum of $Et_3Ge(CHB_{11}H_5Br_6)$.

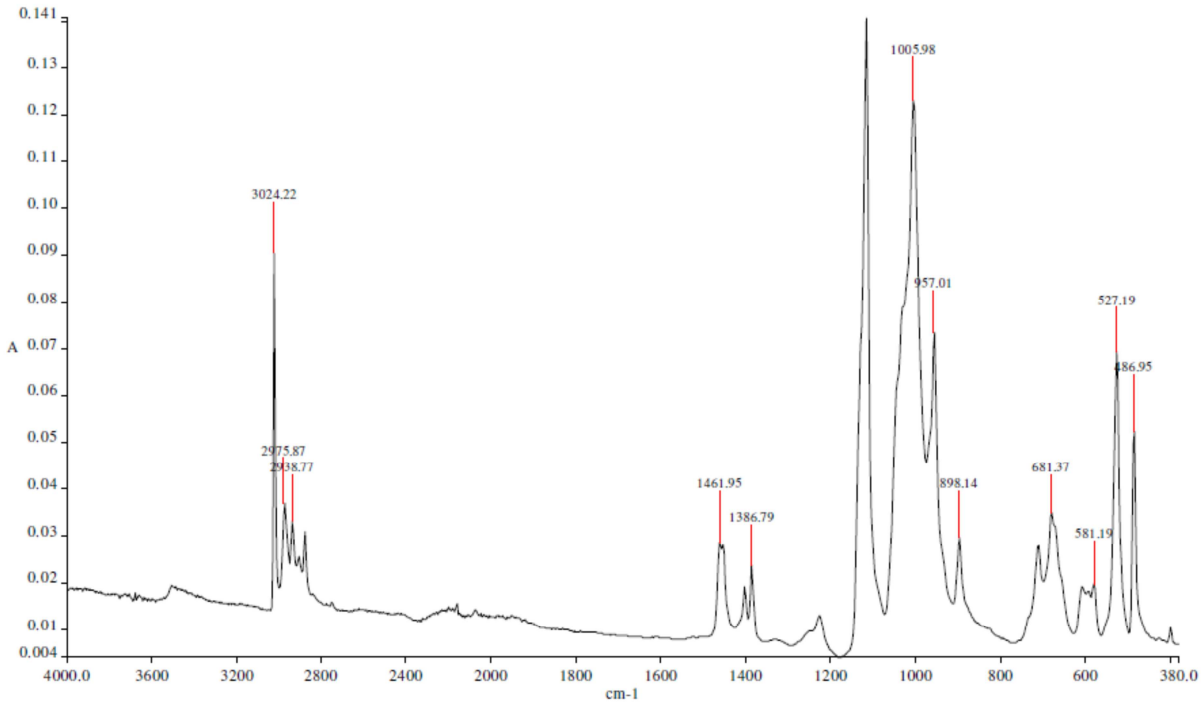

Figure 2.7. FT IR spectrum of $Et_3Ge(CHB_{11}Cl_{11})$ formed by heating $[(Et_3Ge)_2H][CHB_{11}Cl_{11}]$under vacuum at 130 ^{0}C.

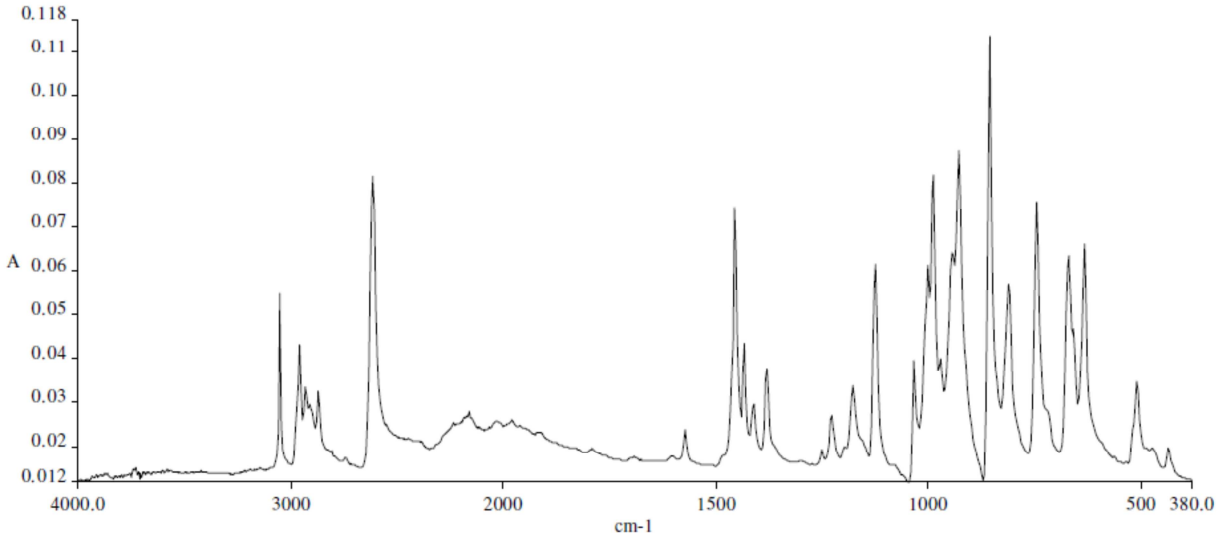

Figure 2.8. ATR IR spectrum of $Et_3Sn(CHB_{11}H_5Br_6)$.

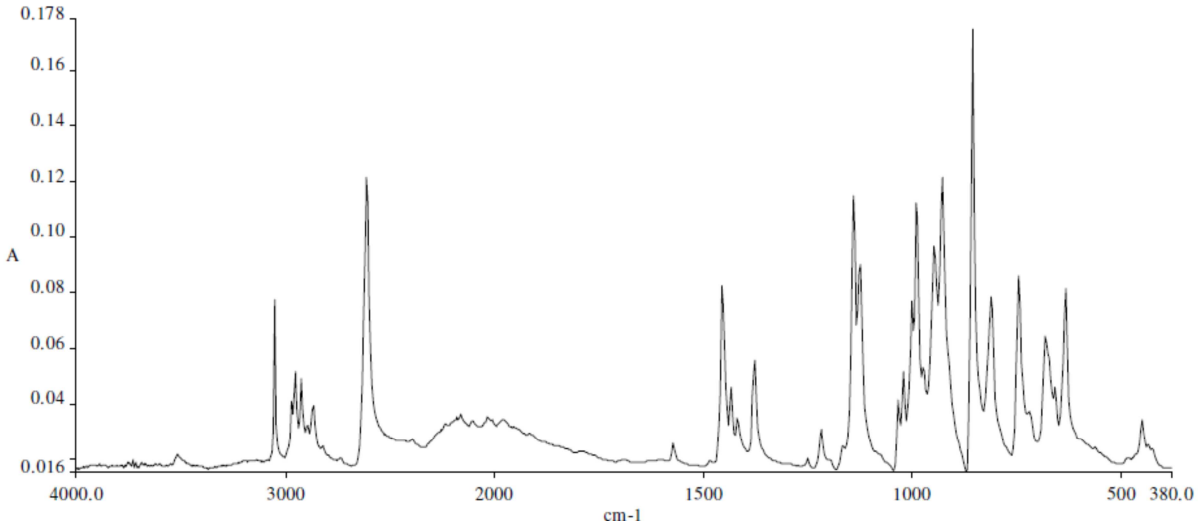

Figure 2.9. ATR IR spectrum of $Et_3Pb(CHB_{11}H_5Br_6)$.

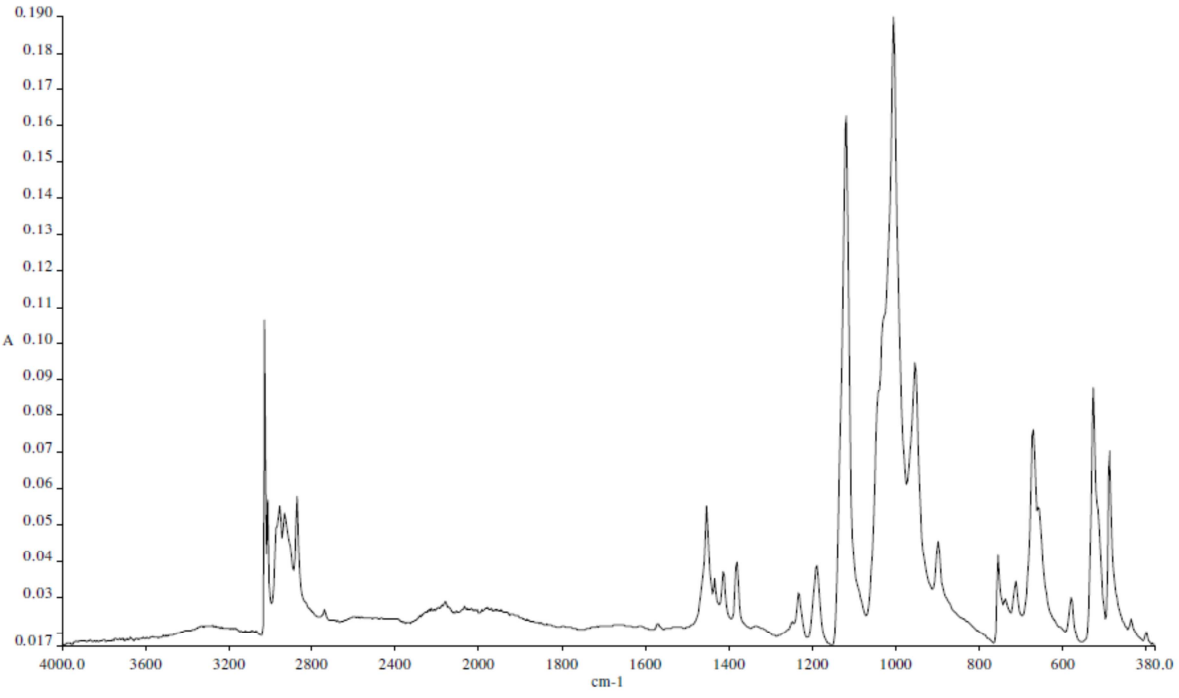

Figure 2.10. ATR IR spectrum of $Et_3Sn(CHB_{11}Cl_{11}) \cdot C_6H_4Cl_2$.

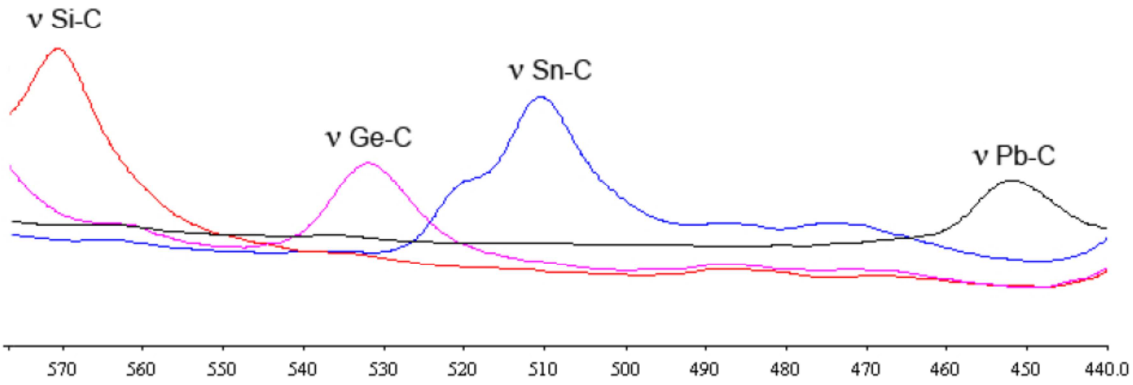

Figure 2.11. ATR IR spectra detail showing peaks arising from methyl group vE-C stretchingmodes in $Et_3E(CHB_{11}H_5Br_6)$ (E = Si, Ge, Sn and Pb). Frequencies are given in the text.

2.8 References:

1. Kato, T.; Reed, C. A., *Angew. Chem. Int. Ed.* **2004**, 43, 2908.
2. Reed, C. A., *Acc. Chem. Res.* **1998**, 31, 325.
3. Kim, K.-C.; Reed, C. A.; Elliott, D. W.; Mueller, L. J.; Tham, F.; Lin, L.; Lambert, J. B.,*Science* **2002**, 297, 825.
4. Lambert, J. B.; Kania, L.; Zhang, S., *Chem. Rev.* **1995**, 95, 1191.
5. Mueller, T., *Adv. Organomet. Chem.* **2005**, 53, 155.
6. Kuppers, T.; Bernhardt, E.; Eujen, R.; Willner, H.; Lehmann, C. W., *Angew. Chem. Int. Ed.* **2007**, 46, 6346.
7. Reed, C. A., *Acc. Chem. Res.* **2010**, 43, 121.
8. Lambert, J. B.; Kuhlmann, B., *J. Chem. Soc., Chem. Commun.* **1992**, 931.
9. Zharov, I.; King, B. T.; Havlas, Z.; Pardi, A.; Michl, J., *J. Am. Chem. Soc.* **2000**, 122, 10253.

10. Zharov, I.; Weng, T.-C.; Orendt, A. M.; Barich, D. H.; Penner-Hahn, J.; Grant, D. M.; Havlas, Z.; Michl, J., *J. Am. Chem. Soc.* **2004**, 126, 12033.

11. Lee, V. Y.; Sekiguchi, A., *Acc. Chem. Res.* **2007**, 4, 410.

12. Lambert, J. B.; Zhao, Y.; Wu, H.; Tse, W. C.; Kuhlmann, B., *J. Am. Chem. Soc.* **1999**, 121,5001.

13. Zhang, Y.; Huynh, K.; Manners, I.; Reed, C. A., *Chem. Commun.* **2008**, 494.

14. Douvris, C.; Ozerov, O. V., *Science* **2008**, 321, 1188.

15. Xie, Z.; Manning, J.; Reed, W. R.; Mathur, R.; Boyd, P. D. W.; Benesi, A.; Reed, C. A., *J. Am. Chem. Soc.* **1996**, 118, 2922.

16. Stoyanov, E. S.; Kim, K.-C.; Reed, C. A., *J. Am. Chem. Soc.* **2006**, 128, 8500.

17. Hoffmann, S. P.; Kato, T.; Tham, F. S.; Reed, C. A., *Chem. Commun.* **2006**, 767.

18. Becker, W. E.; Cook, S. E., *J. Am. Chem. Soc.* **1960**, 82, 6264.

19. Yang, Y.; Panisch, R.; Bolte, M.;Meuller, T. *Organometallics* **2008**, 27, 4847.

20. Sarazin, Y.; Coles, S. J.; Hughes, D. L.; Hursthouse, M. B.; Bochmann, M., *Eur. J. Inorg. Chem.* **2006**, 45, 3211.

21. Kašná, B.; Jambor, R.; Dostál, L.; Císařová, I.; Holeček, J.; Štíbr, B., *Organometallics* **2006**, 25, 5139.

22. Preut, H.; Huber, F., *Acta Crystallogr.* **1979**, B35, 83.

23. Xie, Z.; Bau, R.; Benesi, A.; Reed, C. A., *Organometallics* **1995**, 14, 3933.

24. Preut, H.; Huber, F., *Acta Crystallogr.* **1979**, B35, 744.

25. Preut, H.; Huber, F., *Z. Anorg. Allg. Chem.* **1977**, 435, 234.

26. Stoyanov, E. S.; Hoffmann, S. P.; Juhasz, M.; Reed, C. A., *J. Am. Chem. Soc.* **2006**, 128,3160.

27. Lefferts, J. L.; Molloy, K. C.; Hossain, M. B.; van der Helm, D.; Zuckerman, J. J., *J. Organomet. Chem.* **1982**, 240, 349.

28. Tse, J. S.; Lee, F. L.; Gabe, E. J., *Acta Crystallogr.* **1986**, C42, 1876.

29. Sorensen, T. S. In *Stable Carbocation Chemistry*; Surya Prakash, G. K.; Schleyer, P. v. R., Eds.; Wiley: New York, **1997**; Chapter 3.

30. Perrin, D. D.; Armarego, W. L. F.; Perrin, D. R. *Purification of Laboratory Chemicals*, 2nd ed.; Pergamon Press Ltd.: Sydney, **1980**.

31. See Supporting Information in ref 7.

Chapter Three: Perhalogentaed Carba-*closo*-dodecaborate Anions as Ligand Substituents: Applications in Gold Catalysis

3.1 Introduction:

The success of modern transition-metal catalysis is largely due to the availability of a diverse range of ligand frameworks. One of the most universal aspects of ligand design is the strategic attachment of bulky substituents to influence the activity of catalysts. Sterically demanding substituents kinetically protect the active metal center and, at the same time, promote substrate exchange and low coordination, two processes necessary for turnover. Bulky ligand substituents also influence the selectivity of the metal center for product formation and substrate consumption. For these purposes, the most common groups appended to ancillary ligands are alkyl and aryl groups, such as adamantyl or 2,6-diisopropylphenyl. Far less common is the use of dicarba-*closo*-dodecaborane (C_2B_{10}) clusters[1] as surrogates for alkyl or aryl groups.[2] The three-dimensional aromatic nature of these species and their icosahedral shape lend them properties akin to those of both alkyl and aryl groups. However, owing to the hydridic nature of the B–H vertices, ligands bearing these substituents tend to undergo undesirable B–H activation reactions, such as cyclometalation.[3] It is this tendency for such intramolecular reactions to occur that has limited the synthetic utility of dicarba-*closo*-dodecaborane-bearing ligands in the area of catalysis.

Interestingly, complexes that contain ligands functionalized with related carba-*closo*-dodecaborate anions (CB_{11}^-)[4] directly bound to the coordinating atom through the carborane cage carbon atom have not been reported.[5] Although similar in size to their neutral "dicarba" cousins (C_2B_{10}), isoelectronic (CB_{11}^-) clusters have significantly different properties. The negative charge is delocalized over all of the 12 cage atoms, and as a result, the anion is very weakly coordinating. This weak coordination ability can be enhanced by the substitution of some or all of the B–H vertices for alkyl or halo groups. In the case of alkyl substitution, the cluster becomes more reactive towards substitution and oxidation. On the other hand, exhaustive halogenation of the boron vertices of the cluster introduces a blanket of electron-withdrawing substituents that enhances the inherent weak coordination ability of the anion and also confers upon these molecules exceptional inertness. It has been demonstrated that perhalogenated carborane counteranions are sufficiently unreactive that they can form isolable salts with potent oxidants, such as C_{60}^{+}[6] and CH_3^+.[7] Thus, these clusters can be far more inert than even simple hydrocarbons: CH_3^+ abstracts hydrides from *n*-alkanes with loss of methane at room temperature. It is these properties that have generated increasing interest[8] in the use of perhalogenated carborane anions in silylium catalysis[8i,l] and related processes.[8f] The anion of choice for most applications is the $HCB_{11}Cl_{11}^-$ anion (**1**), since it is readily accessible[8g] and arguably the most inert carborane anion (Scheme 1).

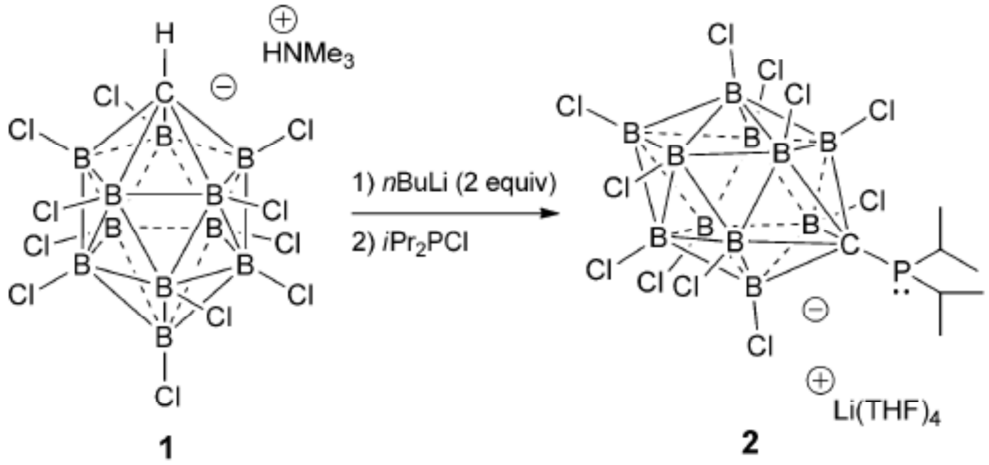

Scheme 3.1 Synthesis of phosphine **2**.

We are interested in using the $HCB_{11}Cl_{11}^-$ cluster (**1**) and related systems not only as weakly coordinating anions, but also as super-bulky, inert, charged ligand substituents. The van der Waals volume (V_{vdW}) of **1** is approximately 350 Å^3,[9] which is more than twice as large as that of an adamantyl group (V_{vdW}=136 Å^3);[1] thus, **1** is an exceptionally large substituent. Appending ligands with such molecular architectures may lead to catalytic systems that display superior activity and stability, particularly when positively charged intermediates are involved. Herein, we report the synthesis of a ligand containing the $CB_{11}Cl_{11}^-$ cluster as a substituent and demonstrate its utility by the preparation of unique single-component Au^I catalysts with unprecedented activity for the hydroamination of alkynes with primary amines.

3.2 Results and Discussion

To begin our investigation into the properties of ligands containing the $CB_{11}Cl_{11}^-$ moiety, we chose to prepare a phosphine. Specifically, we targeted $iPr_2P(CB_{11}Cl_{11})^-Li^+$ (**2**), since the isopropyl groups of this phosphine should give distinct resonances in the ^1H NMR spectrum that are straightforward to interpret (Scheme 1). Additionally, because the $CB_{11}C_{11}^-$ fragment is very large, the intermediate steric bulk of the isopropyl groups should make the phosphorus lone pair accessible for coordination.

Thus, treatment of the trimethylammonium salt of anion **1** with 2 equivalents of *n*BuLi and subsequent quenching of the dianionic intermediate with iPr_2PCl afforded **2** in 98 % yield (Scheme 1). The anionic phosphine **2** is very soluble in common polar solvents (CH_2Cl_2, $CHCl_3$, THF) and is not sensitive to oxygen in solution or the solid state. A single-crystal X-ray diffraction study unambiguously confirmed the structure of **2** and showed a sterically congested environment around the pyramidalized phosphorus center (sum of CPC angles: 325.1°; Figure 1). The bond between the phosphorus atom and the carborane cage carbon atom (P–C1 1.9376(16) Å) is significantly longer than those between the phosphorus atom and the isopropyl groups (P–C2 1.8679(19), P–C3 1.8636(18) Å). The lithium countercation of **2** is coordinated by four THF molecules and does not associate with the halogen substituents on the negatively charged carborane (closest Cl···Li distance: 4.283 Å).

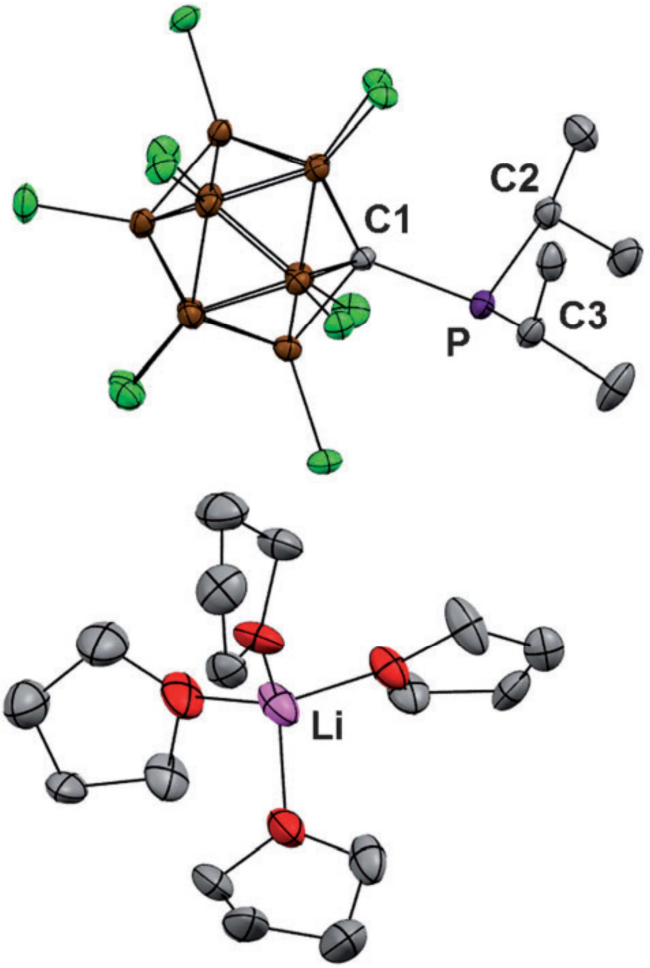

Figure 3.1 Solid-state structure of phosphine **2** (C gray,Ppurple, Cl green,Bbrown, Li pink,Ored). Hydrogen atoms are omitted for clarity;thermal ellipsoids are drawn at the 50%probability level.

There is growing interest in single-component[10] gold catalysts,[11] which can offer a number of advantages over traditional two-component systems that utilize Ag^+ or strong Brønsted acid additives. These additives not only increase the cost of the systems, but can also promote side reactions or different reactivity.[10] Given that our phosphine **2** contains a pendant weakly coordinating anion, we were

intrigued by the idea of combining **2** with a Au^{I} cation. The typical linear geometry of Au^{I} is also important, since the $CB_{11}Cl_{11}$ group of **2** will be fixed in a position close to the metal but removed from the *trans* coordination site (with respect to the phosphine), where substrates usually bind during catalysis.

When the anionic phosphine **2** was treated with chloro(tetrahydrothiophene)gold(I) (ClAu(tht)) in monofluorobenzene (FC_6H_5) at room temperature, a large amount of a white precipitate formed within 5 min (Figure 2). Analysis of the precipitate by ^{31}P NMR spectroscopy showed a phosphorus resonance at δ=+90 ppm, which is significantly shifted downfield from that of the starting material **2** (+77 ppm) and in line with the formation of a gold–phosphine complex. The ^{1}H NMR spectrum clearly showed resonances corresponding to the phosphine ligand as well as coordinated tetrahydrothiophene and thus suggested the formation of the zwitterionic Au complex $\mathbf{3_{(THT)}}$ by ligand coordination and anion metathesis. The driving force for the anion metathesis is the insolubility of LiCl in FC_6H_5. A single-crystal X-ray diffraction study unambiguously confirmed the structure of $\mathbf{3_{(THT)}}$; however, disorder in the P–*i*Pr groups precludes an accurate discussion of the structural parameters of $\mathbf{3_{(THT)}}$. This complex is reminiscent of the single-component zwitterionic Au–tht catalyst supported by an anionic N-heterocyclic carbene[12] that was recently reported by Tamm and co-workers.[13] However, in our case, the charged group is bound directly to the coordinating atom and is therefore much closer to the Au center. Interestingly, when the reaction was performed in THF, a

solvent in which LiCl is soluble, THT was liberated, and an unusual anionic complex **3**$_{(LiCl)}$ was isolated (**3**$_{(LiCl)}$ can also be prepared by the treatment of isolated **3**$_{(THT)}$ with LiCl in THF). In contrast to **3**$_{(THT)}$, we were able to grow single crystals of **3**$_{(LiCl)}$ without significant disorder and thus examined the solid-state structural aspects of this molecule. The Tolman cone angle[14] for the phosphine ligand is 204°, which indicates that this ligand is much more bulky than a standard sterically demanding phosphine ligand, such as P*t*Bu$_3$ (cone angle: 182°). The P–Au bond length is 2.2477(12) Å, which is close to that reported for a neutral *ortho*-dicarba-*closo*-decaborane-substituted phosphine–AuCl complex (2.232(3) Å).[15] The anionic $CB_{11}Cl_{11}$ substituent displays one chloride interaction with the Au ion (closest Au···Cl–B distance: 3.118 Å). This distance is greater than the sum of the covalent Au/Cl radii but in the range of a van der Waals contact (sum of Au/Cl vdW radii: 3.41 Å). For comparison, the chloride ligand (*trans* to the phosphine) is at a distance of 2.2883(12) Å from the metal center. Hence, the carborane substituent retains a significant amount of weakly coordinating character, even though it is forced into a position close to the metal center.

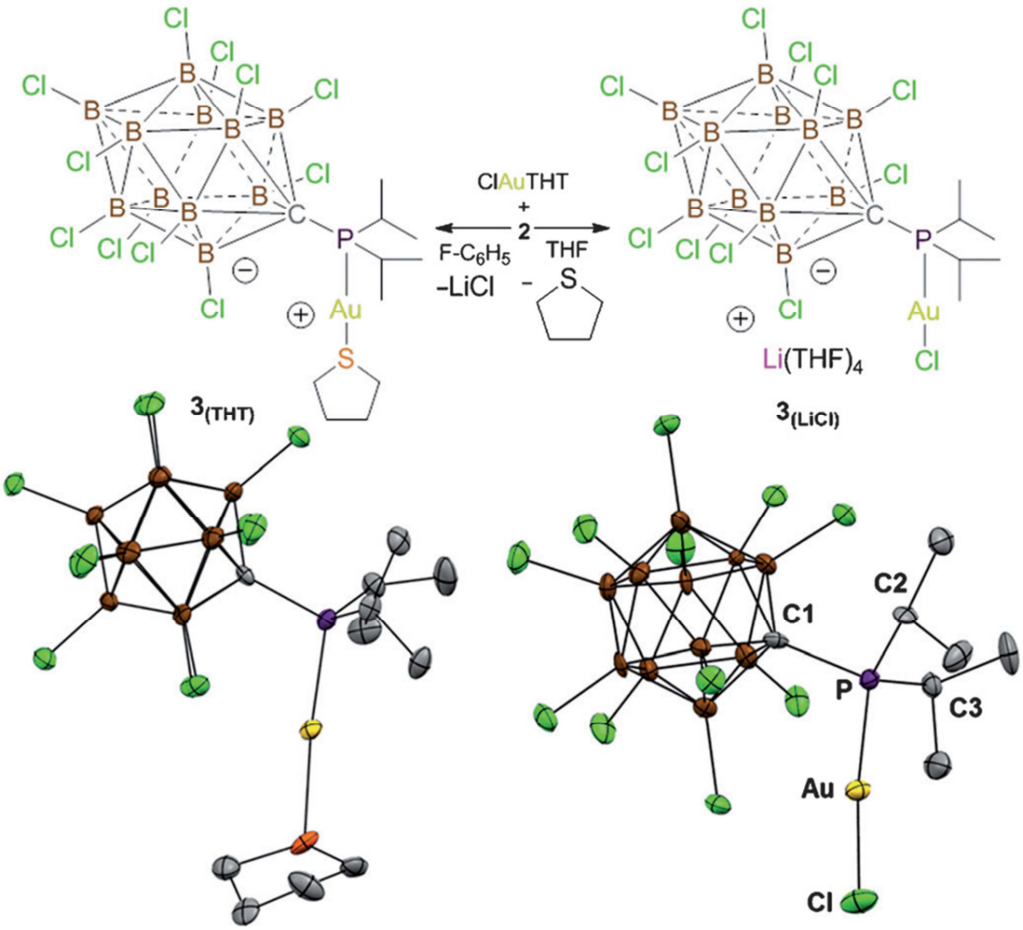

Figure 3.2 Top: Synthesis of complexes **3**$_{(THT)}$ (left) and **3**$_{(LiCl)}$ (right). Bottom: Solid-state structures of **3**$_{(THT)}$ (left) and **3**$_{(LiCl)}$ (right; C gray, P purple, Au gold, Cl green, B brown, S orange). Selected bond lengths [Å] for **3**$_{(LiCl)}$: P—Au 2.2477(12), P—C1 1.943(5), P—C2 1.858(6), P—C3 1.864(5), Au—Cl 2.2883(12). Thermal ellipsoids are drawn at the 50 % probability level; hydrogen atoms in both **3**$_{(THT)}$ and **3**$_{(LiCl)}$ are omitted for clarity.

We next turned our attention to the catalytic properties of complexes **3**, which are air- and light-stable, in the hydroamination[16] of primary amines with alkynes.[17] As a model reaction, we chose the addition of aniline to phenylacetylene. Thus, a

1:1 neat mixture of the amine and the alkyne was added to complex **3**$_{(THT)}$ (0.1 mol %), whereupon an exothermic reaction occurred. We monitored the reaction by ^{1}H NMR spectroscopy and found that the hydroamination was more than 95 % complete after 1 h (Table 1, entry 1). Identical results were obtained with **3**$_{(LiCl)}$ (Table 1, entry 2). Further catalytic tests were carried out only with **3**$_{(THT)}$. When the catalyst loading was decreased to 0.01 % and the mixture was heated at 50 °C for 16 h, the yield of the imine was just as high (Table 1, entry 3). Even at a catalyst loading of 0.004 %, the imine was formed in 88 % yield, which corresponds to a catalyst turnover number (TON) of 22 000 (Table 1, entry 4). The highest reported TON for the gold-catalyzed hydroamination of an alkyne with a primary amine is around 9000, for a multicomponent acid-activated Au system.[17h] Control experiments with ClAu(tht) or $HCB_{11}Cl_{11}^{-}Cs^{+}$/ClAu(tht) at a low catalyst loading (0.1 mol %) afforded the imine in only trace amounts (<5 %). These results demonstrate the benefit of the ligand and show that colloidal gold is unlikely to be responsible for the high activity. A metal-free Brønsted acid catalyzed pathway can also be ruled out, since *i*$Pr_2P(CB_{11}Cl_{11})^{-}$ H_3NPh^{+} does not catalyze the reaction.

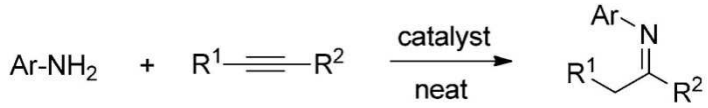

Entry	Cat.	Ar	R^1	R^2	Catalyst loading [%]	*t* [h]	*T* [℃]	Yield [%][a]	TON
1	$3_{(THT)}$	Ph	H	Ph	0.1	1	25	>95	>950
2	$3_{(LiCl)}$	Ph	H	Ph	0.1	1	25	>95	>950
3	$3_{(THT)}$	Ph	H	Ph	0.01	16	50	>95	>9500
4	$3_{(THT)}$	Ph	H	Ph	0.004	16	50	88	22 000
5	$3_{(THT)}$	Mes	H	Ph	0.001	24	50	67	67 000
6	$3_{(THT)}$	Dipp	H	Ph	0.001	24	50	85	85 000
7	$3_{(THT)}$	Ph	H	4-FC_6H_4	0.001	24	50	54	54 000
8	$3_{(THT)}$	Mes	H	4-FC_6H_4	0.001	24	50	75 (60)[b]	75 000
9	$3_{(THT)}$	Dipp	H	4-FC_6H_4	0.001	24	50	92	92 000
10	$3_{(THT)}$	Ph	H	4-$MeOC_6H_4$	0.001	24	50	90	90 000
11	$3_{(THT)}$	Mes	H	4-$MeOC_6H_4$	0.001	24	50	94 (93)[b]	94 000
12	$3_{(THT)}$	Dipp	H	4-$MeOC_6H_4$	0.001	24	50	>95 (88)[b]	>95 000
13	$3_{(THT)}$	Ph	Ph	Ph	0.1	24	80	89.5	895
14	$3_{(THT)}$	Mes	Ph	Ph	0.1	24	80	67	670
15	$3_{(THT)}$	Dipp	Ph	Ph	0.1	24	80	78.5	785
16	$3_{(THT)}$	Ph	H	*n*-C_4H_9	0.2	24	80	86.5	435
17	$3_{(THT)}$	Mes	H	*n*-C_4H_9	0.2	24	80	86	430
18	$3_{(THT)}$	Dipp	H	*n*-C_4H_9	0.2	24	80	>95	>475

Table 3.1 Hydroamination of alkynes with primary amines in the presence of catalysts **3**.[a] The yield was determined by NMR spectroscopy. [b] The yield of the isolated product is given in brackets. Dipp=2,6-diisopropylphenyl, Mes=mesityl (2,4,6-trimethylphenyl).

Because such high catalytic activity is extremely unusual for gold-catalyzed reactions, we examined the hydroamination of phenylacetylene with several different aryl amines at an ultralow loading (0.001 %, 10 ppm). Mesitylamine reacted effectively with phenylacetylene to afford the corresponding imine in 67 % yield after 24 h (TON=67 000; Table 1, entry 5). With bulkier 2,6-diisopropylphenylamine, the reaction was even more efficient and afforded the analogous imine in 85 % yield (TON=85 000; Table 1, entry 6). For the latter reaction, the catalyst was also extremely fast, with an initial turnover frequency of 29 000 in the first hour. Even higher turnover numbers were observed for the analogous reactions with 4-fluorophenylacetylene: a maximum turnover number of 92 000 was reached with 2,6-diisopropylphenylamine (Table 1, entries 7–9). The best results were obtained with 4-methoxyphenylacetylene. With this alkyne, the catalyst converted all three amines into the corresponding imines with turnover numbers of 90 000 or greater (Table 1, entries 10–12).

We postulate that the trend of increased reactivity with increased steric bulk of the amine is related to the decreased binding ability of bulkier amines and the resulting imines, which allows for more facile ligand exchange at the Au center. Catalyst $\mathbf{3}_{(THT)}$ is also effective for the hydroamination of aryl amines with diaryl-substituted alkynes (Table 1, entries 13–15) and terminal alkyl alkynes (Table 1,entries 15–18). Although the activity is lower in these cases, the performance of $\mathbf{3}_{(THT)}$ compares favorably with that of typical Au catalysts, which often require catalyst loadings of 1–10 mol %. A low catalyst loading (0.2 mol %) with an

internal dialkyl alkyne (3-hexyne) or an alkyl amine (*t*BuNH$_2$) as the substrate produced the expected imines only in trace amounts (<5 %).

The two mechanisms generally proposed for gold-catalyzed hydroamination either involve the direct addition of the amine to a coordinated alkyne or a coordination–insertion mechanism. In both pathways, charged intermediates undergo proton-transfer steps that lead to the formation of the functionalized amine. Although we cannot speculate at this time on the exact nature of the mechanism operative in the observed catalysis, it is clear that the anionic $CB_{11}Cl_{11}$ group of phosphine **2** is beneficial for the reaction sequence.

3.3 Conclusion

We postulate that the extraordinary activity of this system might be due in part to the proximity of the anionic $CB_{11}Cl_{11}^-$ group to the Au center during catalysis. This proximity may lead to electrostatic stabilization of the positively charged reaction intermediates. Analogously, the charge on the carborane substituent may also act as an electrostatic tether to prevent phosphine dissociation and subsequent catalyst decomposition. For large-scale applications of homogenous gold catalysis or catalysis with systems based on other precious metals, highly active and efficient catalysts, such as complexes **3**, must be available. Many transition-metal-catalyzed processes involve cationic intermediates that might

benefit from the use of ligands containing a $CB_{11}Cl_{11}^-$ or related substituent. We are currently designing other ligand families that use halogenated carba-*closo*-dodecaborate substituents, as well as expanding on the phosphine system outlined above for use with different transition metals.

3.4 Experimental

Unless otherwise stated, all manipulations were carried out using standard Schlenk or gloveboxtechniques (O_2, H_2O < 1ppm) under a dinitrogen or argon atmosphere. Solvents were dried on K or CaH_2, distilled under argon, and passed through basic alumina before use.Trimethylammonium undecachlorocarborane ($HNMe_3HCB_{11}Cl_{11}$) was prepared by literature methods.[8g] The amines were dried over CaH_2 and distilled before use. The alkynes were driedover molecular sieves and used without further purification. All other reagents were purchasedfrom commercial vendors and used without further purification. Known catalytically producedimines from Table 1 were identified by comparison to their reported spectroscopic data (entries **1-4**,[18]**5**,[19]**6**,[20]**10**,[21]**13**,[22]**14**,[23]**15**,[24]**16**,[25] and **17-18**[26]). Novel compounds (entries **7**, **8**, **9**, **11**, and **12)** were fully characterized. NMR spectra were recorded atroom temperature on Bruker Avance 300MHz, Varian Inova 300MHz, or Varian Inova 400MHz spectrometers. NMR chemical shifts are reported in parts per million (ppm). ^{1}H NMR and ^{13}CNMR chemical shifts were referenced to residual protio

solvent. ^{11}B NMR chemical shifts were externally referenced to BF_3OEt_2. ^{31}P NMR chemical shifts were externally referenced to 80%H_3PO_4 in H_2O. The mass spectra were collected on an Agilent LCTOF Multimode-ESI/APCIwith direct injection.

Synthesis of (2) $Li(THF)_3[P(C_3H_7)_2CB_{11}Cl_{11}]$: $HNMe_3HCB_{11}Cl_{11}$ (1.010g, 1.74mmol) was first deprotonated with 2.1eq (1.46mL, 3.65mmol, 2.5M) of *n*-butyllithium in THF and allowed to stirovernight. The white precipitate was collected on a sintered glass filter and washed with hexane.The solid was subsequently dissolved in fluorobenzene and immediately treated with chlorodiisopropylphosphine (0.322g, 2.11mmol). After stirring the mixture overnight, the lithiumchloride was filtered off and the product was obtained by concentrating the filtrate in vacuo toafford **2** (1.454g, 1.68mmol, 97.0%). Crystals suitable for an X-ray diffraction study were obtained by layering a solution of **2** in $CHCl_3$, with hexanes. m.p. 220℃ (dec.); ^1H NMR (400MHz, $CDCl_3$, 25˚C): *δ*=3.82 (m, 12H, THF), 3.10 (sep, $^3J(H,H)$=4.0 Hz, 2H, CH), 1.98 (m, 12H, THF), 1.51 (dd, $^3J(H,H)$=6.8 Hz; 3J(P,H)=8.0 Hz, 6H, CH_3), 1.35 (dd, $^3J(H,H)$=7.6 Hz,$^3J(P,H)$=23.2 Hz, 6H, CH_3); ^{31}P-(1H-dec) NMR (162 MHz, CDCl3, 25˚C): *δ*= 77.28ppm; ^{13}C-(^1H-dec) NMR (101 MHz, $CDCl_3$, 25˚C): *δ*= 69.98 (CH_2, THF), 25.93 (d, 2J(P,C)=36.4 Hz, CH), 25.72 (CH_2, THF),24.62 (d, 2J(P,C)=39.9 Hz, CH), 24.04 (CH_3); ^{11}B-(^1H-dec) NMR (96 MHz,$CDCl_3$, 25˚C):*δ*= -3.07, -4.71, -

6.63ppm; HRMS: (Multimode-ESI/APCI) [M]- m/z calc'd for$H_{14}B_{11}C_7P_1Cl_{11}$: 637.8345; found: 637.8463.

Note 1: NMR analysis of the amorphous powder indicates 3 coordinated THF molecules. In crystalline form there are 4-coordinated THFs.

Note 2: The small resonance at -9.1 ppm in the ^{11}B spectra is a few percent of the $HCB_{11}Cl_{11}$ anion, likely formed via adventitious water. The traces of $Li^+HCB_{11}Cl_{11}^-$ are removed after formation of complex **3$_{(THT)}$**, since **3$_{(THT)}$** is onlysparingly soluble in F-Benzene.

Synthesis of 3$_{(THT)}$, (THT)Au(P(C$_3$H$_7$)$_2$CB$_{11}$Cl$_{11}$): In a vial equipped with a stir barLi(THF)$_3$[P(C$_3$H$_7$)$_2$CB$_{11}$Cl$_{11}$] (1.100g, 1.277mmol) and ClAu(THT) (377.8mg, 1.180mmol) wereadded and subsequently dissolved in 20mL of fluorobenzene. The mixture was stirred and awhite precipitate rapidly formed. After an hour the capped vial was placed in the freezer (-35˚C) overnight and subsequently collected on a sintered glass filter (the filtrate was not discarded).Extraction of the product from LiCl with CH_2Cl_2 (3 x 10mL), and concentrating under vacuum,afforded 554.0mg of pure **3$_{(THT)}$ (**51% yield, based on ClAuTHT). Concentrating the savedfluorobenzene filtrate to 10mLs and repeating the purification procedure afforded an additional196mg of **3$_{(THT)}$**(total yield = 0.750g, 0.812mmol, 68.9%). Crystals suitable for an X-raydiffraction study were obtained by layering a CH_2Cl_2 solution of **3$_{(THT)}$**with hexanes. m.p. =194℃(dec.); ^1H NMR (400 MHz, CD_2Cl_2, 25˚C): δ= 3.51 (sep, 3J(H,H)=8.0 Hz, 2H, CH), 3.48(sep,

3J(H,H)=8.0 Hz, 2H, CH), 3.42 (m, 4H, THT), 2.20 (m, 4H, THT), 1.63 (dd,3J(H,H)=7.2Hz, 3J(P,H)=12.0 Hz, 6H, CH3), 1.57 (dd, 3J(H,H)=1.2 Hz, 3J(P,H)=7.2 Hz, 6H, CH3); ^{31}P-(^{1}Hdec)NMR (162 MHz, $CDCl_3$, 25˚C): *δ*= 90.90 ppm; ^{13}C-(1H-dec) NMR (101 MHz, CD_2Cl_2,25˚C): *δ*=40.08 (CH_2, THT), 30.94 (CH_2, THT), 29.97 (d, ^{2}J(P,C)=20.0 Hz, CH),28.83 (d,^{2}J(P,C)=19.2 Hz, CH), 21.39 (CH_3), 21.36 (CH_3); ^{11}B-(^{1}H-dec) NMR (96 MHz, CDCl3, 25˚C):
δ= 1.74, -8.08,-10.40ppm; HRMS: (Multimode-ESI/APCI) [M]- m/z calc'd for $H_{23}B_{11}C_{11}P_1Cl_{11}Au$: 923.8534; found: 923.8570.

Note: A solution of **3$_{(THT)}$** in tetrahydrothiophene was used for this experiment. The HRMS datacorresponds to a negative ion formed in flight composed of **3$_{(THT)}$**, a hydrogen atom, and 1electron (likely due to solvent effects).

Synthesis of 3$_{(LiCl)}$,Li(THF)$_2$[ClAu(P(C$_3$H$_7$)$_2$CB$_{11}$Cl$_{11}$)]:3$_{(THT)}$ (0.0276g, 0.032mmol) andLiCl (0.0661g, 1.56mmol) were dissolved in 10mL of THF and allowed to stir overnight. TheTHF was removed in vacuo and the product was extracted from LiCl with CH_2Cl_2. After removalof CH_2Cl_2 in vacuo pure **3$_{(LiCl)}$**was isolated as a white solid (0.0284g, 0.027mmol, 86.7%yield).Crystals suitable for an X-ray diffraction study were obtained by layering a solution of **3$_{(LiCl)}$**inCH_2Cl_2, with hexanes. m.p. = 243℃ (dec.); ^{1}H NMR (400 MHz, CD_2Cl_2, 25˚C):δ=3.80 (m, 8H,THF), 3.47 (sep, ^{3}J(H,H)=8.0 Hz, 2H, CH), 3.44 (sep, ^{3}J(H,H)=8.0 Hz, 2H, CH), 1.95 (m, 8H,THF), 1.63 (dd, ^{3}J(H,H)=7.2 Hz, ^{3}J(P,H)=24.4 Hz, 6H, CH_3),

1.58 (dd, $^{3}J(H,H)=7.2$ Hz,$^{3}J(P,H)=16.4$ Hz, 6H, CH_3); ^{31}P-(^{1}H-dec) NMR (162 MHz, $CDCl_3$, 25˚C):δ=89.49 ppm; ^{13}C-(^{1}H-dec) NMR (101 MHz, CD_2Cl_2, 25˚C):δ=68.85 (CH_2, THF), 30.45 (d, $^{2}J(P,C)=14.3$ Hz, CH),29.53 (d, $^{2}J(P,C)=29.6$ Hz, CH),25.65 (CH_2, THF), 21.37 (CH_3);^{11}B-(^{1}H-dec) NMR (96 MHz,$CDCl_3$, 25˚C):δ=3.65, -6.15, -8.14 ppm; HRMS: (Multimode-ESI/APCI) [M]- m/z calc'd for$H_{14}B_{11}C_7P_1Cl_{11}Au$: 869.7797; found: 869.7837.

Note 1: NMR analysis of the amorphous powder indicates 2 coordinated THF molecules. Incrystalline form there are 4-coordinated THFs.

Note 2: As mentioned in the manuscript, **3$_{(LiCl)}$**can also be prepared directly from **2** and ClAu(THT) in THF. However, using this method, tracesof the $HCB_{11}Cl_{11}$anion will remain in the product and are difficult to remove.

General procedure for catalysis. A standard solution of the appropriate catalyst was prepared,and the desired amount of catalyst was immediately transferred via micropipette to screw capped(PTFE) vials. In experiments with 0.001% loading, for example, a standard catalyst solution(20.0μL, 1.354 x 10^{-3} M; M.W. **3$_{(THT)}$** = 923.20 g/mol) (7.50mg of **3$_{(THT)}$**/6.000mL of CH_2Cl_2) was used.The CH2Cl2 was allowed to evaporate from the open vial in a heating block (50˚C, 10 min), anda stir bar was added. The neat amines and alkynes were then transferred via micropipette (oradded directly if solid) to the screw capped vials, sealed and heated to the indicated temperatureand stirred for the allotted times (Table

1)Yields were calculated by integration ofthe ^{1}H NMR, via direct comparison of the imine formed to the alkyne consumed (average of two runs). The validity of this approach was confirmed by obtaining isolated yields of severalcompounds (entries **8**, **11** and **12**). In these cases the products were isolated via short pathdistillation or by dissolving the catalytic mixture in pentane, followed by filtration, andsubsequent crystallization of the solution at -25˚C.

Imines

(*8*) (E)-N-(1-(4-fluorophenyl)ethylidene)-2,4,6-trimethylaniline

Theoretical Yield = 724.0mg; Isolated Yield = 675.6mg (93.2%). m.p. 60.8-61.7℃; 1H NMR(400 MHz, $CDCl_3$, 25^{o}C): δ=8.04 (m, 2H, Ar), 7.15 (m, 2H, Ar), 6.89 (s, 2H, Ar), 2.30 (s, 3H,CH_3), 2.06 (s, 3H, CH_3), 2.00 (s, 6H, CH_3); ^{13}C-(^{1}H-dec) NMR (101 MHz, $CDCl_3$, 25^{o}C):δ=164.48 (d, $^{1}J(F,C)$=251.49Hz, C,Ar), 164.30 (C, C=N), 146.49 (C, Ar), 135.63 (C,Ar), 132.19 (C, Ar), 129.28 (d, $^{3}J(F,C)$=8.58 Hz, CH, Ar), 128.72 (CH, Ar), 125.75 (C,Ar), 115.45 (d,$^{2}J(F,C)$=21.82 Hz, CH, Ar), 20.93 (CH_3), 18.08 (CH_3), 17.54 (CH_3); ^{19}F-NMR (376 MHz, $CDCl_3$, 25^{o}C): δ= -111.12 ppm; HRMS: (Multimode-ESI/APCI) [M]-m/z calc'd for$H_{18}C_{17}N_1F_1$[H+]: 256.1496; found: 256.1495.

(*9*) (E)-N-(1-(4-fluorophenyl)ethylidene)-2,6-diisopropylaniline

m.p. 109.2-109.7℃; ^{1}H NMR (400 MHz, $CDCl_3$, 25^{o}C): δ=8.08 (m, 2H, Ar), 7.10-7.22 (m, 5H,Ar), 2.77 (sep, $^{3}J(H,H)$=6.8 Hz, 2H, CH), 2.12 (s, 3H, CH_3), 1.19 (d,

$^{3}J(H,H)$=6.8 Hz, 6H, CH_3),1.18 (d, $^{3}J(H,H)$=6.8 Hz, 6H, CH_3); ^{13}C-(^{1}H-dec) NMR (101 MHz, $CDCl_3$, 25^{o}C): δ=164.44 (d,$^{1}J(F,C)$=251.79 Hz, C), 163.73 (C, C=N), 146.71 (C, Ar), 136.32 (C, Ar), 135.45 □C, Ar), 129.40 (d, $^{3}J(F,C)$=8.48 Hz, CH, Ar), 123.62 (CH, Ar), 123.18 (CH, Ar), 115.51 (d,$^{2}J(F,C)$=21.82 Hz, CH, Ar), 28.47 (CH), 23.42 (CH_3), 23.16 (CH_3), 18.22 (CH_3); ^{19}F-NMR (376MHz, CDCl3, 25oC): δ=-111.02 ppm; HRMS: (Multimode-ESI/APCI) [M]- m/z calc'd for $H_{24}C_{20}N_1F_1$[H+]: 298.1966; found: 298.1967.

(*10*) (E)-N-(1-(4-methoxyphenyl)ethylidene)aniline

m.p. 94.1-95.4℃; ^{1}H NMR (400 MHz, $CDCl_3$, 25^{o}C):δ=8.00 (m, 2H, Ar), 7.38 (m, 2H, Ar), 7,12 (m, 1H, Ar), 6.99 (m, 2H, Ar), 6.84 (m, 2H, Ar), 3.88 (s, 3H, OCH_3), 2.23 (s, 3H, CH_3);^{13}C-(^{1}H-dec) NMR (101 MHz, $CDCl_3$, 25^{o}C): δ=164.68 (C=N), 161.78 (C-OMe), 152.18 (C,Ar), 132.44 (C, Ar), 129.16 (CH, Ar), 129.09 (CH, Ar), 123.24 (CH, Ar), 119.85 (CH,Ar), 113.85 (CH, Ar), 55.60 (C, OCH_3), 17.38 (CH_3); HRMS: (Multimode-ESI/APCI) [M]- m/zcalc'd for $H_{15}C_{15}N_1O_1$[H+]: 226.1226; found: 226.1223.

(*11*) (E)-N-(1-(4-methoxyphenyl)ethylidene)-2,4,6-trimethylaniline

Theoretical Yield = 610.0mg; Isolated Yield = 382.2mg (62.9%). brown oil; ^{1}H NMR (400 MHz,$CDCl_3$, 25^{o}C): δ=8.05 (m, 2H, Ar), 7.02 (m, 2H, Ar), 6.93 (s, 2H, Ar), 3.91 (s, 3H, OCH_3), 2.34(s, 3H, CH_3), 2.08 (s, 3H, CH_3), 2.05 (s, 6H, CH_3);^{13}C-(^{1}H-dec) NMR (101 MHz, $CDCl_3$, 25^{o}C):δ=164.65 (C, C=N), 161.71 (C,

C-OMe), 146.90 (C, Ar), 132.27 (C, Ar), 131.90 (C,Ar), 128.92 (CH, Ar), 128.71 (CH, Ar), 125.99 (C, Ar), 113.84 (CH, Ar), 55.61 (C,OCH_3), 20.99 (CH_3), 18.17 (CH_3), 17.40 (CH_3); HRMS: (Multimode-ESI/APCI) [M]- m/z calc'dfor $H_{21}C_{18}N_1O_1$[H+]: 268.1696; found: 268.1697.

(*12*) (E)-2,6-diisopropyl-N-(1-(4-methoxyphenyl)ethylidene)aniline

Theoretical Yield = 767.5mg; Isolated Yield = 672.8mg (87.6%). m.p. 89.6-90.5℃; ^{1}H NMR(400 MHz, $CDCl_3$, 25^{o}C): δ=8.07 (m, 2H, Ar), 7.19 (m, 2H, Ar), 7.12 (m, 1H, Ar), 7.03 (m, 2H,Ar),3.89 (s, 3H, OCH_3), 2.82 (sep, ^{3}J(H,H)=6.8 Hz, 2H, CH), 2.12 (s, 3H, CH_3), 1.20 (d,^{3}J(H,H)=6.8 Hz, 6H, CH_3), 1.19 (d, ^{3}J(H,H)=6.8 Hz, 6H, CH_3); ^{13}C-(^{1}H-dec) NMR (101 MHz,$CDCl_3$, 25^{o}C): δ=163.95 (C, C=N), 161.81 (C-OMe), 147.24 (C, Ar), 136.54 (C,Ar), 132.182 (C, Ar), 129.03 (CH, Ar), 123.42 (CH, Ar) 123.19 (CH, Ar), 113.95 ((CH,Ar), 55.65 (C, OCH_3), 28.52 (CH_3), 23.53 (CH_3), 23.26 (CH_3), 18.15 (CH_3); HRMS:(Multimode-ESI/APCI) [M]- m/z calc'd for $H_{27}C_{21}N_1O_1$[H+]: 310.2165; found: 310.2167.

X-ray Structure:

CCDC 909516 (**2**), 909517 (**3$_{(THT)}$**), and 909518 (**3$_{(LiCl)}$**) contain the supplementary crystallographic data for this paper. These data can beobtainedfree of charge from The Cambridge Crystallographic Data Centre via www.ccdc.cam.ac.uk/data_request/cif.

3.5 References:

1. For a recent review on dicarba-closo-dodecaborane clusters, see:Scholz, M.; Hey-Hawkins, E., *Chem. Rev*. **2011**, 111, 7035.

2. For selected recent examples of ligands containing the C_2B_{10} cluster, see: a) Fey, N.; Haddow, M. F.; Mistry, R.; Norman, N. C.; Orpen, A. G.; Reynolds, T. J.; Pringle, P.G.,*Organometallics* **2012**, 31, 2907; b) Spokoyny, A. M.; Machan, C.W.; Clingerman, D. J.; Rosen, M. S.; Wiester, M. J.; Kennedy, R. D.; Stern, C. L.; Sarjeant, A. A.; Mirkin, C. A., *Nat. Chem*. **2011**, 3, 590; c) van der Vlugt, J. I., *Angew. Chem*. **2010**, 122, 260; *Angew.Chem. Int. Ed*. **2010**, 49, 252; for selected examples of thesynthesis and reactivity of transition-metal systems containinganionic nido boron clusters, see: d) Teixidor, F.; Benakki, R.;Viñas, C.; Kivekäs, R.; Sillanpää, R., *Inorg. Chem*. **1999**, 38, 5916; e) Hewes, J. D.; Kreimendahl, C. W.; Marder, T. B.; Hawthorne,M. F., *J. Am. Chem. Soc*. **1984**, 106, 5757.

3. For a comprehensive list of C_2B_{10} cyclometalation reactions, see Ref. [2a] and references therein.

4. For a comprehensive review on the chemistry of the carba-closododecaborateanion, see: Körbe, S.; Schreiber, P. J.; Michl, J., *Chem. Rev*. **2006**, 106, 5208.

5. For examples of the use of the carba-closo-dodecaborate anionas an X-type ligand with metals directly bound to the carboranecage carbon atom, see: a) Wehmschulte, R. J.; Wojtas, L., *Inorg.Chem*. **2011**, 50, 11300; b) Himmelspach, A.;Zähres, M.; Finze, M., *Inorg. Chem*. **2011**, 50, 3186; c) Himmelspach, A.; Sprenger, J. A. P.; Warneke, J.;Zähres, M.; Finze, M., *Organometallics* **2012**, 31, 1566; d) Finze, M.; Sprenger, J. A. P., *Chem. Eur. J.* **2009**, 15, 9918; e) Ivanov, S. V.; Rockwell, J. J.; Polyakov, O. G.; Gaudinski, C. M.; Anderson,O. P.; Solntsev, K. A.; Strauss, S. H., *J. Am. Chem. Soc*. **1998**, 120, 4224; for examples of the functionalization of the cage carbonatom with potentially coordinating atoms (P,N,O; no transition metal complexes of these molecules have been reported), see:f) Nava, M. J.; Reed, C. A., *Inorg. Chem.* **2010**, 49, 4726;g) Finze, M.; Sprenger,J. A. P.; Schaack, B. B., *Dalton Trans.* **2010**, 39, 2708; h) Vyakaranam, K.; Körbe, S.;Divišová, H.;Michl, J., *J. Am. Chem. Soc*. **2004**, 126, 15795; i) Jelinek, T.;Baldwin, P.;Scheidt, W. A.; Reed, C. A., *Inorg. Chem*. **1993**, 32,1982; for an example of an unusual boron-functionalizedcluster compound with a coordinating acetylide functionality,see: j) Himmelspach, A.; Finze, M.; Raub, S., *Angew. Chem.* **2011**,123, 2676; *Angew. Chem. Int. Ed*. **2011**, 50, 2628.

6. Reed, C. A.; Kim,K.-C.; Bolskar, R. D.; Mueller, L. J., *Science* **2000**, 289, 101.

7. Kato, T.; Reed, C. A., *Angew. Chem*. **2004**, 116, 2968 – 2971; *Angew. Chem. Int. Ed*. **2004**, 43, 2908.

8. For examples of the use of polyhalogenated carboranes asnoncoordinating inert anions, see: a) Stoyanov, E. S.; Stoyanova, I. V.;. Tham, F. S.; Reed, C. A., *Angew. Chem*. **2012**, 124, 9283; *Angew. Chem. Int. Ed*. **2012**, 51, 9149; b) Ramírez-Contreras, R.; Ozerov, O. V., *Dalton Trans*. **2012**, 41, 7842; c) Bolli, C.; Köchner, T.; Knapp, C.,*Z. Anorg. Allg. Chem*.**2012**, 638, 559; d) Volkis, V.; Douvris, C.; Michl, J., *J. Am.Chem. Soc*. **2011**, 133, 7801; e) Fete, M. G.; Havlas, Z.; Michl, J., *J. Am. Chem. Soc*. **2011**, 133, 4123; f) Allemann, O.; Duttwyler, S.; Romanato, P.; Baldridge, K. K.; Siegel, J. S., *Science***2011**, 332, 574; g) Gu, W.; McCulloch, B. J.; Reibenspies, J. H.; Ozerov, O. V., *Chem. Commun*. **2010**, 46, 2820; h) Duttwyler, S.; Douvris, C.; Fackler, N. L. P.; Tham, F. S.; Reed, C. A.; Baldridge, K. K.; Siegel, J. S., *Angew. Chem*. **2010**, 122, 7681; *Angew. Chem. Int. Ed*. **2010**, 49, 7519; i) Douvris, C.; Nagaraja, C. M.; Chen, C.-H.; Foxman, B. M.; Ozerov, O. V., *J. Am. Chem. Soc*. **2010**, 132, 4946; j) Reed, C. A., *Acc. Chem. Res*. **2010**, 43, 121; k) Duttwyler, S.; Zhang, Y.; Linden, A.; Reed, C. A.; Baldridge, K. K.; Siegel, J. S., *Angew. Chem*. **2009**, 121, 3845; *Angew. Chem. Int. Ed.* **2009**, 48, 3787; l) Douvris, C.; Ozerov, O. V., *Science* **2008**, 321, 1188; m) Molinos, E.; Brayshaw, S. K.; Kociok-Köhn, G.; Weller, A. S., *Organometallics* **2007**, 26, 2370; n) Molinos, E.; Brayshaw, S. K.; Kociok-Köhn, G.; Weller, A. S., *Dalton Trans*. **2007**, 4829; o) Köppers, T.; Bernhardt, E.; Eujen, R.; Willner, H.; Lehmann, C. W., *Angew. Chem*. **2007**, 119, 6462; *Angew. Chem. Int. Ed.* **2007**, 46, 6346; p) Ingleson, M. J.; Kociok-Kchn, G.; Weller, A. S., *Inorg. Chim. Acta.* **2005**, 358, 1571; q) Tsang, C. W.; Yang, Q.; Mak, C. T. W.; Xie, Z., *Appl. Organomet. Chem*. **2003**, 17, 449; r) Strauss,S. H. *Spec. Publ. R. Soc. Chem*. **2000**, 253, 44; s) Tsang,C.-W.;Yang, Q.; Sze, E. T.-P.; Mak, T. C. W.; Chan, D. T. W.; Xie, Z., *Inorg. Chem*. **2000**, 39, 5851.

9. The V_{vdw} value of $HCB_{11}Cl_{11}^-$was approximated from crystallographicdata by assuming that the cluster is a perfect sphere.

10. For a recent review on single-component gold catalysts, see:a) Schmidbaur, H.; Schier, A., *Z. Naturforsch. B* **2011**, 66, 329; for a discussion regarding the effects of Ag+ additives onmulticomponent systems, see: b) Wang, D.; Cai, R.; Sharma, S.; Jirak, J.; Thummanapelli, S. K.; Akhmedov, N. G.; Zhang, H.; Liu, X.; Petersen, J. L.; Shi, X., *J. Am. Chem. Soc*. **2012**, 134, 9012.

11. For recent reviews on gold catalysis, see: a) *Modern GoldCatalyzed Synthesis (*Eds.: A. S. K. Hashmi, F. D. Toste), Wiley-VCH, Weinheim, **2012**; b) Gómez-Suárez, A.; Nolan, S., *Angew. Chem*. **2012**, 124, 8278; *Angew. Chem. Int. Ed.* **2012**, 51, 8156; c) Loh,C. C. J.; Enders, D.,*Chem. Eur. J*. **2012**, 18, 10212; d) Garayalde, D.; Nevado, C., *ACS Catal*. **2012**, 2, 1462; e) Lu, B.-L.; Dai, L.; Shi, M., *Chem. Soc. Rev*. **2012**, 41, 3318; f) Liu, L.-P.; Hammond, G. B., *Chem. Soc.Rev*. **2012**, 41, 3129; g) Rudolph, M.; Hashmi, A. S. K., *Chem. Soc.*

Rev. **2012**, 41, 2448; h) Pina, C. D.; Falletta, E.;Rossi, M., *Chem. Soc. Rev*. **2012**, 41, 350; i) Rudolph, M.;Hashmi, A. S. K., *Chem. Commun*. **2011**, 47, 6536; j) Bandini, M., *Chem. Soc. Rev.* **2011**, 40, 1358; k) Malacria, M. Fensterbank, L.; Gandon, V., *Top. Curr. Chem*. **2011**, 302, 157; l) Hashmi, A. S. K., *Angew. Chem*. **2010**, 122, 5360 – 5369; *Angew. Chem. Int. Ed*. **2010**, 49, 5232; m) Gorin, D. J.; Sherry, B. D.; Toste, F. D., *Chem. Rev.* **2008**, 108, 3351; and Ref. [10b].

12. Kösterke, T.; Kösters, J.; Würthwein,E.-U.; Mück-Lichtenfeld,C.; Schulte C; Brinke, T. O.; Lahoz, F.; Hahn, F. E., *Chem. Eur. J*. **2012**, 18, 14594.

13. Kronig, S.; Theuergarten, E.; Daniliuc, C. G.; Jones, P. G.; Tamm, M., *Angew. Chem*. **2012**, 124, 3294; *Angew. Chem. Int. Ed.* **2012**, 51, 3240.

14. Tolman, C. A., *Chem. Rev*. **1977**, 77, 313.

15. McWhannell, M. A.; Rosair, G. M.; Welch, A. J., *Acta Crystallogr. Sect. C* **1998**, 54, 13.

16. For selected reviews on hydroamination reactions, see: a)Klinkenberg, J. L.; Hartwig, J. F., *Angew. Chem*. **2011**, 123, 88; *Angew.Chem. Int. Ed*. **2011**, 50, 86; b) Krossing, I., *Angew.Chem*. **2011**, 123, 11781; *Angew. Chem. Int. Ed.* **2011**, 50,11576; c) Müller, T. E.; Hultzsch,K. C.; Yus, M.; Foubelo, F.; Tada, M., *Chem. Rev*. **2008**, 108, 3795; d) Widenhoefer, R. A.; Han, X., *Eur.J. Org. Chem*. **2006**, 4555.

17. For examples of the gold-catalyzed hydroamination of alkynes,see: a) Fleischer, S.; Werkmeister, S.; Zhou, S.; Junge, K.; Beller, M.,*Chem. Eur. J*. **2012**, 18, 9005; b) Alvarado, E.; Badaj, A. C.; Larocque, T. G.; Lavoie, G .G,*Chem. J*. **2012**, 18, 12112; c) Kinjo, R.; Donnadieu, B.;Bertrand, G.,*Angew. Chem*. **2011**, 123, 5674; *Angew. Chem. Int. Ed*. **2011**, 50, 5560; d) Butler, K. L.; Tragni, M.; Widenhoefer, R. A., *Angew. Chem*. **2012**, 124, 5265; *Angew. Chem. Int. Ed*. **2012**, 51, 5175; e) Hesp, K. D.; Stradiotto, M.,*J. Am. Chem. Soc.***2010**, 132, 18026; f) Leyva-Pérez, A.; Cabrero-Antonino, J. R.;Cantín, A.; Corma, A.,*J. Org. Chem*. **2010**, 75, 7769; g) Lavallo, V.; Frey, G. D.; Donnadieu, B.; Soleilhavoup, M.; Bertrand, G., *Angew. Chem*. **2008**, 120, 5302; *Angew. Chem. Int. Ed*. **2008**, 47, 5224; h) Mizushima, E.;Hayashi, T.;Tanaka, M.,*Org. Lett.* **2003**, 5, 3349; for anexample of a system with a low catalyst loading for the hydrationof alkynes with water (a related process), see: i) Marion, N.;Ramón, R. S.; Nolan, P., *J. Am. Chem. Soc*. **2009**, 131, 448 .

18. Sarma, R.; Prajapati, D.,*Chem. Commun.* **2011**, 47, 9525.

19. Shanbhag, G. V.; Kumbar, S. M.; Joseph, T.; Halligudi, S. B., *Tetrahedron Lett.* **2006**, 47, 141.

20. Zhao, P.; Krug, C.; Hartwig, J. F., *J. Am. Chem. Soc.* **2005**, 127**,** 12066.

21. Imamoto, T.; Iwadate, N.; Yoshida, K., *Org. Lett*. **2006**, 8, 2289.

22. Anderson, L. L. ; Arnold, J.; Bergman, R. G., *Org. Lett.* **2004**, 6, 2519.

23. Zeng, X.; Frey, G. D.; Kousar, S.; Bertrand, G., *Chem. Eur. J.* **2009**, 15, 3056.

24. Greenberg, S.; Stephan, D. W., *Polym. Chem.* **2010**, 1, 1332.

25. Brunet, J.-J.; Chu, N. C.; Diallo,O., *Organometallics* **2005**, 24, 3104.

26. Lorber, C.; Choukroun, R.; Vendier, L.,*Organometallics* **2004**, 23, 1845.

Chapter Four: Anionic Azide Substituted Undecachlorocarborane as Potential Ligands

4.1 Introduction:

The development of homogeneous transition-metal catalysis has been a common topic of intense research in inorganic chemistry. Reactions that require large amounts of energy to proceed are now being done at or near ambient temperatures and pressures due to the rapid development of this field. Nature uses transition metals as catalysts in a variety of ways by incorporating them into proteins or other biological ligands. By incorporating these enzymes into proteins their specificity and reactivity is highly controlled.

As inorganic chemists try to mimic the activity or function of these naturally occurring enzymes, the ligands they choose to modulate the activity and selectivity is vital.[1] Often times the synthesized transition-metal catalysts will be so reactive that they will undergo intramolecular reactions between the ligand and the transition metal.[2] These intramolecular reactions decreases efficiency and lifetime of the catalyst and which then requires increasing the loading amount of catalyst and overall cost.

Often times chemists employ sterically demanding substituents in their ligand design. Common bulky groups utilized are adamantyl, mesityl, diisopropyl phenyl, or terphenyl. By using ligands containing the weakly coordinating perchlorinated1-carba-*closo*-dodecaborate anions, or carboranes, many

intramolecular reactions can be controlled or eliminated. The successful synthesis of the phosphine substituted carborane, its coordination to an Au (I) complex, and the complex's high activity in the hydroamination of amines with alkynes highlighted in Chapter 3 has provided a proof of concept to create and utilize a diverse array of carborane substituted ligands.[3] Exploiting the ability of carboranes that differ by the number and type of substitutents on the eleven B-H vertices a wide variety of C-substituted carborane ligands can be produced for a number of applications.

An obvious choice to quickly expand the library of potential C-substituted carborane ligands would be to synthesize an undecachlorinated carborane azide, $N_3CB_{11}Cl_{11}^-$ or **1** (Figure 4.1). Azides themselves often coordinate strongly to transition-metal catalysts as displayed by their toxicity. Azides are known to inhibit mitochondrial respiration by inhibiting cytochrome oxidase. The electron transport which supports the production of adenosine triphosphate in cytochrome oxidase is disrupted by cyanides, carbon monoxide, and azides in much the same way.[4]

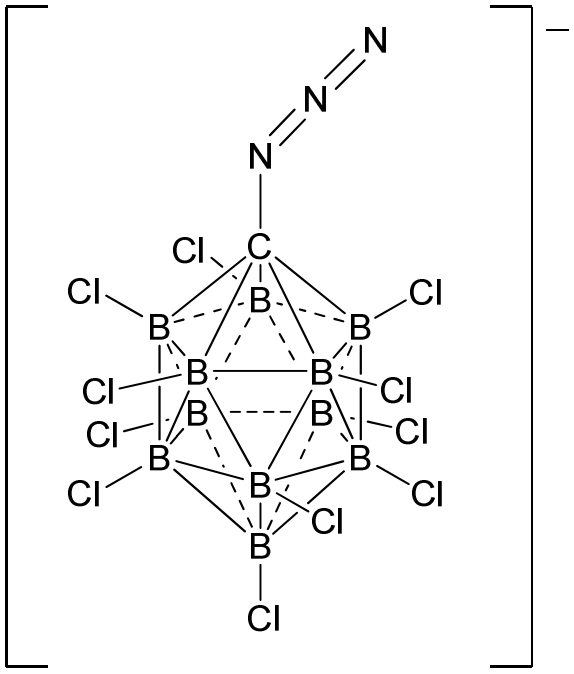

1

Figure 4.1: Azide substituted undecachlorocarborane

Once **1** is isolated it could coordinate to a metal in a variety of coordination modes such as a diazenimido complex, internal azido complex, terminal azido complex, or imido/nitrene complex (Figure 4.2).

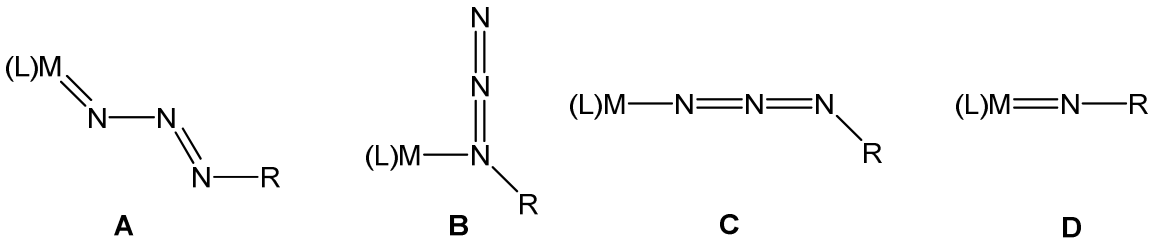

Figure 4.2: Different coordination modes of organic azides.

Azides are also good building blocks to a multitude of various ligands and to another common building block the amine. Azides can be reduced to amines via the Staudinger reaction.[5] An intermediate in this route is a phosphazide and iminophosphorane, which both could also act as ligands as well. Upon hydrolysis of the iminophosphorane in water the amine is synthesized. From the amine additional complexes such as an amido complex or other ligand platforms could be built (Scheme 4.1).

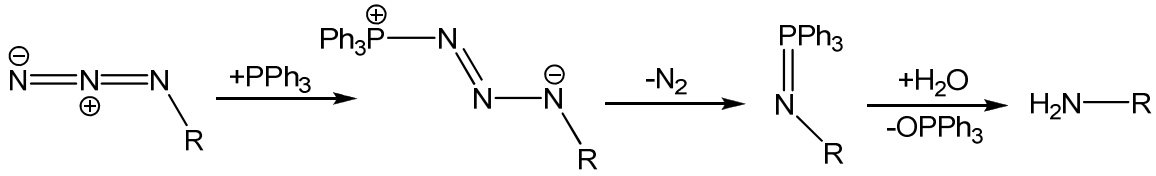

Scheme 4.1: Straudinger reduction of an azide.

Azides can also undergo “Click chemistry”, a term coined by Barry Sharpless of Scripps Reasearch Institute in 2001.[6] While click type chemistry can describe a wide variety of chemical transformations, the reaction between an alkyne and an azide, often utilizing a copper catalyst, tends to dominate the lexicon covered by click chemistry.[7] Sharpless, himself, refers to the Huisgen 1,3-dipolar cycloaddition as “the cream of the crop” for click chemistry. The use of the copper catalyst and the mechanism also serves to illustrate the point of the utility of azides in transition metal chemistry. The 1,2,3-triazole product has become of

particular interest to medicinal chemists and the rapid development of combinatorial libraries.[6] Once synthesis of the azide is completed different triazoles could be synthesized by reacting with different alkynes (Scheme 4.2), which could further increase the number of potential ligands containing the perchlorinated carborane moiety.[7a, 8]

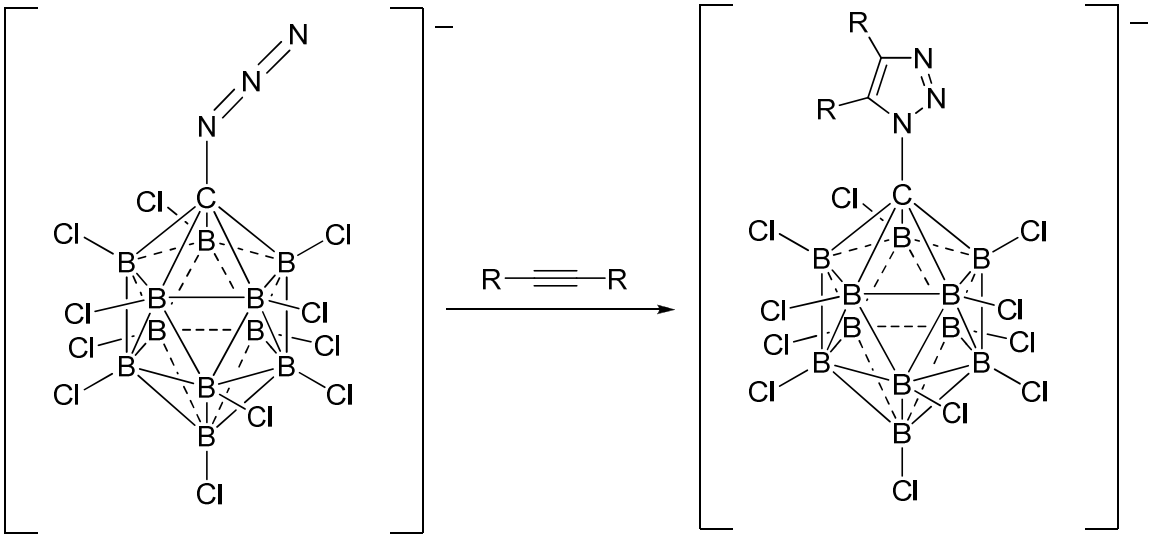

Scheme 4.2: A click reaction on a perchlorinated carborane.

Previous examples anionic carborane azides are more difficult to find in the literature. Only one such compound was found, an anionic permethylated carborane azide was reported by Michl's group.[9] However other work involving neutral carborane substituted azides stem from Blanch *et. al.*[10] and more recently with Kennedy's modified synthesis using 1,2-dicarbadodecaborane.[11] The synthesis of the amine was then carried out using the Staudinger reduction, but also included the isolation and X-ray characterization of the phosphazide

intermediate. The coordination chemistry of the neutral carborane substituted azide and the anionic perchlorocarborane substituted azide could be significantly different. It would be important to explore how the bulk and the electrostatic repulsion of **1** can result in different coordination modes than the neutral 1-azido-2-phenyl-dicarbadodecaborane (Figure 4.3).

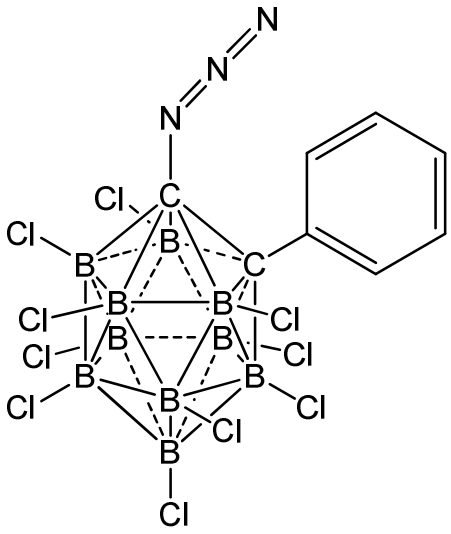

Figure 4.3: 1-azido-2-phenyl-dicarbadodecaborane, a potential azide ligand.

Attempts to synthesis **1** yielded a mixture of two compounds. Through analytical methods of multinuclear nuclear magnetic resonance, electrospray ionization mass spectrometry, and x-ray single crystal diffraction the two compounds were identified. The unanticipated product was a carborane fused heterocycle, **2** (Scheme 4.3). The reaction that must be undergone to synthesize **2** is similar to a click-type reaction, but involves a previously unreported cleavage of a B-Cl

bond of the “inert” perchlorinated carborane anion. Such a reaction has been somewhat ironically nicknamed the “Wright reaction”.

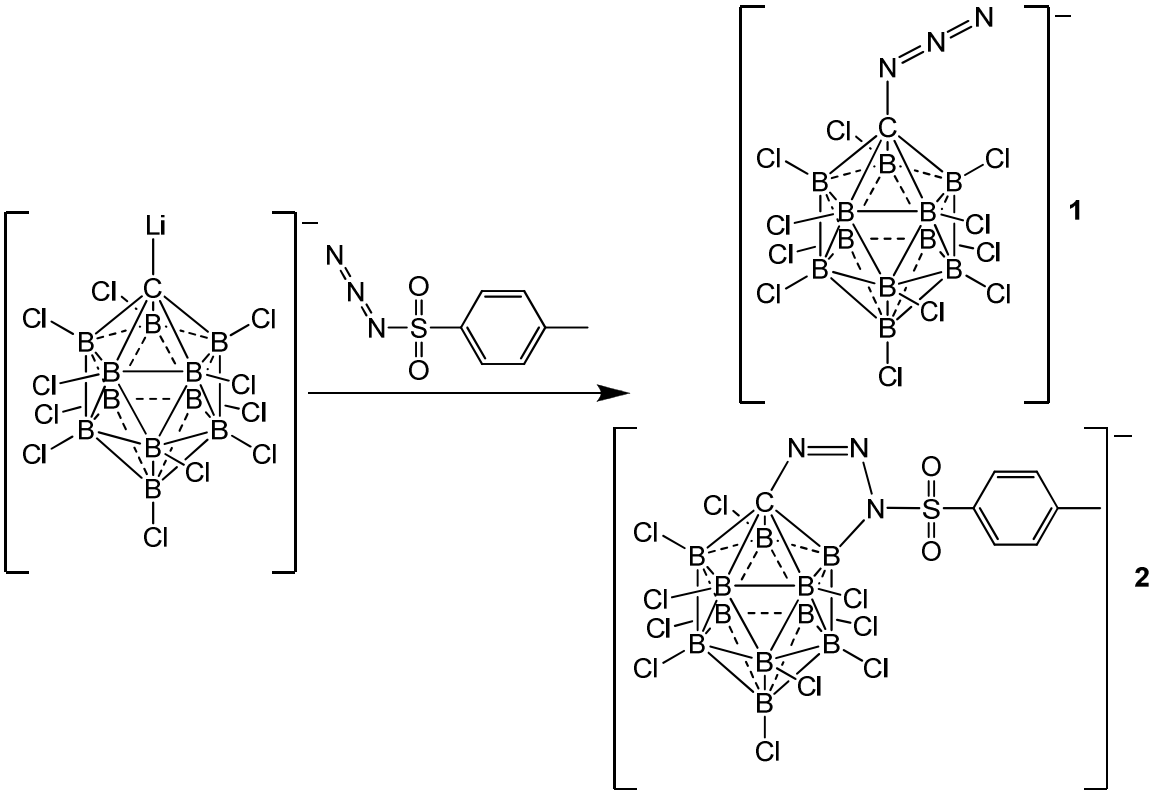

Scheme 4.3: Reaction of the lithiated carborane with tosyl azide gave a mixture of **1** and **2**. The cyclization reaction resulting in **2** is colloquially referred to as the “Wright reaction”.

This chapter reports the synthesis of **1**and a significant byproduct **2**. Attempts to reduce or eliminate production of **2** were unsuccessful. However the separation of **1** proved to be convenient in that it was completed by the continuation toward the synthesis of the amine. The mechanism involved in the Wright reaction is of interest and two possible pathways will be discussed.

4.2 Results and Discussion:

The proposed synthesis of **1** follows the typical electrophilic substitution of carboranes, first the deprotonation of the C-H vertex followed by reaction with an electrophile. In this chapter two different bases are used for the deprotonation. Sodium hydride can be used on the perchlorinated carborane anion as reported by Ozerov due to the halogens increasing the acidity of the C-H vertex.[12] The other base employed is n-butyl lithium, which is commonly used for other carborane anions as well as what Kennedy used on the dicarbadodecaborane.

When a tetrahydrofuran solution of the trimethylammonium undecachlorocarborane is reacted overnight with slightly more than two equivalents of n-butyl lithium a white solid is formed. After separating and washing this white solid the dilithiocarborane species is dissolved in fluorobenzene. The electrophile is 4-methylbenzenesulfonyl azide (tosyl azide) and added slowly to the fluorobenzene solution at room temperature. A precipitate forms almost immediately which should be lithium tosylate. The dilithiocarborane species has two signature ^{11}B NMR peaks which decrease in intensity as tosyl azide is added.

When the reaction is run and monitored by ^{11}B NMR a number of peaks appear (Figure 4.4). These extra peaks were originally thought to have come from advantageous water reacting with the dilithiocarborane. Water could have originated from the tosyl azide since its preparation is done in water ethanol

mixture, and that it was deemed unsafe to distill the organic azide. Other methods of drying the azide will be discussed in the experimental section, however based on the NMR peaks it was suggestive that the C vertex of the carborane was not just reprotonated.

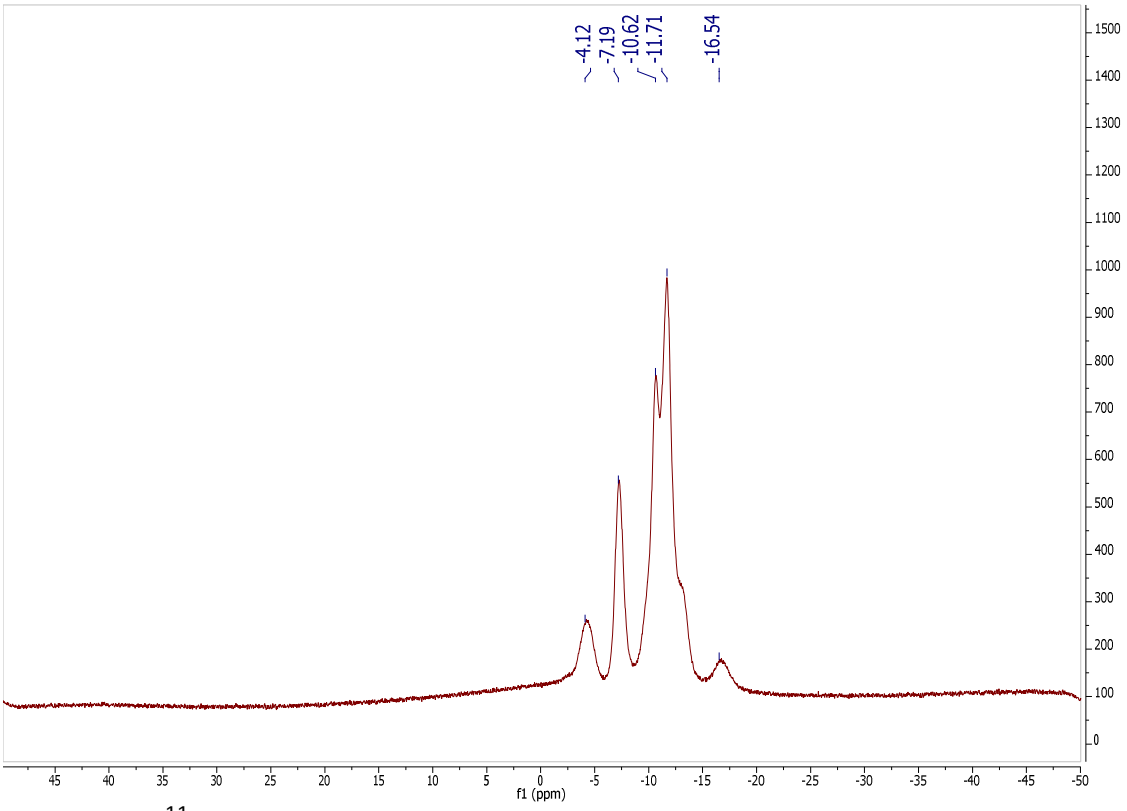

Figure 4.4: ^{11}B NMR of the crude reaction mixture in fluorobenzene.

Electrospray ionization negative ion mass spectrometry was then implemented in the analysis of the mixture. Two products both with complex isotopic distributions indicative of containing large numbers of borons (20% ^{10}B and 80% ^{11}B) and chlorines (75% ^{35}Cl and 25% ^{37}Cl) were observed with a very small amount of the reprotonated carborane (Figures 4.5, 4.6, and 4.7).

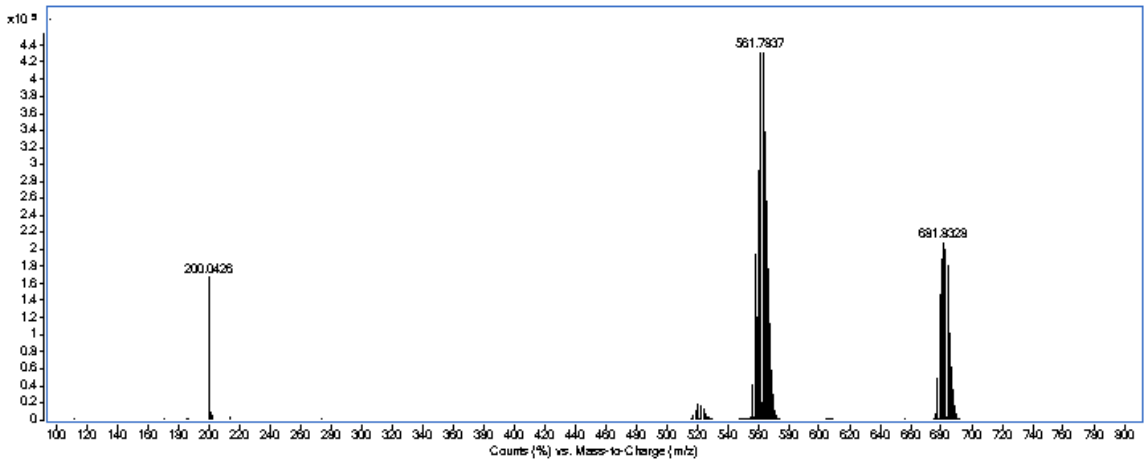

Figure 4.5: Mass spectra of crude reaction mixture.

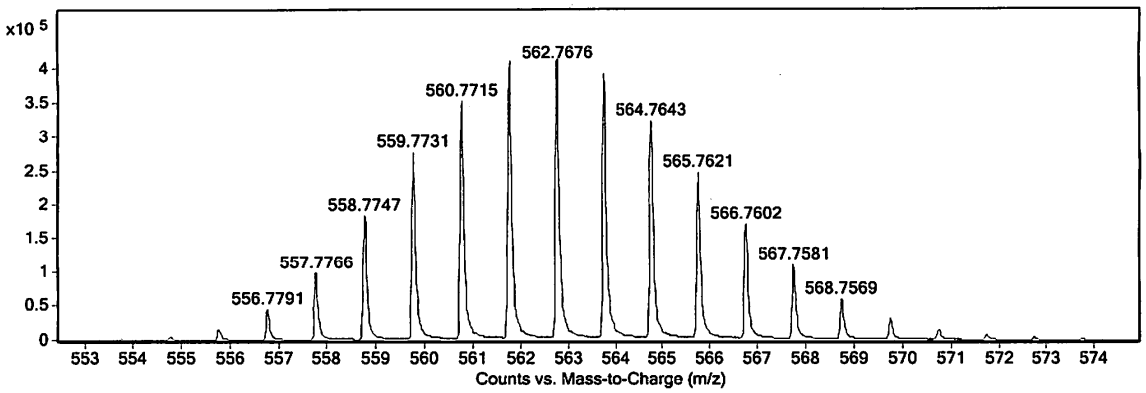

Figure 4.6: Close up of isotope pattern for **1**.

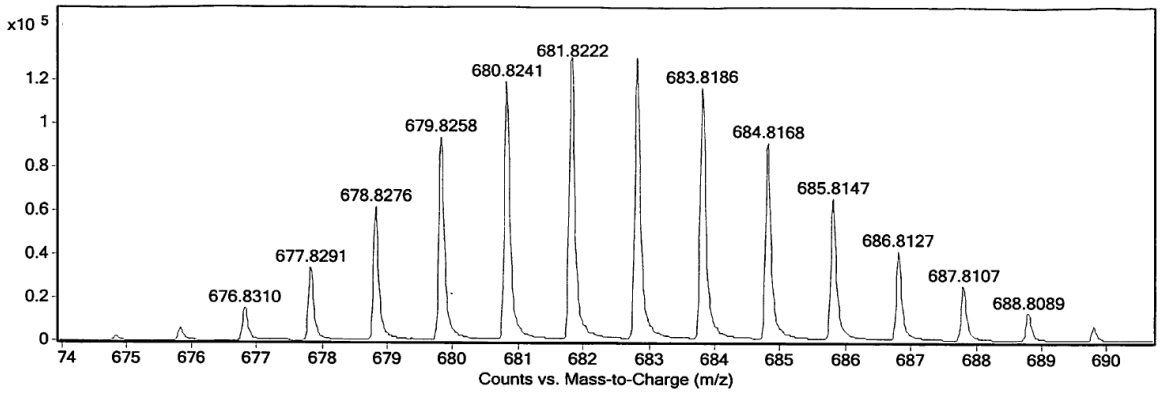

Figure 4.7: Close up of isotope pattern for **2**.

After filtering off the precipitate, it was hypothesized that the two species could be separated by recrystallization. The fluorobenzene solution was layered with hexane and two types of crystals were observable with the aid of a microscope, however only one of the crystals were of sufficient quality for x-ray diffraction structure determination. (Figure 4.8)

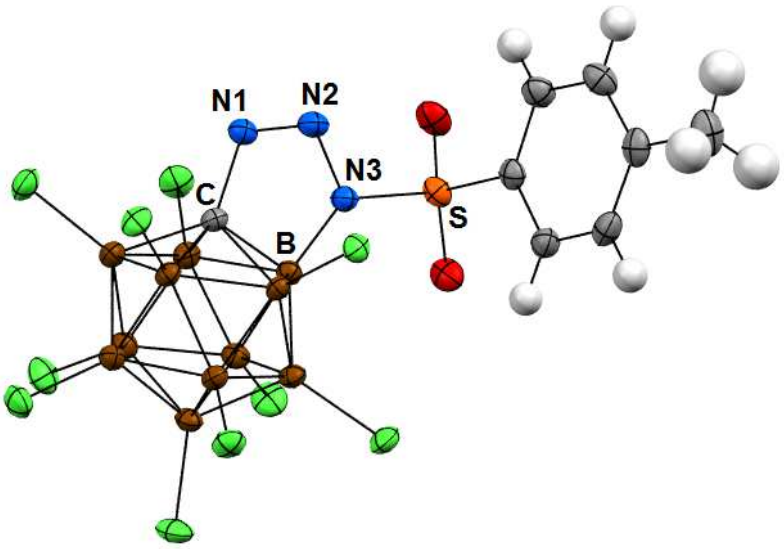

Figure 4.8: X-ray structure of **2**. Cation omitted for clarity.

The crystal selected happened to be the unexpected side product. The X-ray crystal structure in Figure 4.7 as well as the mass observed at 681.8222 in the mass spectra of Figure 4.4 and Figure 4.6 confirms the synthesis of a carborane fused heterocycle. However with both products precipitating out of the fluorobenzene hexane mixture it was unlikely that these two products can be separated by crystallization.

Despite the inability to cleanly synthesize the carborane substituted azide, the unpredicted reaction product was quite interesting. The room temperature cleavage of the B-Cl bond in the carborane is not known and would not be predicted given the inertness of the $[HCB_{11}Cl_{11}]^-$. Also given the popularization of click chemistry, the synthesis of a 1,2,3-triazole is a trending topic.

As with most research, the best projects often results in more questions than answers; and this one result had released a fury of questions. Questions involving the mechanism were immediately asked. Was it a step-wise mechanism (**B**) or an elimination of lithium chloride forming a carboryne-like species before a concerted 3+2 cycloaddition reaction with the azide (**A**)? Two of the possible pathways are in Scheme 4.4. What could the driving force of the reaction be? Can the "Wright reaction" be eliminated to give the azide cleanly? Given our group's desire to synthesize a wide variety of carborane substituted ligands, could this lead to another vertex that can be substituted? What happens if a different organic azide without a leaving group was used (See Chapter 5)?

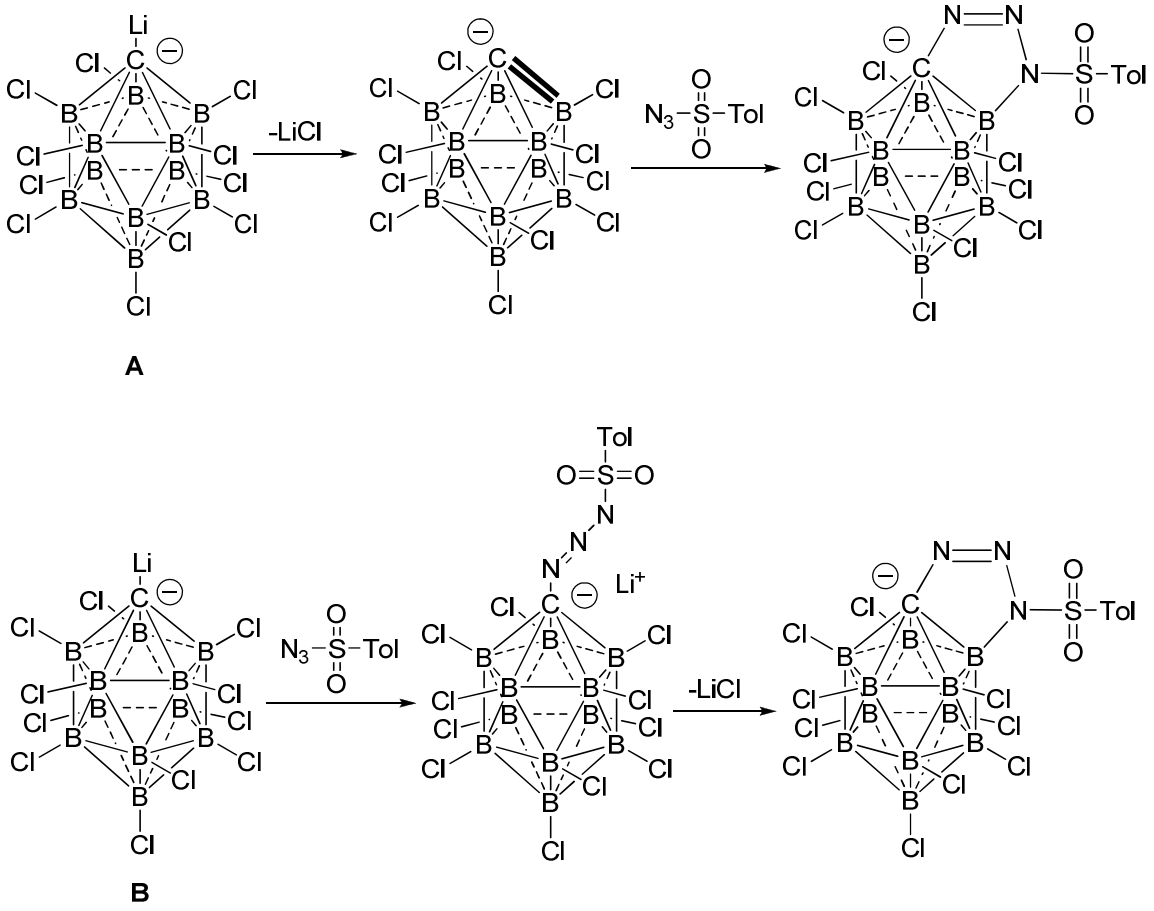

Scheme 4.4: Two possible mechanisms, **A** and **B**, to describe the "Wright reaction".**A** involves the loss of lithium chloride followed by a cycloaddition. **B** is the stepwise approach

Given these two possible mechanisms it is conceivable that reduced temperatures might eliminate the carborane fused heterocycle formation especially if the mechanism followed the proposed formation of a carboryne like intermediate. Elimination of lithium chloride as the first step should be less favorable at lower temperatures and the azide formation should proceed cleanly. At -40 ^{o}C (the freezing point of fluorobenzene), the reaction proceeds and analysis of the reaction mixture by ^{11}B NMR and MS suggests that the ratio between reaction products does not change. Therefore it does not appear that

1could be synthesized without significant byproduct **2** just by reducing the reaction temperature.

The next thought was to lessen the thermodynamic gains of having lithium chloride eliminate could we control the reaction. By having a different salt eliminate with a lower lattice energy then we might force the azide formation.Instead of using n-butyl lithium to deprotonate the carborane, sodium hydride was used.

A large excess of sodium hydride was added to a tetrahydrofuran solution of the trimethylammonium undecachlorocarborane. After stirring the mixture was concentrated invacuo before redissolving in tetrahydrofuran and addition of tosyl azide. With sodium chloride's lattice energy (786kJ/mol) less than lithium chloride (853kJ/mol),[13] could the driving force of the reaction be explained by something as simple as lattice energy of the salt formed? Scheme 4.5 illustrates this proposed route. Unfortunately when this reaction was run at room temperature the resulting ^{11}B NMR indicated that the same ratio of products is similar to all the other reactions.

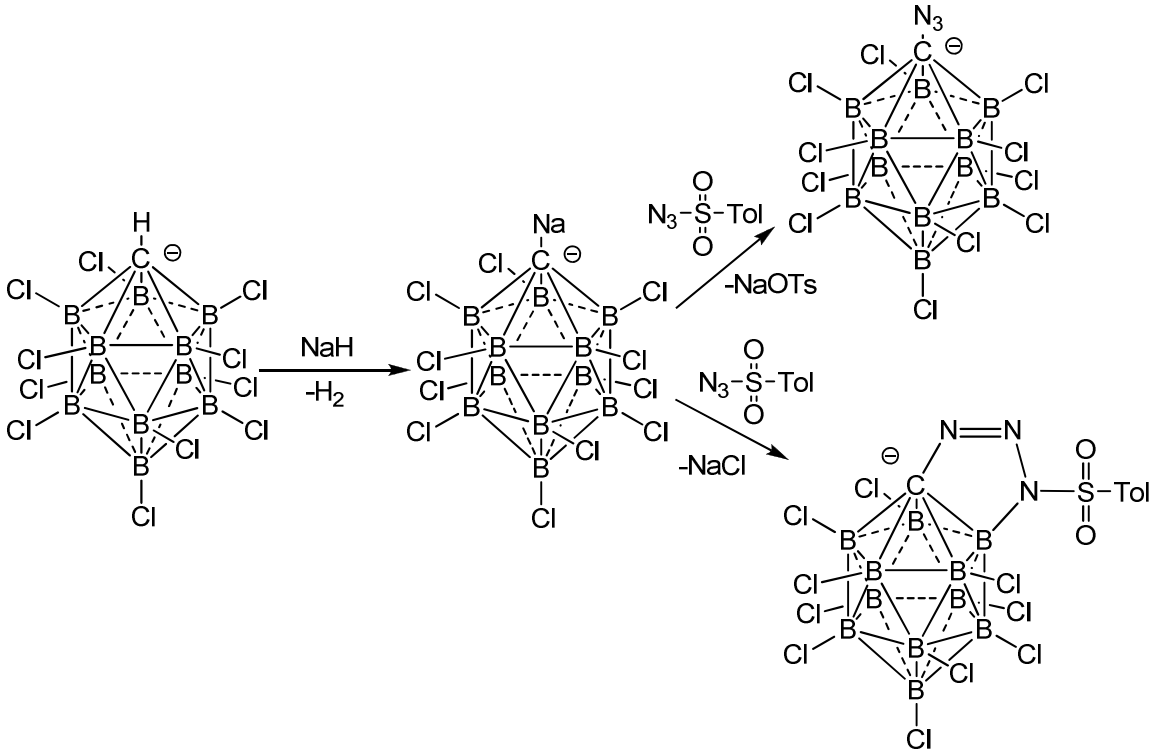

Scheme 4.5: Using sodium hydride to deprotonate the undecachlorocarborane anion followed by reaction with tosyl azide results in mixture of two products.

The cyclization side reaction was not able to be suppressed by lower temperatures, by using a different cation, or by other synthetic tricks such as changing the order of addition. Given these results, instead of focusing on the elimination of a stable salt as a possible driving force, it was hypothesized that the driving force could be the formation of this heterocycle. Given the common use of 3D-aromaticity[14] to describe the carborane and the 2D aromaticity associated with 1,2,3-triazoles one might hypothesize that it is a formation of this 2D-3D hybrid aromatic system that drives the reaction.

Definitions of aromaticity can cause quite a controversy let alone how experimental or computational results can be interpreted. Commonly aromaticity is defined four different ways. Energetically two methods are utilized specifically resonance stabilization energy or aromatic stabilization energy. The geometric structure definition is also used to define aromaticity. When considering geometry the molecule must be cyclic, planar, and have equal bond lengths. The magnetic ring current effects can be measure by nuclear magnetic resonance or calculated computationally using nucleus independent chemical shift (NICS). The fourth criterion sometimes used to define aromaticity is reactivity and whether the molecule undergoes electrophilic aromatic substitution.[15]

The difficulty with each of these becomes apparent when considering the molecule in question, **2**. There would be no easy way to determine the energetic associated with aromaticity, and since geometric considerations are not accurate for 3D molecules or heterocycles those two are not very convincing. However some interesting bond lengths are observed and will be discussed later. NMR is not very beneficial since there are no hydrogens substituted on the ring and cage in question. NICS could be done, but many experimental chemists frown upon definition by computational means only. Finally EAS reactions don't seem like a viable definition either.

In addition to the difficulties in defining aromaticity in order to describe the carborane fused heterocycle as aromatic, a clear distinction between **2** and the

benzo-fused *ortho*-carborane, **3**. First reported in 1968, **3** was subjected to aromaticity measurements involving the reactivity, NMR measurements, and structure. Despite having a diene bonded to the dicarbaborane cluster it is not considered aromatic.[16] Perhaps most damning of evidence against it is the bond alternation between the C-C bonds. They alternate from shorter bonds being more consistent with double bonds (1.331 and 1.340 Å) to longer bonds (1.478, 1.478, 1.452, and 1.654 Å) in Table 4.1 and Table 4.2 the different bond lengths and bond angles are displayed for **2**.

Bond	Bond Lengths
C-B	1.679(3)
C-N_1	1.458(3)
N_1-N_2	1.267(3)
N_2-N_3	1.382(2)
N_3-S	1.6781(19)
B-N_3	1.478(3)
Average C-B(cage)	1.733

Table 4.1: Selected bond lengths of **2**, bond lengths reported in Å.

Angle	Bond Angle
B-C-N_1	105.59(17)
C-N_1-N_2	110.27(17)
N_1-N_2-N_3	114.78(18)
N_2-N_3-B	113.08(18)
N_3-B-C	96.26(16)
N_2-N_3-S	116.28(14)
B-N_3-S	130.63(15)

Table 4.2: Selected bond angles of **2**.

One of the obvious effects observed in the structure of **2** is how the carborane C-B bond shortens an average of 0.54 Å when compared to the other four C-B carborane bonds. The C-N_1 bond corresponds nicely with a single bond (1.454-1.485 Å), where as N_1-N_2 and N_2-N_3 bonds are shorter than what would be expected for a single N-N bond (1.450 Å). The B-N_3 bond is significantly shorter than the accepted B-N single bond of 1.580 Å. The four out of the five bonds that make up the heterocycle are shorter than corresponding single bond, and the fifth bond is on the low end of the range given for C-N single bonds.

Planarity of the ring can be ascertained from the bond angles give. First the hybridization of N_3 is best described as sp^2. The sum of the three angles (N_2-N_3-S, N_2-N_3-B, and B-N_3-S) around the atom total to 359.99˚. Also when the sum of the five interior angles of the heterocycles is taken it almost exactly equals what would be expected for a planar pentagon, 539.99˚ versus 540˚.

The decrease in bond lengths and the planarity as determined by the bond angles suggest dramatic delocalization of electrons in the ring. Despite the difference and asymmetry in bond lengths between the two different N-N bonds, such delocalization might be referred to as aromatic. Determining the number of π electrons would be difficult by conventional Hückel counting. Two would come from the assumed double bond between two nitrogens. Another pair of electrons would come from a nitrogen lone pair as common with aromatic 1,2,3-triazoles. However with normal 1,2,3-triazoles the third pair of electrons come from a C-C

double bond, to give a total of 6, which follows the 4N+2 rule (Figure 4.9). Could the remaining 2 electrons missing from the carborane fused heterocycles come from the carborane cage and its distinct 3 center 2 electron bonds? How might this donation of 2 π electrons affect the 3D aromaticity of the carborane cage?

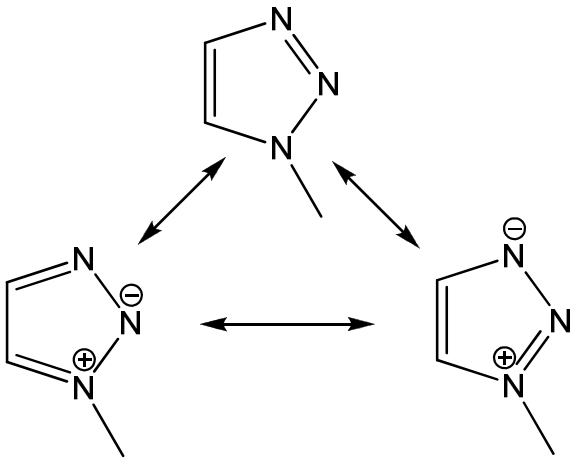

Figure 4.9: Three resonance structures showing the aromaticity of a 1,2,3-triazole.

In the course of studying this side reaction a significant amount of azide had been synthesized, and given the expense of carboranes it was determined that isolation of the azide should be completed. However previously it was discussed that at least using differences in solubility in fluorobenzene and hexane was not a viable option. Since the eventual reduction of the azide to the amine was the original goal further reaction might prove beneficial.

In order to separate the products the mixture was reacted with triphenylphosphine in fluorobenzene. The resulting phosphazide,**3**, precipitated out and was easily separated from **2** by washing with fluorobenzene (Scheme 4.6).

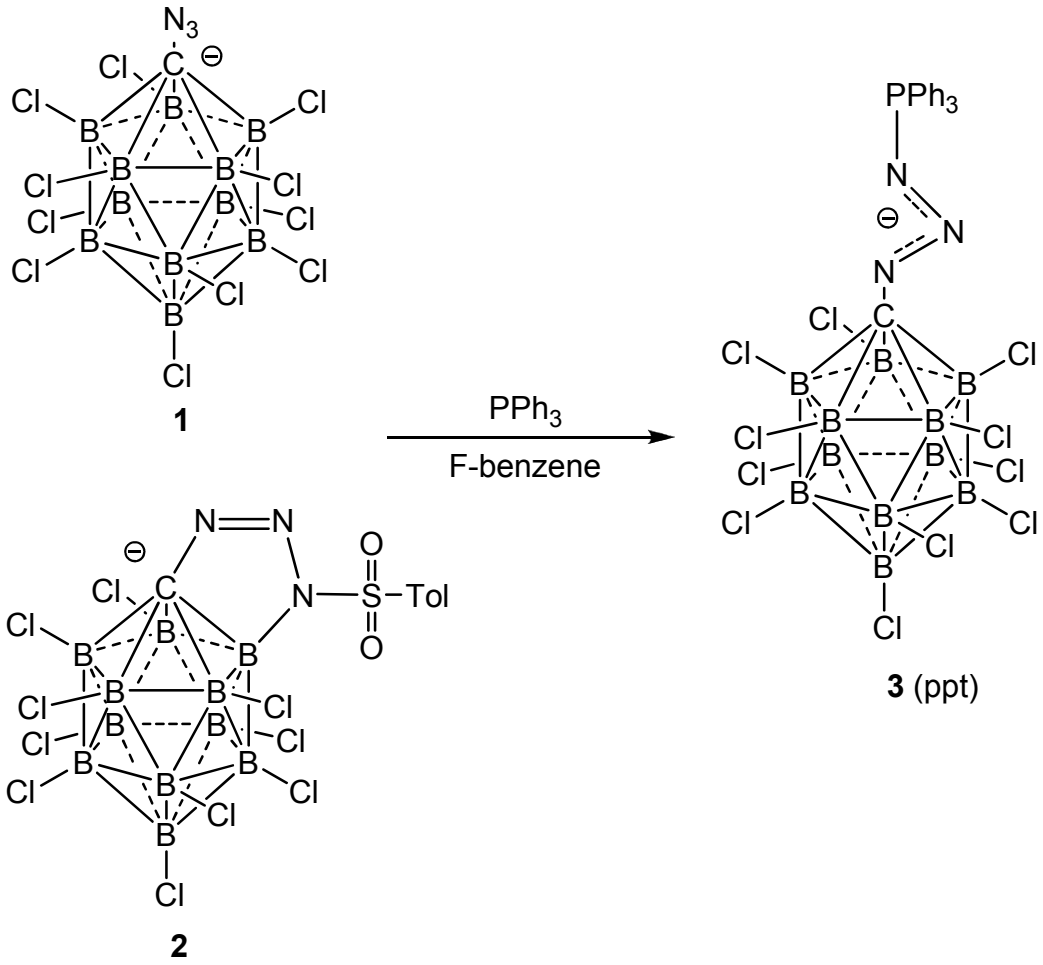

Scheme 4.6: Reaction of mixture of **1** and **2** with triphenylphosphine to yield phosphazide precipitate, **3**. Triphenylphosphine does not react with **2** and **2** is isolated in the supernate.

A X-ray quality crystal of the phosphazide was grown by Professor Lavallo and is presented in Figure 4.10. Javier Farado and Allen Chan were then able to use this method to further characterize the carborane fused heterocycle and the phosphazide.

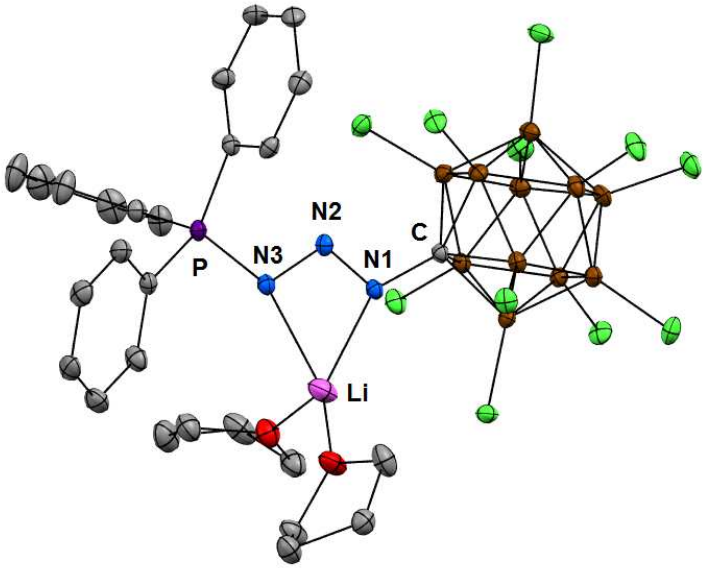

Figure 4.10: X-ray structure of the phosphazide **3**.

Carboranes are often times restrictively expensive and losing a significant percentage to a side product is not an ideal path to synthesize the unchlorocarborane substituted azide, however the use of other carboranes might prove to be successful. A possibly but unlikely path would be to synthesize an azide first from the hydrido parent carborane or the hexachlorocarborane followed by exhaustive chlorination of the B-H vertices(Scheme 4.6). Due to azides reactivity and the harsh conditions required to undecachlorinate the

carborane this pathway is likely to fail, but if other carborane substituted azides prove that the undecachlorocarborane substituted azide is an attractive target then this route should be explored.

4.3 Experimental:

General Considerations:

All manipulations were carried out using standard Schlenk or glovebox technique (O_2, H_2O < 1 ppm) under a dinitrogen or argon atmosphere. Solvents were dried on NaK, K or CaH_2, distilled under argon, and passed through basic alumina before use. Trimethylammonium undecachlorocarborane[17] and tosyl azide[11] were prepared by literature methods. Tosyl azide was furthered dried by passing a dilute diethyl ether solution through a column filled with basic alumina. Before reaction the diethyl ether was removed by placing under vacuum. All other reagents were purchased from commercial vendors and used without further purification. NMR spectra were recorded at room temperature on Bruker Avance 300 MHz, Varian Inova 300MHz, or Bruker Avance 600MHz spectrometers. NMR chemical shifts are reported in parts per million (ppm).^{1}H NMR chemical shifts and^{13}C NMR chemical shifts were referenced to residual protio solvent. ^{11}B NMR chemical shifts were externally referenced to BF_3OEt_2. ^{31}P NMR chemical shifts were externally referenced to 80% H_3PO_4 in H_2O and PPh_3 for the Bruker Avance

300MHz and Bruker Avance 600MHz, respectively. The mass spectra were collected on an Agilent LCTOF Multimode-ESI/APCI with direct injection.

Synthesis of (2) $Li(THF)_4[C_7H_7O_2SN_3CB_{11}Cl_{10}]$ and (3) $Li(THF)_2[Ph_3PN_3CB_{11}Cl_{11}]$: $HNMe_3HCB_{11}Cl_{11}$ (5 g, 8.59 mmol) was first deprotonated with *n*-butyllithium (2.7 eq., 9.3 mL,23.2 mmol, 2.5M in THF) and allowed to stir overnight. The solvent was removed under vacuum, and the precipitate was washed twice with hexanes. The solid was re-dissolved in fluorobenzene and immediately treated with a fluorobenzene solution of tosyl azide (1.1 eq., 1.86 g, 9.45 mmol) at -35^{o}C over 15 minutes. The reaction mixture was stirred and allowed to slowly warm to room temperature overnight, yielding**2** and**3** in solution.^{11}B NMR (96MHz, fluorobenzene, 25^{o}C): δ= -4.12 ppm, -7.19 ppm, -10.62 ppm, -11.71 ppm, -16.54 ppm; HRMS calcd for **2** ($[M]^-$) 681.8190, found: 681.8222.

The LiOTs precipitate was filtered off and triphenylphosphine (1.1 eq., 2.48 g, 9.45 mmol) was added to the solution. The mixture was quickly stirred to dissolve the triphenylphosphine and was left overnight without stirring, after which **3** crystallized from the mixture. The crystals were collected and washed twice with fluorobenzene to give **3**(4.98 g, 5.10 mmol) in 59% yield. ^{11}B NMR (96MHz, THF, 25^{o}C): δ= -3.15 ppm, -11.10 ppm; ^{31}P NMR (121MHz, THF, 25°C): δ=21.05 ppm,

-4.90 ppm; CPMAS ^{31}P NMR (243MHz, 25°C): δ=38.40 ppm; HRMS calcd for **3**([M]$^-$) 562.7697, found: 562.7676.

X-ray Structure:

CCDC 940701 (**2**) and940702 (**3**)contain the supplementary crystallographic data for this paper. These data can beobtainedfree of charge from The Cambridge Crystallographic Data Centre via www.ccdc.cam.ac.uk/data_request/cif.

4.4 Conclusion:

While trying to synthesize an undecachlorocarborane substituted azide $[N_3CB_{11}Cl_{11}]^-$, **1**, an interesting side reaction forming a carborane fused heterocycle, **2**, was discovered. Attempts at understanding the mechanism and driving force were not completely successful. A proposed 2D-3D hybrid aromatic system might be the most controversial but possibly part of the correct driving force. Separation of the two products was easily done by reacting the mixture with triphenylphosphine. Suppressing the side reaction by running the reaction at lower temperatures and switching the cation proved to be unsuccessful.

Since the synthesis of the **1** is hindered by the production of **2**, Chapter 5 sets out to explore the use of different organic azides to see if exclusive synthesis of the triazole fused carborane can be accomplished. Since tosylate is a good leaving group, what happens if organic azides that do not have good leaving groups are reacted? Chapter 5 answers this by testing phenyl azide, mesityl

azide, 2-methylphenyl azide, 4-methoxyphenyl azide, 4-fluorophenyl azide, butyl azide, and adamantyl azide.

4.5 References

1. (a) Williams, R. J. P., *J. Inorg. Biochem.* **2008,** 102, 1; (b) Dennard, A. E.; Williams, R. J. P., *Transition Metal Chem.* **1966,** 2, 115; (c) Irving, H. M.; Williams, R. J. P., *J. Chem. Soc.* **1953**, 3192.

2. (a) Hong, S. H.; Wenzel, A. G.; Salguero, T. T.; Day, M. W.; Grubbs, R. H., *J. Am. Chem. Soc.* **2007,** 129, 7961; (b) Hong, S. H.; Chlenov, A.; Day, M. W.; Grubbs, R. H., *Angew. Chem. Int. Ed.* **2007,** 46, 5148; (c) Brookhart, M.; Green, M. L. H.; Parkin, G., *Proc. Natl. Acad. Sci. U. S. A.* **2007,** 104, 6908; (d) Mohr, F.; Priver, S. H.; Bhargava, S. K.; Bennett, M. A., *Coord. Chem. Rev.* **2006,** 250, 1851.

3. Lavallo, V.; Wright, J. H.; Tham, F. S.; Quinlivan, S., *Angew. Chem. Int. Ed.* **2013,** 52, 3172.

4. Bowler, M. W.; Montgomery, M. G.; Leslie, A. G. W.; Walker, *Proc. Natl. Acad. Sci. U. S. A.* **2006,** 103, 8646.

5. (a) Gololobov, Y. G.; Zhmurova, I. N.; Kasukhin, L. F., *Tetrahedron* **1981,** 37, 437; (b) Staudinger, H.; Meyer, J., *Helvetica Chimica Acta* **1919,** 2, 635.

6. Kolb, H. C.; Finn, M. G.; Sharpless, K. B., *Angew. Chem. Int. Ed.* **2001,** 40, 2004.

7. (a) Scott, S. O.; Gavey, E. L.; Lind, S. J.; Gordon, K. C.; Crowley, J. D., *Dalton Trans.* **2011,** 40, 12117; (b) Aizpurua, J. M.; Sagartzazu-Aizpurua, M.; Azcune, I.; Miranda, J. I.; Monasterio, Z.; Garcia-Lecina, E.; Fratila, R. M., *Synthesis* **2011,** 17, 2737; (c) Hanelt, S.; Liebscher, J., *Synlett.* **2008,** 7, 1058.

8. (a) Ol'shevskaya, V. A.; Makarenkov, A. V.; Kononova, E. G.; Petrovskii, P. V.; Verbitskiy, E. V.; Rusinov, G. L.; Charushin, V. N.; Hey-Hawkins, E.; Kalinin, V. N., *Polyhedron* **2012,** 42, 302; (b) Zhao, P.; Li, N.; Salmon, L.; Liu, N.; Ruiz, J.; Astruc, D., *Chem. Commun.* **2013,** 49, 3218; (c) Wang, D.; Denux, D.; Ruiz, J.; Astruc, D., *Adv. Synth. Catal.* **2013,** 355, 129.

9. Vyakaranam, K.; Havlas, Z.; Michl, J., *J. Am. Chem. Soc.* **2007,** 129, 4172.

10. Hawthorne, M. F.; Andrews, T. D.; Garrett, P. M.; Olsen, F. P.; Reintjes, M.; Tebbe, F. N.; Warren, L. F., Jr.; Wegner, P. A.; Young, D. C., *Inorg. Synth.* **1967,** 10, 91.

11. Kennedy, R. D., *Chem. Commun.* **2010,** 46, 4782.

12. Ramirez-Contreras, R.; Ozerov, O. V., *Dalton Trans.* **2012,** 41, 7842.

13. Seitz, F., *The Modern Theory of Solids*. McGraw Hill: New York, **1940**.

14. (a) Chen, Z.; King, R. B., *Chem. Rev.* **2005,** 105, 3613; (b) King, R. B., *Chem. Rev.* **2001,** 101, 1119.

15. (a) Sastry, G. N.; Venuvanalingam, P.; Kolandaivel, P. In *On the measures of aromaticity*, Taylor & Francis: **2011**; pp 31-53; (b) Stanger, A., *J. Org. Chem.* **2006,** 71, 883; (c) Fallah-Bagher-Shaidaei, H.; Wannere, C. S.; Corminboeuf, C.; Puchta, R.; Schleyer, P. v. R., *Org. Lett.* **2006,** 8, 863; (d) Kertesz, M.; Choi, C. H.; Yang, S., *Chem. Rev.* **2005,** 105, 3448; (e) Chen, Z.; Wannere, C. S.; Corminboeuf, C.; Puchta, R.; Schleyer, P. v. R., *Chem. Rev.* **2005,**105, 3842; (f) Gomes, J. A. N. F.; Mallion, R. B., *Chem. Rev.* **2001,** 101, 1349; (g) Schleyer, P. v. R.; Maerker, C.; Dransfeld, A.; Jiao, H.; van, E. H. N. J. R., *J. Am. Chem. Soc.* **1996,** 118, 6317; (h) Mallion, R. B., *Pure Appl. Chem.* **1980,** 52, 1541.

16.(a) Copley, R. C. B.; Fox, M. A.; Gill, W. R.; Howard, J. A. K.; MacBride, J. A. H.; Peace, R. J.; Rivers, G. P.; Wade, K., *Chem. Commun.* **1996,** 17, 2033;(b) Wu, S.; Jones, M., Jr., *Inorg. Chem.* **1988,** 27, 2005;(c) Matteson, D. S.; Hota, N. K., *J. Amer. Chem. Soc.* **1971,** 93, 2893;(d) Hota, N. K.; Matteson, D. S., *J. Amer. Chem. Soc.* **1968,** 90, 3570.

17. Reed, C. A., *Acc. Chem. Res.* **2010,** 43, 121.

Chapter Five: Click-Like Reactions with the Inert $HCB_{11}Cl_{11}^-$ Anion Lead to Carborane-Fused Heterocycles with Unusual Aromatic Character

5.1 Abstract:

The chlorinated carba-closo-dodecaborate anion $HCB_{11}Cl_{11}^-$ is an exceptionally stable molecule and has previously been reported to be substitutionally inert at the B−Cl vertices. We present here the discovery of base induced cycloaddition reactions between this carborane anion andorganic azides that leads to selective C and B functionalization of the cluster. A single crystal X-ray diffraction study reveals bond lengths in the heterocyclic portion of the ring that are shortened, which suggests electronic delocalization. Molecular orbital analysis of the ensuing heterocycles reveals that two of the bonding orbitals of these systems resemble two of the doubly occupied π-MOs of a simple 5-membered Hückel-aromatic, even though they are entangled in the carborane skeleton. Nucleus independent chemical shift analysis indicates that both the carborane cluster portion of the molecule and the carborane fused heterocyclic region display aromatic character. Computational methods indicate that the reaction likely follows a stepwise addition cyclization pathway.

5.2 Introduction:

Since their preparation and structural elucidation in the 1960s, icosahedral boron[1] and carborane[2] cluster compounds have captivated the imagination of the

scientific community. With respect to the carboranes[3] and from an organic chemistry point of view, the hyper-coordinate carbon atoms seemingly defy the octet rule (Figure 5.1). The

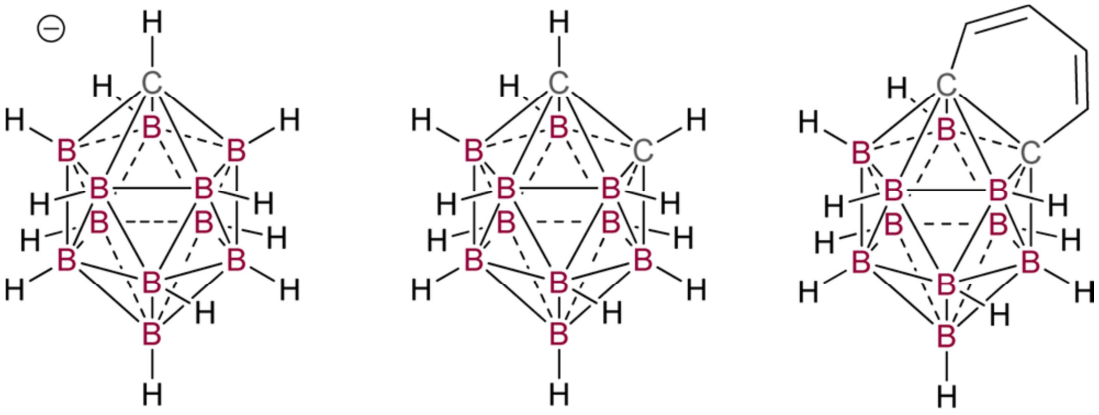

1 **2** **3**

Figure 5.1.Isoelectronic and 3-D aromatic parent icosahedral carboranes $HCB_{11}H_{11}^{-}$**1**, $H_2C_2B_{10}H_{10}$**2**. Conjugation between the delocalized carborane skeletal electrons of **3** and its cluster fused 2-D π−system has been a matter of debate.

core of these clusters, which cannot be described by classical 2-center-2-electron bonding models, feature a completely delocalized web of 26 skeletal electrons involved in 3-center-2-electron bonding between tangential ptype orbitals, as well as radial sp orbitals at the cluster vertices. Such polyhedra are said to possess 3-D aromaticity,[4] and analogies are often made to classical 2-D aromatic systems, such as benzene. Indeed, similar to benzene, icosahedral carborane clusters display exceptional thermal stability, and the parent hydride derivatives **1** and **2** undergo reactions akin to electrophilic aromatic substitution at the B−H vertices.

A question that has long been asked is whether significant conjugation (or possibly aromaticity) can exist between a 3-D aromatic carborane and a fused 2-D π-ring system.[5] While π- donor−acceptor interactions are well documented for exocluster substituents of icosahedral carboranes,[3,6] extended conjugation or aromaticity is a matter of debate, as exemplified by the benzo-fused ortho-carborane **3**.[5] This molecule features localized C−C double bonds and also displays a carborane C− C bond length comparable to the parent carborane **2**.

Of the icosahedral carboranes the carba-closo-dodecaborate cluster $HCB_{11}H_{11}^{-}$[13b] has historically received much less attention than its neutral and isoelectronic cousin orthocarborane $H_2C_2B_{10}H_{10}$**2**.[3a,7] However, in the past 20 years or so there has been consistent growing interest in the use of this molecule and its derivatives for a variety of applications.[3b] The most familiar use of these molecules is as counter-anions for a variety of reactive cationic species.[8] The negative charge of these clusters is delocalized throughout the 12 cage atoms, resulting in a very weakly coordinating anion. This weak coordinative ability can be enhanced by halogenation of the cluster's boron vertices. Halogenation of the cage bestows these carborane anions with extraordinary inertness. As demonstratedby Reed and co-workers,[9] polyhalogenated carborane anions are sufficiently unreactive that they resist decomposition even when paired with some of the most potent electron deficient species. Other groups have capitalized on these properties to generate very useful catalytic processes for the transition-metal free activation and functionalization of persistent aliphatic

fluorocarbons[8h,l] and fluoroaromatics,[8g] respectively. The anion of choice for most applications is the $HCB_{11}Cl_{11}^-$ anion (**4**), which is particularly renowned for its weak coordinative abilities, ease of access,[10] and it is arguably the least reactive of the per-halogenated carba-closo-dodecaborates. Recently we reported a novel application of the carba-closo-dodecaborate anion core, namely, utilizing these species as super bulky, negatively charged, and weakly coordinating ligand R-groups.[11]Specifically, we demonstrated that a phosphine ligand bearing a $CB_{11}Cl_{11}^-$R-group, afforded anionic and zwitterionic single component gold catalysts that display the highest activity ever reported for the hydroamination of alkynes with primary aryl amines. This carborane ligand R-group is derived from the parent $HCB_{11}Cl_{11}^-$anion via deprotonation of the mildly acidic C−H vertex and subsequent reaction with an appropriate electrophile (Figure 5.2).

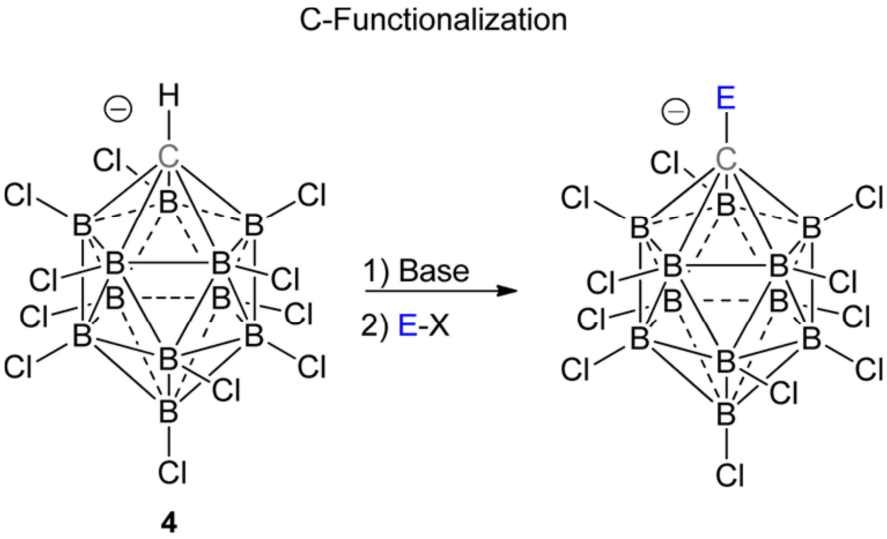

Figure 5.2. C-vertex of the perchlorinated carba-closo-dodecaborate anion ($HCB_{11}Cl_{11}$−) 4 can be deprotonated and functionalized with electrophiles. However, the B−Cl vertices are reportedly unreactive to any form of functionalization.

In contrast to the reactive C−H site, which allows for facile C- functionalization, [3b, 12] the cluster B−Cl vertices of 4 are reported to be completely unreactive. In fact these B−Cl bonds are “supposedly” inert toward nucleophilic substitution, potent Brønsted bases, and oxidizing or reducing agents.[13] The inability to functionalize the B−Cl vertices of this cluster limits the molecular complexity that one can achieve when designing sophisticated building blocks for ligand design and other applications.

Here we report the discovery of a base-induced “click-like” cycloaddition reaction between the $HCB_{11}Cl_{11}^-$ anion and organic azides that leads to selective C and B functionalization of the cluster. Further, evidence is presented that the ensuing heterocycles, which resemble 1,2,3-triazoles but with cluster fused C−B backbones, display aromatic characteristics.

5.3 Results and Discussion:

Synthesis and Characterization. We reasoned that it might be possible to induce B−Cl substitution on the $HCB_{11}Cl_{11}^-$ anion **4** by using the intramolecular advantage coupled with the formation of a delocalized, or possibly aromatic, system. Specifically, we envisioned the nucleophilic addition of the lithio-carborane **5** to a 1,3-dipole, such as an organic azide,[14] to generate a high energy dianionic intermediate **6** that might be able to attack one of the adjacent boron atoms of the cluster (Figure 5.3).

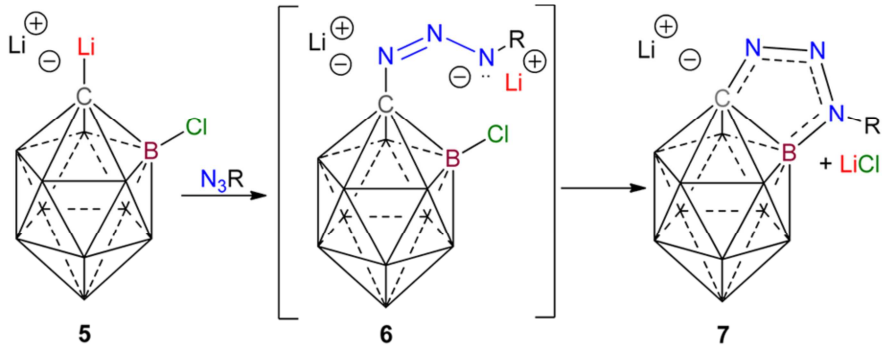

5 **6** **7**

Entry	N_3R	Time (h)	% yield	(**7**)
1	Ph	16	95.0	7a
2	4-FC_6H_4	16	94.5	7b
3	4-$MeOC_6H_4$	16	95.0	7c
4	2-MeC_6H_4	16	85.0	7d
5	Mes	24	84.0	7e
6	*n*-C_4H_9	16	0	
7	Ad	7 (d)	15	7f

Figure 5.3. Lithio-carborane **5** undergoes cycloaddition reactions with organic azides that results in selective B−Cl functionalization, and produces the anionic heterocycles **7** (unlabeled icosahedron vertices = B−Cl).

Because of the inherent anionic charge of the CB_{11} cluster core, heterocycles **7** might display enhanced exocluster delocalization, relative to neutral systems based on ortho-carborane **2**. Thus, carborane **4** was lithiated with n-BuLi to generate **5**, and subsequently treated with a fluorobenzene solution of phenyl azide (N_3Ph). As indicated by ^{11}B Nuclear Magnetic Resonance (NMR) spectroscopy, no functionalization of the lithiated carborane **5** occurred at room temperature. However, upon heating the reaction mixture at 120℃ for 16 h, a new compound (**7a**) formed (Figure 5.3, entry 1). The ^{11}B spectrum of **7a** shows

seven distinct resonances, indicating disruption of the pseudo C_{5v} symmetry in the cluster framework, suggesting B substitution. Two-dimensional ^{11}B-^{11}B correlation NMR spectroscopy confirmed that all seven resonances were interconnected in a single molecule. The natural abundance ^{15}N NMR spectra shows two resonances at 459 and 334 ppm, which are in the range (250−500 ppm, referenced to NH_3) expected for a 2-D aromatic N-heterocycle.[15] We postulate that the third ^{15}N resonance is not observable because of the presence of a B−N linkage, which induces quadrupolar broadening of the signal. High Resolution Mass Spectrometry confirmed the identity of **7a**.

To explore the scope of the cycloaddition reaction, we next tested several electronically and sterically differentiated azide reaction partners. Aryl azides, featuring an electron donating para-methoxy or electron withdrawing para-fluoro substituent afforded the heterocycles **7b** and **7c** in excellent yields (Figure 5.3, entries 2 and 3). The reaction also tolerates sterically demanding mono- and diortho substituted aryl azides to form bulky heterocycles **7d** and **7e**, respectively (Figure 5.3, entries 4 and 5). Interestingly, when n-Butyl azide is used as an electrophile no heterocycle is formed (Figure 5.3, entry 6); instead clean C-alkylation occurs with liberation of LiN_3, affording the previously synthesized n-butylated carborane anion.[12a] In contrast when adamantyl azide is used, an electrophile where backside attack is precluded, the heterocycle **7f** forms after extended heating as indicated by HRMS and ^{11}B NMR (Figure 5.3, entry 8), but

we have not yet devised a method to isolate it from organic impurities (presumably formed by thermal decomposition of N_3Ad).

To investigate the molecular structure of these heterocycles a single crystal X-ray diffraction study was carried out on **7a** (cesium salt metathesis provided crystals of high quality). In the solid-state **7a** acts as a ligand, binding the cesium cation in an η^2-fashion, via N1 and N2 (CCDC 884593). All 5 atoms of the heterocyclic portion of the molecule are coplanar (sum of internal pentagon angles = 540°), and the nitrogen bearing the phenyl group (N3) is perfectly sp^2 hybridized (sum of angles = 360°), which suggests conjugation with the two other nitrogen atoms (Figure 5.4).

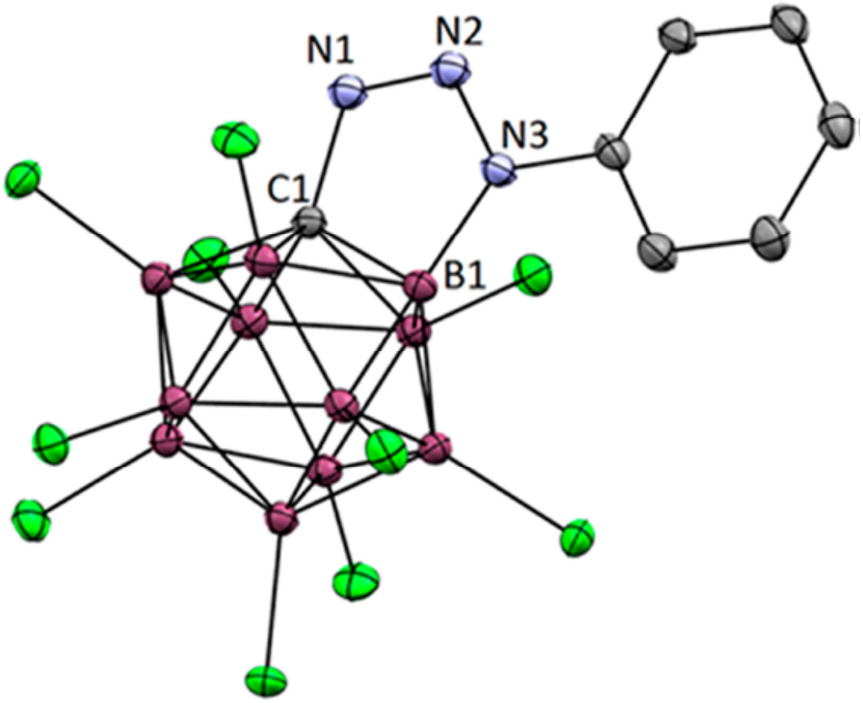

Figure 5.4.Solid-state structure of the anionic heterocycle **7a**. Countercation, solvent molecules, and hydrogen atoms omitted for clarity. Thermal ellipsoids drawn at the 50% probability level. Color coding (C-gray, N-blue, B-magenta, Cl-green).

Indeed, the N_1-N_2(1.2823 (15) Å) and N2−N3(1.3538 (15) Å) bond lengths are significantly shorter than standard N−N single bonds (1.450 Å).[16] Although the exocluster bound carbon−nitrogen distance (C1−N1 = 1.4460 (15) Å) is only slightly shorter than one would typically expect for a C−N single bond (1.454−1.485 Å),[17] the analogous N−B bond (B1−N3 = 1.4878 (16) Å) is short, which suggests multiple bond character (B−N single and double bond lengths 1.580 and 1.400 Å, respectively).[18] Interestingly, the C−B portion of the pentagon is dramatically shortened (C1−B1 = 1.6696 (18) Å) with respect to the other C−B linkages in the cluster (average C−B bond lengths = 1.7362 Å). Such a bond contraction is not observed with related neutral and diene-like benzocarboranes.[5a]

Computational Study.

To gain further insight into the electronic structure of heterocycles **7** and probe the possibility of extended delocalization between the 2-D π-system of the heterocycle and the 3-D cluster framework, we performed various quantum chemical calculations, using **7a** as a model compound. The validity of the computational protocol used (B3PW91/6-31++G**) was confirmed by the insignificant average absolute error in distances (<2%) and bond angles (±0.2°), relative to the observed solid-state structure, allowing an accurate prediction of various geometrical, bonding, and electronic properties of **7a**. Close inspection of the molecular orbitals (MOs) of heterocycle **7a** reveals significant mixing between

the carborane cage and the outer rings (5-member heterocycle and phenyl), indicating a strong interplay between the different systems. Of particular interest are three occupied π-type MOs (orbitals 96, 121, and 124). Two of these MOs (MOs 96 and 121, Figure 5.5(a)) contain

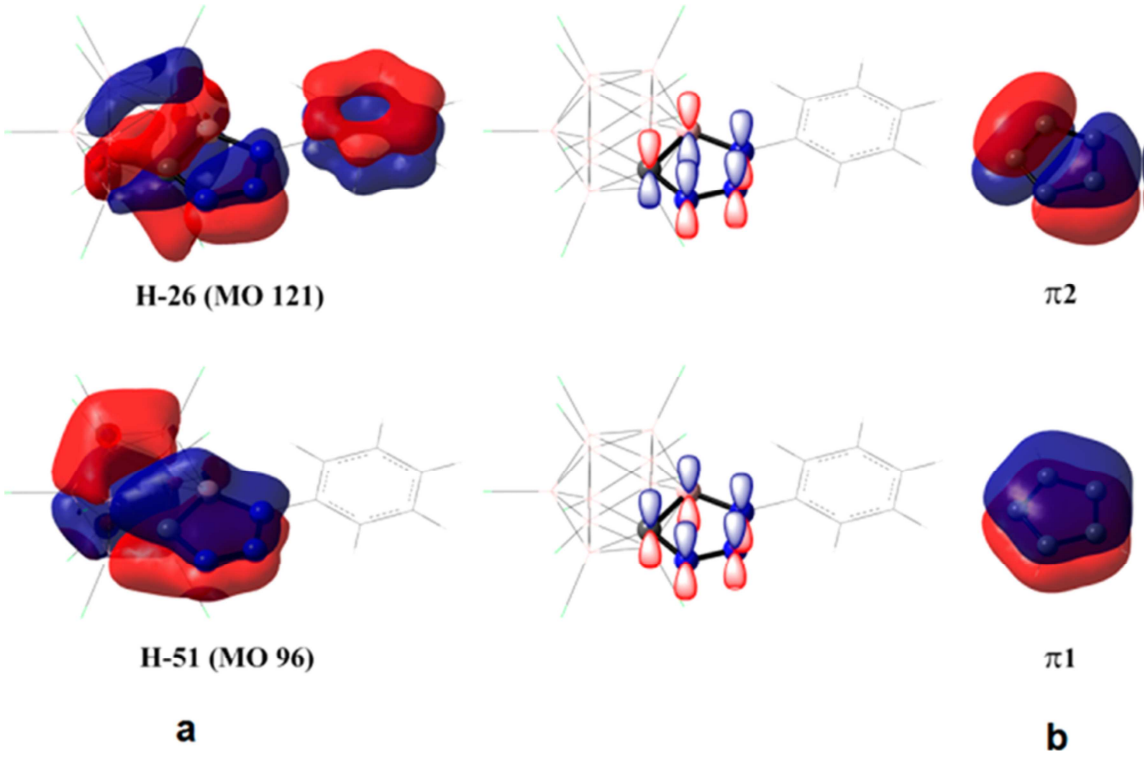

Figure 5.5.Molecular Orbitals. Bonding MOs (a) 96 and 121 of **7a** resemble two doubly occupied MOs (π1 and π2) (b) of a simple 5-membered ring aromatic. Chlorine orbital contributions omitted for clarity (For complete MOs, see Appendix E)

areas of constructive bonding that resemble two of the doubly occupied π MOs (π1 and π2, Figure 5.5b) of a simple 5-membered Hückel-aromatic.

However, these MOs differ in that the atomic p-π orbitals of carbon and boron, which are used to complete the 5-membered ring π-bonding combinations, are at the same time strongly mixed with adjacent cluster orbitals to form extended

delocalized MOs. The third π-bonding type MO, orbital 124, is delocalized over the entire molecule (Appendix E). The highest occupied molecular orbital (HOMO) of the system has significant cluster orbital contributions, whereas the lowest unoccupied molecular orbital (LUMO) resides almost entirely outside of the 3-D framework (Appendix E). The ultraviolet−visible spectrum displays a strong absorption band (λ_{max} = 313.0 nm), which corresponds to a HOMO−LUMO transition (π→π* excitation) and is supportive of extended delocalization between the cluster, heterocycle, and pendant benzene ring.

We next performed both an Atoms In Molecules (AIM)[19] and a Nucleus Independent Chemical Shift (NICS)[20] analysis. The AIM analysis confirms the presence of a ring critical point at the center of mass of the heterocycle and the carborane cage, which is supportive of delocalization of the 2-D π-system of the heterocycle, and the 3-D aromatic cluster respectively.[21] Values of magnetism based on Schleyer's NICS method indicate that the 5-membered heterocyclic portion of the molecule has appreciable aromatic character (NICS(0) = −7.8, NICS(1) = −8.8, and NICS(1)zz = −19.3 ppm respectively). For comparison, benzene as the benchmark 2-D π-aromatic has a NICS(1)zz value of −29.2 ppm. Likewise, NICS measurements (NICS (0) = −27.8 ppm) taken at the center of the carborane region of the molecule indicate **7a** also retains its 3-D aromaticity ($HCB_{11}Cl_{11}^-$ NICS(0) = −30.8 ppm).

Calculated Reaction Pathway.

Mechanistically, the formation of heterocycles **7** can be rationalized by either a stepwise addition cyclization pathway, as initially postulated, or a concerted reaction between the azide and a carboryne-like intermediate[22] formed by the initial elimination of LiCl from the lithiocarborane. The latter pathway is ruled out since formation of such a C−B carboryne is kinetically nonaccessible ($\Delta E^{\ddagger}$ = 53.8 kcal.mol^{-1}) and thermodynamically unfavorable by 52.5 kcal.mol^{-1} (Figure 5.6). Hence, this unusual reaction likely follows a stepwise addition cyclization pathway (Figure 5.7).

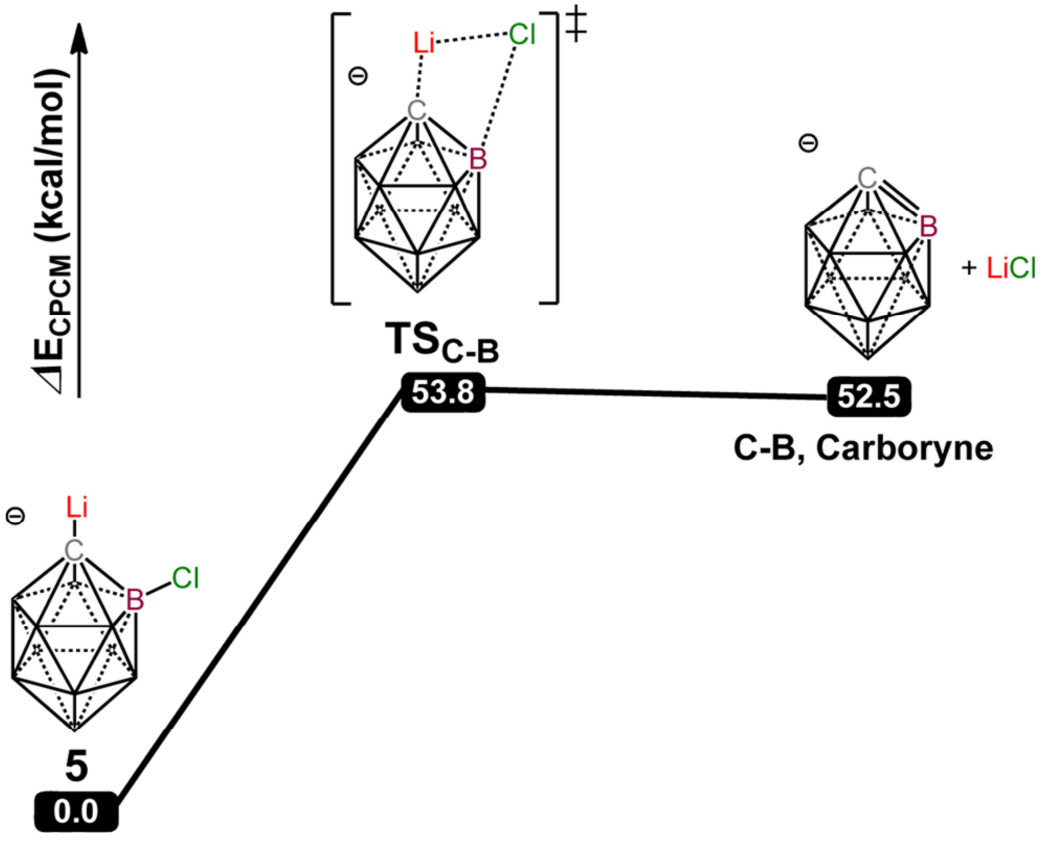

Figure 5.6.Calculated reaction pathway leading to C−B carboryne. For clarity, most B−Cl linkages are not shown.

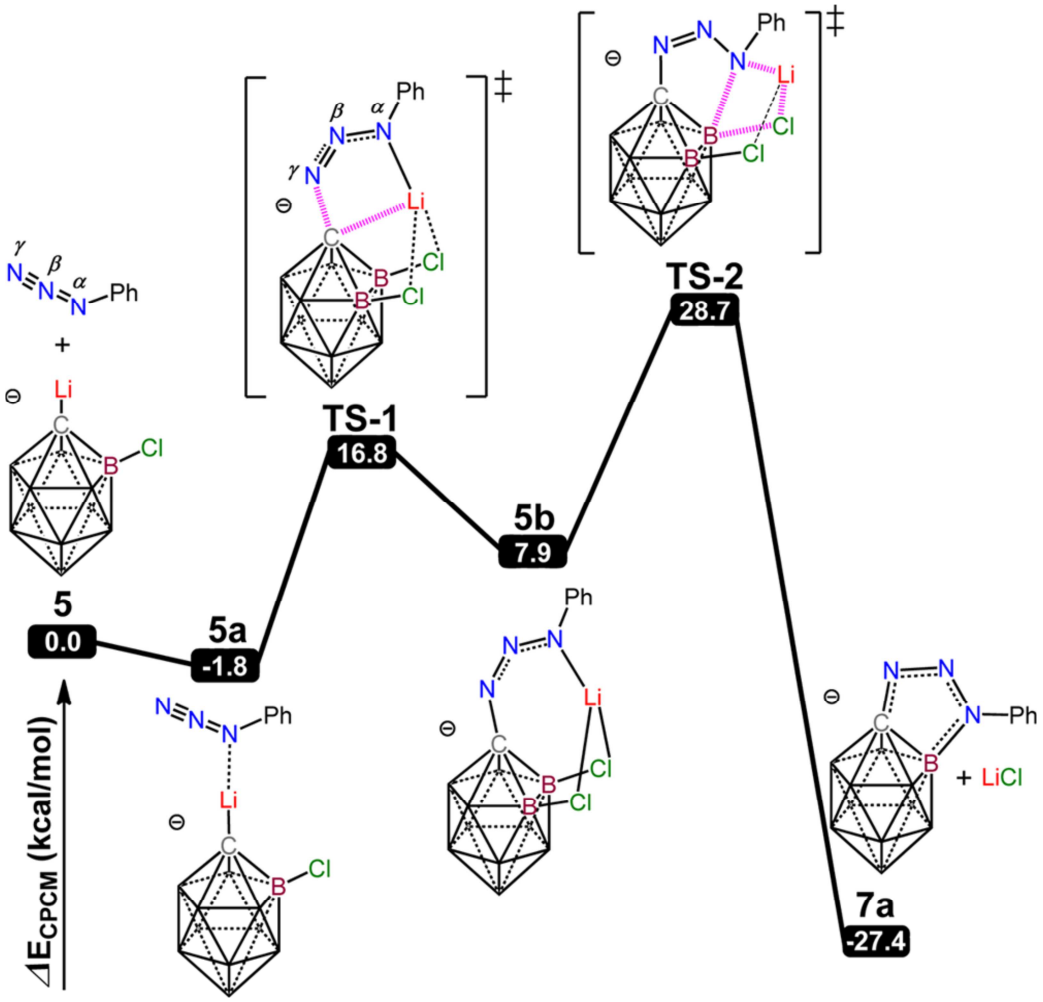

Figure 5.7.Calculated reaction pathway, leading to heterocycle **7a**. For clarity, most B−Cl linkages are not shown.

The C-nucleophilic lithiated carborane 5 first associates with the phenyl azide to form adduct **5a**. The formation of the latter is exothermic by only 1.8 kcal mol^{-1}. Then electrophilic attack of the terminal N atom (γ-nitrogen) of the weakly coordinated phenyl azide to the nucleophilic carbon occurs, and leads to intermediate **5b** via a late transition state, TS-1. The C−Li bond length, in TS-1, is substantially increased with respect to **5a** (2.906 vs 2.048 Å). This relative long

distance is the result of the interaction between the lithium atom and the two neighboring chlorides. At the same time, the distance between the γ-nitrogen of the azide and the carbon is significantly decreased by 2.33 Å, being 2.08 Å in TS-1 and 4.41 Å in **5a**. In the vibrational mode corresponding to the imaginary frequency of TS-1, the dominant motions involve the stretching of Li atom toward the carbon of the carborane, and the concomitant bending of the N3 framework again toward the carbon of the carborane. The transformation of **5a** to **5b** requires a relative low energy barrier (18.6 kcal.mol−1) and is endoergic (9.7 kcal.mol^{-1}). It should be noted that TS-1 is indeed the true transition state that connects intermediates **5a** and **5b**, as it is the result of the IRC calculations. Moreover, based on natural population analysis, NPA, in TS-1 the γ-nitrogen of the azide acquires an almost zero natural charge, the β-nitrogen a positive natural charge (0.116 |e|), and the α-nitrogen that is bonded to the phenyl group has a strong negative charge of −0.50 |e|. This shows an allylic-like character of the azide and is the result of its coordination to the carborane. This allylic-like nature of the azide is even more pronounced in the intermediate **5b** (NPA's of α-, β-, and γ- nitrogen, −0.51, 0.05, and −0.31 |e| respectively). (For complete NPA charges, Appendix E)

The next step corresponds to the nucleophilic attack of α- nitrogen to the typically inert B−Cl vertex of the cluster with simultaneous elimination of lithium chloride (TS-2). The activation barrier is needed for this process is 20.8 kcal.mol^{-1}. In the vibrational mode corresponding to the imaginary frequency of TS-2, the dominant

motions involve the stretching of B−N(phenyl) bond, along with a simultaneous stretching of the B−Cl bond (leading to bond dissociation). It is worth noting that the forming N−B bond is 2.125 Å long, and the corresponding B−Cl linkage is elongated by 0.16 Å with respect to the intermediate **5b**. In addition, NPA analysis clearly shows the nature of the nucleophilic attack. Hence, in TS-2 the α-nitrogen of the azide acquires a strong negative charge of −0.49 |e| and the boron a positive one (0.20 |e|). More interestingly, the relative high activation barrier of this step is presumably due to the high accumulation of negative charges on each atom of the CNNN framework increasing the electrostatic repulsion between carborane and the phenylazide (Appendix E); this step being the rate-determining in the reaction. This is in line with the experimental finding of a slow reaction, and the need for heat to achieve the cycloaddition. However, the high stability of the final product **7a** (−35.3 kcal.mol^{-1}), as well as the overall exothermicity of the reaction (−27.4 kcal.mol^{-1}), is the thermodynamic driving force for this process.

5.4: Conclusion

The reactions outlined above demonstrate a viable strategy to functionalize the typically inert B−Cl vertices of the $HCB_{11}Cl_{11}^-$ anion. Mechanistically, the reaction occurs via a novel stepwise addition cyclization pathway, that features a nucleophilic substitution reaction of a carborane B−Cl bond. This methodology allows access to structurally and electronically complex molecular fragments that

have potential use as ligand building blocks, weakly coordinating anions, or components of advanced materials. Further, evidence presented in this study supports the notion that aromaticity can occur in two separate but fused 3-dimensional and 2-dimensional systems, such as an icosahedral carborane and a Hückel aromatic.

5.5 Experimental:

General Considerations.

All manipulations were carried out using standard Schlenk or glovebox technique (O_2, H_2O < 1 ppm) under a dinitrogen or argon atmosphere. Solvents were dried on K or CaH_2, distilled under argon, and passed through basic alumina before use. Trimethyl ammonium undecachlorocarborane and organic azides were prepared by literature methods.[10,23] All other reagents were purchased from commercial vendors and used without further purification. NMR spectra were recorded at room temperature on Brüker Avance 600 MHz, Varian Inova 400 MHz, or Varian Inova 300 MHz spectrometers. NMR chemical shifts are reported in parts per million (ppm). ^{1}H NMR and ^{13}C NMR chemical shifts were referenced to the NMR solvent peaks. ^{11}B NMR chemical shifts were externally referenced to BF3OEt2. Natural abundance ^{15}N NMR chemical shifts were externally referenced to NH_3. The mass spectra were collected on an Agilent LCTOF Multimode-ESI/APCI with direct injection. The UV/vis spectra was obtained on a Varian Cary 50 UV/vis spectrophotometer.

Quantum Chemical Calculations.

All density functional theory (DFT) calculations were carried out using the Gaussian09 program suite.[24] The entire gas-phase potential energy surface (PES) for the mechanism was computed at the B3PW91 level of theory,[25,26] while the 6-31G++(d,p) basis set was used for all atoms. To study the solvent effects, single point CPCM[27] calculations were conducted using fluorobenzene (dielectric constant, ε = 5.42) as solvent on the gas-phase optimized geometries of B3PW91, using the larger 6-311+ +G(2d,2p) basis set for all atoms. All energies given in the text are CPCM electronic energies. The nature of the species connected by a given transition state structure was confirmed by intrinsic reaction coordinate (IRC) calculations, while intrinsic reaction paths (IRPs) [28] were traced from the various transition structures to make sure that no further intermediates exist. Time-dependent density functional theory (TD-DFT)[29−31] calculations were performed on the equilibrium ground state geometries employing the same density functional and basis set used in geometry optimizations. The Davidson algorithm was used, in which the error tolerance in the square of the excitation energies and trial-vector orthonormality criterion were set to 10^{-8} and 10^{-10}, respectively. Analysis of the electron distribution function was made on the basis of QTAIM (quantum theory of atoms in molecules),[19] while the search and topological analysis of ring critical points (RCPs) were done using Multiwfn program.[32] Nucleus- Independent Chemical Shifts (NICS) values were computed at the same level of theory according to the procedure described by the Schleyer

group.[33] The magnetic shielding tensor element was calculated for a ghost atom located at the center of the heterocycle ring (NICS(0)) and along the z-axis ($NICS(1)_{zz}$).[34] It has been shown that the latter is a more reliable descriptor of aromaticity of a given system.[35] Negative (diatropic) NICS values indicate aromaticity, while positive (paratropic) values imply antiaromaticity. NMR shielding tensors were computed by the gauge-including atomic orbital method (GIAO),[36–40] as implemented in the GAUSSIAN09 series of programs using the same theoretical protocol used in geometry optimizations. The natural bond orbital (NBO) population analysis was performed using Weinhold's methodology.[41,42] More information available in Appendix E.

Synthesis of Heterocycles 7.

$Li(THF)_3$[closo-PhN_3-$CB_{11}Cl_{10}$] (**7a**). $HNMe_3HCB_{11}Cl_{11}$ (2.00 g, 3.44 mmol) was dissolved in tetrahydrofuran (THF, 100 mL) in a Schlenk flask. Subsequent addition of nbutyllithium (2.89 mL, 7.22 mmol, 2.5 M in hexanes, over 15 min) afforded a white precipitate of the dilithio species, and the mixture was allowed to stir for 12 h. The suspension was then concentrated to 1.0 mL, then hexanes (200 mL) was added and the reaction stirred for 5 min. After allowing the precipitate to settle (15 min), the supernatant was removed via cannula filtration and discarded. The white powder was dried under high vacuum for 30 min and subsequently dissolved in fluorobenzene (40 mL). The solution was transferred to a thick walled high pressure Schlenk tube containing phenyl azide (879.4 mg,

7.383 mmol) and placed behind a blast shield where the reaction was heated for 16 h at 120 ℃. After cooling the darkened reaction mixture to ambient temperature it was brought into a glovebox, and the precipitate was collected on a sintered glass filter. The solid was extracted with boiling fluorobenzene (3 × 100 mL) until only LiCl remained on the filter. The combined fluorobenzene fractions were concentrated to dryness, washed with hexane (3 × 20 mL), then diethyl ether (3 × 10 mL), and the off-white powder was collected on a clean sintered glass filter to afford pure **7a** (2.7 g, 3.27 mmol, 95% yield, mp 231 ℃ (dec.)). X-ray quality crystals of **7a**(Cs+) were grown, after cesium salt metathesis in H_2O, and subsequent dissolution of the precipitate in diethyl ether and layering with hexanes. HRMS: (Multimode-ESI/APCI) [M]−m/z calc'd for $H_5B_{11}C_7N_3Cl_{10}$ 603.8419, found: 603.8422. ^{1}H NMR($CDCl_3$, 300 MHz): δ = 7.34 (m, 1H), 7.47(m, 2H), 7.68(m, 2H); Note: ^{1}H NMR analysis indicates the lithium countercation of 7a retains three coordinated THF molecules.^{11}B NMR (THF-d8, 192 MHz): δ =−1.98, −8.98, −12.05, −12.65, −15.16, −15.88; ^{13}C NMR (THF, 151 MHz): δ = 141.46, 130.38, 126.98, 119.25, 85.31 ($C_{carborane}$); ^{15}N NMR (THF-d8, 61 MHz): δ = 458.67, 333.55. UV: λmax = 313.4 nm (CH_3CN).

Li(THF)$_3$[closo-4-FC$_6$H$_4$N$_3$-CB$_{11}$Cl$_{10}$] (7b).7b was prepared in an analogous manner as **7a**. HRMS: (Multimode-ESI/APCI) [M]−m/z calc'd for $H_4B_{11}C_7N_3FCl_{10}$ 621.8325, found: 621.8351. ^{1}H NMR ($CDCl_3$, 300 MHz): δ = 7.14 (m, 2H), 7.64 (m, 2H), Note: 1H NMR analysis indicates the lithium countercation retains three

coordinated THF molecules. ^{11}B NMR ($CDCl_3$, 96 MHz): δ = −5.38, −9.65, −13.06, −16.78; 13C NMR ($CDCl_3$, 101 MHz): δ = 161.53 (d, 1J(F, C) = 278 Hz), 136.05, 120.96 (d, 3J(F, C) = 8.5 Hz), 116.94 (d, 2J(F, C) = 23.0 Hz); Note: Ccarborane was not observed; ^{19}F NMR ($CDCl_3$, 282 MHz): δ = −114.9 (tt, 3J(H, F) = 8.4 Hz, 4J(H, F) = 4.5 Hz); offwhite powder with 94.6% yield.

$Li(THF)_3$[closo-4-$MeOC_6H_4N_3$-$CB_{11}Cl_{10}$] (7c).7c was prepared in an analogous manner as **7a**. HRMS: (Multimode-ESI/APCI) [M]−m/z calc'd for $H_7B_{11}C_8N_3OCl_{10}$ 633.8525, found: 635.8539. ^{1}H NMR- ($CDCl_3$, 300 MHz): δ = 3.84 (s, 3H), 6.97 (d, J = 9 Hz, 2H), 7.58 (d, J = 9 Hz, 2H), Note: ^{1}H NMR analysis indicates the lithium countercation retains three coordinated THF molecules. ^{11}B NMR ($CDCl_3$, 96 MHz): δ = −5.42, −9.82, −13.07, −17.02; 13C NMR ($CDCl_3$, 101 MHz): δ = 158.05, 133.68, 119.75, 114.71, 84.31 ($C_{carborane}$), 54.70; dark brown solid with 97.3% yield.

$Li(THF)_3$[closo-2-$MeC_6H_4N_3$-$CB_{11}Cl_{10}$] (7d).7d was prepared in an analogous manner as **7a**. HRMS: (Multimode-ESI/APCI) [M]-m/z calc'd for $H_7B_{11}C_8N_3Cl_{10}$ 617.8576, found: 617.8578. ^{1}H NMR ($CDCl_3$, 300 MHz): δ = 2.480 (s, 3H), 7.32 (m, 3H), 7.67 (m, 1H) Note: ^{1}H NMR analysis indicates the lithium countercation retains three coordinated THF molecules. ^{11}B NMR (THF, 96 MHz): δ = −6.59, −10.52, −13.43,-16.11, −17.37; ^{13}C NMR (THF, 101 MHz): δ = 141.78, 135.57,

130.53, 129.69, 127.64, 122.75, 87.09 ($C_{carborane}$), 23.05; dark brown solid with 82.0% yield.

$Li(THF)_3$[closo-MesitylN_3-$CB_{11}Cl_{10}$] (7e).7e was prepared in an analogous manner as **7a**. HRMS: (Multimode-ESI/APCI) [M]−m/z calc'd for $H_{11}B_{11}C1_0N_3Cl_{10}$645.8890, found: 645.8909. ^{1}H NMR ($CDCl_3$, 300 MHz): δ = 2.30 (s, 3H), 2.47 (s, 6H), 6.94 (s, 2H), Note: ^{1}H NMR analysis indicates the lithium countercation retains three coordinated THF molecules. ^{11}B NMR ($CDCl_3$, 96 MHz): δ = −2.50, −5.09, −10.17, −13.09, −17.50; 13C NMR ($CDCl_3$, 101 MHz): δ = 139.1, 135.5, 134.8, 131.1, 22.2, 20.8; Note: Ccarborane was not observed. Dark brown oil with 84.2%yield

$Li(THF)_3$[closo-AdamantylN_3-$CB_{11}Cl_{10}$] (7f). 7f was prepared in an analogous manner as **7a**, except heating was continued for 1 week. HRMS: (Multimode-ESI/APCI) [M]−m/z calc'd for $H_4B_{11}C_7N_3FCl_{10}$ 661.9193, found: 661.9204.

X-ray Structure.

CCDC 884593 (**7a**)contain the supplementary crystallographic data for this paper. These data can beobtainedfree of charge from The Cambridge Crystallographic Data Centre via www.ccdc.cam.ac.uk/data_request/cif.

5.6 References

1. Pitochelli, A. R.; Hawthorne, F. M., *J. Am. Chem. Soc*. **1960**, 82, 3228.

2. (a) Knoth, W. H., *J. Am. Chem. Soc*. **1967**, 89, 1274. (b) Heying, T. L.; Ager, J. W.; Clark, S. L.; Mangold, D. J.; Goldstein, H. L.; Hillman, M.; Polak, R. J.; Szymanski, J. W., *Inorg. Chem*. **1963**, 2, 1089. (c) Fein, M. M.; Bobinski, J.; Mayes, N.; Schwartz, N.; Cohen, M. S., *Inorg. Chem*. **1963**, 2, 1111.

3. For reviews on the isoelectronic carborane clusters C_2B_{10} and CB_{11}−, see refs 3a and 3b respectively. (a) Scholz, M.; Hey-Hawkins, E., *Chem. Rev*. **2011**, 111, 7035. (b) Körbe, S.; Schreiber, P. J.; Michl, J., *Chem. Rev*. **2006**, 106, 5208.

4. (a) Chen, Z.; King, R. B., *Chem. Rev.* **2005**, 105, 3613. (b) King, R. B. *Chem. Rev*. **2001**, 101, 1119.

5. (a) Copley, R. C. B.; Fox, M. A.; Gill, W. R.; Howard, J. A. K.; MacBride, J. A. H.; Peace, R. J.; Rivers, G. P.; Wade, K., *Chem. Commun*. **1996**, 2033. (b) Matteson, D. S.; Hota, N. K., *J. Am. Chem. Soc.* **1971**, 93, 2893. (c) Hota, N. K.; Matteson, D. S., *J. Am. Chem. Soc*. **1968**, 90, 3570. (d) Wu, S-h.; Jones, M., *Inorg. Chem*. **1988**, 27, 2005.

6. (a) Weber, L.; Kahlert, J.; Brockhinke, R.; Böhling, L.; Brockhinke, A.; Stammler, H.-G.; Neumann, B.; Harder, R. A.; Fox, M. A., *Chem.Eur. J*. **2012**, 18, 8347. (b) Dash, B. P.; Satapathy, R.;Gaillard, E. R.; Norton, K. M.; Maguire,J. A.; Chug, N.; Hosmane, N. S., *Inorg. Chem*. **2011**, 50, 5485. (c) Fox, M.; Nervi, C.; Crivello, A.; Batsanov, A.; Howard, J. K.; Wade, K.; Low, P. J., *Solid State Electrochem*. **2009**, 13, 1483. (d) Boyd, L. A.; Clegg, W.; Copley, R. C. B.; Davidson, M. G.; Fox, M. A.; Hibbert, T. G.; Howard, J. A. K.; Mackinnon, A.; Peace, R. J.; Wade, K., *Dalton Trans.* **2004**, 2786.

7. For recent examples of applications utilizing ortho- carborane, see 7a−c. (a) Spokoyny, A. M.; Machan, C. W.; Clingerman, D. J.; Rosen, M. S.; Wiester, M. J.; Kennedy, R. D.; Stern, C. L.; Sarjeant, A. A.; Mirkin, C. A., *Nat. Chem*. **2011**, 3, 590. (b) Spokoyny, A. M.; Reuter, M. G.; Stern, C. L.; Ratner, M. A.; Seideman, T.; Mirkin, C. A., *J. Am. Chem. Soc*. **2009**, 131, 9482. (c) Kusari, U.; Li, Y.; Bradley, M. G.; Sneddon, L. G., *J. Am. Chem. Soc*. **2004**, 126, 8662.

8. (a) Kaleta, J.; Tarabek, J.; Akdag, A.; Pohl, R.; Michl, J., *Inorg. Chem*. **2012**, 51, 10819. (b) Stoyanov, E. S.; Gunbas, G.; Hafezi, N.; Mascal, M.; Stoyanova, I. V.; Tham, F. S.; Reed, C. A., *J. Am. Chem. Soc*. **2012**, 134, 707. (c) Volkis, V.; Douvris, C.; Michl, J*., J. Am. Chem. Soc*. **2011**, 133, 7801. (d) Fete, M. G.; Havlas, Z. k.; Michl, J., *J. Am. Chem. Soc.* **2011**, 133, 4123. (e) Tsurumaki, E.; Hayashi, S.-Y.; Tham, F. S.; Reed, C. A.; Osuka, A., *J. Am. Chem. Soc*. **2011**, 133, 11956. (f) Stoyanov, E. S.; Stoyanova, I. V.; Reed, C. A., *J. Am. Chem. Soc.* **2011**, 133, 8452. (g) Allemann, O.; Duttwyler, S.; Romanato,

P.; Baldridge, K. K.; Siegel, J. S., *Science* **2011**, 332, 574. (h) Douvris, C.; Nagaraja, C. M.; Chen, C.-H.; Foxman, B. M.; Ozerov, O. V., *J. Am. Chem. Soc*. **2010**, 132, 4946. (i) Stoyanov, E. S.; Stoyanova, I. V.; Tham, F. S.; Reed, C. A., *J. Am. Chem. Soc.* **2010**, 132, 4062. (j) Valášek, M.; Štursa, J.; Pohl, R.; Michl, J., *Inorg. Chem*. **2010**, 49, 10247. (k) Stoyanov, E. S.; Stoyanova, I. V.; Tham, F. S.; Reed, C. A., *J. Am. Chem. Soc*. **2009**, 131, 17540. (l) Douvris, C.; Ozerov, O. V., *Science* **2008**, 321, 1188. (m) Stoyanov, E. S.; Stoyanova, I. V.; Tham, F. S.; Reed, C. A. *J. Am. Chem. Soc*. **2008**, 130, 12128. (n) Molinos, E.; Brayshaw, S. K.; Kociok-Köhn, G.; Weller, A. S., *Organometallics* **2007**, 26, 2370. (o) Molinos, E.; Brayshaw, S. K.; Kociok-Kohn, G.; Weller, A. S., Dalton Trans. **2007,** 4829. (p) Douglas, T. M.; Molinos, E.; Brayshaw, S. K.; Weller, A. S., *Organometallics* **2007**, 26, 463. (q) Clarke, A. J.; Ingleson, M. J.; Kociok-Koehn, G.; Mahon, M. F.; Patmore, N. J.; Rourke, J. P.; Ruggiero, G. D.; Weller, A. S., *J. Am. Chem. Soc.* **2004**, 126, 1503.

9. Reed, C. A., *Acc. Chem. Res*. **2009**, 43, 121.

10. Gu, W.; McCulloch, B. J.; Reibenspies, J. H.; Ozerov, O. V., *Chem. Commun.* **2010**, 46, 2820.

11. Lavallo, V.; Wright, J. H., II; Tham, F. S.; Quinlivan, S., *Angew. Chem. Int. Ed.* **2013**, 52, 3172.

12. (a) Ramirez-Contreras, R.; Ozerov, O. V., *Dalton Trans*. **2012**, 41, 7842. (b) Himmelspach, A.; Sprenger, J. A. P.; Warneke, J.; Zähres, M.; Finze, M., *Organometallics* **2011**, 31, 1566. (c) Finze, M.; Sprenger, J. A. P.; Schaack, B. B., *Dalton Trans.* **2010**, 39, 2708.

13. Boeré, R. T.; Bolli, C.; Finze, M.; Himmelspach, A.; Knapp, C.; Roemmele, T. L., *Chem.-Eur. J.* **2013**, 19, 1784.

14. For an example of a cycloaddition reaction of an organic azide with a boron cluster, see: Küpper, S.; Carroll, P. J.; Sneddon, L. G., *J. Am. Chem. Soc*. **1992**, 114, 4914.

15. Witanowski, M. Nitrogen NMR; Witanowski, M., Webb, G. A., Eds.; Plenum Press: London, U.K., **1973**; pp 163.

16. CRC Handbook of Chemistry and Physics, 92nd ed.; CRC Press: Boca Raton, FL, **2011**.

17. Allen, F. H.; Kennard, O.; Watson, D. G.; Brammer, L.; Orpen, A. G.; Taylor, R., *J. Chem. Soc*., *Perkin Trans. 2* **1987**, S1.

18. Bosdet, M. J. D.; Piers, W. E., *Can.J. Chem*. **2009**, 87, 8.

19. Bader, R. F. W. *Atoms in Molecules: A Quantum Theory*; Oxford University Press: New York, **1990**.

20. Chen, Z. F.; Wannere, C. S.; Corminboeuf, C.; Puchta, R.; Schleyer, P. v. R., *Chem. Rev*. **2005**, 105, 3842.

21. Poater, J.; Duran, M.; Solà, M.; Silvi, B., *Chem. Rev*. **2005**, 105, 3911.

22. (a) Ren, S.; Qiu, Z.; Xie, Z., *J. Am. Chem. Soc*. **2012**, 134, 3242. (b) Wang, S. R.; Qiu, Z.; Xie, Z., *J. Am. Chem. Soc.* **2011**, 133, 5760. (c) Qiu, Z.; Ren, S.; Xie, Z. *Acc. Chem. Res*. **2011**, 44, 299. (d) Wang, S. R.; Qiu, Z.; Xie, Z*., J. Am. Chem. Soc*. **2010**, 132, 9988.

23. Spencer, L. P.; Altwer, R.; Wei, P.; Gelmini, L.; Gauld, J.; Stephan, D. W., *Organometallics* **2003**, 22, 3841.

24. Frisch, M. J.; Trucks, G. W.; Schlegel, H. B.; Scuseria, G. E.; Robb, M. A.; Cheeseman, J. R.; Scalmani, G.; Barone, V.; Mennucci, B.; Petersson, G. A.; Nakatsuji, H.; Caricato, M.; Li, X.; Hratchian, H. P.; Izmaylov, A. F.; Bloino, J.; Zheng, G.; Sonnenberg, J. L.; Hada, M.; Ehara, M.; Toyota, K.; Fukuda, R.; Hasegawa, J.; Ishida, M.; Nakajima, T.; Honda, Y.; Kitao, O.; Nakai, H.; Vreven, T.; Montgomery, Jr., J. A.; Peralta, J. E.; Ogliaro, F.; Bearpark, M.; Heyd, J. J.; Brothers, E.; Kudin, K. N.; Staroverov, V. N.; Kobayashi, R.; Normand, J.; Raghavachari, K.; Rendell, A.; Burant, J. C.; Iyengar, S. S.; Tomasi, J.; Cossi, M.; Rega, N.; Millam, J. M.; Klene, M.; Knox, J. E.; Cross, J. B.; Bakken, V.; Adamo, C.; Jaramillo, J.; Gomperts, R.; Stratmann, R. E.; Yazyev, O.; Austin, A. J.; Cammi, R.; Pomelli, C.; Ochterski, J. W.; Martin, R. L.; Morokuma, K.; Zakrzewski, V. G.; Voth, G. A.; Salvador, P.; Dannenberg, J. J.; Dapprich, S.; Daniels, A. D.; Farkas, Ö.; Foresman, J. B.; Ortiz, J. V.; Cioslowski, J.; Fox, D. J. *Gaussian 09*, Revision A.02; Gaussian, Inc.: Wallingford, CT, **2009**.

25. Becke, A. D., *J. Chem. Phys*. **1993**, 98, 5648.

26. Perdew, J. P.; Wang, Y., *Phys. Rev. B* **1992**, 45, 13244.

27. (a) Barone, V.; Cossi, M. *J. Phys. Chem*. *A* **1998**, 102, 1995. (b) Cossi, M.; Rega, N.; Scalmani, G.; Barone, V., *J. Comput. Chem*. **2003**, 24, 669.

28. (a) Gonzalez, C.; Schlegel, H. B. *J. Chem. Phys*. **1989**, 90, 2154. (b) Gonzalez, C.; Schlegel, H. B., *J. Phys. Chem*. **1990**, 94, 5523.

29. Gisbergen, S. J. A.; Kootstra, F.; Schipper, P. R. T.; Gritsenko, O. V.; Snijders, J. G.; Baerends, E. J., *J. Phys. Rev*. A **1998**, 57, 1556.

30. Jamorski, C.; Casida, M. E.; Salahub, D. R., *J. Chem. Phys.* **1996**, 104, 5134.

31. Bauernschmitt, R.; Ahlrichs, R., *Chem. Phys. Lett*. **1996**, 256, 454.

32. Lu, T.; Chen, F., *J. Comput. Chem*. **2012**, 33, 580.

33. Schleyer, P. v. R.; Maerker, C.; Dransfeld, A.; Jiao, H.; Hommes, N. J. R. v. R., *J. Am. Chem. Soc*. **1996**, 118, 6317.

34. Fallah-Bagher-Shaidaei, H.; Wannere, C. S.; Corminboeuf, C.; Puchta, R.; Schleyer, P. v. R., *Org. Lett*. **2006**, 8, 863.

35. Stanger, A. J., *Org. Chem*. **2006**, 71, 883.

36. London, F. J., *Phys. Radium* **1937**, 8, 397.

37. McWeeny, R., *Phys. Rev*. **1962**, 126, 1028.

38. Ditchfield, R., *Mol. Phys*. **1974**, 27, 789.

39. Wolinski, K.; Hinton, J. F.; Pulay, P., *J. Am. Chem. Soc*. **1990**, 112, 8251.

40. Cheeseman, J. R.; Trucks, G. W.; Keith, T. A.; Frisch, M. J.. *J. Chem. Phys*. **1996**, 104, 5497.

41. Reed, A. E.; Agrtiss, L. A.; Weinhold, *F., Chem*. Rev. **1988**, 88, 899.

42. Weinhold, F. In *The Encyclopedia of Computational Chemistry*; Schleyer, P. v. R., Ed.; John Wiley & Sons: Chichester, U.K., **1998**; p 1792.

Chapter Six: Triazolium Carborane Zwitterion and the Formation of its Radical Anion.

6.1 Introduction:

Triazoles are aromatic five member heterocyclic compounds that contain three nitrogen atoms. There are two possible constitutional isomers which differ by the location of the nitrogens around the ring (Figure 6.1). The two isomers are the 1,2,3-triazole and 1,2,4-triazole which describes the location of the three nitrogen atoms around the pentagon.

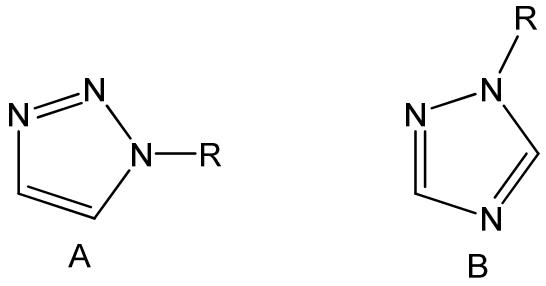

Figure 6.1: Constitutional isomers of triazoles. A is the 1,2,3-triazole. B is the 1,2,4-triazole.

Triazoles are present in a number of natural products that are important in agricultural fungicides[1] and appear in antifungal medicines[2] (Figure 6.2). As click chemistry has gained popularity the number and diversity of these triazoles have increased.[3] With this increase of triazoles their application has spread into not just other areas of medicine such as anticonvulsants,[4] but into other areas of science such as optics,[5] redox sensing,[6] catalysis,[7] and combinatorial chemistry.[8]

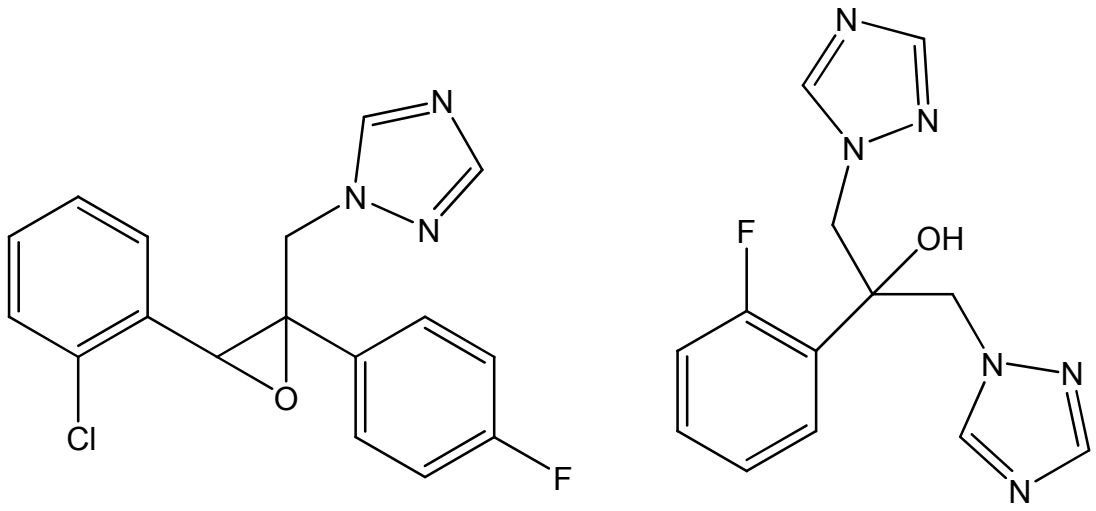

Epoxiconazole Fluconazole

Figure 6.2: Two examples of triazoles antifungal properties. Epoxiconazole is a fungicide for agricultural use, whereas fluconazole is a prescription antifungal drug.

More recently triazoles have been utilized in stabilizing transition metals. By conducting click chemistry on an alkyne with a polyethylene glycol tail a PEGylated triazole was synthesized and used to stabilize gold nanoparticles.[9] A palladium cage was self assembled by coordination with a bistriazole in studying metallosupramolecular chemistry.[10] Most interesting for the development of transition metal catalysts is the synthesis of pyridyl-triazole ligands via click chemistry (Figure 6.3). Once coordinated to palladium these catalysts proved to be efficient for the Suzuki-Miyaura, Sonogashira, and Heck reactions.[7]

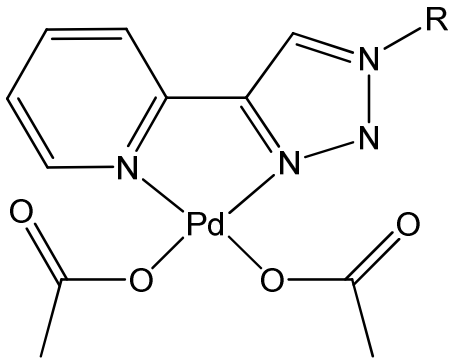

Figure 6.3 Example of palladium catalyst containing a triazole from reference 4.

Triazoles can also be alkylated or protonated result to form a triazolium salts. These triazolium salts are most prevalent in ionic liquids. Additionally work by Strauss has incorporated triazoliums with carboranes ($CB_{11}H_{12}^-$) and dodecaborates ($B_{12}X_{12}^{2-}$) through metathesis reactions for highly specialized ionic liquids for battery and other electrochemical applications. They have developed a large library of both water soluble and insoluble triazolium carboranes and triazolium dodecaborates.[11]

Perhaps most interestingly to the goals of the Lavallo lab, triazolium salts have been utilized as a N-heterocyclic carbene precursor. The 1,2,4-triazolium salts in the presence of a base can act as organocatalysts. A commercially available Rovis triazolium salt has been shown to catalyze a highly enantioselective Stetter reaction.[12] The application of 1,2,3-triazoliums as carbene precursor has also been shown to be a viable ligand for transition metals (Scheme 6.1).[13]

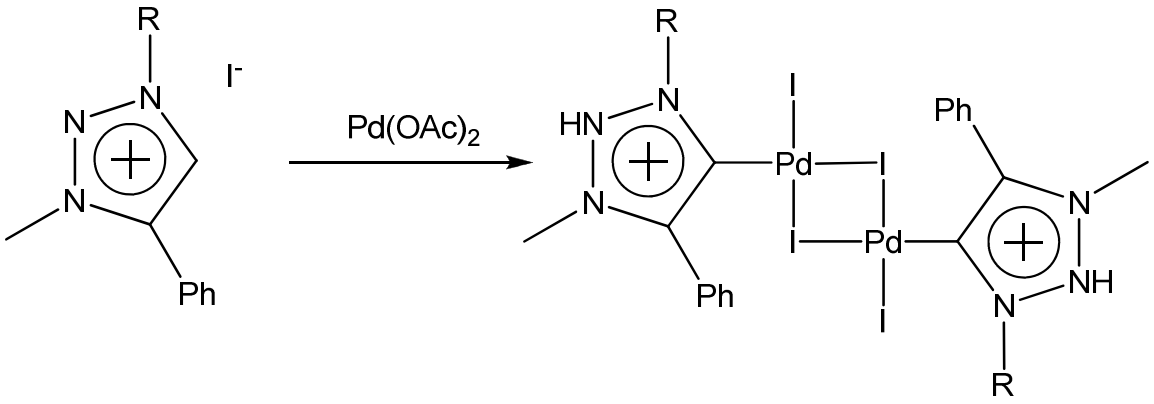

Scheme 6.1 C-H activation of a triazolium salt by palladium to yield a carbene transition metal catalyst.[13]

Only recently have chemists been able to isolate and characterize N-heterocyclic nitrenium ions as ligands for transition metals.[14] N-heterocyclic nitrenium ions are isoelectronically equivalent to the popularized N-heterocyclic carbenes that have become so prevalent in organometallic chemistry and transition metal catalysis. Since the discovery of N-heterocyclic carbenes in 1991,[15] other isovalent analogues have been synthesized and used as ligands for transition metals. Silicon,[16] germanium,[17] boron,[18] gallium,[19] phosphorus,[20] and arsenic[21] analogues have been explored, with nitrogen missing until 2011 (Figure 6.4).

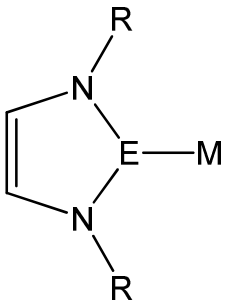

Figure 6.4: Generic N-heterocyclic carbene transition metal analogue. E can be C, Si, Ge, B^-, Ga^-, N^+, P^+, As^+. When E is N^+ it is a nitrenium ion.

With the recent discovery of click-type reaction of organic azides with undecachlorinated carborane anions resulting in the synthesis of a triazole fused carborane **1**(Figure 6.5), the development of triazole and triazolium chemistry can be further developed.[22] The effect of having a negative charge fused on the ring result in the triazole being anionic, whereas the triazolium with be a zwitterion **2** (Figure 6.5). These unusual charges for these molecules could open new applications. One could easily see how a zwitterionic nitrenium could have profound effects on its coordinate to a transition metal.

The unique molecular architectures of **1** and **2** are of particular interest given the recent development of halogenated 1-carba-*closo*-dodecaborate anions and triazolium cations use in catalysis, ionic liquids, high energetic material, and electrochemical applications. A single molecular component with both of these moieties could improve and open new applications.

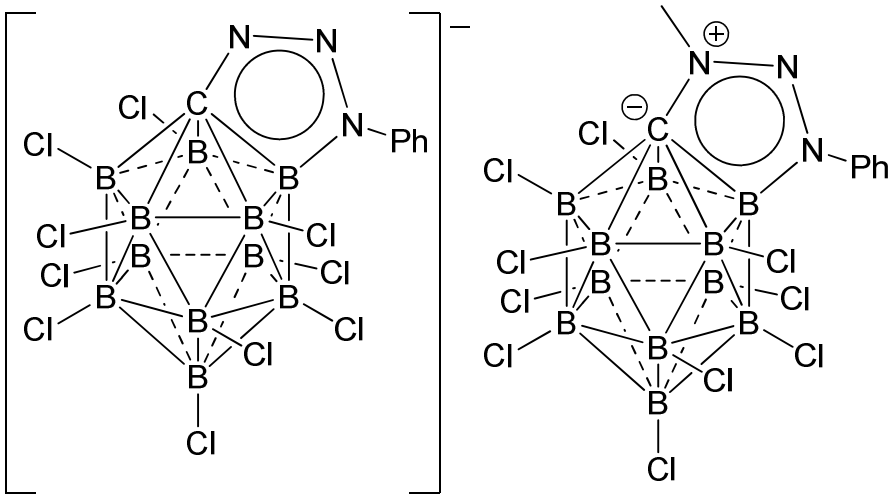

Figure 6.5 Carborane fused triazole **1** andtriazolium carborane zwitterion **2**.

The effects of having a carborane fused triazole has been explored with quantum mechanical calculations detailed in Chapter 5. In summary the calculations predict **1** to possess very interesting electronic properties. In particular it was shown through various theoretical methods to display aromatic characteristics that we described as extending through both the 2D heterocycle and the 3D cage.

The methylation of **1** would result in a triazolium-carborane zwitterion **2**. This molecule's electrochemistry would be extremely interesting. If **2** or similar compounds are used as ionic liquids in batteries the redox potentials must provide adequate range to be useful.[23] Also as an intellectual curiosity and to potentially develop nitrenium based ligands, the understanding of the how the 2D

aromatic system of triazolium affects the electrochemical properties of the 3D aromatic carborane is of interest.

This chapter reports the synthesis of the triazolium carborane zwitterion, **2**, and its characterization. Discussions involving the electronic structure and the nature of **1** will then be extended to speculation of these properties for **2**. The electrochemistry of **2** was studied by cyclic voltammetry, which lead to the attempts to synthesize the species radical anion, **3** (Figure 6.6).

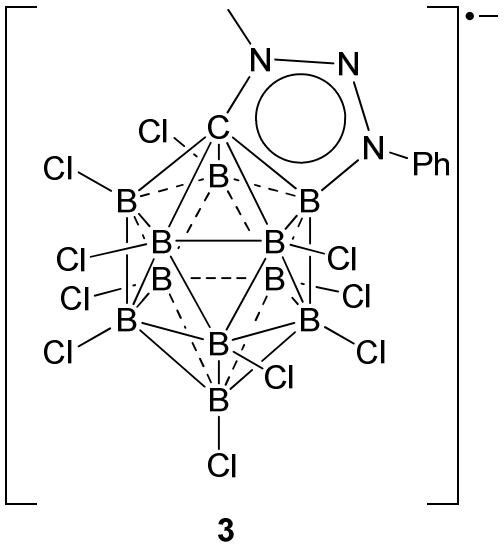

3

Figure 6.6 The triazolium carborane radical anion **3**.

6.2 Results and Discussion

The synthesis of **2** was accomplished by reacting $Li(THF)_3$**1** with methyl triflate in methylene chloride (Scheme 6.2).

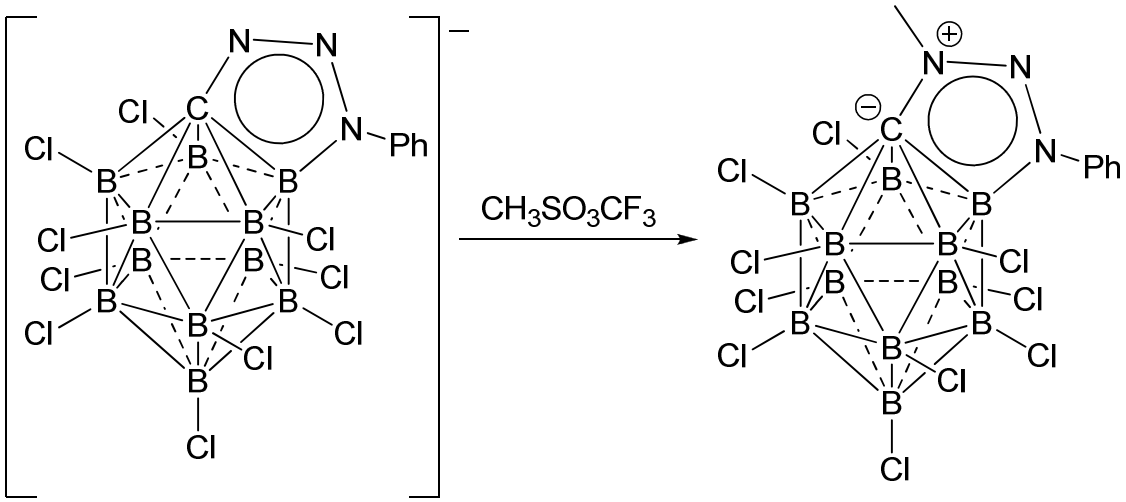

1 **2**

Scheme 6.2: Methylation of **1** with methyl triflate to form **2**.

After addition of methyl triflate to the off white slurry slowly turned yellow as it was stirred overnight. After filtering off the triflate salt and concentrating in vacuo. X-ray quality crystals were grown of **2** from layering a fluorobenzene solution with hexane (Figure 6.7).

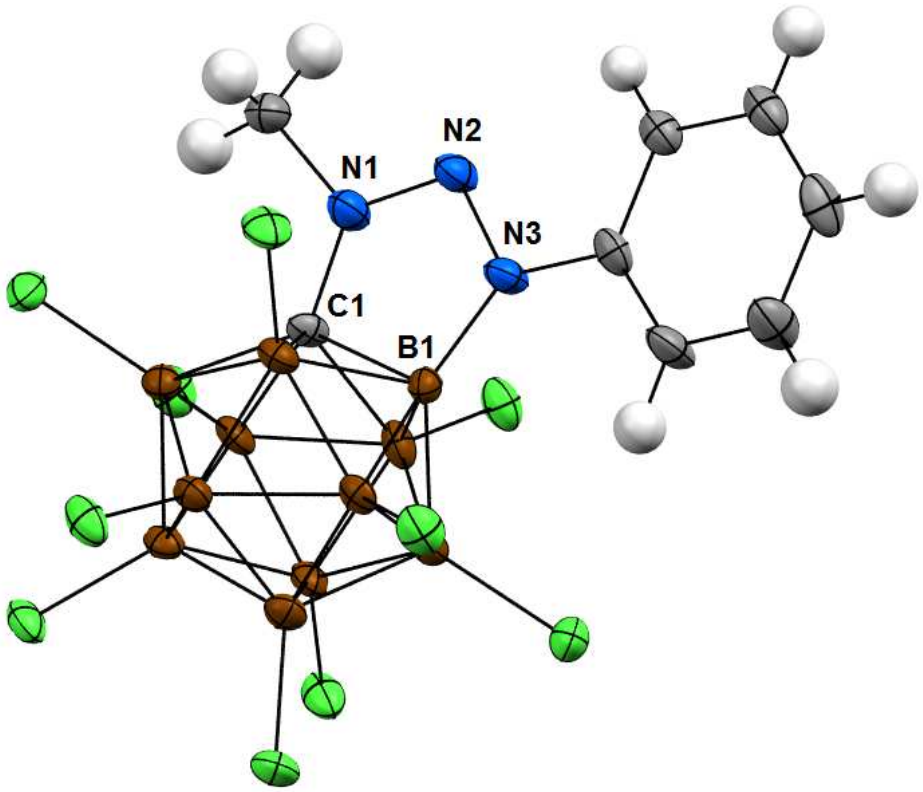

Figure 6.7: X-ray structure of **2**, Carbon: gray, Boron: brown, Chlorine: Green, Nitrogen: blue, Hydrogen: white.

To further understand the reduction-oxidation properties of the newly formed **2**, cyclic voltammetry studies was conducted on **2**. Also in order to understand how the charge might influence the redox properties cyclic voltammetry was also run on **1**. With the assistance of Christopher Hondros, a third year graduate student in Professor Bocian's lab at UC Riverside, the electrochemistry of these compounds were evaluated in both tetrahydrofuran and methylene chloride. Due to the window constraints of these solvents no noticeable reversible reduction or

oxidation occurred for **1**. This result is consistent with the redox properties of most halogenated carboranes.[23]

The cyclic voltammogram of **2** in methylene chloride indicates reversible reduction at -0.87V from Fc/Fc^+ (Figure 6.8). Additional CV work was done by David Weinberger, a visiting scientist from Dr. Guy Betrand's group at UCSD. At reduction potentials above -2.50V there are irreversible one-electron steps evident.

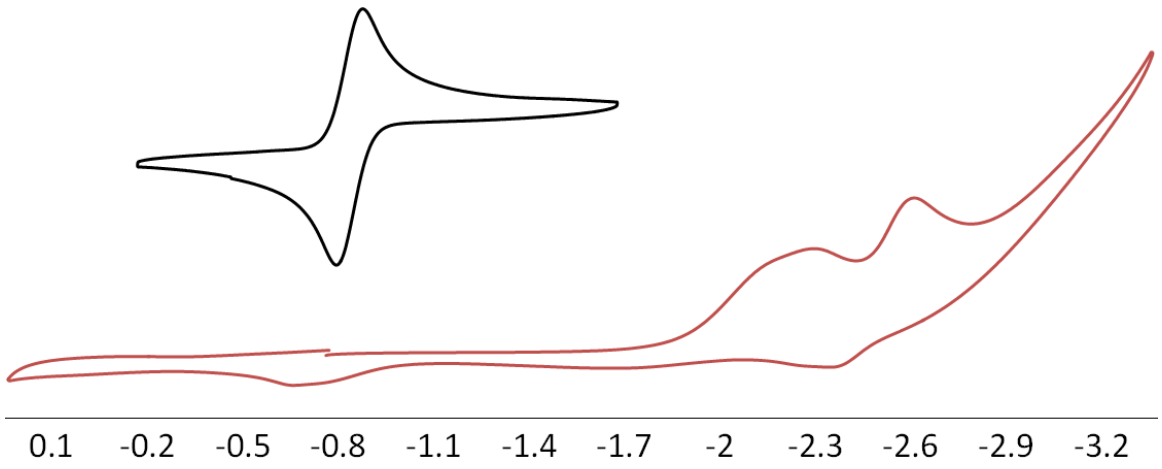

Figure 6.8: Cyclic voltammogram of**1** (red, bottom) and**2**(black, top) in methylene chloride.

Given the reversible reduction of **2**, it should be possible to isolate a chemically reduced radical anion **3**. While initial attempts used potassium metal saw a slight color change, a reducing agent with a redox potential that more closely matches the observed -0.87V of **2** was used. The 19 electron cobaltocene complex with an oxidation potential of 1.33V (to Fc/Fc^+),[24] was selected as a more appropriate

reducing agent. Matt Asay recently joined the Lavallo lab and began work with Jess Estrada on the reduction of **2**. They were able to successfully synthesize **3**, as evident from the detection of the cobaltocenium cation in the ^{1}H NMR and the detection of a radical species with EPR. One broad signal at g = 2.003 with the peak to peak width of the signal is 29.8 G and 28.2 G at 120K was observed, which is in line with the formation of the carborane radical anion **3**. Finally upon slow diffusion of a THF solution with hexane X-ray quality crystals of **3**were obtained. (Figure 6.9)

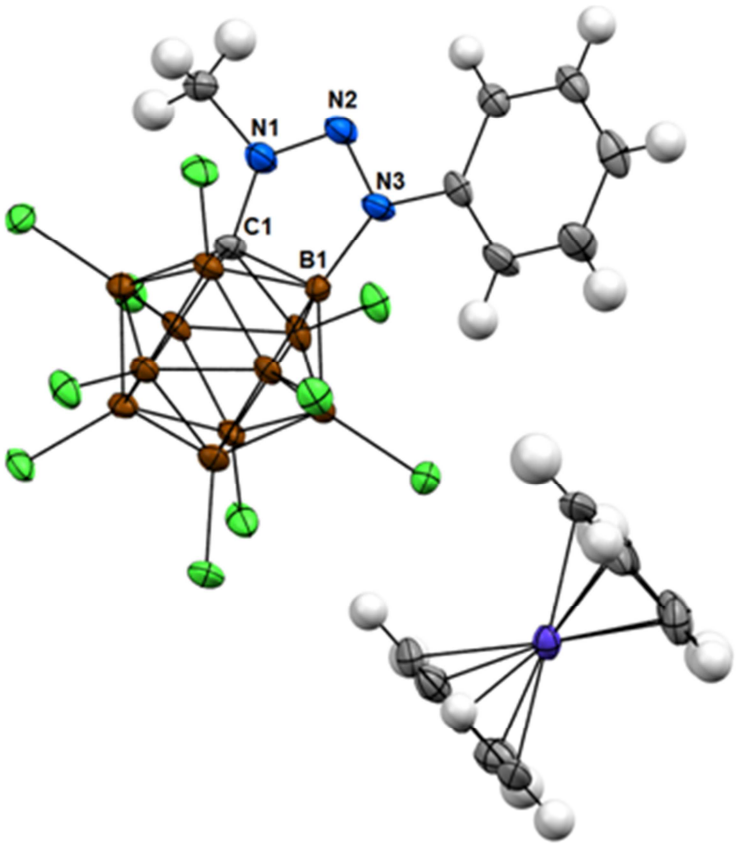

Figure 6.9: X-ray structure of **3**, Carbon: gray, Boron: brown, Chlorine: Green, Nitrogen: blue, Cobalt: purple, Hydrogen: white.

Before discussing the X-ray structures some valuable information can be obtained by understanding the differences observed in the electrochemistry of the undecachlorocarborane anion $[CHB_{11}Cl_{11}]^-$, **1**, and **2.** The undecachlorocarborane anion is fairly resistant to reduction and oxidation. This is part of the reason why such its utility as weakly coordinating anions and as a counteranions in ionic liquids for electrochemical cells is being explored. However it has been reported that it can be reversibly oxidized in liquid SO_2 at 2.85V and reduced in acetonitrile at -2.59V.[23] As one would expect **2** is much more easily reduced. The neutral zwitterion would conceivably be much easier to gain an electron as opposed to the anionic undecahlorocarborane and **1**.

Since the carborane fused heterocycles are unique it is practically impossible to compare bond lengths and angles of other molecules or radicals. The most effective comparison is between the anionic heterocycle, zwitterionic heterocycle, and radical anion heterocycle.

All three heterocycles have internal bond angles of close to 540˚ as one expects with a planar pentagon. Also **1**, **2**, and **3** each have the three angles around N_3 sum to 360˚ indicative of a sp^2 hybridized nitrogen. This will allow for a good comparison of the three heterocycle's bond lengths.

Table 6.1 directly compares the bond lengths of the five bonds of the triazole along with the exocyclic bonds between the phenyl group and methyl group for **1**, **2**, and **3**.

	1	**2**	**3**
Bond	Bond Length	Bond Length	Bond Length
C-B	1.6696(18)	1.675(4)	1.666(6)
C-N_1	1.4460(15)	1.413(3)	1.413(5)
N_1-N_2	1.2823(15)	1.307(3)	1.386(5)
N_2-N_3	1.3538(15)	1.302(3)	1.391(5)
B-N_3	1.4878(16)	1.514(4)	1.472(6)
N_3-C_{phenyl}	1.4222(16)	1.430(4)	1.413(5)
N_1-C_{methyl}	N/A	1.475(4)	1.429(5)

Table 6.1 Bond lengths of select bonds (in Å) of **1**, **2**,and **3**.

One immediate observation from the bond lengths is that they do not change significantly for the ring with the largest change is about 0.1Å (10pm). The fact that it is a fused planar ring can prevent large increases in bond length. The most significant change was between N_1-N_2 of the anion, **1**, and radical anion, **3**. The N_1-N_2 bond length in **3** increased indicating a weaker bond with a lower bond order however the 1.386Å is still close to 0.1Å shorter than a standard N-N single bond.

Next it is interesting how upon methylation the two N-N bonds of the heterocycle equalize. Also when the zwitterion is reduced to **3**these bonds are close to 0.1Å longer, but the radical anion maintains the bond equalization between the two N-N bonds. This bond equalization could be indicative of additional aromatic character.

The methylation also shortened the C-N_1 bond as observed by comparing **1** with **2**. This bond then remains short when **2** is reduced to **3**. The shortening of the C-

N_1 bond upon methylation could be explained by simple electrostatics. The positive charge being localized on N_1 and the negative charge being localized on the most electronegative element of the cage, C, shortens the bond. However this argument cannot explain why the length does not change between **2** and **3**.

The one bond that was more or less consistent through all three structures was the C-B bond. This could suggest a limit to the 2D-3D aromaticity advocated previously, however there were some noticeable changes in the average of the other four C-B bond lengths of the carborane cage. **1** had an average bond length of 1.750Å, longer than **2** average bond length of 1.736Å, and almost identical to the length in **3** of 1.751Å.

The last three bonds I have yet to discuss are the B-N_3 and the two exocyclic bonds. The two applicable bonds for **1** and **2** (B-N_3 and N_3-C_{phenyl}) had longer lengths after methylation. However upon reduction all three bonds (B-N_3, N_3-C_{phenyl}, N_1-C_{methyl}) were shorter than both **1** and **2**. This is very interesting behavior without an easily identifiable reason.

Based on all of these observations it can be hypothesized that upon methylation of the heterocycle the positive charge is better delocalized through the three nitrogen atoms. Scheme 6.2 indicated how resonance can delocalize the positive charge and forced the bonds to become equal in length. The bond length equalization is also seen in the radical which could also be explained by the radical being delocalized instead of the positive charge. Also noteworthy is how

the other carborane C-B bonds change with methylation (shorten) and reduction (elongate).

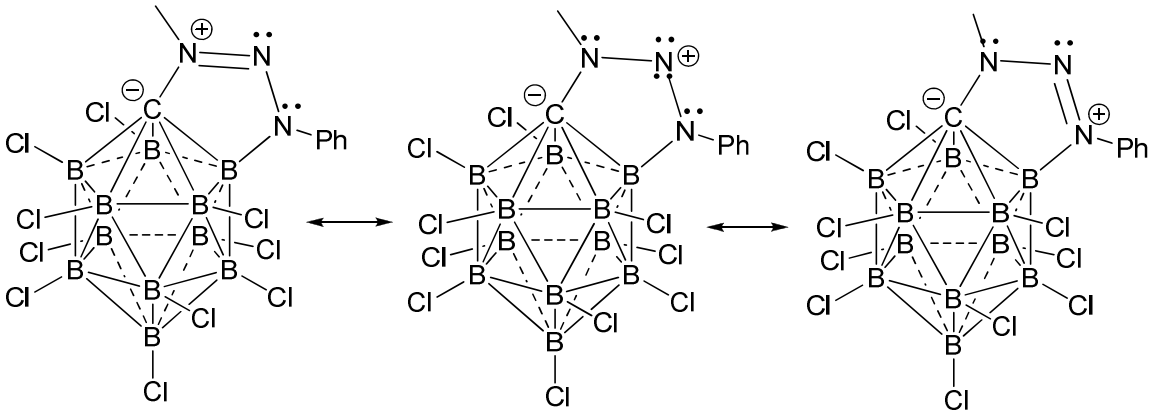

Scheme 6.3: Three different resonances showing the delocalization of the positive charge among all the nitrogens of **2**.

6.3 Experimental:

General Considerations:

All manipulations were carried out using standard Schlenk or glovebox technique (O_2, H_2O < 1 ppm) under a dinitrogen or argon atmosphere. Solvents were dried on NaK, K, or CaH_2, distilled under argon, and passed through basic alumina before use. $Li(THF)_3$**1** was prepared by literature methods.[22]All other reagents were purchased from commercial vendors and used without further purification. NMRspectra were recorded at room temperature on Bruker Avance 600MHz, Varian Inova 400 MHz, or Varian Inova 300 MHzspectrometers. NMR chemical shifts are reported in parts per million(ppm). ^{1}H NMR and ^{13}C NMR chemical

shifts were referenced to theNMR solvent peaks. ^{11}B NMR chemical shifts were externallyreferenced to BF_3OEt_2. The mass spectra were collected on an Agilent LCTOF Multimode-ESI/APCI with direct injection. Melting point measurements were performed on a Büchi Melting Point B-545.

Cyclic voltammetry:

The samples were contained in a three-compartment cell equipped with a Pt wire working electrode, a Pt mesh counter electrode, and a Ag/Ag^+ (butyronitrile) reference electrode. The solvent was CH_2Cl_2 containing 0.1 M Bu_4NPF_6 as the supporting electrolyte. All reported potentials are with respect to ferrocene/ferrocenium = 0.0 V.

Synthesis of *closo*-CH_3-PhN_3-$CB_{11}Cl_{10}$(2):

$Li(THF)_3$[*closo*-PhN_3-$CB_{11}Cl_{11}$] (0.0608g, 0.0734mmol) was made into a slurry with 8mL of fluorobenzene. MeOTf (0.0474g, 0.288mmol) was added and allowed to stir overnight. Fluorobenzene was removed in vacuo. The resulting yellow solid is washed with water and *closo*-CH_3-PhN_3-$CB_{11}Cl_{10}$**(2)** remained. (0.0398g, 0.0642mmole, 87.5%yield, 242.2˚C mp (decomp.)). X-ray quality crystals were grown by vapor diffusion of hexane in a solution of fluorobenzene. ^{1}H NMR(400MHz, C_6D_6, 25˚C): δ=3.00 (s, 3H, CH_3), 6.81 (m, 3H, CH-phenyl),

7.50 (m, 2H, CH-phenyl); ^{11}B {^{1}H} NMR (193MHz, $(CD_3)_2CO$, 25˚C): δ= -7.05, -12.88, -13.69, -16.08, -17.96, -20.65ppm; ^{13}C {^{1}H} NMR (75MHz, $(CD_3)_2CO$, 25˚C): δ= 138.06 (C-phenyl), 133.69 (CH-phenyl), 132.19 (CH-phenyl), 121.89 (CH-phenyl), 43.84 (CH_3); UV-Vis (THF) λ_{max}/nm (ε)= 360 (6053).HRMS: (Multimode-ESI/APCI) [M-H]−m/zcalc'd for $H_7B_{11}C_8N_3Cl_{10}$ 617.8566, found: 617.8591.

Synthesis of $CoCp_2$ [*closo*-CH_3-PhN_3-$CB_{11}Cl_{10}$](3):

In a glovebox, *closo*-CH_3-PhN_3-$CB_{11}Cl_{10}$, **2**, (g, mmole) was weighed in a reaction vessel with stir bar and dissolved in 7mL of diethyl ether. $CoCp_2$ (g, mmole) was weighed in a vial and dissolved in diethyl ether (2mL). The cobaltocene solution was added to the **2**/ether solution dropwise. The mixture was stirred for 12 hours and a green/brown precipitate formed. The supernate was removed, and the remaining solid was washed with diethyl ether (3x5mL). The solid was then dissolved in a minimal quantity of THF and filtered. Dark green crystal plates of **3** were grown from the THF solution by slow diffusion with hexane (g, mmole, % yield, 63.3˚C mp (decomp)). Due to the paramagnetic nature of **3** ^{1}H NMR only shows solvent residual peaks and a singlet for the colbaltocenium counteraction in a window of 100ppm to -100ppm. No other NMR spectra were recorded. UV-vis (THF) λ_{max}.nm (ε)= 346 (39787) the weak signal at ~400nm is from the colbaltocenium caountercation.

6.4 Conclusions

The synthesis of a triazolium carborane zwitterion, **2**, was accomplished by methylation of the previously reported carborane fused triazole, **1**. Both of these molecules exhibit unique charges because of the carborane moiety. Manipulation of these charges on the carborane fused heterocycles hold significant promise toward the discovery of new ligand systems for transition metal catalysis.

The electrochemical activity of **2** proved to be much more active than that of **1** as observed by cyclic voltammetry. Cyclic voltammetry work was done simultaneously by myself and David Weinberger of UCSD. His results are reported. A reversible reduction was observed at -0.87V for **2**, so the synthesis of the radical anion, **3**, was targeted. Matt Asay and Jess Estrada of the Lavallo group carried out the synthesis and characterization of **3**. The X-ray structures and the potential aromatic characteristics are included in the discussion.

6.5 Future Work

Based on differences in the bond lengths determined for **1**, **2**, and **3** information regarding resonance and aromaticity can be speculated. Based on the hypotheses drawn from the X-ray structures computational work similar to the work done in Chapter 5 should be carried out. Specific calculations such as

Nucleus Independent Chemical Shift,[25] Atoms in Molecules,[26] and other methods used to determine aromaticity should be conducted and scrutinized.

Whether or not these molecules are aromatic they certainly contain interesting electrical properties. The electrical properties and overall neutral charge of **2** is of particular interest. Cyclic voltammetry in a different solvent such as liquid sulfur dioxide could provide additional insights onto the oxidation of **1** and **2**.

Also quantum mechanical calculations can be used to calculate the HOMO, SOMO, and LUMO of **1**, **2**, and **3**. This will provide a detailed illustration of the frontier orbitals and how the different atoms contribute to these orbitals. Optimized structures can then be used to calculate ionization energy and electron affinity. The calculated ionization energy and electron affinity have been shown by Knapp[23] to correlate well with oxidation potential and reduction potential, respectively. In silico experimentation can direct the synthesis of additional carborane fused heterocycles and triazolium carborane zwitterions that possess specific redox chemisty.

Coordination to transition metals that will not reduce **2** should be carried out to produce another example of a N-heterocyclic nitrenium ligand. To assist with the coordination via the chelating effect, a heterocycle similar to the pyridyl-triazole in Figure 6.3 could be synthesized (Scheme 6.4).

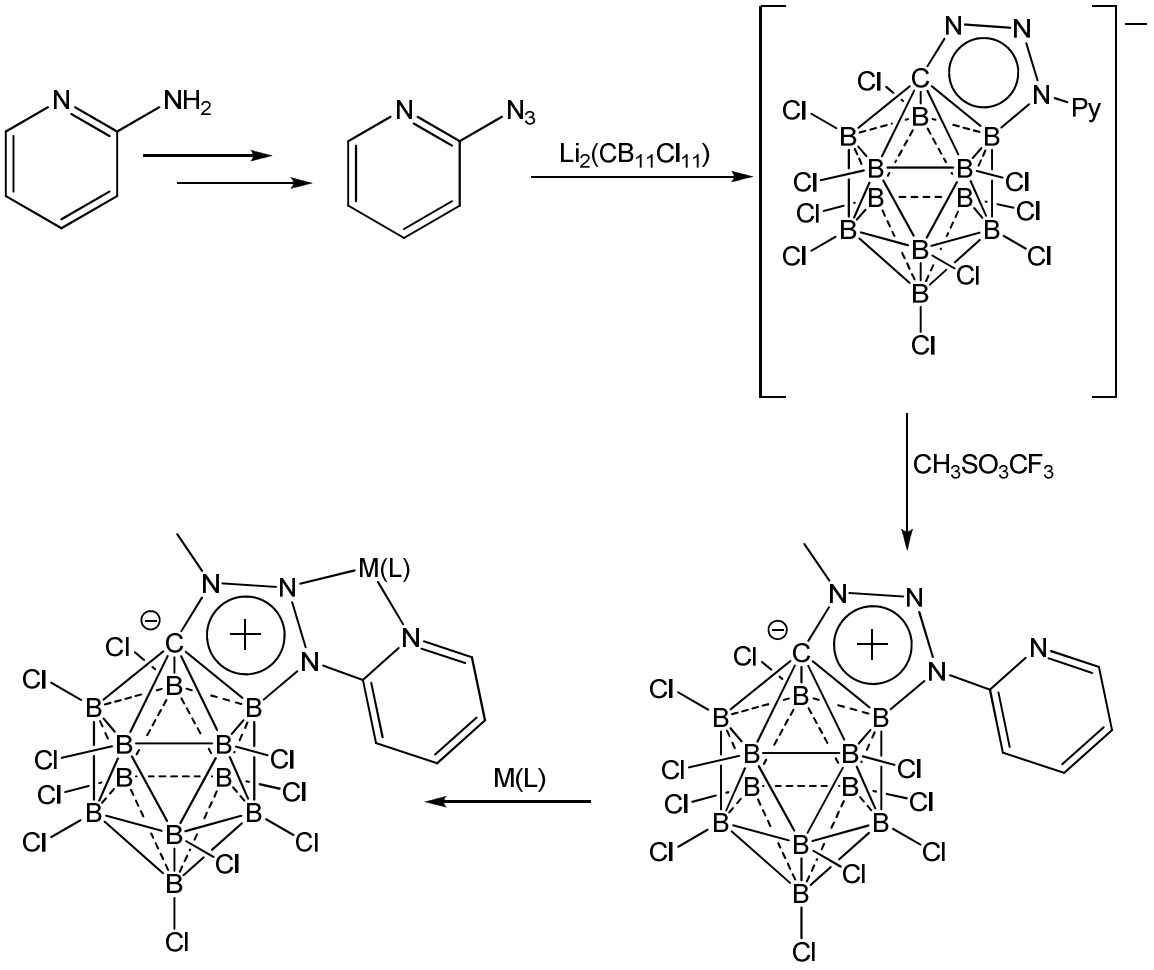

Scheme 6.4: Possible synthesis of a N-heterocyclic nitrenium ligand

Gandelman and coworkers[14] utilized two chelating phosphine arms to form a PNP pincer ligand framework which ultimately isolated the first nitrenium complexes. The CO stretching frequency (ν_{CO}) of the two nitrenium complexes with carbonyls were 2019 and 2024cm^{-1}, compared to free CO at 2143cm^{-1}. This indicates the weak σ-donating ability, but significant π-accepting capability. Given the triazolium carborane reduction potential and insights on triazolium ligand bonding specific metal complexes can be targeted. If an additional chelating arm

is required or desired a phosphine could be built off of the triazolium carborane zwitterion. This method would require development of different techniques to alkylate the triazole, which would be important for moving forward on other projects.

Finally toward the development of specialized ionic liquids or zwitterionic liquids,[27] for use in advancing electrochemical technology, the carborane fused heterocycles produced offer numerous variables that can be experimented with. Given how the triazolium carborane produced in this chapter failed to melt, but rather decomposed at over 240 ˚C indicates that significant work needs to be done to explore this possible application. However the uniqueness of the triazolium carborane zwitterion and the ability of these to be used in highly specialized applications make the development of this field worthwhile.

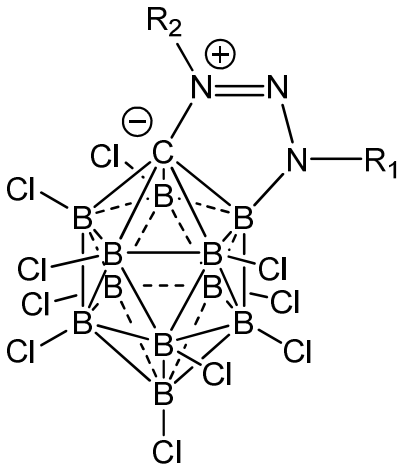

Figure 6.10 Triazolium carborane zwitterion with different substituents can provide unique zwitterionic liquids whose properties can be fine tuned.

Chapter 5 showed how a variety of organic azides, mostly aromatic, can be used to synthesize the anionic carborane fused triazoles in high yields.[22]The R_1 group off the triazole can provide an opportunity to build a large library with different melting points, solubility, and stability similar to Strauss's work (Figure 6.10).[11] Alkylationof different R_2 groups can provide a second opportunity to introduce diverse products to make different triazolium carborane zwitterions. These different zwitterionic liquids should be explored as a solution to preventing solvent's component ions migrating along a potential gradient. Theoretical and experimental studies involving the electrochemistry of each new anionic carborane fused heterocycle and carborane triazolium zwitterion can provide insight into these novel molecules and their relatively unexplored electronic structure.

6.6 References

1. Hauthal, H. G., *Nachr. Chem. Tech. Lab.* **1993,** 41, 566.

2. Humphrey, M. J.; Jevons, S.; Tarbit, M. H., *Antimicrob. Agents Chemother.* **1985,** 28, 648.

3. Kolb, H. C.; Finn, M. G.; Sharpless, K. B., *Angew. Chem. Int. Ed.* **2001,** 40, 2004.

4. Kadaba, P. K., *J. Med. Chem.* **1988,** 31, 196.

5. Zhu, Y.; Guang, S.; Su, X.; Xu, H.; Xu, D., *Dyes Pigm.* **2013,** 97, 175.

6. Thakur, A.; Mandal, D.; Ghosh, S., *Anal. Chem.* **2013,** 85, 1665.

7. Wang, D.; Denux, D.; Ruiz, J.; Astruc, D., *Adv. Synth. Catal.* **2013,** 355, 129.

8. (a) Bhatia, M. S.; Zarekar, B. E.; Choudhari, P. B.; Ingale, K. B.; Bhatia, N. M., *Med. Chem. Res.* **2011,** 20, 116; (b) Leeb, L.; Gmeiner, P.; Loeber, S., *QSAR Comb. Sci.* **2007,** 26, 1145; (c) Pagliai, F.; Pirali, T.; Del, G. E.; Di, B. R.; Tron, G. C.; Sorba, G.; Genazzani, A. A., *J. Med. Chem.* **2006,** 49, 467; (d) Pokhodylo, N. T.; Matiychuk, V. S.; Obushak, M. D., *J. Comb. Chem.* **2009,** 11, 481; (e) Tan, L. P.; Wu, H.; Yang, P.-Y.; Kalesh, K. A.; Zhang, X.; Hu, M.; Srinivasan, R.; Yao, S. Q., *Org. Lett.* **2009,** 11, 5102; (f) Tornoe, C. W.; Sanderson, S. J.; Mottram, J. C.; Coombs, G. H.; Meldal, M., *J. Comb. Chem.* **2004,** 6, 312; (g) Woodard, S. S.; Jerome, K. D., *Comb. Chem. High Throughput Screening* **2011,** 14, 132.

9. Zhao, P.; Li, N.; Salmon, L.; Liu, N.; Ruiz, J.; Astruc, D., *Chem. Commun.* **2013,** 49, 3218.

10. Scott, S. O.; Gavey, E. L.; Lind, S. J.; Gordon, K. C.; Crowley, J. D., *Dalton Trans.* **2011,** 40, 12117.

11. (a) Belletire, J. L.; Schneider, S.; Wight, B. A.; Strauss, S. L.; Shackelford, S. A., *Synthetic Commun.* **2012,** 42, 155; (b) Shackelford, S. A.; Belletire, J. L.; Boatz, J. A.; Schneider, S.; Wheaton, A. K.; Wight, B. A.; Hudgens, L. M.; Ammon, H. L.; Strauss, S. H., *Org. Lett.* **2009,** 11, 2623.

12. (a) Kerr, M. S.; Rovis, T., *J. Am. Chem. Soc.* **2004,** 126, 8876; (b) Reynolds, N. T.; Read, d. A. J.; Rovis, T., *J. Am. Chem. Soc.* **2004,** 126, 9518.

13. Mathew, P.; Neels, A.; Albrecht, M., *J. Am. Chem. Soc.* **2008,** 130, 13534.

14. (a) Tulchinsky, Y.; Iron, M. A.; Botoshansky, M.; Gandelman, M., *Nat. Chem.* **2011,** 3, 525-531; (b) Choudhury, J., *Angew. Chem. Int. Ed.* **2011,** 50, 10772.

15. Arduengo, A. J.; Harlow, R. L.; Kline, M., *J. Am. Chem. Soc.* **1991,** 113, 361.

16. (a) Denk, M.; Lennon, R.; Hayashi, R.; West, R.; Belyakov, A. V.; Verne, H. P.; Haaland, A.; Wagner, M.; Metzler, N., *J. Am. Chem. Soc.* **1994,** 116, 2691; (b) Yoo, H.; Carroll, P. J.; Berry, D. H., *J. Am. Chem. Soc.* **2006,** 128, 6038.

17. Herrmann, W. A.; Denk, M.; Behm, J.; Scherer, W.; Klingan, F.-R.; Bock, H.; Solouki, B.; Wagner, M., *Angew. Chem. Int. Ed.* **1992,** 31, 1485.

18. (a) Segawa, Y.; Yamashita, M.; Nozaki, K., *Science* **2006,** 314, 113; (b) Segawa, Y.; Yamashita, M.; Nozaki, K., *J. Am. Chem. Soc.* **2009,** 131, 9201.

19. (a) Schmidt, E. S.; Jockisch, A.; Schmidbaur, H., *J. Am. Chem. Soc.* **1999,** 121, 9758; (b) Baker, R. J.; Jones, C.; Platts, J. A., *J. Am. Chem. Soc.* **2003,** 125, 10534.

20. (a) Denk, M. K.; Gupta, S.; Ramachandran, R., *Tetrahedron Lett.* **1996,** 37, 9025; (b) Caputo, C. A.; Brazeau, A. L.; Hynes, Z.; Price, J. T.; Tuononen, H. M.; Jones, N. D., *Organometallics* **2009,** 28, 5261.

21. (a) Carmalt, C. J.; Lomeli, V.; McBurnett, B. G.; Cowley, A. H., *Chem. Commun.* **1997,** 21, 2095; (b) Burck, S.; Daniels, J.; Gans-Eichler, T.; Gudat, D.; Naettinen, K.; Nieger, M., *Z. Anorg. Allg. Chem.* **2005,** 631, 1403.

22. Wright, J. H., II; Kefalidis, C. E.; Tham, F. S.; Maron, L.; Lavallo, V., *Inorg. Chem.* **2013,** 52, 6223.

23. Boere, R. T.; Bolli, C.; Finze, M.; Himmelspach, A.; Knapp, C.; Roemmele, T. L., *Chem. Eur. J.* **2013,** 19, 1784.

24. Connelly, N. G.; Geiger, W. E., *Chem. Rev.* **1996,** 96, 877.

25. Schleyer, P. v. R.; Maerker, C.; Dransfeld, A.; Jiao, H.; van, E. H. N. J. R., *J. Am. Chem. Soc.* **1996,** 118, 6317.

26. Poater, J.; Duran, M.; Sola, M.; Silvi, B., *Chem. Rev.* **2005,** 105, 3911.

27. Yoshizawa-Fujita, M.; Narita, A.; Ohno, H. In *Zwitterionic liquids*, John Wiley & Sons, Inc.: **2011**; pp 301

Appendix A

X-Ray Structure Determination of $[Et_3Ge]^+[CB_{11}H_6Br_6]^-$

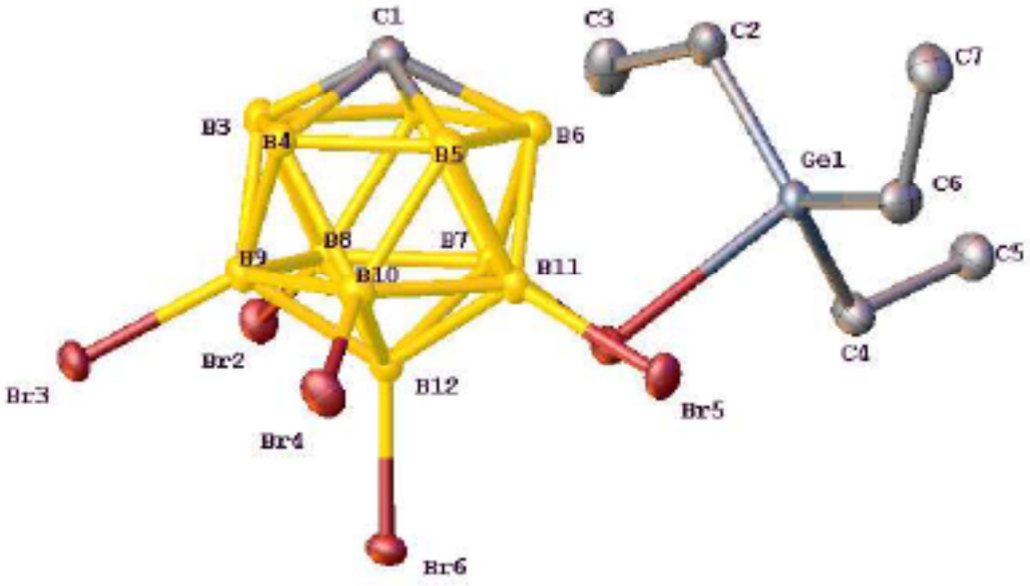

Appendix A.1 Experimental:

A colorless fragment of a prism (0.26 x 0.24 x 0.12 mm^3) was used for the single crystal x-ray diffraction study of $[[C_2H_5]_3Ge]^+[CH_6B_{11}Br_6]^-$ (sample cr331_0m). The crystal was coated with perfluoropolyethers (PFPE) oil and mounted on to a cryo-loop glass fiber. X-ray intensity data were collected at 100(2) K on a Bruker APEX2 (**ref. 1**) platform-CCD x-ray diffractometer system (Mo-radiation, λ = 0.71073 Å, 50KV/40mA power). The CCD detector was placed at a distance of 5.0550 cm from the crystal.

A total of 3600 frames were collected for a sphere of reflections (with scan width of 0.3^o in ω, starting ω and 2θ angles of -30^o, and ϕ angles of 0^o, 90^o, 120^o, 180^o,

240°, and 270° for every 600 frames, 30 sec/frame exposure time). The frames were integrated using the Bruker SAINT software package (**ref. 2**) and using a narrow-frame integration algorithm. Based on a triclinic crystal system, the integrated frames yielded a total of 50425 reflections at a maximum 2θ angle of 58.26° (0.73 Å resolution), of which 12266 were independent reflections (R_{int} = 0.0289, R_{sig} = 0.0248, redundancy = 4.1, completeness = 99.8%) and 10586 (86.3%) reflections were greater than 2σ(I). The unit cell parameters were, **a** = 7.7749(3) Å, **b** = 16.2008(6) Å, **c** = 19.5985(7) Å, **α** = 110.8189(5)°, **β** = 96.8267(5)°, **γ**= 92.3583(5)°, V = 2281.81(15) Å^3, Z = 4, calculated density D_c = 2.259 g/cm^3. Absorption corrections were applied (absorption coefficient μ = 11.841 mm^{-1}; max/min transmission = 0.3307/0.1488) to the raw intensity data using the SADABS program (**ref. 3**).

The Bruker SHELXTL software package (**ref. 4**) was used for phase determination and structure refinement. The distribution of intensities (E^2-1 = 0.962) and no systematic absent reflections indicated two possible space groups, P-1 and P1. The space group P-1 (#2) was later determined to be correct. Direct methods of phase determination followed by two Fourier cycles of refinement led to an electron density map from which most of the non-hydrogen atoms were identified in the asymmetry unit of the unit cell. With subsequent isotropic refinement, all of the non-hydrogen atoms were identified. There were two cations of $[[C_2H_5]_3Ge]^+$ and two anions of $[CH_6B_{11}Br_6]^-$present in the asymmetry unit of the unit cell. One of the two cations was disordered (disordered site

occupancy factor ratio was 74%/26%). The DELU, SIMU, DFIX, SADI and EADP restraints were used to stabilize the final refinement of the disordered cation.

Atomic coordinates, isotropic and anisotropic displacement parameters of all the non-hydrogen atoms were refined by means of a full matrix least-squares procedure on F^2. The H-atoms were included in the refinement in calculated positions riding on the atoms to which they were attached. The refinement converged at R1 = 0.0205, wR2 = 0.0454, with intensity, $I>2\sigma(I)$. The largest peak/hole in the final difference map was 0.951/-0.624 e/Å^3.

Appendix A.2: Structure Data

A.2.1 Crystal data and structure refinement for $[Et_3Ge]^+[CB_{11}H_6Br_6]^-$

Identification code	cr331_0m	
Empirical formula	C7 H21 B11 Br6 Ge	
Formula weight	776.20	
Temperature	100(2) K	
Wavelength	0.71073 Å	
Crystal system	Triclinic	
Space group	P-1	
Unit cell dimensions	a = 7.7749(3) Å	α= 110.8189(5)°.
	b = 16.2008(6) Å	β= 96.8267(5)°.
	c = 19.5985(7) Å	γ = 92.3583(5)°.
Volume	2281.81(15) Å^3	
Z	4	
Density (calculated)	2.259 Mg/m^3	
Absorption coefficient	11.841 mm^{-1}	
F(000)	1440	
Crystal size	0.26 x 0.24 x 0.12 mm^3	
Theta range for data collection	2.05 to 29.13°.	

Index ranges	-10<=h<=10, -22<=k<=22, -26<=l<=26
Reflections collected	50425
Independent reflections	12266 [R(int) = 0.0289]
Completeness to theta = 29.13°	99.8 %
Absorption correction	Semi-empirical from equivalents
Max. and min. transmission	0.3307 and 0.1488
Refinement method	Full-matrix least-squares on F^2
Data / restraints / parameters	12266 / 183 / 524
Goodness-of-fit on F^2	1.019
Final R indices [I>2sigma(I)]	R1 = 0.0205, wR2 = 0.0454
R indices (all data)	R1 = 0.0278, wR2 = 0.0473
Largest diff. peak and hole	0.951 and -0.624 e.$Å^{-3}$

A.2.2. Atomic coordinates (x 10^4) and equivalent isotropic displacement parameters ($Å^2$x 10^3) for $[Et_3Ge]^+[CB_{11}H_6Br_6]^-$. U(eq) is defined as one third of the trace of the orthogonalized U^{ij} tensor.

	x	y	z	U(eq)
C(1)	9364(3)	5690(2)	1705(1)	17(1)
B(2)	7908(3)	4900(2)	1070(1)	16(1)
B(3)	7364(3)	6006(2)	1502(1)	17(1)
B(4)	8522(3)	6434(2)	2415(1)	17(1)
B(5)	9786(3)	5594(2)	2548(1)	17(1)
B(6)	9407(3)	4641(2)	1719(1)	16(1)
B(7)	7183(3)	4277(2)	1577(1)	13(1)
B(8)	5898(3)	5098(2)	1430(1)	15(1)
B(9)	6291(3)	6050(2)	2264(1)	14(1)
B(10)	7790(3)	5791(2)	2912(1)	15(1)
B(11)	8340(3)	4685(2)	2485(1)	15(1)
B(12)	6159(3)	4962(2)	2313(1)	14(1)
Br(1)	6199(1)	3016(1)	1110(1)	16(1)
Br(2)	3679(1)	4776(1)	785(1)	19(1)
Br(3)	4464(1)	6835(1)	2578(1)	18(1)

Br(4)	7751(1)	6318(1)	3975(1)	21(1)
Br(5)	8924(1)	3906(1)	3025(1)	20(1)
Br(6)	4233(1)	4499(1)	2654(1)	18(1)
Ge(1)	8296(1)	2042(1)	363(1)	15(1)
C(2)	8811(3)	2664(2)	-275(1)	21(1)
C(3)	7192(4)	2810(2)	-732(1)	29(1)
C(4)	6602(3)	1018(2)	-60(1)	21(1)
C(5)	7400(3)	232(2)	-584(1)	24(1)
C(6)	10083(3)	1975(2)	1114(1)	22(1)
C(7)	11924(3)	2268(2)	1054(1)	26(1)
C(1A)	3948(3)	10664(2)	6907(1)	16(1)
B(2A)	2743(3)	9882(2)	6155(1)	17(1)
B(3A)	1880(3)	10881(2)	6666(1)	16(1)
B(4A)	2830(3)	11199(2)	7608(1)	15(1)
B(5A)	4279(3)	10400(2)	7680(1)	15(1)
B(6A)	4238(3)	9589(2)	6784(1)	17(1)
B(7A)	2113(3)	9063(2)	6498(1)	17(1)
B(8A)	633(3)	9843(2)	6409(1)	15(1)
B(9A)	686(3)	10665(2)	7313(1)	15(1)
B(10A)	2177(3)	10367(2)	7939(1)	14(1)
B(11A)	3055(3)	9368(2)	7432(1)	15(1)
B(12A)	805(3)	9524(2)	7206(1)	14(1)
Br(2A)	-1430(1)	9484(1)	5669(1)	21(1)
Br(3A)	-1299(1)	11309(1)	7638(1)	19(1)
Br(4A)	1882(1)	10644(1)	8971(1)	18(1)
Br(5A)	3726(1)	8486(1)	7855(1)	20(1)
Br(6A)	-1071(1)	8837(1)	7388(1)	19(1)
Br(1A)	1655(2)	7775(1)	5873(1)	18(1)
Ge(1A)	4059(2)	7223(1)	5062(1)	16(1)
C(2A)	4092(12)	8055(6)	4563(5)	21(1)
C(3A)	2336(15)	8128(10)	4159(7)	28(2)
C(4A)	2844(19)	6069(5)	4505(5)	25(1)
C(5A)	2024(11)	5556(5)	4921(5)	41(2)
C(6A)	6067(5)	7312(2)	5775(2)	19(1)

C(7A)	5948(5)	6745(3)	6244(2)	33(1)
Br(1D)	1254(7)	7800(4)	5864(4)	18(1)
Ge(1D)	3834(7)	7175(4)	5201(3)	22(1)
C(2D)	4220(30)	7985(18)	4704(16)	28(4)
C(3D)	2600(40)	8020(30)	4190(20)	29(5)
C(4D)	2660(60)	6042(15)	4553(14)	25(1)
C(5D)	2520(30)	5368(16)	4930(17)	35(4)
C(6D)	5395(16)	7193(9)	6033(7)	42(4)
C(7D)	6898(15)	6640(8)	5844(6)	44(4)

A.2.3 Bond lengths [Å] and angles [°] for $[Et_3Ge]^+[CB_{11}H_6Br_6]^-$

C(1)-B(2)	1.697(3)
C(1)-B(3)	1.703(3)
C(1)-B(4)	1.705(3)
C(1)-B(5)	1.708(3)
C(1)-B(6)	1.712(3)
B(2)-B(7)	1.768(3)
B(2)-B(3)	1.782(4)
B(2)-B(8)	1.784(4)
B(2)-B(6)	1.795(4)
B(3)-B(9)	1.776(4)
B(3)-B(8)	1.778(4)
B(3)-B(4)	1.782(4)
B(4)-B(9)	1.773(4)
B(4)-B(10)	1.778(4)
B(4)-B(5)	1.785(4)
B(5)-B(11)	1.775(4)
B(5)-B(10)	1.777(4)
B(5)-B(6)	1.782(4)
B(6)-B(7)	1.761(3)
B(6)-B(11)	1.781(3)
B(7)-B(11)	1.774(3)
B(7)-B(12)	1.775(3)
B(7)-B(8)	1.779(3)
B(7)-Br(1)	1.994(2)
B(8)-B(9)	1.787(3)
B(8)-B(12)	1.810(3)
B(8)-Br(2)	1.946(2)
B(9)-B(10)	1.794(3)
B(9)-B(12)	1.798(3)
B(9)-Br(3)	1.954(2)
B(10)-B(11)	1.782(3)
B(10)-B(12)	1.783(3)

B(10)-Br(4)	1.955(2)
B(11)-B(12)	1.796(3)
B(11)-Br(5)	1.950(2)
B(12)-Br(6)	1.937(2)
Br(1)-Ge(1)	2.5351(3)
Ge(1)-C(2)	1.929(2)
Ge(1)-C(6)	1.935(2)
Ge(1)-C(4)	1.937(2)
C(2)-C(3)	1.532(3)
C(4)-C(5)	1.532(3)
C(6)-C(7)	1.520(3)
C(1A)-B(6A)	1.700(3)
C(1A)-B(4A)	1.702(3)
C(1A)-B(2A)	1.703(3)
C(1A)-B(3A)	1.708(3)
C(1A)-B(5A)	1.710(3)
B(2A)-B(7A)	1.763(4)
B(2A)-B(8A)	1.775(4)
B(2A)-B(3A)	1.780(4)
B(2A)-B(6A)	1.794(4)
B(3A)-B(9A)	1.779(3)
B(3A)-B(8A)	1.780(4)
B(3A)-B(4A)	1.786(4)
B(4A)-B(10A)	1.773(3)
B(4A)-B(9A)	1.777(3)
B(4A)-B(5A)	1.783(4)
B(5A)-B(11A)	1.766(4)
B(5A)-B(10A)	1.772(3)
B(5A)-B(6A)	1.776(4)
B(6A)-B(7A)	1.759(4)
B(6A)-B(11A)	1.777(4)
B(7A)-B(11A)	1.772(3)
B(7A)-B(8A)	1.783(4)
B(7A)-B(12A)	1.783(4)

B(7A)-Br(1A)	2.000(3)
B(7A)-Br(1D)	2.015(6)
B(8A)-B(9A)	1.792(3)
B(8A)-B(12A)	1.804(3)
B(8A)-Br(2A)	1.946(2)
B(9A)-B(10A)	1.792(3)
B(9A)-B(12A)	1.793(3)
B(9A)-Br(3A)	1.942(2)
B(10A)-B(11A)	1.783(3)
B(10A)-B(12A)	1.786(3)
B(10A)-Br(4A)	1.953(2)
B(11A)-B(12A)	1.803(3)
B(11A)-Br(5A)	1.950(2)
B(12A)-Br(6A)	1.940(2)
Br(1A)-Ge(1A)	2.5790(19)
Ge(1A)-C(2A)	1.927(4)
Ge(1A)-C(6A)	1.931(4)
Ge(1A)-C(4A)	1.933(4)
C(2A)-C(3A)	1.526(6)
C(4A)-C(5A)	1.525(7)
C(6A)-C(7A)	1.520(4)
Br(1D)-Ge(1D)	2.566(5)
Ge(1D)-C(6D)	1.903(12)
Ge(1D)-C(2D)	1.925(9)
Ge(1D)-C(4D)	1.936(10)
C(2D)-C(3D)	1.525(9)
C(4D)-C(5D)	1.527(10)
C(6D)-C(7D)	1.503(9)

B(2)-C(1)-B(3)	63.19(14)
B(2)-C(1)-B(4)	115.68(18)
B(3)-C(1)-B(4)	63.05(15)
B(2)-C(1)-B(5)	115.87(17)
B(3)-C(1)-B(5)	115.77(18)

B(4)-C(1)-B(5)	63.05(14)
B(2)-C(1)-B(6)	63.54(14)
B(3)-C(1)-B(6)	116.08(17)
B(4)-C(1)-B(6)	115.45(17)
B(5)-C(1)-B(6)	62.82(14)
C(1)-B(2)-B(7)	102.94(17)
C(1)-B(2)-B(3)	58.58(14)
B(7)-B(2)-B(3)	107.14(17)
C(1)-B(2)-B(8)	104.17(17)
B(7)-B(2)-B(8)	60.10(14)
B(3)-B(2)-B(8)	59.81(14)
C(1)-B(2)-B(6)	58.62(14)
B(7)-B(2)-B(6)	59.22 v(14)
B(3)-B(2)-B(6)	108.22(17)
B(8)-B(2)-B(6)	108.24(17)
C(1)-B(3)-B(9)	104.09(17)
C(1)-B(3)-B(8)	104.19(17)
B(9)-B(3)-B(8)	60.37(14)
C(1)-B(3)-B(2)	58.24(14)
B(9)-B(3)-B(2)	108.28(17)
B(8)-B(3)-B(2)	60.17(14)
C(1)-B(3)-B(4)	58.52(14)
B(9)-B(3)-B(4)	59.75(14)
B(8)-B(3)-B(4)	108.09(17)
B(2)-B(3)-B(4)	107.85(17)
C(1)-B(4)-B(9)	104.18(17)
C(1)-B(4)-B(10)	104.13(17)
B(9)-B(4)-B(10)	60.69(14)
C(1)-B(4)-B(3)	58.43(14)
B(9)-B(4)-B(3)	59.96(14)
B(10)-B(4)-B(3)	108.47(17)
C(1)-B(4)-B(5)	58.56(14)
B(9)-B(4)-B(5)	108.50(17)
B(10)-B(4)-B(5)	59.84(14)

B(3)-B(4)-B(5)	108.21(17)
C(1)-B(5)-B(11)	104.38(17)
C(1)-B(5)-B(10)	104.03(17)
B(11)-B(5)-B(10)	60.22(14)
C(1)-B(5)-B(6)	58.68(14)
B(11)-B(5)-B(6)	60.08(14)
B(10)-B(5)-B(6)	108.18(18)
C(1)-B(5)-B(4)	58.39(14)
B(11)-B(5)-B(4)	108.21(18)
B(10)-B(5)-B(4)	59.89(14)
B(6)-B(5)-B(4)	108.16(18)
C(1)-B(6)-B(7)	102.68(17)
C(1)-B(6)-B(11)	103.98(17)
B(7)-B(6)-B(11)	60.11(14)
C(1)-B(6)-B(5)	58.50(14)
B(7)-B(6)-B(5)	107.00(17)
B(11)-B(6)-B(5)	59.74(14)
C(1)-B(6)-B(2)	57.84(14)
B(7)-B(6)-B(2)	59.64(14)
B(11)-B(6)-B(2)	108.32(17)
B(5)-B(6)-B(2)	107.57(17)
B(6)-B(7)-B(2)	61.14(14)
B(6)-B(7)-B(11)	60.51(14)
B(2)-B(7)-B(11)	109.84(17)
B(6)-B(7)-B(12)	109.88(17)
B(2)-B(7)-B(12)	109.91(17)
B(11)-B(7)-B(12)	60.80(14)
B(6)-B(7)-B(8)	110.02(17)
B(2)-B(7)-B(8)	60.39(14)
B(11)-B(7)-B(8)	110.15(17)
B(12)-B(7)-B(8)	61.23(14)
B(6)-B(7)-Br(1)	124.95(15)
B(2)-B(7)-Br(1)	123.13(15)
B(11)-B(7)-Br(1)	120.73(15)

B(12)-B(7)-Br(1)	116.15(15)
B(8)-B(7)-Br(1)	117.58(15)
B(3)-B(8)-B(7)	106.84(17)
B(3)-B(8)-B(2)	60.02(14)
B(7)-B(8)-B(2)	59.51(14)
B(3)-B(8)-B(9)	59.78(14)
B(7)-B(8)-B(9)	106.64(17)
B(2)-B(8)-B(9)	107.69(17)
B(3)-B(8)-B(12)	107.76(17)
B(7)-B(8)-B(12)	59.28(13)
B(2)-B(8)-B(12)	107.63(17)
B(9)-B(8)-B(12)	59.99(13)
B(3)-B(8)-Br(2)	123.23(15)
B(7)-B(8)-Br(2)	121.42(15)
B(2)-B(8)-Br(2)	121.47(15)
B(9)-B(8)-Br(2)	123.18(15)
B(12)-B(8)-Br(2)	121.26(15)
B(4)-B(9)-B(3)	60.29(14)
B(4)-B(9)-B(8)	108.12(17)
B(3)-B(9)-B(8)	59.85(14)
B(4)-B(9)-B(10)	59.81(14)
B(3)-B(9)-B(10)	108.03(17)
B(8)-B(9)-B(10)	108.04(17)
B(4)-B(9)-B(12)	107.70(17)
B(3)-B(9)-B(12)	108.33(17)
B(8)-B(9)-B(12)	60.64(13)
B(10)-B(9)-B(12)	59.50(13)
B(4)-B(9)-Br(3)	123.07(15)
B(3)-B(9)-Br(3)	122.52(15)
B(8)-B(9)-Br(3)	120.81(15)
B(10)-B(9)-Br(3)	121.77(15)
B(12)-B(9)-Br(3)	120.26(15)
B(5)-B(10)-B(4)	60.27(14)
B(5)-B(10)-B(11)	59.82(14)

B(4)-B(10)-B(11)	108.19(17)
B(5)-B(10)-B(12)	108.32(17)
B(4)-B(10)-B(12)	108.14(17)
B(11)-B(10)-B(12)	60.50(14)
B(5)-B(10)-B(9)	107.89(17)
B(4)-B(10)-B(9)	59.50(14)
B(11)-B(10)-B(9)	108.50(17)
B(12)-B(10)-B(9)	60.36(14)
B(5)-B(10)-Br(4)	121.10(15)
B(4)-B(10)-Br(4)	121.11(16)
B(11)-B(10)-Br(4)	121.72(15)
B(12)-B(10)-Br(4)	122.11(15)
B(9)-B(10)-Br(4)	121.92(15)
B(7)-B(11)-B(5)	106.77(17)
B(7)-B(11)-B(6)	59.38(14)
B(5)-B(11)-B(6)	60.17(14)
B(7)-B(11)-B(10)	106.66(17)
B(5)-B(11)-B(10)	59.97(14)
B(6)-B(11)-B(10)	108.06(17)
B(7)-B(11)-B(12)	59.63(13)
B(5)-B(11)-B(12)	107.86(17)
B(6)-B(11)-B(12)	108.03(17)
B(10)-B(11)-B(12)	59.77(13)
B(7)-B(11)-Br(5)	121.97(15)
B(5)-B(11)-Br(5)	121.99(16)
B(6)-B(11)-Br(5)	120.18(15)
B(10)-B(11)-Br(5)	123.47(15)
B(12)-B(11)-Br(5)	122.48(16)
B(7)-B(12)-B(10)	106.58(17)
B(7)-B(12)-B(11)	59.57(13)
B(10)-B(12)-B(11)	59.73(14)
B(7)-B(12)-B(9)	106.33(17)
B(10)-B(12)-B(9)	60.13(14)
B(11)-B(12)-B(9)	107.71(17)

B(7)-B(12)-B(8)	59.49(13)
B(10)-B(12)-B(8)	107.54(17)
B(11)-B(12)-B(8)	107.78(17)
B(9)-B(12)-B(8)	59.38(13)
B(7)-B(12)-Br(6)	121.72(15)
B(10)-B(12)-Br(6)	123.31(15)
B(11)-B(12)-Br(6)	121.75(15)
B(9)-B(12)-Br(6)	122.97(15)
B(8)-B(12)-Br(6)	121.19(15)
B(7)-Br(1)-Ge(1)	111.76(7)
C(2)-Ge(1)-C(6)	120.36(10)
C(2)-Ge(1)-C(4)	116.64(11)
C(6)-Ge(1)-C(4)	114.90(11)
C(2)-Ge(1)-Br(1)	101.60(7)
C(6)-Ge(1)-Br(1)	103.03(8)
C(4)-Ge(1)-Br(1)	93.64(7)
C(3)-C(2)-Ge(1)	113.60(18)
C(5)-C(4)-Ge(1)	110.50(16)
C(7)-C(6)-Ge(1)	115.37(17)
B(6A)-C(1A)-B(4A)	115.44(17)
B(6A)-C(1A)-B(2A)	63.63(15)
B(4A)-C(1A)-B(2A)	115.49(18)
B(6A)-C(1A)-B(3A)	116.08(18)
B(4A)-C(1A)-B(3A)	63.19(14)
B(2A)-C(1A)-B(3A)	62.93(15)
B(6A)-C(1A)-B(5A)	62.77(14)
B(4A)-C(1A)-B(5A)	63.00(14)
B(2A)-C(1A)-B(5A)	115.70(18)
B(3A)-C(1A)-B(5A)	115.78(17)
C(1A)-B(2A)-B(7A)	102.93(17)
C(1A)-B(2A)-B(8A)	104.46(17)
B(7A)-B(2A)-B(8A)	60.52(15)
C(1A)-B(2A)-B(3A)	58.68(14)
B(7A)-B(2A)-B(3A)	107.71(17)

B(8A)-B(2A)-B(3A)	60.09(14)
C(1A)-B(2A)-B(6A)	58.12(14)
B(7A)-B(2A)-B(6A)	59.28(14)
B(8A)-B(2A)-B(6A)	108.47(17)
B(3A)-B(2A)-B(6A)	108.00(17)
C(1A)-B(3A)-B(9A)	103.94(17)
C(1A)-B(3A)-B(2A)	58.39(14)
B(9A)-B(3A)-B(2A)	108.08(18)
C(1A)-B(3A)-B(8A)	104.03(17)
B(9A)-B(3A)-B(8A)	60.48(14)
B(2A)-B(3A)-B(8A)	59.82(14)
C(1A)-B(3A)-B(4A)	58.24(14)
B(9A)-B(3A)-B(4A)	59.79(14)
B(2A)-B(3A)-B(4A)	107.65(17)
B(8A)-B(3A)-B(4A)	108.05(17)
C(1A)-B(4A)-B(10A)	104.23(17)
C(1A)-B(4A)-B(9A)	104.28(17)
B(10A)-B(4A)-B(9A)	60.66(14)
C(1A)-B(4A)-B(5A)	58.74(14)
B(10A)-B(4A)-B(5A)	59.78(14)
B(9A)-B(4A)-B(5A)	108.49(17)
C(1A)-B(4A)-B(3A)	58.57(14)
B(10A)-B(4A)-B(3A)	108.44(17)
B(9A)-B(4A)-B(3A)	59.89(14)
B(5A)-B(4A)-B(3A)	108.43(17)
C(1A)-B(5A)-B(11A)	104.30(17)
C(1A)-B(5A)-B(10A)	103.92(17)
B(11A)-B(5A)-B(10A)	60.52(14)
C(1A)-B(5A)-B(6A)	58.34(14)
B(11A)-B(5A)-B(6A)	60.22(14)
B(10A)-B(5A)-B(6A)	108.36(17)
C(1A)-B(5A)-B(4A)	58.27(13)
B(11A)-B(5A)-B(4A)	108.36(17)
B(10A)-B(5A)-B(4A)	59.84(14)

B(6A)-B(5A)-B(4A)	107.84(17)
C(1A)-B(6A)-B(7A)	103.20(18)
C(1A)-B(6A)-B(5A)	58.89(14)
B(7A)-B(6A)-B(5A)	107.27(17)
C(1A)-B(6A)-B(11A)	104.25(17)
B(7A)-B(6A)-B(11A)	60.16(14)
B(5A)-B(6A)-B(11A)	59.61(14)
C(1A)-B(6A)-B(2A)	58.25(14)
B(7A)-B(6A)-B(2A)	59.49(14)
B(5A)-B(6A)-B(2A)	108.08(17)
B(11A)-B(6A)-B(2A)	108.19(18)
B(6A)-B(7A)-B(2A)	61.23(15)
B(6A)-B(7A)-B(11A)	60.41(14)
B(2A)-B(7A)-B(11A)	109.78(18)
B(6A)-B(7A)-B(8A)	109.68(18)
B(2A)-B(7A)-B(8A)	60.08(14)
B(11A)-B(7A)-B(8A)	109.91(17)
B(6A)-B(7A)-B(12A)	109.63(17)
B(2A)-B(7A)-B(12A)	109.27(17)
B(11A)-B(7A)-B(12A)	60.95(14)
B(8A)-B(7A)-B(12A)	60.77(14)
B(6A)-B(7A)-Br(1A)	121.69(17)
B(2A)-B(7A)-Br(1A)	123.32(17)
B(11A)-B(7A)-Br(1A)	118.80(17)
B(8A)-B(7A)-Br(1A)	121.23(17)
B(12A)-B(7A)-Br(1A)	118.59(17)
B(6A)-B(7A)-Br(1D)	130.6(2)
B(2A)-B(7A)-Br(1D)	124.5(3)
B(11A)-B(7A)-Br(1D)	122.1(3)
B(8A)-B(7A)-Br(1D)	113.2(2)
B(12A)-B(7A)-Br(1D)	111.9(2)
Br(1A)-B(7A)-Br(1D)	8.99(16)
B(2A)-B(8A)-B(3A)	60.09(14)
B(2A)-B(8A)-B(7A)	59.40(14)

B(3A)-B(8A)-B(7A)	106.82(18)
B(2A)-B(8A)-B(9A)	107.69(17)
B(3A)-B(8A)-B(9A)	59.72(14)
B(7A)-B(8A)-B(9A)	106.70(17)
B(2A)-B(8A)-B(12A)	107.80(17)
B(3A)-B(8A)-B(12A)	107.67(17)
B(7A)-B(8A)-B(12A)	59.62(14)
B(9A)-B(8A)-B(12A)	59.80(13)
B(2A)-B(8A)-Br(2A)	121.10(15)
B(3A)-B(8A)-Br(2A)	123.13(16)
B(7A)-B(8A)-Br(2A)	121.28(16)
B(9A)-B(8A)-Br(2A)	123.50(16)
B(12A)-B(8A)-Br(2A)	121.48(15)
B(4A)-B(9A)-B(3A)	60.31(14)
B(4A)-B(9A)-B(8A)	107.93(17)
B(3A)-B(9A)-B(8A)	59.80(14)
B(4A)-B(9A)-B(10A)	59.56(14)
B(3A)-B(9A)-B(10A)	107.91(17)
B(8A)-B(9A)-B(10A)	107.92(17)
B(4A)-B(9A)-B(12A)	107.64(17)
B(3A)-B(9A)-B(12A)	108.23(17)
B(8A)-B(9A)-B(12A)	60.42(14)
B(10A)-B(9A)-B(12A)	59.75(13)
B(4A)-B(9A)-Br(3A)	120.42(16)
B(3A)-B(9A)-Br(3A)	121.50(16)
B(8A)-B(9A)-Br(3A)	123.09(16)
B(10A)-B(9A)-Br(3A)	121.15(15)
B(12A)-B(9A)-Br(3A)	122.61(15)
B(5A)-B(10A)-B(4A)	60.38(14)
B(5A)-B(10A)-B(11A)	59.58(14)
B(4A)-B(10A)-B(11A)	108.04(17)
B(5A)-B(10A)-B(12A)	108.41(17)
B(4A)-B(10A)-B(12A)	108.13(17)
B(11A)-B(10A)-B(12A)	60.71(14)

B(5A)-B(10A)-B(9A)	108.28(17)
B(4A)-B(10A)-B(9A)	59.78(14)
B(11A)-B(10A)-B(9A)	108.54(17)
B(12A)-B(10A)-B(9A)	60.13(14)
B(5A)-B(10A)-Br(4A)	120.76(15)
B(4A)-B(10A)-Br(4A)	121.80(15)
B(11A)-B(10A)-Br(4A)	120.94(15)
B(12A)-B(10A)-Br(4A)	121.81(15)
B(9A)-B(10A)-Br(4A)	122.44(15)
B(5A)-B(11A)-B(7A)	107.13(17)
B(5A)-B(11A)-B(6A)	60.17(14)
B(7A)-B(11A)-B(6A)	59.43(14)
B(5A)-B(11A)-B(10A)	59.90(14)
B(7A)-B(11A)-B(10A)	106.92(17)
B(6A)-B(11A)-B(10A)	107.83(17)
B(5A)-B(11A)-B(12A)	107.88(17)
B(7A)-B(11A)-B(12A)	59.82(14)
B(6A)-B(11A)-B(12A)	107.93(17)
B(10A)-B(11A)-B(12A)	59.73(14)
B(5A)-B(11A)-Br(5A)	122.29(16)
B(7A)-B(11A)-Br(5A)	121.85(16)
B(6A)-B(11A)-Br(5A)	121.27(16)
B(10A)-B(11A)-Br(5A)	122.83(15)
B(12A)-B(11A)-Br(5A)	121.69(15)
B(7A)-B(12A)-B(10A)	106.32(17)
B(7A)-B(12A)-B(9A)	106.68(17)
B(10A)-B(12A)-B(9A)	60.12(14)
B(7A)-B(12A)-B(11A)	59.23(14)
B(10A)-B(12A)-B(11A)	59.56(14)
B(9A)-B(12A)-B(11A)	107.62(17)
B(7A)-B(12A)-B(8A)	59.62(14)
B(10A)-B(12A)-B(8A)	107.70(17)
B(9A)-B(12A)-B(8A)	59.78(13)
B(11A)-B(12A)-B(8A)	107.60(17)

B(7A)-B(12A)-Br(6A)	123.03(16)
B(10A)-B(12A)-Br(6A)	121.92(15)
B(9A)-B(12A)-Br(6A)	122.17(16)
B(11A)-B(12A)-Br(6A)	121.70(15)
B(8A)-B(12A)-Br(6A)	122.16(15)
B(7A)-Br(1A)-Ge(1A)	112.00(12)
C(2A)-Ge(1A)-C(6A)	116.5(3)
C(2A)-Ge(1A)-C(4A)	116.4(4)
C(6A)-Ge(1A)-C(4A)	118.8(5)
C(2A)-Ge(1A)-Br(1A)	101.2(4)
C(6A)-Ge(1A)-Br(1A)	103.06(13)
C(4A)-Ge(1A)-Br(1A)	94.7(4)
C(3A)-C(2A)-Ge(1A)	114.9(6)
C(5A)-C(4A)-Ge(1A)	118.7(6)
C(7A)-C(6A)-Ge(1A)	116.7(3)
B(7A)-Br(1D)-Ge(1D)	104.4(3)
C(6D)-Ge(1D)-C(2D)	121.6(10)
C(6D)-Ge(1D)-C(4D)	117.5(12)
C(2D)-Ge(1D)-C(4D)	113.3(12)
C(6D)-Ge(1D)-Br(1D)	98.7(4)
C(2D)-Ge(1D)-Br(1D)	101.3(10)
C(4D)-Ge(1D)-Br(1D)	97.5(16)
C(3D)-C(2D)-Ge(1D)	112.5(15)
C(5D)-C(4D)-Ge(1D)	113.3(17)
C(7D)-C(6D)-Ge(1D)	114.4(8)

Appendix A.3 References

1. *APEX 2,* version 2010.3-0, Bruker (2010), Bruker AXS Inc., Madison, Wisconsin, USA.

2. *SAINT,* version V7.60A, Bruker (2009), Bruker AXS Inc., Madison, Wisconsin, USA.

3. *SADABS,* version 2008/1, Bruker (2008), Bruker AXS Inc., Madison, Wisconsin, USA.

4. *SHELXTL,* version 2008/4, Bruker (2008), Bruker AXS Inc., Madison, Wisconsin, USA.

Appendix B

X-Ray Structure Determination of $[Et_3Sn]^+[CB_{11}H_6Br_6]^-$

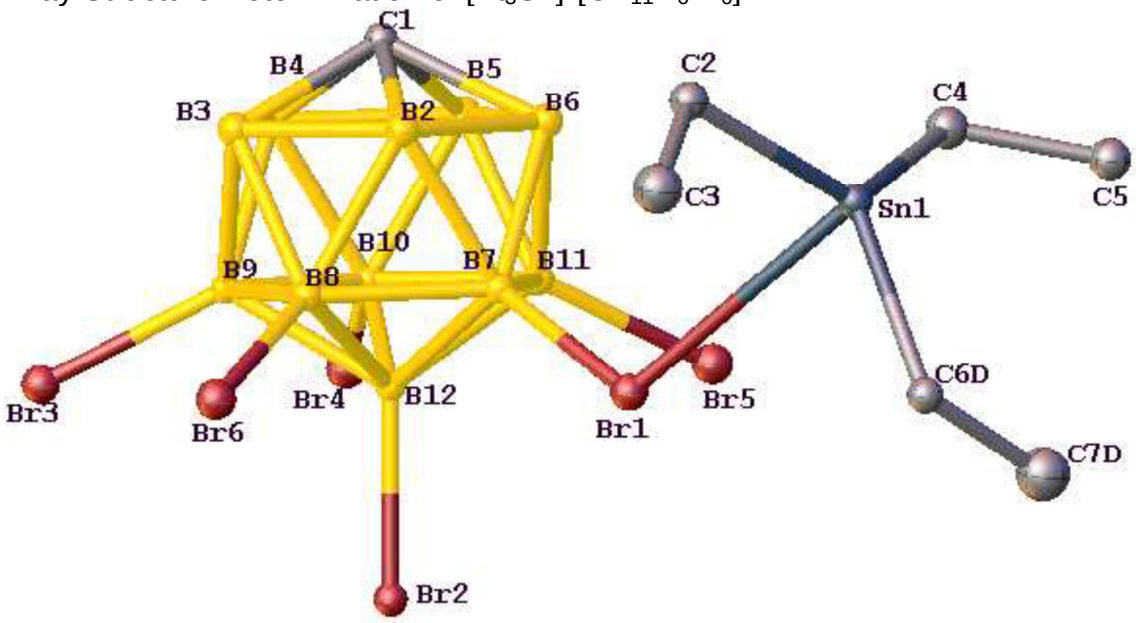

Appendix B.1 Experimental:

A colorless fragment of a prism (0.51 x 0.42 x 0.37 mm^3) was used for the single crystal x-ray diffraction study of $[[C_2H_5]_3Sn]^+[CH_6B_{11}Br_6]^-$ (sample cr348_0m). The crystal was coated with paratone oil and mounted on to a cryo-loop glass fiber. X-ray intensity data were collected at 100(2) K on a Bruker APEX2 (**ref. 1**) platform-CCD x-ray diffractometer system (Mo-radiation, λ = 0.71073 Å, 50KV/40mA power). The CCD detector was placed at a distance of 5.0800 cm from the crystal.

A total of 4800 frames were collected for a hemisphere of reflections (with scan width of 0.3° in ω, starting ω and 2θ angles at –30° and –45°, ϕ angles of 0°, 90°, 180°, and 270° for every 600 frames, 20 sec/frame exposure time). The frames were integrated using the Bruker SAINT software package (**ref. 2**) and using a narrow-frame integration algorithm. Based on an orthorhombic crystal system, the integrated frames yielded a total of 80941 reflections at a maximum 2θ angle of 71.26° (0.61 Å resolution), of which 10432 were independent reflections (R_{int} = 0.0394, R_{sig} = 0.0258, redundancy = 7.8, completeness = 99.8%) and 9698 (93.0%) reflections were greater than 2σ(I). The unit cell parameters were, **a** = 12.7355(4) Å, **b** = 13.2053(4) Å, **c** = 13.4694(4) Å, **α** = **β** = **γ**= 90°**,** V = 2265.23(12) $Å^3$, Z = 4, calculated density D_c = 2.411 g/cm^3. Absorption

corrections were applied (absorption coefficient μ = 11.703 mm^{-1}; max/min transmission = 0.0986/0.0658) to the raw intensity data using the SADABS program (**ref. 3**).

The Bruker SHELXTL software package (**ref. 4**) was used for phase determination and structure refinement. The distribution of intensities (E^2-1 = 0.735) and systematic absent reflections indicated one possible space group, P2(1)2(1)2(1). The space group P2(1)2(1)2(1) (#19) was later determined to be correct. Direct methods of phase determination followed by two Fourier cycles of refinement led to an electron density map from which most of the non-hydrogen atoms were identified in the asymmetry unit of the unit cell. With subsequent isotropic refinement, all of the non-hydrogen atoms were identified. There was one cation of $[[C_2H_5]_3Sn]^+$ (where one of the three C_2H_5-groups was refined with disorder and the disordered site occupancy factor ratio was 75%/25%) and one anion of $[CH_6B_{11}Br_6]^-$ present in the asymmetry unit of the unit cell. The CIF validation report of an Alert level B was a false alarm because the structure could not properly fit on a mirror plane perpendicular to the **b**-axis of the Pnma space group suggested. The final structure was refined as a racemic twin with Flack parameter, x = 0.575(4). SADI, DELU, SIMU, EADP, and DFIX restraints were used to stabilize the refinement of the disordered C_2H_5-group.

Atomic coordinates, isotropic and anisotropic displacement parameters of all the non-hydrogen atoms were refined by means of a full matrix least-squares procedure on F^2. The H-atoms were included in the refinement in calculated positions riding on the atoms to which they were attached. The refinement converged at R1 = 0.0232, wR2 = 0.0495, with intensity, I>2σ(I). The largest peak/hole in the final difference map was 1.693/-0.976 e/$Å^3$. The high electron density peak/hole was probably due to absorption correction and Fourier truncation errors.

Appendix B.2: Structure Data

B.2.1 Crystal data and structure refinement for $[Et_3Sn]^+[CB_{11}H_6Br_6]^-$

Identification code	cr348_0m
Empirical formula	C7 H21 B11 Br6 Sn
Formula weight	822.30
Temperature	100(2) K

Wavelength	0.71073 Å	
Crystal system	Orthorhombic	
Space group	P2(1)2(1)2(1) (#19)	
Unit cell dimensions	a = 12.7355(4) Å	α= 90°.
	b = 13.2053(4) Å	β= 90°.
	c = 13.4694(4) Å	γ= 90°.
Volume	2265.23(12) $Å^3$	
Z	4	
Density (calculated)	2.411 Mg/m^3	
Absorption coefficient	11.703 mm^{-1}	
F(000)	1512	
Crystal size	0.51 x 0.42 x 0.37 mm^3	
Theta range for data collection	2.16 to 35.63°.	
Index ranges	-20<=h<=20, -21<=k<=21, -22<=l<=22	
Reflections collected	80941	
Independent reflections	10432 [R(int) = 0.0394]	
Completeness to theta = 35.63°	99.8 %	
Absorption correction	Semi-empirical from equivalents	
Max. and min. transmission	0.0986 and 0.0658	
Refinement method	Full-matrix least-squares on F^2	
Data / restraints / parameters	10432 / 52 / 247	
Goodness-of-fit on F^2	1.056	
Final R indices [I>2sigma(I)]	R1 = 0.0232, wR2 = 0.0495	
R indices (all data)	R1 = 0.0277, wR2 = 0.0505	
Absolute structure parameter	0.575(4)	
Largest diff. peak and hole	1.693 and -0.976 e.$Å^{-3}$	

B.2.2. Atomic coordinates (x 10^4) and equivalent isotropic displacement parameters ($Å^2$x 10^3) for $[Et_3Sn]^+[CB_{11}H_6Br_6]^-$. U(eq) is defined as one third of the trace of the orthogonalized U^{ij} tensor.

	x	y	z	U(eq)
C(1)	2703(2)	5968(2)	76(2)	10(1)

B(2)	2279(2)	5036(2)	856(2)	11(1)
B(3)	2037(2)	6336(2)	1106(2)	11(1)
B(4)	1880(2)	6980(2)	-45(2)	10(1)
B(5)	2041(2)	6078(2)	-1019(2)	12(1)
B(6)	2279(2)	4872(2)	-464(2)	11(1)
B(7)	1163(2)	4540(2)	239(2)	9(1)
B(8)	1001(2)	5438(2)	1220(2)	10(1)
B(9)	765(2)	6641(2)	664(2)	8(1)
B(10)	764(2)	6482(2)	-656(2)	10(1)
B(11)	1016(2)	5175(2)	-919(2)	10(1)
B(12)	226(2)	5523(2)	121(2)	8(1)
Br(1)	693(1)	3126(1)	415(1)	13(1)
Br(2)	-1301(1)	5306(1)	138(1)	11(1)
Br(3)	-99(1)	7660(1)	1314(1)	14(1)
Br(4)	-122(1)	7308(1)	-1509(1)	15(1)
Br(5)	436(1)	4507(1)	-2081(1)	15(1)
Br(6)	402(1)	5077(1)	2497(1)	15(1)
Sn(1)	2375(1)	1636(1)	-9(1)	11(1)
C(2)	3129(2)	2093(2)	1328(2)	14(1)
C(3)	2656(2)	1543(2)	2217(2)	23(1)
C(4)	2706(2)	2127(2)	-1495(2)	17(1)
C(5)	2593(2)	1271(2)	-2250(2)	16(1)
C(6)	1213(3)	451(4)	18(4)	18(1)
C(7)	124(3)	722(3)	-329(3)	27(1)
C(6D)	1193(10)	526(10)	342(8)	12(2)
C(7D)	609(9)	176(9)	-585(9)	27(1)

B.2.3 Bond lengths [Å] and angles [°] for $[Et_3Sn]^+[CB_{11}H_6Br_6]^-$.

C(1)-B(3)	1.698(3)
C(1)-B(5)	1.705(3)
C(1)-B(4)	1.706(3)
C(1)-B(2)	1.706(3)
C(1)-B(6)	1.707(3)

C(1)-H(1)	0.954(10)
B(2)-B(7)	1.772(3)
B(2)-B(3)	1.776(3)
B(2)-B(8)	1.781(3)
B(2)-B(6)	1.792(4)
B(2)-H(2)	1.1200
B(3)-B(9)	1.771(3)
B(3)-B(4)	1.778(3)
B(3)-B(8)	1.781(3)
B(3)-H(3)	1.1200
B(4)-B(9)	1.769(3)
B(4)-B(10)	1.769(3)
B(4)-B(5)	1.783(3)
B(4)-H(4)	1.1200
B(5)-B(11)	1.774(3)
B(5)-B(10)	1.780(4)
B(5)-B(6)	1.785(4)
B(5)-H(5)	1.1200
B(6)-B(7)	1.764(3)
B(6)-B(11)	1.767(3)
B(6)-H(6)	1.1200
B(7)-B(12)	1.771(3)
B(7)-B(11)	1.782(3)
B(7)-B(8)	1.788(3)
B(7)-Br(1)	1.975(2)
B(8)-B(9)	1.781(3)
B(8)-B(12)	1.783(3)
B(8)-Br(6)	1.940(2)
B(9)-B(12)	1.785(3)
B(9)-B(10)	1.791(3)
B(9)-Br(3)	1.947(2)
B(10)-B(12)	1.780(3)
B(10)-B(11)	1.791(3)
B(10)-Br(4)	1.946(2)

B(11)-B(12)	1.784(3)
B(11)-Br(5)	1.942(2)
B(12)-Br(2)	1.966(2)
Br(1)-Sn(1)	2.9652(3)
Sn(1)-C(2)	2.128(2)
Sn(1)-C(4)	2.146(2)
Sn(1)-C(6D)	2.154(8)
Sn(1)-C(6)	2.154(3)
C(2)-C(3)	1.524(4)
C(2)-H(2A)	0.9900
C(2)-H(2B)	0.9900
C(3)-H(3A)	0.9800
C(3)-H(3B)	0.9800
C(3)-H(3C)	0.9800
C(4)-C(5)	1.528(3)
C(4)-H(4A)	0.9900
C(4)-H(4B)	0.9900
C(5)-H(5A)	0.9800
C(5)-H(5B)	0.9800
C(5)-H(5C)	0.9800
C(6)-C(7)	1.507(6)
C(6)-H(6A)	0.9900
C(6)-H(6B)	0.9900
C(7)-H(7A)	0.9800
C(7)-H(7B)	0.9800
C(7)-H(7C)	0.9800
C(6D)-C(7D)	1.524(9)
C(6D)-H(6C)	0.9900
C(6D)-H(6D)	0.9900
C(7D)-H(7D)	0.9800
C(7D)-H(7E)	0.9800
C(7D)-H(7F)	0.9800

B(3)-C(1)-B(5)	115.78(16)

B(3)-C(1)-B(4)	63.00(14)
B(5)-C(1)-B(4)	63.05(14)
B(3)-C(1)-B(2)	62.92(14)
B(5)-C(1)-B(2)	115.96(16)
B(4)-C(1)-B(2)	115.39(16)
B(3)-C(1)-B(6)	115.65(16)
B(5)-C(1)-B(6)	63.08(14)
B(4)-C(1)-B(6)	115.39(16)
B(2)-C(1)-B(6)	63.33(14)
B(3)-C(1)-H(1)	117.3(8)
B(5)-C(1)-H(1)	116.5(8)
B(4)-C(1)-H(1)	117.0(8)
B(2)-C(1)-H(1)	117.6(8)
B(6)-C(1)-H(1)	117.3(8)
C(1)-B(2)-B(7)	103.42(16)
C(1)-B(2)-B(3)	58.31(13)
B(7)-B(2)-B(3)	107.91(17)
C(1)-B(2)-B(8)	104.14(16)
B(7)-B(2)-B(8)	60.44(13)
B(3)-B(2)-B(8)	60.08(13)
C(1)-B(2)-B(6)	58.37(13)
B(7)-B(2)-B(6)	59.32(13)
B(3)-B(2)-B(6)	107.75(17)
B(8)-B(2)-B(6)	108.03(17)
C(1)-B(2)-H(2)	125.6
B(7)-B(2)-H(2)	122.8
B(3)-B(2)-H(2)	121.5
B(8)-B(2)-H(2)	122.1
B(6)-B(2)-H(2)	121.7
C(1)-B(3)-B(9)	104.35(16)
C(1)-B(3)-B(2)	58.77(13)
B(9)-B(3)-B(2)	108.32(17)
C(1)-B(3)-B(4)	58.72(13)
B(9)-B(3)-B(4)	59.78(13)

B(2)-B(3)-B(4)	108.43(17)
C(1)-B(3)-B(8)	104.49(16)
B(9)-B(3)-B(8)	60.19(13)
B(2)-B(3)-B(8)	60.08(13)
B(4)-B(3)-B(8)	108.09(17)
C(1)-B(3)-H(3)	125.0
B(9)-B(3)-H(3)	122.4
B(2)-B(3)-H(3)	121.1
B(4)-B(3)-H(3)	121.4
B(8)-B(3)-H(3)	122.3
C(1)-B(4)-B(9)	104.10(16)
C(1)-B(4)-B(10)	104.29(16)
B(9)-B(4)-B(10)	60.80(13)
C(1)-B(4)-B(3)	58.27(13)
B(9)-B(4)-B(3)	59.91(13)
B(10)-B(4)-B(3)	108.54(16)
C(1)-B(4)-B(5)	58.45(14)
B(9)-B(4)-B(5)	108.68(16)
B(10)-B(4)-B(5)	60.12(14)
B(3)-B(4)-B(5)	108.02(17)
C(1)-B(4)-H(4)	125.5
B(9)-B(4)-H(4)	122.1
B(10)-B(4)-H(4)	122.0
B(3)-B(4)-H(4)	121.5
B(5)-B(4)-H(4)	121.3
C(1)-B(5)-B(11)	103.96(17)
C(1)-B(5)-B(10)	103.89(17)
B(11)-B(5)-B(10)	60.54(14)
C(1)-B(5)-B(4)	58.50(13)
B(11)-B(5)-B(4)	107.99(17)
B(10)-B(5)-B(4)	59.54(13)
C(1)-B(5)-B(6)	58.52(13)
B(11)-B(5)-B(6)	59.55(14)
B(10)-B(5)-B(6)	107.91(17)

B(4)-B(5)-B(6)	107.89(17)
C(1)-B(5)-H(5)	125.4
B(11)-B(5)-H(5)	122.4
B(10)-B(5)-H(5)	122.5
B(4)-B(5)-H(5)	121.6
B(6)-B(5)-H(5)	121.6
C(1)-B(6)-B(7)	103.72(16)
C(1)-B(6)-B(11)	104.13(16)
B(7)-B(6)-B(11)	60.60(13)
C(1)-B(6)-B(5)	58.39(13)
B(7)-B(6)-B(5)	108.08(17)
B(11)-B(6)-B(5)	59.90(14)
C(1)-B(6)-B(2)	58.30(13)
B(7)-B(6)-B(2)	59.78(13)
B(11)-B(6)-B(2)	108.46(17)
B(5)-B(6)-B(2)	107.91(16)
C(1)-B(6)-H(6)	125.6
B(7)-B(6)-H(6)	122.5
B(11)-B(6)-H(6)	122.1
B(5)-B(6)-H(6)	121.5
B(2)-B(6)-H(6)	121.4
B(6)-B(7)-B(12)	108.17(16)
B(6)-B(7)-B(2)	60.90(14)
B(12)-B(7)-B(2)	108.14(16)
B(6)-B(7)-B(11)	59.80(14)
B(12)-B(7)-B(11)	60.29(13)
B(2)-B(7)-B(11)	108.72(16)
B(6)-B(7)-B(8)	108.96(16)
B(12)-B(7)-B(8)	60.15(13)
B(2)-B(7)-B(8)	60.02(13)
B(11)-B(7)-B(8)	108.81(16)
B(6)-B(7)-Br(1)	122.98(14)
B(12)-B(7)-Br(1)	119.95(14)
B(2)-B(7)-Br(1)	122.50(15)

B(11)-B(7)-Br(1)	121.19(15)
B(8)-B(7)-Br(1)	120.26(14)
B(2)-B(8)-B(3)	59.84(13)
B(2)-B(8)-B(9)	107.69(16)
B(3)-B(8)-B(9)	59.64(13)
B(2)-B(8)-B(12)	107.19(16)
B(3)-B(8)-B(12)	107.24(16)
B(9)-B(8)-B(12)	60.12(13)
B(2)-B(8)-B(7)	59.54(13)
B(3)-B(8)-B(7)	107.01(16)
B(9)-B(8)-B(7)	107.49(16)
B(12)-B(8)-B(7)	59.44(13)
B(2)-B(8)-Br(6)	122.04(15)
B(3)-B(8)-Br(6)	122.13(15)
B(9)-B(8)-Br(6)	121.68(15)
B(12)-B(8)-Br(6)	122.24(14)
B(7)-B(8)-Br(6)	122.49(15)
B(4)-B(9)-B(3)	60.31(14)
B(4)-B(9)-B(8)	108.50(16)
B(3)-B(9)-B(8)	60.17(13)
B(4)-B(9)-B(12)	107.25(16)
B(3)-B(9)-B(12)	107.56(16)
B(8)-B(9)-B(12)	60.00(13)
B(4)-B(9)-B(10)	59.60(14)
B(3)-B(9)-B(10)	107.91(17)
B(8)-B(9)-B(10)	108.26(17)
B(12)-B(9)-B(10)	59.70(13)
B(4)-B(9)-Br(3)	121.45(15)
B(3)-B(9)-Br(3)	121.52(14)
B(8)-B(9)-Br(3)	121.51(15)
B(12)-B(9)-Br(3)	122.60(15)
B(10)-B(9)-Br(3)	121.81(15)
B(4)-B(10)-B(5)	60.34(14)
B(4)-B(10)-B(12)	107.48(16)

B(5)-B(10)-B(12)	107.45(16)
B(4)-B(10)-B(9)	59.59(14)
B(5)-B(10)-B(9)	107.89(17)
B(12)-B(10)-B(9)	60.01(13)
B(4)-B(10)-B(11)	107.85(17)
B(5)-B(10)-B(11)	59.57(14)
B(12)-B(10)-B(11)	59.95(13)
B(9)-B(10)-B(11)	108.02(16)
B(4)-B(10)-Br(4)	122.17(15)
B(5)-B(10)-Br(4)	122.37(15)
B(12)-B(10)-Br(4)	121.55(15)
B(9)-B(10)-Br(4)	121.45(16)
B(11)-B(10)-Br(4)	121.82(15)
B(6)-B(11)-B(5)	60.54(14)
B(6)-B(11)-B(7)	59.59(13)
B(5)-B(11)-B(7)	107.78(17)
B(6)-B(11)-B(12)	107.41(16)
B(5)-B(11)-B(12)	107.53(17)
B(7)-B(11)-B(12)	59.55(13)
B(6)-B(11)-B(10)	108.19(17)
B(5)-B(11)-B(10)	59.90(14)
B(7)-B(11)-B(10)	107.42(16)
B(12)-B(11)-B(10)	59.72(13)
B(6)-B(11)-Br(5)	121.49(15)
B(5)-B(11)-Br(5)	121.61(15)
B(7)-B(11)-Br(5)	122.13(15)
B(12)-B(11)-Br(5)	122.37(15)
B(10)-B(11)-Br(5)	121.97(15)
B(7)-B(12)-B(10)	108.39(16)
B(7)-B(12)-B(8)	60.41(13)
B(10)-B(12)-B(8)	108.63(16)
B(7)-B(12)-B(11)	60.15(13)
B(10)-B(12)-B(11)	60.34(13)
B(8)-B(12)-B(11)	108.91(16)

B(7)-B(12)-B(9)	108.06(15)
B(10)-B(12)-B(9)	60.29(12)
B(8)-B(12)-B(9)	59.88(13)
B(11)-B(12)-B(9)	108.55(16)
B(7)-B(12)-Br(2)	124.00(14)
B(10)-B(12)-Br(2)	119.43(14)
B(8)-B(12)-Br(2)	121.89(14)
B(11)-B(12)-Br(2)	121.98(15)
B(9)-B(12)-Br(2)	119.71(14)
B(7)-Br(1)-Sn(1)	112.64(7)
C(2)-Sn(1)-C(4)	127.93(9)
C(2)-Sn(1)-C(6D)	108.9(3)
C(4)-Sn(1)-C(6D)	123.2(3)
C(2)-Sn(1)-C(6)	120.13(16)
C(4)-Sn(1)-C(6)	111.74(17)
C(6D)-Sn(1)-C(6)	11.9(3)
C(2)-Sn(1)-Br(1)	88.56(6)
C(4)-Sn(1)-Br(1)	96.93(7)
C(6D)-Sn(1)-Br(1)	84.5(5)
C(6)-Sn(1)-Br(1)	88.97(15)
C(3)-C(2)-Sn(1)	110.54(16)
C(3)-C(2)-H(2A)	109.5
Sn(1)-C(2)-H(2A)	109.5
C(3)-C(2)-H(2B)	109.5
Sn(1)-C(2)-H(2B)	109.5
H(2A)-C(2)-H(2B)	108.1
C(2)-C(3)-H(3A)	109.5
C(2)-C(3)-H(3B)	109.5
H(3A)-C(3)-H(3B)	109.5
C(2)-C(3)-H(3C)	109.5
H(3A)-C(3)-H(3C)	109.5
H(3B)-C(3)-H(3C)	109.5
C(5)-C(4)-Sn(1)	112.28(15)
C(5)-C(4)-H(4A)	109.1

Sn(1)-C(4)-H(4A)	109.1
C(5)-C(4)-H(4B)	109.1
Sn(1)-C(4)-H(4B)	109.1
H(4A)-C(4)-H(4B)	107.9
C(4)-C(5)-H(5A)	109.5
C(4)-C(5)-H(5B)	109.5
H(5A)-C(5)-H(5B)	109.5
C(4)-C(5)-H(5C)	109.5
H(5A)-C(5)-H(5C)	109.5
H(5B)-C(5)-H(5C)	109.5
C(7)-C(6)-Sn(1)	117.1(3)
C(7)-C(6)-H(6A)	108.0
Sn(1)-C(6)-H(6A)	108.0
C(7)-C(6)-H(6B)	108.0
Sn(1)-C(6)-H(6B)	108.0
H(6A)-C(6)-H(6B)	107.3
C(7D)-C(6D)-Sn(1)	111.6(7)
C(7D)-C(6D)-H(6C)	109.3
Sn(1)-C(6D)-H(6C)	109.3
C(7D)-C(6D)-H(6D)	109.3
Sn(1)-C(6D)-H(6D)	109.3
H(6C)-C(6D)-H(6D)	108.0
C(6D)-C(7D)-H(7D)	109.5
C(6D)-C(7D)-H(7E)	109.5
H(7D)-C(7D)-H(7E)	109.5
C(6D)-C(7D)-H(7F)	109.5
H(7D)-C(7D)-H(7F)	109.5
H(7E)-C(7D)-H(7F)	109.5

Symmetry transformations used to generate equivalent atoms:

Appendix B.3 References

1. *APEX 2,* version 2009.5-1, Bruker (2009), Bruker AXS Inc., Madison,

Wisconsin, USA.

2. *SAINT,* version V7.60A, Bruker (2009), Bruker AXS Inc., Madison, Wisconsin, USA.

3. *SADABS,* version 2008/1, Bruker (2008), Bruker AXS Inc., Madison, Wisconsin, USA.

4. *SHELXTL,* version 2008/4, Bruker (2008), Bruker AXS Inc., Madison, Wisconsin, USA.

Appendix C

X-Ray Structure Determination of $[Et_3Pb]^+[CB_{11}H_6Br_6]^-$

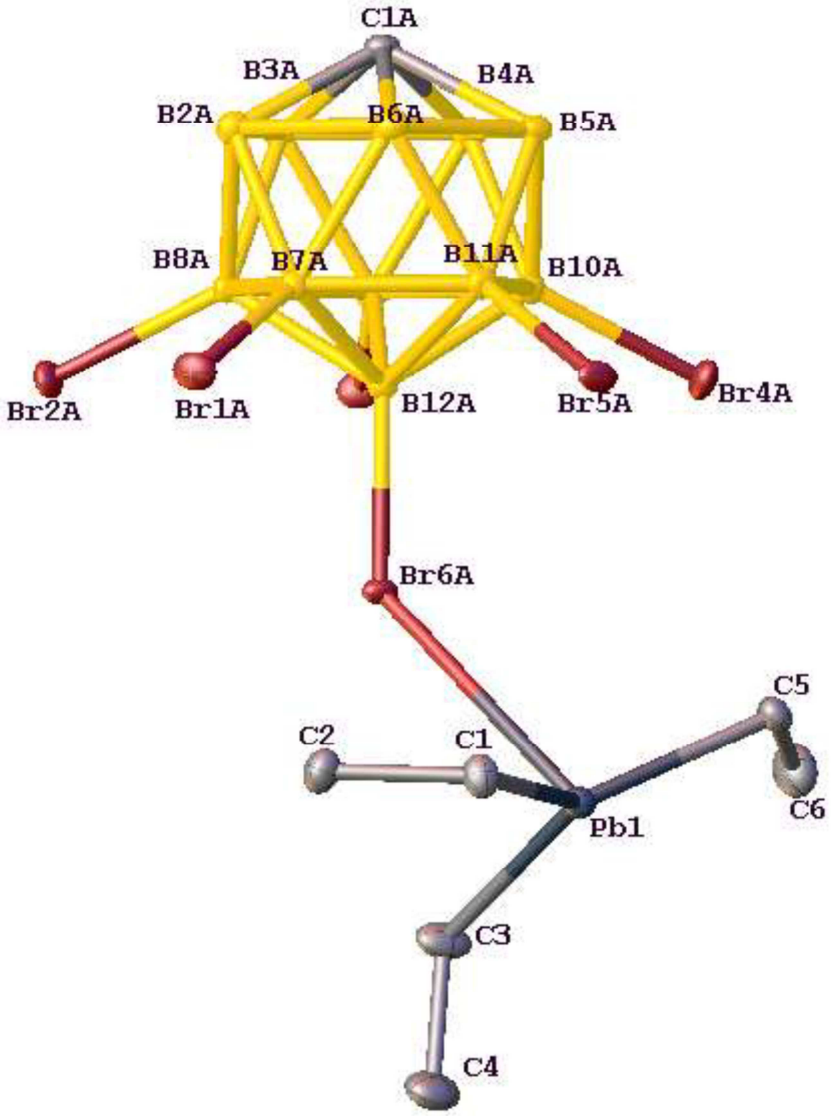

Appendix C.1 Experimental:

A colorless fragment of a prism (0.34 x 0.22 x 0.16 mm^3) was used for the single crystal x-ray diffraction study of $[[C_2H_5]_3Pb]^+[CH_6B_{11}Br_6]^-$ (sample cr369_0m). The crystal was coated with paratone oil and mounted on to a cryo-loop glass fiber. X-ray intensity data were collected at 100(2) K on a Bruker APEX2 (**ref. 1**) platform-CCD x-ray diffractometer system (Mo-radiation, λ = 0.71073 Å,

50KV/30mA power). The CCD detector was placed at a distance of 5.0510 cm from the crystal.

A total of 3000 frames were collected for a sphere of reflections (with scan width of 0.3^o in ω, starting ω and 2θ angles at -30^o, and ϕ angles of 0^o, 90^o, 120^o, 180^o, and 270^o for every 600 frames, 20 sec/frame exposure time). The frames were integrated using the Bruker SAINT software package (**ref. 2**) and using a narrow-frame integration algorithm. Based on an orthorhombic crystal system, the integrated frames yielded a total of 42663 reflections at a maximum 2θ angle of 59.14^o (0.72 Å resolution), of which 6412 were independent reflections (R_{int} = 0.0363, R_{sig} = 0.0222, redundancy = 6.7, completeness = 99.8%) and 6261 (97.6%) reflections were greater than $2\sigma(I)$. The unit cell parameters were, **a** = 12.7512(5) Å, **b** = 13.3623(5) Å, **c** = 13.3961(5) Å, $\alpha = \beta = \gamma = 90^o$, V = 2282.50(15) $Å^3$, Z = 4, calculated density D_c = 2.650 g/cm^3. Absorption corrections were applied (absorption coefficient μ = 17.887 mm^{-1}; max/min transmission = 0.1668/0.0641) to the raw intensity data using the SADABS program (**ref. 3**).

The Bruker SHELXTL software package (**ref. 4**) was used for phase determination and structure refinement. The distribution of intensities (E^2-1 = 0.728) and systematic absent reflections indicated one possible space group, P2(1)2(1)2(1). The space group P2(1)2(1)2(1) (#19) was later determined to be correct. Direct methods of phase determination followed by two Fourier cycles of refinement led to an electron density map from which most of the non-hydrogen atoms were identified in the asymmetry unit of the unit cell. With subsequent isotropic refinement, all of the non-hydrogen atoms were identified. There was one cation of $[[C_2H_5]_3Pb]^+$ and one anion of $[CH_6B_{11}Br_6]^-$ present in the asymmetry unit of the unit cell. The CIF validation report of an Alert level B was a false alarm because the structure could not properly fit on a mirror plane perpendicular to the **b**-axis of the Pnma space group suggested. The final structure was refined as a racemic twin with Flack parameter, x = 0.382(3).

Atomic coordinates, isotropic and anisotropic displacement parameters of all the non-hydrogen atoms were refined by means of a full matrix least-squares procedure on F^2. The H-atoms were included in the refinement in calculated positions riding on the atoms to which they were attached. The refinement converged at R1 = 0.0136, wR2 = 0.0326, with intensity, $I>2\sigma(I)$. The largest peak/hole in the final difference map was 0.730/-0.976 e/$Å^3$.

Appendix C.2: Structure Data

C.2.1 Crystal data and structure refinement for $[Et_3Pb]^+[CB_{11}H_6Br_6]^-$.

Identification code	cr369_0m	
Empirical formula	C7 H21 B11 Br6 Pb	
Formula weight	910.80	
Temperature	100(2) K	
Wavelength	0.71073 Å	
Crystal system	Orthorhombic	
Space group	P2(1)2(1)2(1) (#19)	
Unit cell dimensions	a = 12.7512(5) Å	α= 90°.
	b = 13.3623(5) Å	β= 90°.
	c = 13.3961(5) Å	γ = 90°.
Volume	2282.50(15) $Å^3$	
Z	4	
Density (calculated)	2.650 Mg/m^3	
Absorption coefficient	17.887 mm^{-1}	
F(000)	1640	
Crystal size	0.34 x 0.22 x 0.16 mm^3	
Theta range for data collection	2.15 to 29.57°.	
Index ranges	-17<=h<=17, -18<=k<=18, -18<=l<=18	
Reflections collected	42663	
Independent reflections	6412 [R(int) = 0.0363]	
Completeness to theta = 29.57°	99.8 %	
Absorption correction	Semi-empirical from equivalents	
Max. and min. transmission	0.1668 and 0.0641	
Refinement method	Full-matrix least-squares on F^2	
Data / restraints / parameters	6412 / 0 / 233	
Goodness-of-fit on F^2	1.015	
Final R indices [I>2sigma(I)]	R1 = 0.0136, wR2 = 0.0326	
R indices (all data)	R1 = 0.0145, wR2 = 0.0328	
Absolute structure parameter	0.382(3)	

Largest diff. peak and hole 0.730 and -0.976 e.Å^{-3}

C.2.2. Atomic coordinates (x 10^4) and equivalent isotropic displacement parameters (Å^{2}x 10^3) for $[Et_3Pb]^+[CB_{11}H_6Br_6]^-$. U(eq) is defined as one third of the trace of the orthogonalized U^{ij} tensor.

_	x	y	z	U(eq)
C(1A)	2307(2)	10950(2)	9945(2)	10(1)
B(2A)	2959(2)	11334(2)	8898(2)	11(1)
B(3A)	3106(2)	11969(2)	10066(2)	10(1)
B(4A)	2977(2)	11074(2)	11039(2)	11(1)
B(5A)	2768(2)	9876(2)	10475(2)	11(1)
B(6A)	2750(2)	10037(2)	9151(2)	11(1)
B(7A)	4012(2)	10471(2)	8774(2)	9(1)
B(8A)	4223(2)	11666(2)	9341(2)	9(1)
B(9A)	4237(2)	11500(2)	10665(2)	10(1)
B(10A)	4026(2)	10205(2)	10928(2)	9(1)
B(11A)	3885(2)	9574(2)	9760(2)	10(1)
B(12A)	4800(2)	10569(2)	9874(2)	9(1)
Br(1A)	4605(1)	10135(1)	7480(1)	15(1)
Br(2A)	5055(1)	12700(1)	8682(1)	14(1)
Br(3A)	5108(1)	12344(1)	11520(1)	15(1)
Br(4A)	4633(1)	9553(1)	12092(1)	15(1)
Br(5A)	4384(1)	8189(1)	9573(1)	13(1)
Br(6A)	6325(1)	10370(1)	9841(1)	11(1)
Pb(1)	7621(1)	8360(1)	9972(1)	10(1)
C(1)	7330(2)	7852(2)	8407(2)	15(1)
C(2)	7413(3)	8727(2)	7691(2)	16(1)
C(3)	8840(2)	9573(2)	9992(3)	21(1)
C(4)	9917(2)	9237(2)	9668(3)	26(1)
C(5)	6906(2)	7900(2)	11414(2)	13(1)
C(6)	7416(3)	8465(2)	12265(2)	23(1)

C.2.3 Bond lengths [Å] and angles [°] for $[Et_3Pb]^+[CB_{11}H_6Br_6]^-$.

C(1A)-B(4A)	1.705(4)
C(1A)-B(5A)	1.706(4)
C(1A)-B(3A)	1.708(4)
C(1A)-B(2A)	1.709(4)
C(1A)-B(6A)	1.715(4)
C(1A)-H(1A)	0.97(3)
B(2A)-B(8A)	1.774(4)
B(2A)-B(7A)	1.777(4)
B(2A)-B(6A)	1.786(4)
B(2A)-B(3A)	1.790(4)
B(2A)-H(2A)	1.1200
B(3A)-B(9A)	1.765(4)
B(3A)-B(8A)	1.771(4)
B(3A)-B(4A)	1.777(4)
B(3A)-H(3A)	1.1200
B(4A)-B(9A)	1.776(4)
B(4A)-B(10A)	1.778(4)
B(4A)-B(5A)	1.789(4)
B(4A)-H(4A)	1.1200
B(5A)-B(11A)	1.763(4)
B(5A)-B(10A)	1.770(4)
B(5A)-B(6A)	1.787(4)
B(5A)-H(5A)	1.1200
B(6A)-B(11A)	1.772(4)
B(6A)-B(7A)	1.783(4)
B(6A)-H(6A)	1.1200
B(7A)-B(8A)	1.789(4)
B(7A)-B(12A)	1.789(4)
B(7A)-B(11A)	1.791(4)
B(7A)-Br(1A)	1.943(3)

B(8A)-B(9A)	1.788(4)
B(8A)-B(12A)	1.790(4)
B(8A)-Br(2A)	1.952(3)
B(9A)-B(12A)	1.785(4)
B(9A)-B(10A)	1.787(4)
B(9A)-Br(3A)	1.954(3)
B(10A)-B(11A)	1.787(4)
B(10A)-B(12A)	1.789(4)
B(10A)-Br(4A)	1.947(3)
B(11A)-B(12A)	1.776(4)
B(11A)-Br(5A)	1.973(3)
B(12A)-Br(6A)	1.963(3)
Br(5A)-Pb(1)#1	3.1167(3)
Br(6A)-Pb(1)	3.1582(3)
Pb(1)-C(5)	2.223(3)
Pb(1)-C(1)	2.235(2)
Pb(1)-C(3)	2.245(3)
Pb(1)-Br(5A)#2	3.1167(3)
C(1)-C(2)	1.516(4)
C(1)-H(1B)	0.9900
C(1)-H(1C)	0.9900
C(2)-H(2B)	0.9800
C(2)-H(2C)	0.9800
C(2)-H(2D)	0.9800
C(3)-C(4)	1.509(4)
C(3)-H(3B)	0.9900
C(3)-H(3C)	0.9900
C(4)-H(4B)	0.9800
C(4)-H(4C)	0.9800
C(4)-H(4D)	0.9800
C(5)-C(6)	1.515(4)
C(5)-H(5B)	0.9900
C(5)-H(5C)	0.9900
C(6)-H(6B)	0.9800

C(6)-H(6C)	0.9800
C(6)-H(6D)	0.9800

B(4A)-C(1A)-B(5A)	63.28(17)
B(4A)-C(1A)-B(3A)	62.74(17)
B(5A)-C(1A)-B(3A)	115.2(2)
B(4A)-C(1A)-B(2A)	115.61(19)
B(5A)-C(1A)-B(2A)	115.2(2)
B(3A)-C(1A)-B(2A)	63.16(17)
B(4A)-C(1A)-B(6A)	115.9(2)
B(5A)-C(1A)-B(6A)	62.99(17)
B(3A)-C(1A)-B(6A)	115.5(2)
B(2A)-C(1A)-B(6A)	62.90(17)
B(4A)-C(1A)-H(1A)	115(2)
B(5A)-C(1A)-H(1A)	119.0(19)
B(3A)-C(1A)-H(1A)	114.4(18)
B(2A)-C(1A)-H(1A)	118(2)
B(6A)-C(1A)-H(1A)	120.4(19)
C(1A)-B(2A)-B(8A)	104.05(19)
C(1A)-B(2A)-B(7A)	104.5(2)
B(8A)-B(2A)-B(7A)	60.52(17)
C(1A)-B(2A)-B(6A)	58.70(16)
B(8A)-B(2A)-B(6A)	108.4(2)
B(7A)-B(2A)-B(6A)	60.06(17)
C(1A)-B(2A)-B(3A)	58.40(15)
B(8A)-B(2A)-B(3A)	59.59(16)
B(7A)-B(2A)-B(3A)	108.1(2)
B(6A)-B(2A)-B(3A)	108.1(2)
C(1A)-B(2A)-H(2A)	125.2
B(8A)-B(2A)-H(2A)	122.4
B(7A)-B(2A)-H(2A)	122.2
B(6A)-B(2A)-H(2A)	121.2
B(3A)-B(2A)-H(2A)	121.6
C(1A)-B(3A)-B(9A)	104.33(19)

C(1A)-B(3A)-B(8A)	104.2(2)
B(9A)-B(3A)-B(8A)	60.75(15)
C(1A)-B(3A)-B(4A)	58.53(16)
B(9A)-B(3A)-B(4A)	60.19(17)
B(8A)-B(3A)-B(4A)	108.8(2)
C(1A)-B(3A)-B(2A)	58.44(16)
B(9A)-B(3A)-B(2A)	108.3(2)
B(8A)-B(3A)-B(2A)	59.75(17)
B(4A)-B(3A)-B(2A)	108.2(2)
C(1A)-B(3A)-H(3A)	125.4
B(9A)-B(3A)-H(3A)	122.1
B(8A)-B(3A)-H(3A)	122.1
B(4A)-B(3A)-H(3A)	121.1
B(2A)-B(3A)-H(3A)	121.5
C(1A)-B(4A)-B(9A)	104.0(2)
C(1A)-B(4A)-B(3A)	58.72(16)
B(9A)-B(4A)-B(3A)	59.57(16)
C(1A)-B(4A)-B(10A)	104.0(2)
B(9A)-B(4A)-B(10A)	60.36(17)
B(3A)-B(4A)-B(10A)	108.0(2)
C(1A)-B(4A)-B(5A)	58.39(16)
B(9A)-B(4A)-B(5A)	107.6(2)
B(3A)-B(4A)-B(5A)	107.8(2)
B(10A)-B(4A)-B(5A)	59.50(17)
C(1A)-B(4A)-H(4A)	125.3
B(9A)-B(4A)-H(4A)	122.6
B(3A)-B(4A)-H(4A)	121.5
B(10A)-B(4A)-H(4A)	122.5
B(5A)-B(4A)-H(4A)	121.8
C(1A)-B(5A)-B(11A)	104.2(2)
C(1A)-B(5A)-B(10A)	104.3(2)
B(11A)-B(5A)-B(10A)	60.76(16)
C(1A)-B(5A)-B(6A)	58.73(16)
B(11A)-B(5A)-B(6A)	59.88(16)

B(10A)-B(5A)-B(6A)	108.8(2)
C(1A)-B(5A)-B(4A)	58.33(16)
B(11A)-B(5A)-B(4A)	108.3(2)
B(10A)-B(5A)-B(4A)	59.92(17)
B(6A)-B(5A)-B(4A)	108.3(2)
C(1A)-B(5A)-H(5A)	125.4
B(11A)-B(5A)-H(5A)	122.3
B(10A)-B(5A)-H(5A)	122.0
B(6A)-B(5A)-H(5A)	121.1
B(4A)-B(5A)-H(5A)	121.4
C(1A)-B(6A)-B(11A)	103.43(19)
C(1A)-B(6A)-B(7A)	103.96(19)
B(11A)-B(6A)-B(7A)	60.51(16)
C(1A)-B(6A)-B(2A)	58.40(16)
B(11A)-B(6A)-B(2A)	107.7(2)
B(7A)-B(6A)-B(2A)	59.70(17)
C(1A)-B(6A)-B(5A)	58.27(16)
B(11A)-B(6A)-B(5A)	59.39(16)
B(7A)-B(6A)-B(5A)	108.0(2)
B(2A)-B(6A)-B(5A)	107.6(2)
C(1A)-B(6A)-H(6A)	125.6
B(11A)-B(6A)-H(6A)	122.8
B(7A)-B(6A)-H(6A)	122.3
B(2A)-B(6A)-H(6A)	121.7
B(5A)-B(6A)-H(6A)	121.7
B(2A)-B(7A)-B(6A)	60.24(17)
B(2A)-B(7A)-B(8A)	59.65(17)
B(6A)-B(7A)-B(8A)	107.8(2)
B(2A)-B(7A)-B(12A)	107.4(2)
B(6A)-B(7A)-B(12A)	107.26(19)
B(8A)-B(7A)-B(12A)	60.03(15)
B(2A)-B(7A)-B(11A)	107.3(2)
B(6A)-B(7A)-B(11A)	59.43(16)
B(8A)-B(7A)-B(11A)	107.35(19)

B(12A)-B(7A)-B(11A)	59.46(15)
B(2A)-B(7A)-Br(1A)	121.84(18)
B(6A)-B(7A)-Br(1A)	121.91(18)
B(8A)-B(7A)-Br(1A)	121.76(18)
B(12A)-B(7A)-Br(1A)	122.21(18)
B(11A)-B(7A)-Br(1A)	122.53(18)
B(3A)-B(8A)-B(2A)	60.66(16)
B(3A)-B(8A)-B(9A)	59.48(17)
B(2A)-B(8A)-B(9A)	108.0(2)
B(3A)-B(8A)-B(7A)	108.4(2)
B(2A)-B(8A)-B(7A)	59.83(16)
B(9A)-B(8A)-B(7A)	108.2(2)
B(3A)-B(8A)-B(12A)	107.38(19)
B(2A)-B(8A)-B(12A)	107.6(2)
B(9A)-B(8A)-B(12A)	59.87(16)
B(7A)-B(8A)-B(12A)	59.99(16)
B(3A)-B(8A)-Br(2A)	121.58(19)
B(2A)-B(8A)-Br(2A)	121.30(18)
B(9A)-B(8A)-Br(2A)	122.08(19)
B(7A)-B(8A)-Br(2A)	121.41(17)
B(12A)-B(8A)-Br(2A)	122.47(18)
B(3A)-B(9A)-B(4A)	60.23(17)
B(3A)-B(9A)-B(12A)	107.82(19)
B(4A)-B(9A)-B(12A)	107.9(2)
B(3A)-B(9A)-B(10A)	108.1(2)
B(4A)-B(9A)-B(10A)	59.86(17)
B(12A)-B(9A)-B(10A)	60.10(16)
B(3A)-B(9A)-B(8A)	59.78(17)
B(4A)-B(9A)-B(8A)	108.1(2)
B(12A)-B(9A)-B(8A)	60.13(16)
B(10A)-B(9A)-B(8A)	108.3(2)
B(3A)-B(9A)-Br(3A)	121.76(18)
B(4A)-B(9A)-Br(3A)	122.29(18)
B(12A)-B(9A)-Br(3A)	121.42(19)

B(10A)-B(9A)-Br(3A)	121.95(18)
B(8A)-B(9A)-Br(3A)	121.0(2)
B(5A)-B(10A)-B(4A)	60.58(17)
B(5A)-B(10A)-B(9A)	108.0(2)
B(4A)-B(10A)-B(9A)	59.78(17)
B(5A)-B(10A)-B(11A)	59.42(16)
B(4A)-B(10A)-B(11A)	107.8(2)
B(9A)-B(10A)-B(11A)	107.46(19)
B(5A)-B(10A)-B(12A)	107.3(2)
B(4A)-B(10A)-B(12A)	107.7(2)
B(9A)-B(10A)-B(12A)	59.91(16)
B(11A)-B(10A)-B(12A)	59.55(16)
B(5A)-B(10A)-Br(4A)	121.55(19)
B(4A)-B(10A)-Br(4A)	121.61(18)
B(9A)-B(10A)-Br(4A)	122.13(18)
B(11A)-B(10A)-Br(4A)	122.05(18)
B(12A)-B(10A)-Br(4A)	122.32(19)
B(5A)-B(11A)-B(6A)	60.74(17)
B(5A)-B(11A)-B(12A)	108.2(2)
B(6A)-B(11A)-B(12A)	108.4(2)
B(5A)-B(11A)-B(10A)	59.82(16)
B(6A)-B(11A)-B(10A)	108.7(2)
B(12A)-B(11A)-B(10A)	60.28(16)
B(5A)-B(11A)-B(7A)	108.7(2)
B(6A)-B(11A)-B(7A)	60.06(16)
B(12A)-B(11A)-B(7A)	60.21(16)
B(10A)-B(11A)-B(7A)	108.7(2)
B(5A)-B(11A)-Br(5A)	122.99(18)
B(6A)-B(11A)-Br(5A)	122.18(18)
B(12A)-B(11A)-Br(5A)	120.07(18)
B(10A)-B(11A)-Br(5A)	121.40(18)
B(7A)-B(11A)-Br(5A)	120.35(17)
B(11A)-B(12A)-B(9A)	108.0(2)
B(11A)-B(12A)-B(10A)	60.18(16)

B(9A)-B(12A)-B(10A)	59.99(16)
B(11A)-B(12A)-B(7A)	60.33(16)
B(9A)-B(12A)-B(7A)	108.3(2)
B(10A)-B(12A)-B(7A)	108.71(19)
B(11A)-B(12A)-B(8A)	108.00(19)
B(9A)-B(12A)-B(8A)	60.01(15)
B(10A)-B(12A)-B(8A)	108.13(19)
B(7A)-B(12A)-B(8A)	59.98(16)
B(11A)-B(12A)-Br(6A)	123.22(17)
B(9A)-B(12A)-Br(6A)	120.41(18)
B(10A)-B(12A)-Br(6A)	121.83(18)
B(7A)-B(12A)-Br(6A)	121.85(18)
B(8A)-B(12A)-Br(6A)	120.57(17)
B(11A)-Br(5A)-Pb(1)#1	111.43(9)
B(12A)-Br(6A)-Pb(1)	129.19(8)
C(5)-Pb(1)-C(1)	131.52(11)
C(5)-Pb(1)-C(3)	118.25(12)
C(1)-Pb(1)-C(3)	110.22(12)
C(5)-Pb(1)-Br(5A)#2	86.67(8)
C(1)-Pb(1)-Br(5A)#2	95.81(8)
C(3)-Pb(1)-Br(5A)#2	88.72(8)
C(5)-Pb(1)-Br(6A)	93.97(7)
C(1)-Pb(1)-Br(6A)	96.87(7)
C(3)-Pb(1)-Br(6A)	75.48(7)
Br(5A)#2-Pb(1)-Br(6A)	162.417(7)
C(2)-C(1)-Pb(1)	110.35(17)
C(2)-C(1)-H(1B)	109.6
Pb(1)-C(1)-H(1B)	109.6
C(2)-C(1)-H(1C)	109.6
Pb(1)-C(1)-H(1C)	109.6
H(1B)-C(1)-H(1C)	108.1
C(1)-C(2)-H(2B)	109.5
C(1)-C(2)-H(2C)	109.5
H(2B)-C(2)-H(2C)	109.5

C(1)-C(2)-H(2D)	109.5
H(2B)-C(2)-H(2D)	109.5
H(2C)-C(2)-H(2D)	109.5
C(4)-C(3)-Pb(1)	114.35(19)
C(4)-C(3)-H(3B)	108.7
Pb(1)-C(3)-H(3B)	108.7
C(4)-C(3)-H(3C)	108.7
Pb(1)-C(3)-H(3C)	108.7
H(3B)-C(3)-H(3C)	107.6
C(3)-C(4)-H(4B)	109.5
C(3)-C(4)-H(4C)	109.5
H(4B)-C(4)-H(4C)	109.5
C(3)-C(4)-H(4D)	109.5
H(4B)-C(4)-H(4D)	109.5
H(4C)-C(4)-H(4D)	109.5
C(6)-C(5)-Pb(1)	109.85(18)
C(6)-C(5)-H(5B)	109.7
Pb(1)-C(5)-H(5B)	109.7
C(6)-C(5)-H(5C)	109.7
Pb(1)-C(5)-H(5C)	109.7
H(5B)-C(5)-H(5C)	108.2
C(5)-C(6)-H(6B)	109.5
C(5)-C(6)-H(6C)	109.5
H(6B)-C(6)-H(6C)	109.5
C(5)-C(6)-H(6D)	109.5
H(6B)-C(6)-H(6D)	109.5
H(6C)-C(6)-H(6D)	109.5

Symmetry transformations used to generate equivalent atoms:

#1 x-1/2,-y+3/2,-z+2 #2 x+1/2,-y+3/2,-z+2

Appendix C.3 References

1. *APEX 2,* version 2009.5-1, Bruker (2009), Bruker AXS Inc., Madison, Wisconsin, USA.

2. *SAINT,* version V7.60A, Bruker (2009), Bruker AXS Inc., Madison, Wisconsin, USA.

3. *SADABS,* version 2008/1, Bruker (2008), Bruker AXS Inc., Madison, Wisconsin, USA.

4. *SHELXTL,* version 2008/4, Bruker (2008), Bruker AXS Inc., Madison, Wisconsin, USA.

Appendix D

X-Ray Structure Determination of $[Et_3Sn]^+[CHB_{11}Cl_{11}]^-$

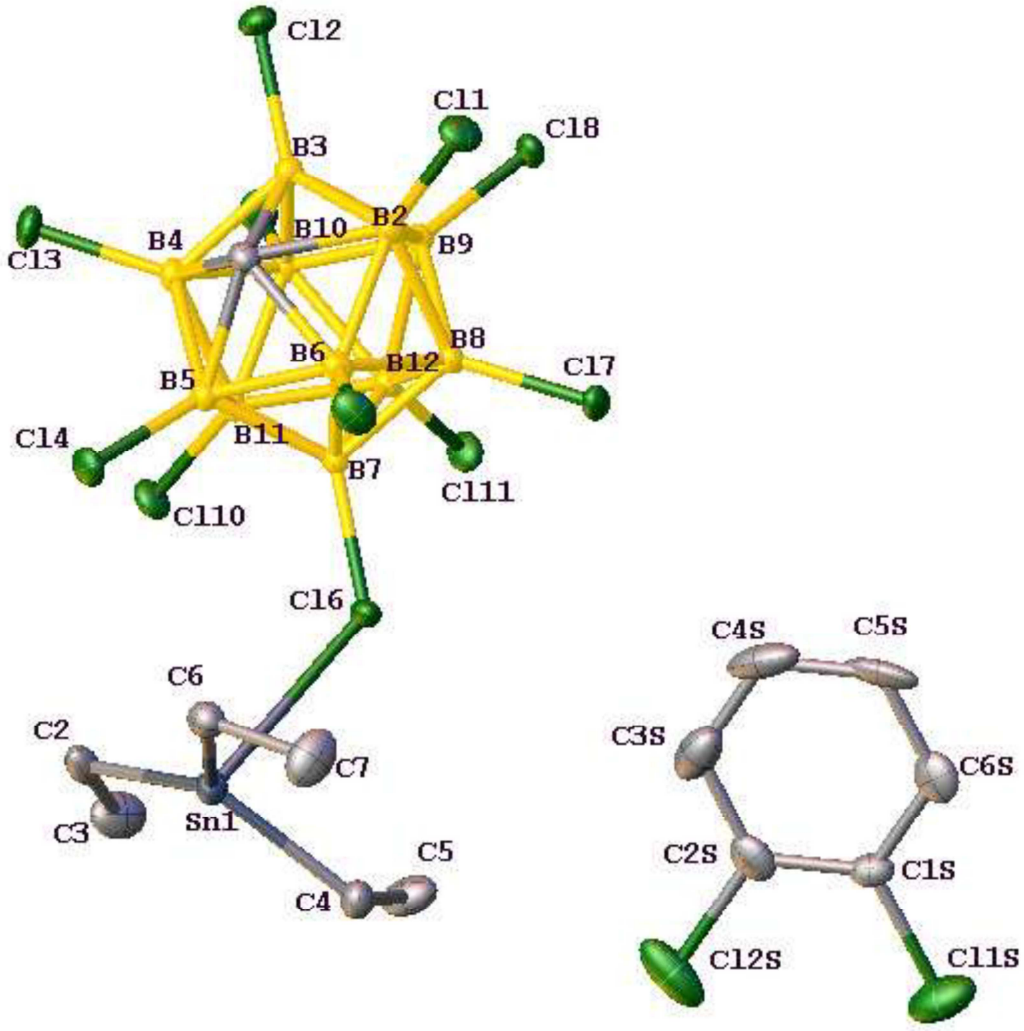

Appendix D.1 Experimental:

A colorless prism fragment (0.45 x 0.25 x 0.23 mm^3) was used for the single crystal x-ray diffraction study of $[[C_2H_5]_3Sn]^+[CHB_{11}Cl_{11}]^-.C_6H_4Cl_2$ (sample cr359r_0m). The crystal was coated with paratone oil and mounted on to a cryo-loop glass fiber. X-ray intensity data were collected at 100(2) K on a Bruker APEX2 (**ref. 1**) platform-CCD x-ray diffractometer system (Mo-radiation, λ = 0.71073 Å, 50KV/40mA power). The CCD detector was placed at a distance of 5.0450 cm from the crystal.

A total of 2400 frames were collected for a hemisphere of reflections (with scan width of 0.3^{o} in ω, starting ω and 2θ angles at –30^{o}, and ϕ angles of 0^{o}, 90^{o}, 180^{o}, and 270^{o} for every 600 frames, 20 sec/frame exposure time). The frames were integrated using the Bruker SAINT software package (**ref. 2**) and using a narrow-frame integration algorithm. Based on a monoclinic crystal system, the integrated frames yielded a total of 43590 reflections at a maximum 2θ angle of 59.14^{o} (0.72 Å resolution), of which 8282 were independent reflections (R_{int} = 0.0265, R_{sig} = 0.0193, redundancy = 5.3, completeness = 99.9%) and 7322 (88.4%) reflections were greater than 2σ(I). The unit cell parameters were, **a** = 10.4002(12) Å, **b** = 18.4874(20) Å, **c** = 15.3879(17) Å, **β** = 94.2242(16)^{o}**,** V = 2950.6(6) Å^{3}, Z = 4, calculated density D_c = 1.804 g/cm^{3}. Absorption corrections were applied (absorption coefficient μ = 1.958 mm^{-1}; max/min transmission = 0.6594/0.4741) to the raw intensity data using the SADABS program (**ref. 3**).

The Bruker SHELXTL software package (**ref. 4**) was used for phase determination and structure refinement. The distribution of intensities (E^2-1 = 0.942) and systematic absent reflections indicated one possible space group, P2(1)/n. The space group P2(1)/n (#14) was later determined to be correct. Direct methods of phase determination followed by two Fourier cycles of refinement led to an electron density map from which most of the non-hydrogen atoms were identified in the asymmetry unit of the unit cell. With subsequent isotropic refinement, all of the non-hydrogen atoms were identified. There were one cation of $[[C_2H_5]_3Sn]^+$, one anion of $[CHB_{11}Cl_{11}]^-$, and one disordered ODCB solvent molecule present in the asymmetry unit of the unit cell. The DELU, SIMU, and SADI restraints were used to stabilize the refinement of the disordered solvent molecule (disordered site occupancy factor ratio was 50%/50%) located on an inversion center.

Atomic coordinates, isotropic and anisotropic displacement parameters of all the non-hydrogen atoms were refined by means of a full matrix least-squares procedure on F^2. The H-atoms were included in the refinement in calculated positions riding on the atoms to which they were attached. The refinement converged at R1 = 0.0190, wR2 = 0.0438, with intensity I>2σ (I). The largest peak/hole in the final difference map was 0.525/-0.314 e/Å^{3}.

Appendix D.2: Structure Data

D.2.1 Crystal data and structure refinement for $[Et_3Sn]^+[CHB_{11}Cl_{11}]^-$.

Identification code	cr359r_0m	
Empirical formula	C10 H18 B11 Cl12 Sn	
Formula weight	801.24	
Temperature	100(2) K	
Wavelength	0.71073 Å	
Crystal system	Monoclinic	
Space group	P2(1)/n (#14)	
Unit cell dimensions	a = 10.4002(12) Å	α= 90°.
	b = 18.487(2) Å	β= 94.2242(16)°.
	c = 15.3879(17) Å	γ = 90°.
Volume	2950.6(6) $Å^3$	
Z	4	
Density (calculated)	1.804 Mg/m^3	
Absorption coefficient	1.958 mm^{-1}	
F(000)	1548	
Crystal size	0.45 x 0.25 x 0.23 mm^3	
Theta range for data collection	1.72 to 29.57°.	
Index ranges	-14<=h<=14, -25<=k<=25, -21<=l<=21	
Reflections collected	43590	
Independent reflections	8282 [R(int) = 0.0265]	
Completeness to theta = 29.57°	99.9 %	
Absorption correction	Semi-empirical from equivalents	
Max. and min. transmission	0.6594 and 0.4741	
Refinement method	Full-matrix least-squares on F^2	
Data / restraints / parameters	8282 / 95 / 340	
Goodness-of-fit on F^2	1.041	
Final R indices [I>2sigma(I)]	R1 = 0.0190, wR2 = 0.0438	
R indices (all data)	R1 = 0.0241, wR2 = 0.0457	
Largest diff. peak and hole	0.525 and -0.314 e.$Å^{-3}$	

D.2.2. Atomic coordinates (x 10^4) and equivalent isotropic displacement parameters (Å^{2}x 10^3) for $[Et_3Sn]^+[CHB_{11}Cl_{11}]^-$. U(eq) is defined as one third of the trace of the orthogonalized U^{ij} tensor.

	x	y	z	U(eq)
C(1)	7136(1)	4299(1)	3359(1)	14(1)
B(2)	8071(1)	3991(1)	2565(1)	15(1)
B(3)	7059(1)	4772(1)	2395(1)	14(1)
B(4)	5657(1)	4645(1)	2989(1)	14(1)
B(5)	5803(1)	3788(1)	3524(1)	14(1)
B(6)	7295(1)	3382(1)	3265(1)	15(1)
B(7)	5819(1)	3109(1)	2715(1)	13(1)
B(8)	7220(1)	3223(1)	2119(1)	14(1)
B(9)	7062(1)	4086(1)	1590(1)	13(1)
B(10)	5568(1)	4496(1)	1844(1)	13(1)
B(11)	4792(1)	3883(1)	2544(1)	13(1)
B(12)	5666(1)	3537(1)	1670(1)	13(1)
Cl(1)	9763(1)	4088(1)	2657(1)	22(1)
Cl(2)	7742(1)	5640(1)	2326(1)	22(1)
Cl(3)	4980(1)	5384(1)	3515(1)	22(1)
Cl(4)	5250(1)	3679(1)	4575(1)	20(1)
Cl(5)	8187(1)	2864(1)	4060(1)	24(1)
Cl(6)	5194(1)	2211(1)	2851(1)	19(1)
Cl(7)	8030(1)	2480(1)	1671(1)	21(1)
Cl(8)	7716(1)	4283(1)	565(1)	18(1)
Cl(9)	4689(1)	5082(1)	1111(1)	22(1)
Cl(10)	3091(1)	3815(1)	2544(1)	20(1)
Cl(11)	4868(1)	3112(1)	748(1)	22(1)
Sn(1)	3931(1)	1680(1)	4314(1)	17(1)
C(2)	2360(2)	2419(1)	4166(1)	24(1)
C(3)	1393(2)	2239(1)	3401(1)	37(1)
C(4)	3840(2)	699(1)	3566(1)	21(1)
C(5)	3271(2)	742(1)	2634(1)	32(1)

C(6)	5581(1)	1767(1)	5219(1)	21(1)
C(7)	6467(2)	1120(1)	5161(1)	36(1)
C(1S)	5220(2)	-434(1)	-266(1)	19(1)
C(2S)	4482(2)	40(1)	191(1)	25(1)
C(3S)	4985(2)	707(1)	459(1)	38(1)
C(4S)	6215(4)	894(2)	268(2)	44(1)
C(5S)	6957(5)	422(3)	-179(4)	40(2)
C(6S)	6465(3)	-240(2)	-454(2)	27(1)
Cl(1S)	4613(1)	-1259(1)	-618(1)	45(1)
Cl(2S)	2946(1)	-196(1)	434(1)	50(1)

D.2.3 Bond lengths [Å] and angles [°] for $[Et_3Sn]^+[CHB_{11}Cl_{11}]^-$.

C(1)-B(6)	1.711(2)
C(1)-B(5)	1.712(2)
C(1)-B(2)	1.714(2)
C(1)-B(3)	1.718(2)
C(1)-B(4)	1.723(2)
C(1)-H(1)	0.950(9)
B(2)-Cl(1)	1.7638(15)
B(2)-B(9)	1.776(2)
B(2)-B(8)	1.783(2)
B(2)-B(6)	1.791(2)
B(2)-B(3)	1.795(2)
B(3)-Cl(2)	1.7619(15)
B(3)-B(9)	1.774(2)
B(3)-B(10)	1.786(2)
B(3)-B(4)	1.792(2)
B(4)-Cl(3)	1.7609(15)
B(4)-B(10)	1.779(2)
B(4)-B(11)	1.782(2)
B(4)-B(5)	1.787(2)
B(5)-B(7)	1.768(2)

B(5)-Cl(4)	1.7685(15)
B(5)-B(11)	1.782(2)
B(5)-B(6)	1.795(2)
B(6)-Cl(5)	1.7628(16)
B(6)-B(7)	1.771(2)
B(6)-B(8)	1.784(2)
B(7)-B(12)	1.788(2)
B(7)-B(8)	1.790(2)
B(7)-B(11)	1.792(2)
B(7)-Cl(6)	1.8020(15)
B(8)-Cl(7)	1.7779(15)
B(8)-B(9)	1.793(2)
B(8)-B(12)	1.805(2)
B(9)-B(12)	1.783(2)
B(9)-B(10)	1.798(2)
B(9)-Cl(8)	1.7990(15)
B(10)-Cl(9)	1.7686(15)
B(10)-B(11)	1.795(2)
B(10)-B(12)	1.796(2)
B(11)-Cl(10)	1.7735(15)
B(11)-B(12)	1.794(2)
B(12)-Cl(11)	1.7751(15)
Cl(6)-Sn(1)	2.8623(4)
Sn(1)-C(2)	2.1294(15)
Sn(1)-C(6)	2.1356(15)
Sn(1)-C(4)	2.1455(15)
C(2)-C(3)	1.527(3)
C(2)-H(2A)	0.9900
C(2)-H(2B)	0.9900
C(3)-H(3A)	0.9800
C(3)-H(3B)	0.9800
C(3)-H(3C)	0.9800
C(4)-C(5)	1.513(2)
C(4)-H(4A)	0.9900

C(4)-H(4B)	0.9900
C(5)-H(5A)	0.9800
C(5)-H(5B)	0.9800
C(5)-H(5C)	0.9800
C(6)-C(7)	1.515(2)
C(6)-H(6A)	0.9900
C(6)-H(6B)	0.9900
C(7)-H(7A)	0.9800
C(7)-H(7B)	0.9800
C(7)-H(7C)	0.9800
C(1S)-C(2S)	1.3900
C(1S)-C(6S)	1.394(4)
C(1S)-Cl(1S)	1.7217(17)
C(2S)-C(3S)	1.3900
C(2S)-Cl(2S)	1.723(2)
C(3S)-C(4S)	1.377(4)
C(3S)-H(3D)	0.9500
C(4S)-C(5S)	1.381(5)
C(4S)-H(4C)	0.9500
C(5S)-C(6S)	1.381(5)
C(5S)-H(5D)	0.9500
C(6S)-H(6C)	0.9500

B(6)-C(1)-B(5)	63.26(9)
B(6)-C(1)-B(2)	63.07(9)
B(5)-C(1)-B(2)	115.51(10)
B(6)-C(1)-B(3)	115.52(10)
B(5)-C(1)-B(3)	114.96(10)
B(2)-C(1)-B(3)	63.08(9)
B(6)-C(1)-B(4)	115.48(10)
B(5)-C(1)-B(4)	62.70(9)
B(2)-C(1)-B(4)	115.33(10)
B(3)-C(1)-B(4)	62.75(9)
B(6)-C(1)-H(1)	117.7(4)

B(5)-C(1)-H(1)	117.2(4)
B(2)-C(1)-H(1)	117.8(4)
B(3)-C(1)-H(1)	117.2(4)
B(4)-C(1)-H(1)	116.7(4)
C(1)-B(2)-Cl(1)	121.64(10)
C(1)-B(2)-B(9)	103.80(10)
Cl(1)-B(2)-B(9)	125.53(10)
C(1)-B(2)-B(8)	104.29(10)
Cl(1)-B(2)-B(8)	125.17(10)
B(9)-B(2)-B(8)	60.48(8)
C(1)-B(2)-B(6)	58.39(8)
Cl(1)-B(2)-B(6)	120.47(10)
B(9)-B(2)-B(6)	107.84(10)
B(8)-B(2)-B(6)	59.88(8)
C(1)-B(2)-B(3)	58.59(8)
Cl(1)-B(2)-B(3)	120.04(10)
B(9)-B(2)-B(3)	59.57(8)
B(8)-B(2)-B(3)	108.34(10)
B(6)-B(2)-B(3)	107.95(10)
C(1)-B(3)-Cl(2)	121.53(10)
C(1)-B(3)-B(9)	103.68(10)
Cl(2)-B(3)-B(9)	125.96(10)
C(1)-B(3)-B(10)	104.35(10)
Cl(2)-B(3)-B(10)	124.86(10)
B(9)-B(3)-B(10)	60.67(8)
C(1)-B(3)-B(4)	58.76(8)
Cl(2)-B(3)-B(4)	119.83(10)
B(9)-B(3)-B(4)	107.85(10)
B(10)-B(3)-B(4)	59.63(8)
C(1)-B(3)-B(2)	58.33(8)
Cl(2)-B(3)-B(2)	120.45(10)
B(9)-B(3)-B(2)	59.68(8)
B(10)-B(3)-B(2)	108.57(10)
B(4)-B(3)-B(2)	108.10(10)

C(1)-B(4)-Cl(3)	120.91(10)
C(1)-B(4)-B(10)	104.45(10)
Cl(3)-B(4)-B(10)	125.62(10)
C(1)-B(4)-B(11)	104.25(10)
Cl(3)-B(4)-B(11)	125.64(10)
B(10)-B(4)-B(11)	60.55(8)
C(1)-B(4)-B(5)	58.34(8)
Cl(3)-B(4)-B(5)	119.96(10)
B(10)-B(4)-B(5)	108.34(10)
B(11)-B(4)-B(5)	59.92(8)
C(1)-B(4)-B(3)	58.50(8)
Cl(3)-B(4)-B(3)	120.05(10)
B(10)-B(4)-B(3)	60.02(8)
B(11)-B(4)-B(3)	108.31(10)
B(5)-B(4)-B(3)	107.84(10)
C(1)-B(5)-B(7)	103.76(10)
C(1)-B(5)-Cl(4)	121.31(10)
B(7)-B(5)-Cl(4)	125.73(10)
C(1)-B(5)-B(11)	104.73(10)
B(7)-B(5)-B(11)	60.63(8)
Cl(4)-B(5)-B(11)	125.04(10)
C(1)-B(5)-B(4)	58.97(8)
B(7)-B(5)-B(4)	108.08(10)
Cl(4)-B(5)-B(4)	119.98(10)
B(11)-B(5)-B(4)	59.92(8)
C(1)-B(5)-B(6)	58.35(8)
B(7)-B(5)-B(6)	59.62(8)
Cl(4)-B(5)-B(6)	119.99(10)
B(11)-B(5)-B(6)	108.63(10)
B(4)-B(5)-B(6)	108.34(10)
C(1)-B(6)-Cl(5)	121.95(10)
C(1)-B(6)-B(7)	103.65(10)
Cl(5)-B(6)-B(7)	124.81(10)
C(1)-B(6)-B(8)	104.38(10)

Cl(5)-B(6)-B(8)	125.44(10)
B(7)-B(6)-B(8)	60.48(8)
C(1)-B(6)-B(2)	58.54(8)
Cl(5)-B(6)-B(2)	121.44(10)
B(7)-B(6)-B(2)	107.73(10)
B(8)-B(6)-B(2)	59.85(9)
C(1)-B(6)-B(5)	58.39(8)
Cl(5)-B(6)-B(5)	119.53(10)
B(7)-B(6)-B(5)	59.44(8)
B(8)-B(6)-B(5)	108.17(10)
B(2)-B(6)-B(5)	107.77(10)
B(5)-B(7)-B(6)	60.95(8)
B(5)-B(7)-B(12)	108.29(10)
B(6)-B(7)-B(12)	108.68(10)
B(5)-B(7)-B(8)	109.09(10)
B(6)-B(7)-B(8)	60.12(8)
B(12)-B(7)-B(8)	60.60(8)
B(5)-B(7)-B(11)	60.08(8)
B(6)-B(7)-B(11)	109.26(10)
B(12)-B(7)-B(11)	60.15(8)
B(8)-B(7)-B(11)	109.22(10)
B(5)-B(7)-Cl(6)	123.40(10)
B(6)-B(7)-Cl(6)	120.93(10)
B(12)-B(7)-Cl(6)	120.24(10)
B(8)-B(7)-Cl(6)	118.83(9)
B(11)-B(7)-Cl(6)	122.45(9)
Cl(7)-B(8)-B(2)	121.91(10)
Cl(7)-B(8)-B(6)	121.49(10)
B(2)-B(8)-B(6)	60.28(9)
Cl(7)-B(8)-B(7)	122.29(10)
B(2)-B(8)-B(7)	107.23(10)
B(6)-B(8)-B(7)	59.41(8)
Cl(7)-B(8)-B(9)	122.82(10)
B(2)-B(8)-B(9)	59.55(8)

B(6)-B(8)-B(9)	107.42(10)
B(7)-B(8)-B(9)	106.69(10)
Cl(7)-B(8)-B(12)	122.47(10)
B(2)-B(8)-B(12)	107.25(10)
B(6)-B(8)-B(12)	107.36(10)
B(7)-B(8)-B(12)	59.64(8)
B(9)-B(8)-B(12)	59.41(8)
B(3)-B(9)-B(2)	60.75(9)
B(3)-B(9)-B(12)	108.32(10)
B(2)-B(9)-B(12)	108.55(10)
B(3)-B(9)-B(8)	108.86(10)
B(2)-B(9)-B(8)	59.96(8)
B(12)-B(9)-B(8)	60.65(8)
B(3)-B(9)-B(10)	59.99(8)
B(2)-B(9)-B(10)	108.88(10)
B(12)-B(9)-B(10)	60.21(8)
B(8)-B(9)-B(10)	109.10(10)
B(3)-B(9)-Cl(8)	119.20(10)
B(2)-B(9)-Cl(8)	121.52(10)
B(12)-B(9)-Cl(8)	122.59(10)
B(8)-B(9)-Cl(8)	123.40(10)
B(10)-B(9)-Cl(8)	119.62(10)
Cl(9)-B(10)-B(4)	121.56(10)
Cl(9)-B(10)-B(3)	121.17(10)
B(4)-B(10)-B(3)	60.35(8)
Cl(9)-B(10)-B(11)	122.32(10)
B(4)-B(10)-B(11)	59.82(8)
B(3)-B(10)-B(11)	107.99(10)
Cl(9)-B(10)-B(12)	122.77(10)
B(4)-B(10)-B(12)	107.53(10)
B(3)-B(10)-B(12)	107.23(10)
B(11)-B(10)-B(12)	59.94(8)
Cl(9)-B(10)-B(9)	122.24(10)
B(4)-B(10)-B(9)	107.37(10)

B(3)-B(10)-B(9)	59.35(8)
B(11)-B(10)-B(9)	107.37(10)
B(12)-B(10)-B(9)	59.49(8)
Cl(10)-B(11)-B(4)	122.08(10)
Cl(10)-B(11)-B(5)	121.28(9)
B(4)-B(11)-B(5)	60.17(8)
Cl(10)-B(11)-B(7)	121.82(10)
B(4)-B(11)-B(7)	107.21(10)
B(5)-B(11)-B(7)	59.29(8)
Cl(10)-B(11)-B(12)	122.39(10)
B(4)-B(11)-B(12)	107.46(10)
B(5)-B(11)-B(12)	107.39(10)
B(7)-B(11)-B(12)	59.82(8)
Cl(10)-B(11)-B(10)	122.50(10)
B(4)-B(11)-B(10)	59.63(8)
B(5)-B(11)-B(10)	107.81(10)
B(7)-B(11)-B(10)	107.61(10)
B(12)-B(11)-B(10)	60.05(8)
Cl(11)-B(12)-B(9)	122.12(10)
Cl(11)-B(12)-B(7)	121.88(10)
B(9)-B(12)-B(7)	107.20(10)
Cl(11)-B(12)-B(11)	121.58(9)
B(9)-B(12)-B(11)	108.07(10)
B(7)-B(12)-B(11)	60.03(8)
Cl(11)-B(12)-B(10)	121.88(10)
B(9)-B(12)-B(10)	60.30(8)
B(7)-B(12)-B(10)	107.75(10)
B(11)-B(12)-B(10)	60.01(8)
Cl(11)-B(12)-B(8)	121.07(10)
B(9)-B(12)-B(8)	59.94(8)
B(7)-B(12)-B(8)	59.76(8)
B(11)-B(12)-B(8)	108.45(10)
B(10)-B(12)-B(8)	108.62(10)
B(7)-Cl(6)-Sn(1)	126.73(5)

C(2)-Sn(1)-C(6)	126.52(6)
C(2)-Sn(1)-C(4)	118.79(6)
C(6)-Sn(1)-C(4)	114.53(6)
C(2)-Sn(1)-Cl(6)	95.07(4)
C(6)-Sn(1)-Cl(6)	95.38(4)
C(4)-Sn(1)-Cl(6)	82.67(4)
C(3)-C(2)-Sn(1)	113.57(11)
C(3)-C(2)-H(2A)	108.9
Sn(1)-C(2)-H(2A)	108.9
C(3)-C(2)-H(2B)	108.9
Sn(1)-C(2)-H(2B)	108.9
H(2A)-C(2)-H(2B)	107.7
C(2)-C(3)-H(3A)	109.5
C(2)-C(3)-H(3B)	109.5
H(3A)-C(3)-H(3B)	109.5
C(2)-C(3)-H(3C)	109.5
H(3A)-C(3)-H(3C)	109.5
H(3B)-C(3)-H(3C)	109.5
C(5)-C(4)-Sn(1)	117.58(11)
C(5)-C(4)-H(4A)	107.9
Sn(1)-C(4)-H(4A)	107.9
C(5)-C(4)-H(4B)	107.9
Sn(1)-C(4)-H(4B)	107.9
H(4A)-C(4)-H(4B)	107.2
C(4)-C(5)-H(5A)	109.5
C(4)-C(5)-H(5B)	109.5
H(5A)-C(5)-H(5B)	109.5
C(4)-C(5)-H(5C)	109.5
H(5A)-C(5)-H(5C)	109.5
H(5B)-C(5)-H(5C)	109.5
C(7)-C(6)-Sn(1)	111.38(10)
C(7)-C(6)-H(6A)	109.4
Sn(1)-C(6)-H(6A)	109.4
C(7)-C(6)-H(6B)	109.4

Sn(1)-C(6)-H(6B)	109.4
H(6A)-C(6)-H(6B)	108.0
C(6)-C(7)-H(7A)	109.5
C(6)-C(7)-H(7B)	109.5
H(7A)-C(7)-H(7B)	109.5
C(6)-C(7)-H(7C)	109.5
H(7A)-C(7)-H(7C)	109.5
H(7B)-C(7)-H(7C)	109.5
C(2S)-C(1S)-C(6S)	119.91(14)
C(2S)-C(1S)-Cl(1S)	120.93(7)
C(6S)-C(1S)-Cl(1S)	119.15(17)
C(1S)-C(2S)-C(3S)	120.0
C(1S)-C(2S)-Cl(2S)	120.35(8)
C(3S)-C(2S)-Cl(2S)	119.65(8)
C(4S)-C(3S)-C(2S)	119.59(16)
C(4S)-C(3S)-H(3D)	120.2
C(2S)-C(3S)-H(3D)	120.2
C(3S)-C(4S)-C(5S)	120.7(3)
C(3S)-C(4S)-H(4C)	119.7
C(5S)-C(4S)-H(4C)	119.7
C(4S)-C(5S)-C(6S)	120.3(3)
C(4S)-C(5S)-H(5D)	119.9
C(6S)-C(5S)-H(5D)	119.9
C(5S)-C(6S)-C(1S)	119.5(3)
C(5S)-C(6S)-H(6C)	120.2
C(1S)-C(6S)-H(6C)	120.2

Symmetry transformations used to generate equivalent atoms:

Appendix D.3 References

1. *APEX 2,* version 2009.5-1, Bruker (2009), Bruker AXS Inc., Madison, Wisconsin, USA.

2. *SAINT,* version V7.60A, Bruker (2009), Bruker AXS Inc., Madison, Wisconsin, USA.

3. *SADABS,* version 2008/1, Bruker (2008), Bruker AXS Inc., Madison, Wisconsin, USA.

4. *SHELXTL,* version 2008/4, Bruker (2008), Bruker AXS Inc., Madison, Wisconsin, USA.

Appendix E
Computational Details for Chapter 5

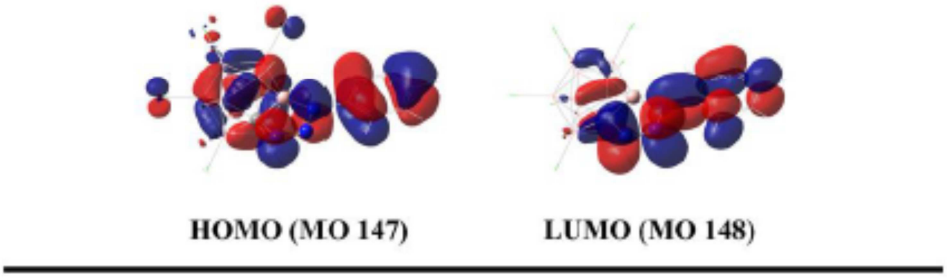

HOMO (MO 147) LUMO (MO 148)

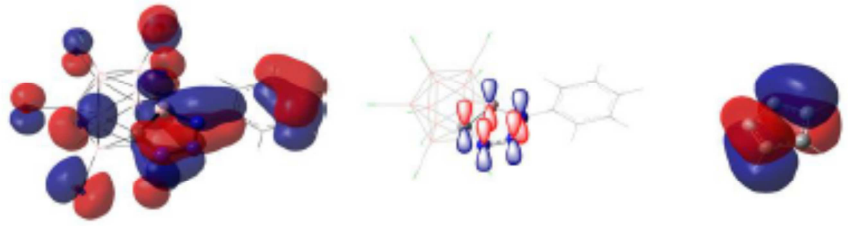

H-23 (MO 124) π3

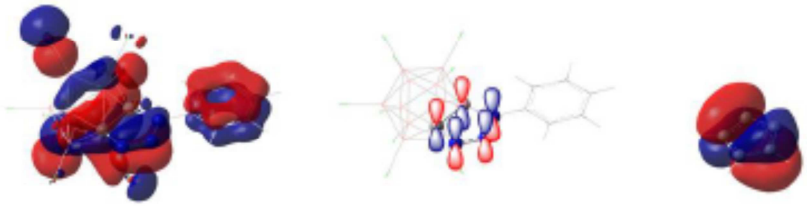

H-26 (MO 121) π2

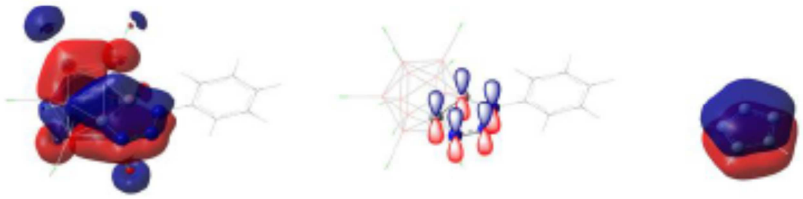

H-51 (MO 96) π1

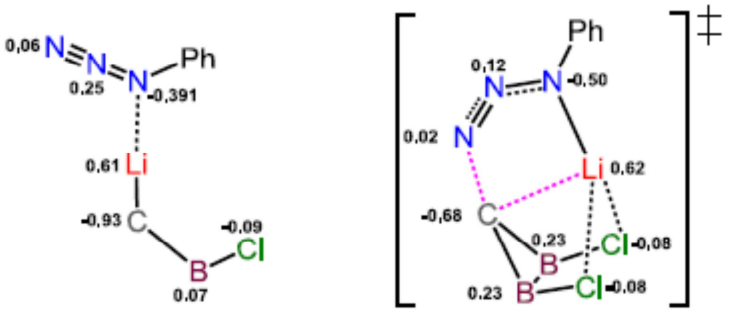

5a

TS-1

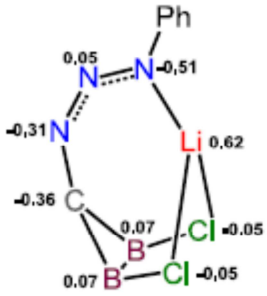

5b

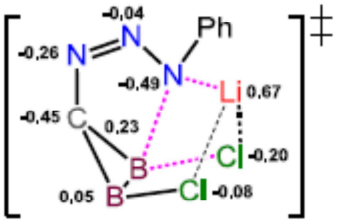

TS-2

7a

Energies (in a.u.) along with Cartesian Coordinates of the Optimized Structures

Compound 5

ECPCM= -5381.76360572
B,0,-0.701729,1.283443,0.872829
B,0,-0.701729,1.283443003,-0.8728289955
B,0,-0.959259,-0.354966,-1.427939
B,0,-1.114895,-1.37636,-0.0000000024
B,0,-0.959259,-0.354966005,1.4279389988
Cl,0,-1.559599,2.664351,-1.727104
Cl,0,-1.931985,-0.672559,-2.906167
Cl,0,-2.224029,-2.785635,-0.0000000049
Cl,0,-1.931985,-0.6725590101,2.9061669977
Cl,0,-1.559599,2.664350994,1.7271040093
B,0,0.689703,0.366414,1.466356
B,0,0.843016,1.423484,0.0000000025
B,0,0.689703,0.3664140051,-1.4663559987
B,0,0.43848,-1.332241,-0.903027
B,0,0.43848,-1.3322410031,0.9030269954

Cl,0,1.824998,2.922398,0.0000000051
Cl,0,1.52965,0.761005,-2.998199
Cl,0,1.037803,-2.730069,-1.847332
Cl,0,1.037803,-2.7300690064,1.8473319905
Cl,0,1.52965,0.7610049895,2.9981990027
B,0,1.544327,-0.231758,-0.0000000004
Cl,0,3.318335,-0.48344,-0.0000000008
C,0,-1.675686,0.219364,0.0000000004
Li,0,-3.062594,1.700421,0.000000003

Intermediate 5a
ECPCM= -5777.56540426
B,0,0.2532793647,0.5446675457,1.2181577549
B,0,0.2570389908,1.2157310683,-0.3947864877
B,0,0.507493652,-0.087218321,-1.5339697409
B,0,0.6627747325,-1.5770536664,-0.6072510618
B,0,0.5027478197,-1.1824205403,1.1020537378
Cl,0,-0.9606095692,2.5281080551,-0.7796130517
Cl,0,-0.3248097328,-0.0737138678,-3.1298046975
Cl,0,0.0242304241,-3.1266053906,-1.2527339462
Cl,0,-0.3344599374,-2.301499644,2.2356271378
Cl,0,-0.9702493898,1.198890776,2.4146635556
B,0,1.8575031461,-0.1074060828,1.5926336598
B,0,1.6886836271,1.4270114846,0.6422289055
B,0,1.8632925916,1.0174419634,-1.1146875452
B,0,2.1329336995,-0.764842666,-1.2449343326
B,0,2.1302752708,-1.457654763,0.4229087889
Cl,0,2.1799668175,3.0188529888,1.3054170998
Cl,0,2.5516213041,2.1838559279,-2.2879905088
Cl,0,3.1262104801,-1.4693448724,-2.5586821578
Cl,0,3.1198027457,-2.887331042,0.8534957702
Cl,0,2.5401461743,-0.117061489,3.249306782
B,0,2.855323451,0.1640025237,0.1199452019
Cl,0,4.6238777521,0.433095808,0.235548961
C,0,-0.3502875707,-0.3278648113,-0.090421659
Li,0,-2.1779444145,0.5271026372,0.2597835413
N,0,-4.1075682264,-0.1217892303,-0.1277956293
N,0,-4.1901812437,-1.2536372099,-0.6432647599
N,0,-4.1768888136,-2.2872493689,-1.1046236447
C,0,-5.3305852459,0.579961072,0.0787014084
C,0,-6.5820291128,0.0699636585,-0.2813021113
C,0,-5.2267057024,1.8411224054,0.6732566113
C,0,-7.7254783648,0.829541408,-0.0424534549
H,0,-6.6703497435,-0.9084485652,-0.7452194549

C,0,-6.3772390653,2.5883009076,0.9058737037
H,0,-4.2523742398,2.233454032,0.9503440053
C,0,-7.6309458481,2.0884605308,0.5502862653
H,0,-8.6953755886,0.429843711,-0.3247088945
H,0,-6.2886495089,3.5672891521,1.3675938994
H,0,-8.5258953878,2.6754789864,0.7332526717

TS-1
ECPCM= -5777.53571394
B,0,0.8853510143,0.4873911399,1.6319486647
B,0,0.9257826202,1.1878560971,0.0255275579
B,0,1.0515634762,-0.1169329563,-1.1446570371
B,0,1.1203956534,-1.6435989347,-0.2470104044
B,0,0.985845318,-1.2599575143,1.4782560339
Cl,0,-0.0407805317,2.6946255535,-0.356821168
Cl,0,0.2248564063,0.0010962627,-2.726506912
Cl,0,0.4212892248,-3.1410995001,-0.9172403273
Cl,0,0.0904753383,-2.3225247499,2.6047533549
Cl,0,-0.1287329933,1.2495569233,2.9519223625
B,0,2.4360978806,-0.3049487747,1.9639164617
B,0,2.3873248318,1.2484378086,1.0452803517
B,0,2.5029944912,0.862440582,-0.714187548
B,0,2.6305139516,-0.9234363594,-0.879880836
B,0,2.5897131723,-1.6445545571,0.7741894037
Cl,0,2.9983648778,2.7861437176,1.7314684411
Cl,0,3.256901426,1.9965903611,-1.8752154603
Cl,0,3.5430985243,-1.6748906442,-2.2216884715
Cl,0,3.45825348,-3.1558426254,1.1736297845
Cl,0,3.1177849615,-0.3959022221,3.6160136123
B,0,3.4428698502,-0.0873724716,0.4896158865
Cl,0,5.2247034417,0.0413850751,0.5901958925
C,0,0.1799046757,-0.3079345418,0.3115745332
Li,0,-1.5394786822,1.857406486,1.2067009682
N,0,-3.0188340989,0.7572453835,0.6543633019
N,0,-2.6733855467,-0.4015081401,0.1836888453
N,0,-1.72433813,-1.0540570414,-0.0552138009
C,0,-4.403891419,0.9880575746,0.6899158775
C,0,-5.3744841551,0.0650164133,0.2657215751
C,0,-4.830037057,2.2311980447,1.1843464674
C,0,-6.7264822252,0.3871364608,0.3390505906
H,0,-5.0588671565,-0.8997424737,-0.119450154
C,0,-6.184374714,2.5440406841,1.2537350053
H,0,-4.0918147535,2.9588938022,1.515284575
C,0,-7.1459148807,1.6248314982,0.83163451

H,0,-7.4613323703,-0.3413778911,0.0053698358
H,0,-6.4875455316,3.5138305857,1.6399618505
H,0,-8.2030546806,1.8683666842,0.8848115459

Intermediate 5b

ECPCM= -5777.54990252
B,0,0.8853510143,0.4873911399,1.6319486647
B,0,0.9257826202,1.1878560971,0.0255275579
B,0,1.0515634762,-0.1169329563,-1.1446570371
B,0,1.1203956534,-1.6435989347,-0.2470104044
B,0,0.985845318,-1.2599575143,1.4782560339
Cl,0,-0.0407805317,2.6946255535,-0.356821168
Cl,0,0.2248564063,0.0010962627,-2.726506912
Cl,0,0.4212892248,-3.1410995001,-0.9172403273
Cl,0,0.0904753383,-2.3225247499,2.6047533549
Cl,0,-0.1287329933,1.2495569233,2.9519223625
B,0,2.4360978806,-0.3049487747,1.9639164617
B,0,2.3873248318,1.2484378086,1.0452803517
B,0,2.5029944912,0.862440582,-0.714187548
B,0,2.6305139516,-0.9234363594,-0.879880836
B,0,2.5897131723,-1.6445545571,0.7741894037
Cl,0,2.9983648778,2.7861437176,1.7314684411
Cl,0,3.256901426,1.9965903611,-1.8752154603
Cl,0,3.5430985243,-1.6748906442,-2.2216884715
Cl,0,3.45825348,-3.1558426254,1.1736297845
Cl,0,3.1177849615,-0.3959022221,3.6160136123
B,0,3.4428698502,-0.0873724716,0.4896158865
Cl,0,5.2247034417,0.0413850751,0.5901958925
C,0,0.1799046757,-0.3079345418,0.3115745332
Li,0,-1.5394786822,1.857406486,1.2067009682
N,0,-3.0188340989,0.7572453835,0.6543633019
N,0,-2.6733855467,-0.4015081401,0.1836888453
N,0,-1.72433813,-1.0540570414,-0.0552138009
C,0,-4.403891419,0.9880575746,0.6899158775
C,0,-5.3744841551,0.0650164133,0.2657215751
C,0,-4.830037057,2.2311980447,1.1843464674
C,0,-6.7264822252,0.3871364608,0.3390505906
H,0,-5.0588671565,-0.8997424737,-0.119450154
C,0,-6.184374714,2.5440406841,1.2537350053
H,0,-4.0918147535,2.9588938022,1.515284575
C,0,-7.1459148807,1.6248314982,0.83163451
H,0,-7.4613323703,-0.3413778911,0.0053698358
H,0,-6.4875455316,3.5138305857,1.6399618505
H,0,-8.2030546806,1.8683666842,0.8848115459

TS-2

ECPCM= -5777.51680132
B,0,-0.3211686568,-0.3733312785,1.4735985372
B,0,-0.9633116403,0.7915800866,0.2470219984
B,0,-0.4794308789,-0.0873408657,-1.2912720606
B,0,0.3828480811,-1.6738708097,-0.9895583429
B,0,0.462399927,-1.866728095,0.7817805668
Cl,0,-1.7449076375,2.5572086534,0.7822120066
Cl,0,-1.5160685276,0.0217295058,-2.744779686
Cl,0,0.1093077335,-3.064827217,-2.0574202428
Cl,0,0.2751293546,-3.4441649952,1.57838033
Cl,0,-1.2993111507,-0.5535787794,3.0106882999
B,0,1.4702215567,-0.5516683493,1.439793933
B,0,0.7047978779,1.0246129083,1.1029628443
B,0,0.5656075161,1.2301922559,-0.6690452971
B,0,1.3065735121,-0.2212250953,-1.4367408826
B,0,1.8942653313,-1.3299185993,-0.1285209805
Cl,0,1.0357492822,2.3284825057,2.2926181318
Cl,0,0.7034602944,2.8066922354,-1.5124713636
Cl,0,2.1287705261,-0.1303944759,-3.0234394096
Cl,0,3.3246972168,-2.3853609569,-0.3183150124
Cl,0,2.427064545,-0.8271124825,2.9279064162
B,0,2.0301028822,0.4385857491,0.0582037671
Cl,0,3.6184865853,1.2596337329,0.0551156566
C,0,-0.8538592299,-1.1097372285,0.0341364412
Li,0,-2.8323306024,0.9819835291,2.0028113903
N,0,-2.9393352936,0.1551047918,0.1311630961
N,0,-3.1094121035,-1.1583924331,0.0788669141
N,0,-2.0626227352,-1.8682199329,0.0401808695
C,0,-4.1811665886,0.845686378,0.0044529221
C,0,-5.2629290452,0.5072445357,0.8356999238
C,0,-4.3324591223,1.8847718244,-0.9235740393
C,0,-6.4701770859,1.2038200338,0.7452703855
H,0,-5.1661552194,-0.3415756228,1.5106970167
C,0,-5.5371193515,2.5757334749,-1.0040604844
H,0,-3.5008966561,2.1310311293,-1.5738042904
C,0,-6.6096452528,2.2451707014,-0.1700189175
H,0,-7.3007719123,0.9231617234,1.3880613835
H,0,-5.6418049003,3.3774289675,-1.7304234925
H,0,-7.5464176316,2.7912204946,-0.2404613287

Compound 7a
ECPCM= -5309.78398764
B,0,0.0207704292,-0.5070248754,-1.472931744
B,0,0.9772157269,-0.1216562596,0.
B,0,0.0207704292,-0.5070248754,1.472931744
B,0,-1.5038352607,-1.2533799266,0.9030198232
B,0,-1.5038352607,-1.2533799266,-0.9030198232
Cl,0,0.8474671377,-1.1431468122,2.9118879647
Cl,0,-2.2369884324,-2.6006545598,1.7962703776
Cl,0,-2.2369884324,-2.6006545598,-1.7962703776
Cl,0,0.8474671377,-1.1431468122,-2.9118879647
B,0,-1.4502907209,0.4558630544,-1.4555123571
B,0,0.1334534388,1.1672453039,-0.9083028325
B,0,0.1334534388,1.1672453039,0.9083028325
B,0,-1.4502907209,0.4558630544,1.4555123571
B,0,-2.4011491138,-0.0000082121,0.
Cl,0,0.97021357,2.4346767478,-1.859248027
Cl,0,0.97021357,2.4346767478,1.859248027
Cl,0,-2.2320111764,0.9631494417,2.9790544791
Cl,0,-4.18794212,0.0496981876,0.
Cl,0,-2.2320111764,0.9631494417,-2.9790544791
B,0,-1.383573787,1.5029919455,0.
Cl,0,-2.1228741357,3.1312227203,0.
C,0,-0.0482228371,-1.4436254384,0.
N,0,2.2547948333,-0.8944907039,0.
N,0,2.0306025101,-2.2287939004,0.
N,0,0.8172275611,-2.5887266928,0.
C,0,3.5955322529,-0.4583616582,0
C,0,4.6553870064,-1.3763898858,0.
C,0,3.8657297406,0.9139026271,0.
C,0,5.9671143115,-0.9122836401,0.
H,0,4.4411206024,-2.4381911992,0.
C,0,5.184361818,1.3620891959,0.
H,0,3.0527499259,1.6321209751,0.
C,0,6.244287965,0.4562593113,0.
H,0,6.7809343075,-1.633015996,0.
H,0,5.3758899265,2.4316111394,0.
H,0,7.2714697995,0.8102590736,0.

Compound 4
NICS(0)= -30.8 ppm
B,0,-0.8951986453,-1.2322937992,0.7374866996
B,0,0.,-1.534494075,-0.7760697925
B,0,1.4603442042,-0.4743047699,-0.7757502924

B,0,1.4485625788,0.4706145393,0.7382318373
Cl,0,-1.7840823779,-2.4566894121,1.6785905289
Cl,0,0.0000000003,-3.1467744001,-1.5477296982
Cl,0,2.9935545117,-0.9725176847,-1.5475212737
Cl,0,2.8871289039,0.9379767188,1.6799485374
B,0,0.,1.5227811245,0.7370193278
B,0,-1.4485625789,0.4706145387,0.738231837
B,0,-1.4603442042,-0.4743047701,-0.7757502918
B,0,0.0000000001,-0.0001194428,-1.7152074693
B,0,0.9027680448,1.2419573584,-0.7766464829
Cl,0,-2.8871289041,0.9379767183,1.6799485373
Cl,0,-2.9935545121,-0.9725176848,-1.5475212723
Cl,0,0.0000000002,-0.0002437439,-3.5033412397
Cl,0,1.8503356031,2.5463617629,-1.5479420896
Cl,0,0.0000000001,3.0360030475,1.6781546252
B,0,-0.9027680448,1.2419573587,-0.7766464844
Cl,0,-1.8503356028,2.5463617628,-1.5479420923
B,0,0.8951986453,-1.2322937988,0.7374867002
Cl,0,1.784082378,-2.4566894138,1.6785905265
H,0,-0.0000000004,0.0005067566,2.6067083082
C,0,0.,0.0001313088,1.5211770135

TSC-B
ECPCM= -5381.6778871
B,0,0.7697436878,1.0552706583,-0.6797949645
B,0,1.4832944977,-0.497044435,-0.7772864046
B,0,0.0282740504,-1.5104451027,-0.876282636
B,0,-1.437081288,-0.4489807566,-0.8783789227
B,0,-0.9278966094,1.2505765502,-0.781504798
Cl,0,2.9512687908,-0.8539942025,-1.7241156363
Cl,0,0.0361281145,-2.9994317051,-1.8552837658
Cl,0,-2.8525390793,-0.9080619963,-1.8581181985
Cl,0,-1.7240086092,2.5349027447,-1.7251247016
Cl,0,1.7494524306,2.35022501,-4.2699338256
B,0,-0.0446506047,1.5368628348,0.7668938607
B,0,1.4797217918,0.4328490344,0.7688303243
B,0,0.8995070142,-1.2970847152,0.6938796033
B,0,-0.9132920246,-1.2651288077,0.6272728794
B,0,-1.5072216697,0.4476050518,0.6901812545
Cl,0,2.9673097808,0.9499063884,1.5896283661
Cl,0,1.7896886759,-2.6190215741,1.4907030359
Cl,0,-1.8721797048,-2.5877991147,1.3491282645
Cl,0,-3.0417701252,0.8819101305,1.4849792432
Cl,0,-0.0181193106,3.1124211962,1.5860143977

B,0,-0.0367581699,-0.0543308933,1.624235971
Cl,0,-0.0682075724,-0.0952679689,3.4099529893
C,0,0.0445042008,0.0518410092,-1.5357561076
Li,0,0.6149548824,0.7387933737,-3.5427587587

C-B, Carboryne
ECPCM= -4913.85770027
B,0,1.4626588775,-0.3266669534,0.90822971
B,0,0.0667021627,-1.2649913998,1.4801169631
B,0,-0.6618141178,-1.6922617541,0.0000000082
B,0,0.0667021258,-1.2649913998,-1.4801169648
B,0,1.4626588548,-0.3266669534,-0.9082297464
Cl,0,0.165133047,-2.3614608343,2.8943478254
Cl,0,0.1651329749,-2.3614608343,-2.8943478295
Cl,0,3.0148074339,-0.3728102229,-1.7832206529
Cl,0,3.0148074783,-0.3728102229,1.7832205777
B,0,0.8331398564,1.0845818657,-0.0000000104
B,0,-0.0328770688,0.5106156703,1.4888793282
B,0,-1.4602355567,-0.4790119639,0.9374460075
B,0,-1.4602355801,-0.4790119639,-0.9374459711
B,0,-0.0328771059,0.5106156703,-1.4888793274
Cl,0,-0.0768871994,1.4840438684,2.9847722606
Cl,0,-2.9938809202,-0.6082150039,1.8398890185
Cl,0,-2.993880966,-0.6082150039,-1.8398889439
Cl,0,-0.0768872738,1.4840438684,-2.9847722587
Cl,0,1.697046209,2.6513063117,-0.0000000211
B,0,-0.9593196692,0.9773615815,0.000000012
Cl,0,-1.991077873,2.439809846,0.0000000248
C,0,0.8112620449,-1.5857981657,-0.0000000101

Phenyl-azide
ECPCM= -395.798950757
N,0,1.2395634792,0.1393464037,-2.2090939784
N,0,2.0038367719,0.5375458123,-1.4631655779
N,0,2.7189991416,1.0636998829,-0.6093378991
C,0,4.0418490545,0.5859743925,-0.4460821802
C,0,4.8065849925,1.2223588381,0.5372780086
C,0,4.5918679893,-0.4578745628,-1.2001642032
C,0,6.1174200506,0.8137975989,0.7632317445
H,0,4.3606335035,2.0290513457,1.1105245628
C,0,5.9058373482,-0.8566409847,-0.963166174
H,0,4.0018529115,-0.9557144253,-1.9651255781
C,0,6.6741588905,-0.226047941,0.0159577964
H,0,6.7068584173,1.3114115947,1.5280949582

H,0,6.3290505347,-1.6668544627,-1.5503420243
H,0,7.6974365145,-0.5420989524,0.1949336349

LiCl
ECPCM= -467.822167486
Li,0,0.5780315304,-1.33093523,-0.00863223
Cl,0,-1.4791997104,-1.33093523,-0.00863

Appendix F
X-Ray Structure Determination of $C_8H_8N_3Cl_{10}$

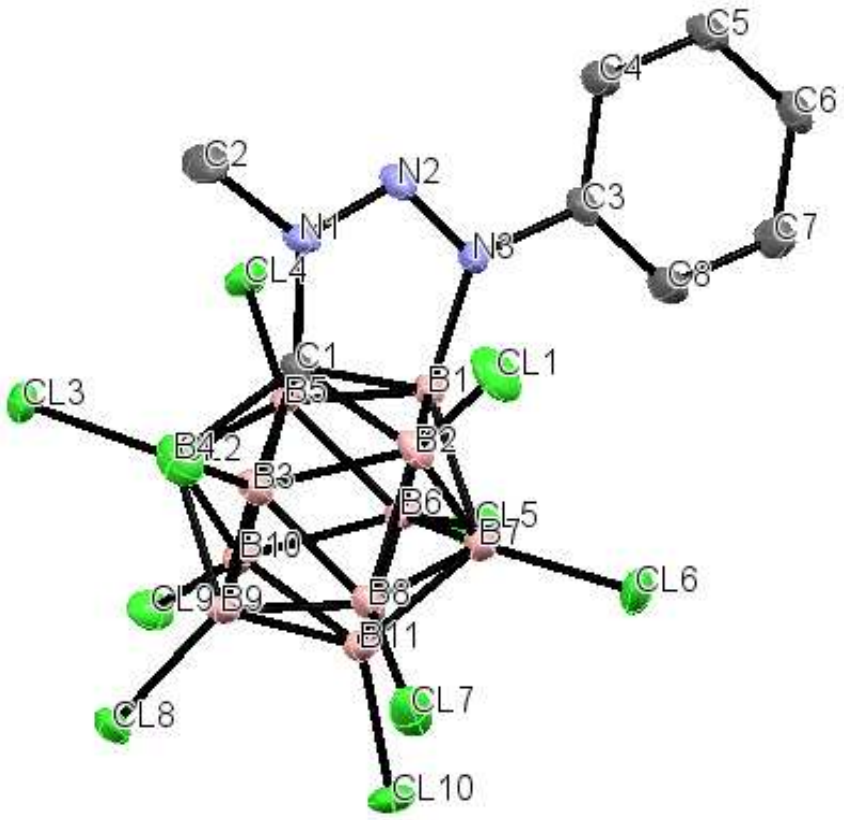

Appendix F.1 Experimental

A light yellow prism fragment (0.38 x 0.36 x 0.14 mm^3) was used for the single crystal x-ray diffraction study of $C_8H_8B_{11}N_3Cl_{11}$ (sample vL29_0m). The crystal was coated with paratone oil and mounted on to a cryo-loop glass fiber. X-ray intensity data were collected at 100(2) K on a Bruker APEX2 (**ref. 1**) platform-CCD x-ray diffractometer system (fine focus Mo-radiation, λ = 0.71073 Å, 50KV/35 mA power). The CCD detector was placed at a distance of 5.1000 cm from the crystal.

A total of 4800 frames were collected for a sphere of reflections (with scan width of 0.3° in ω, starting ω and 2θ angles at –30°, and ϕ angles of 0°, 90°, 120°, 180°, 240° and 270° for every 600 frames, and 1200 frames with ϕ-scan from 0-360°,

30 sec/frame exposure time). The frames were integrated using the Bruker SAINT software package (**ref. 2**) and using a narrow-frame integration algorithm. Based on a monoclinic crystal system, the integrated frames yielded a total of 31989 reflections at a maximum 2θ angle of 59.14^{o} (0.72 Å resolution), of which 6704 were independent reflections (R_{int} = 0.0318, R_{sig} = 0.0274, redundancy = 4.8, completeness = 99.9%) and 6353 (94.8%) reflections were greater than 2σ(I). The unit cell parameters were, **a** = 9.0006(6) Å, **b** = 28.8333 (19) Å, **c** = 9.2444(6) Å, **β** = 93.473(1)^{o}**,** V = 2394.7(3) Å^{3}, Z = 4, calculated density D_c = 1.719 g/cm^{3}. Absorption corrections were applied (absorption coefficient μ = 1.171 mm^{-1}; max/min transmission = 0.8542/0.6633) to the raw intensity data using the SADABS program (**ref. 3**).

The Bruker SHELXTL software package (**ref. 4**) was used for phase determination and structure refinement. The distribution of intensities (E^2-1 = 0.779) and systematic absent reflections indicated two possible space groups, C2/c and Cc. The space group Cc (#9) was later determined to be correct. Direct methods of phase determination followed by two Fourier cycles of refinement led to an electron density map from which most of the non-hydrogen atoms were identified in the asymmetry unit of the unit cell. With subsequent isotropic refinement, all of the non-hydrogen atoms were identified. There was one molecule of $C_8H_8B_{11}N_3Cl_{11}$ present in the asymmetry unit of the unit cell.

Atomic coordinates, isotropic and anisotropic displacement parameters of all the non-hydrogen atoms were refined by means of a full matrix least-squares procedure on F^2. The H-atoms were included in the refinement in calculated positions riding on the atoms to which they were attached. The Flack parameter, x = -0.01(6). for the Cc space group. The refinement converged at R1 = 0.0419, wR2 = 0.1114, with intensity I>2σ (I). The largest peak/hole in the final difference map was 1.048/-0.350 e/Å^{3}. The high electron density peak/hole ratio (2.99) is probably due to absorption correction error.

Appendix F.2 Structure Data

F.2.1 Crystal data and structure refinement for $C_8H_8N_3B_{11}Cl_{10}$.

Identification code	vl29_0m
Empirical formula	C8 H8 B11 Cl10 N3

Formula weight	619.58	
Temperature	100(2) K	
Wavelength	0.71073 Å	
Crystal system	Monoclinic	
Space group	Cc	
Unit cell dimensions	a = 9.0006(6) Å	α= 90°.
	b = 28.8333(19) Å	β= 93.4730(10)°.
	c = 9.2444(6) Å	γ = 90°.
Volume	2394.7(3) $Å^3$	
Z	4	
Density (calculated)	1.719 Mg/m^3	
Absorption coefficient	1.171 mm^{-1}	
F(000)	1208	
Crystal size	0.38 x 0.36 x 0.14 mm^3	
Theta range for data collection	2.37 to 29.57°.	
Index ranges	-12<=h<=12, -40<=k<=40, -12<=l<=12	
Reflections collected	31989	
Independent reflections	6704 [R(int) = 0.0318]	
Completeness to theta = 29.57°	99.9 %	
Absorption correction	Semi-empirical from equivalents	
Max. and min. transmission	0.8542 and 0.6633	
Refinement method	Full-matrix least-squares on F^2	
Data / restraints / parameters	6704 / 2 / 290	
Goodness-of-fit on F^2	1.062	
Final R indices [I>2sigma(I)]	R1 = 0.0419, wR2 = 0.1114	
R indices (all data)	R1 = 0.0449, wR2 = 0.1134	
Absolute structure parameter	-0.01(6)	
Largest diff. peak and hole	1.048 and -0.350 $e.Å^{-3}$	

F.2.2 Atomic coordinates (x 10^4) and equivalent isotropic displacement parameters (Å^{2}x 10^3) for $C_8H_8N_3B_{11}Cl_{10}$. U(eq) is defined as one third of the trace of the orthogonalized U^{ij} tensor.

	x	y	z	U(eq)
C(1)	7583(3)	6620(1)	5490(3)	16(1)
N(1)	7308(3)	6758(1)	4031(3)	20(1)
N(2)	6205(3)	6541(1)	3340(3)	21(1)
N(3)	5596(3)	6233(1)	4147(3)	16(1)
C(3)	4365(3)	5973(1)	3522(3)	18(1)
C(8)	3794(4)	5621(1)	4302(4)	31(1)
C(7)	2598(5)	5365(1)	3718(4)	35(1)
C(6)	1987(4)	5468(1)	2346(4)	27(1)
C(5)	2570(4)	5826(1)	1569(3)	27(1)
C(4)	3771(4)	6083(1)	2137(3)	24(1)
C(2)	8071(4)	7130(1)	3271(4)	33(1)
B(1)	6304(3)	6205(1)	5672(3)	15(1)
B(2)	8227(4)	6040(1)	5654(4)	18(1)
B(3)	9264(4)	6520(1)	6448(3)	18(1)
B(4)	7950(4)	6959(1)	7017(3)	16(1)
B(5)	6090(4)	6754(1)	6569(3)	15(1)
B(6)	5774(4)	6230(1)	7516(3)	16(1)
B(7)	7073(4)	5794(1)	6960(4)	19(1)
B(8)	8930(4)	6002(1)	7450(4)	19(1)
B(9)	8796(4)	6562(1)	8277(3)	18(1)
B(10)	6853(4)	6702(1)	8353(3)	17(1)
B(11)	7442(4)	6114(1)	8608(3)	18(1)
Cl(1)	8835(1)	5762(1)	4107(1)	31(1)
Cl(2)	10966(1)	6689(1)	5766(1)	28(1)
Cl(3)	8371(1)	7554(1)	6905(1)	24(1)
Cl(4)	4713(1)	7139(1)	5874(1)	22(1)
Cl(5)	3978(1)	6090(1)	8055(1)	26(1)
Cl(6)	6641(1)	5196(1)	6961(1)	30(1)

Cl(7)	10400(1)	5614(1)	7936(1)	30(1)
Cl(8)	10140(1)	6745(1)	9650(1)	24(1)
Cl(9)	6139(1)	7047(1)	9728(1)	25(1)
Cl(10)	7392(1)	5848(1)	10331(1)	28(1)

F.2.3 Bond lengths [Å] and angles [°] for $C_8H_8N_3B_{11}Cl_{10}$.

C(1)-N(1)	1.413(3)
C(1)-B(1)	1.675(4)
C(1)-B(3)	1.730(4)
C(1)-B(4)	1.732(4)
C(1)-B(5)	1.764(4)
C(1)-B(2)	1.775(5)
N(1)-N(2)	1.307(3)
N(1)-C(2)	1.475(4)
N(2)-N(3)	1.302(3)
N(3)-C(3)	1.430(4)
N(3)-B(1)	1.514(4)
C(3)-C(8)	1.363(4)
C(3)-C(4)	1.394(4)
C(8)-C(7)	1.388(5)
C(8)-H(8)	0.9500
C(7)-C(6)	1.383(5)
C(7)-H(7)	0.9500
C(6)-C(5)	1.381(5)
C(6)-H(6)	0.9500
C(5)-C(4)	1.387(4)
C(5)-H(5)	0.9500
C(4)-H(4)	0.9500
C(2)-H(2A)	0.9800
C(2)-H(2B)	0.9800
C(2)-H(2C)	0.9800
B(1)-B(7)	1.790(5)

B(1)-B(2)	1.796(5)
B(1)-B(6)	1.800(4)
B(1)-B(5)	1.803(4)
B(2)-B(8)	1.744(5)
B(2)-Cl(1)	1.756(3)
B(2)-B(7)	1.786(5)
B(2)-B(3)	1.803(5)
B(3)-Cl(2)	1.760(3)
B(3)-B(9)	1.770(5)
B(3)-B(8)	1.793(5)
B(3)-B(4)	1.830(5)
B(4)-Cl(3)	1.761(3)
B(4)-B(9)	1.772(4)
B(4)-B(10)	1.788(5)
B(4)-B(5)	1.799(5)
B(5)-B(10)	1.754(5)
B(5)-Cl(4)	1.755(3)
B(5)-B(6)	1.780(4)
B(6)-Cl(5)	1.767(3)
B(6)-B(11)	1.789(5)
B(6)-B(7)	1.811(5)
B(6)-B(10)	1.818(5)
B(7)-Cl(6)	1.767(3)
B(7)-B(11)	1.794(5)
B(7)-B(8)	1.807(5)
B(8)-Cl(7)	1.770(3)
B(8)-B(9)	1.792(5)
B(8)-B(11)	1.794(5)
B(9)-Cl(8)	1.781(3)
B(9)-B(10)	1.800(5)
B(9)-B(11)	1.814(5)
B(10)-Cl(9)	1.766(3)
B(10)-B(11)	1.788(4)
B(11)-Cl(10)	1.771(3)

N(1)-C(1)-B(1)	102.4(2)
N(1)-C(1)-B(3)	129.2(2)
B(1)-C(1)-B(3)	114.5(2)
N(1)-C(1)-B(4)	129.3(2)
B(1)-C(1)-B(4)	114.8(2)
B(3)-C(1)-B(4)	63.81(18)
N(1)-C(1)-B(5)	112.5(2)
B(1)-C(1)-B(5)	63.16(18)
B(3)-C(1)-B(5)	114.8(2)
B(4)-C(1)-B(5)	61.93(18)
N(1)-C(1)-B(2)	112.6(2)
B(1)-C(1)-B(2)	62.69(18)
B(3)-C(1)-B(2)	61.88(18)
B(4)-C(1)-B(2)	114.7(2)
B(5)-C(1)-B(2)	114.5(2)
N(2)-N(1)-C(1)	114.6(2)
N(2)-N(1)-C(2)	118.5(2)
C(1)-N(1)-C(2)	126.8(2)
N(3)-N(2)-N(1)	112.3(2)
N(2)-N(3)-C(3)	118.0(2)
N(2)-N(3)-B(1)	113.6(2)
C(3)-N(3)-B(1)	128.4(2)
C(8)-C(3)-C(4)	121.3(3)
C(8)-C(3)-N(3)	119.0(3)
C(4)-C(3)-N(3)	119.8(3)
C(3)-C(8)-C(7)	119.9(3)
C(3)-C(8)-H(8)	120.0
C(7)-C(8)-H(8)	120.0
C(6)-C(7)-C(8)	119.9(3)
C(6)-C(7)-H(7)	120.1
C(8)-C(7)-H(7)	120.1
C(5)-C(6)-C(7)	119.7(3)
C(5)-C(6)-H(6)	120.1

C(7)-C(6)-H(6)	120.1
C(6)-C(5)-C(4)	120.9(3)
C(6)-C(5)-H(5)	119.5
C(4)-C(5)-H(5)	119.5
C(5)-C(4)-C(3)	118.3(3)
C(5)-C(4)-H(4)	120.9
C(3)-C(4)-H(4)	120.9
N(1)-C(2)-H(2A)	109.5
N(1)-C(2)-H(2B)	109.5
H(2A)-C(2)-H(2B)	109.5
N(1)-C(2)-H(2C)	109.5
H(2A)-C(2)-H(2C)	109.5
H(2B)-C(2)-H(2C)	109.5
N(3)-B(1)-C(1)	97.0(2)
N(3)-B(1)-B(7)	141.1(3)
C(1)-B(1)-B(7)	107.4(2)
N(3)-B(1)-B(2)	110.9(2)
C(1)-B(1)-B(2)	61.38(18)
B(7)-B(1)-B(2)	59.75(19)
N(3)-B(1)-B(6)	139.4(3)
C(1)-B(1)-B(6)	106.9(2)
B(7)-B(1)-B(6)	60.60(18)
B(2)-B(1)-B(6)	109.3(2)
N(3)-B(1)-B(5)	109.4(2)
C(1)-B(1)-B(5)	60.83(18)
B(7)-B(1)-B(5)	108.9(2)
B(2)-B(1)-B(5)	111.6(2)
B(6)-B(1)-B(5)	59.23(17)
B(8)-B(2)-Cl(1)	129.4(2)
B(8)-B(2)-C(1)	103.7(2)
Cl(1)-B(2)-C(1)	118.5(2)
B(8)-B(2)-B(7)	61.6(2)
Cl(1)-B(2)-B(7)	126.3(2)
C(1)-B(2)-B(7)	103.4(2)

B(8)-B(2)-B(1)	107.6(2)
Cl(1)-B(2)-B(1)	118.5(2)
C(1)-B(2)-B(1)	55.94(17)
B(7)-B(2)-B(1)	59.94(19)
B(8)-B(2)-B(3)	60.71(19)
Cl(1)-B(2)-B(3)	120.3(2)
C(1)-B(2)-B(3)	57.84(18)
B(7)-B(2)-B(3)	109.7(2)
B(1)-B(2)-B(3)	105.5(2)
C(1)-B(3)-Cl(2)	121.6(2)
C(1)-B(3)-B(9)	103.1(2)
Cl(2)-B(3)-B(9)	125.9(2)
C(1)-B(3)-B(8)	103.5(2)
Cl(2)-B(3)-B(8)	126.3(2)
B(9)-B(3)-B(8)	60.39(18)
C(1)-B(3)-B(2)	60.27(18)
Cl(2)-B(3)-B(2)	120.4(2)
B(9)-B(3)-B(2)	107.1(2)
B(8)-B(3)-B(2)	58.02(19)
C(1)-B(3)-B(4)	58.15(17)
Cl(2)-B(3)-B(4)	120.3(2)
B(9)-B(3)-B(4)	58.95(18)
B(8)-B(3)-B(4)	107.2(2)
B(2)-B(3)-B(4)	108.7(2)
C(1)-B(4)-Cl(3)	122.2(2)
C(1)-B(4)-B(9)	102.9(2)
Cl(3)-B(4)-B(9)	125.7(2)
C(1)-B(4)-B(10)	104.1(2)
Cl(3)-B(4)-B(10)	125.1(2)
B(9)-B(4)-B(10)	60.74(19)
C(1)-B(4)-B(5)	59.90(17)
Cl(3)-B(4)-B(5)	120.4(2)
B(9)-B(4)-B(5)	107.2(2)
B(10)-B(4)-B(5)	58.55(18)

C(1)-B(4)-B(3)	58.04(17)
Cl(3)-B(4)-B(3)	120.7(2)
B(9)-B(4)-B(3)	58.85(18)
B(10)-B(4)-B(3)	107.8(2)
B(5)-B(4)-B(3)	108.4(2)
B(10)-B(5)-Cl(4)	128.8(2)
B(10)-B(5)-C(1)	104.1(2)
Cl(4)-B(5)-C(1)	118.46(19)
B(10)-B(5)-B(6)	61.91(18)
Cl(4)-B(5)-B(6)	125.9(2)
C(1)-B(5)-B(6)	104.0(2)
B(10)-B(5)-B(4)	60.39(18)
Cl(4)-B(5)-B(4)	120.24(19)
C(1)-B(5)-B(4)	58.17(17)
B(6)-B(5)-B(4)	109.9(2)
B(10)-B(5)-B(1)	108.0(2)
Cl(4)-B(5)-B(1)	118.6(2)
C(1)-B(5)-B(1)	56.00(16)
B(6)-B(5)-B(1)	60.30(17)
B(4)-B(5)-B(1)	105.7(2)
Cl(5)-B(6)-B(5)	120.6(2)
Cl(5)-B(6)-B(11)	123.3(2)
B(5)-B(6)-B(11)	106.4(2)
Cl(5)-B(6)-B(1)	123.9(2)
B(5)-B(6)-B(1)	60.47(17)
B(11)-B(6)-B(1)	105.4(2)
Cl(5)-B(6)-B(7)	122.6(2)
B(5)-B(6)-B(7)	108.9(2)
B(11)-B(6)-B(7)	59.78(18)
B(1)-B(6)-B(7)	59.43(18)
Cl(5)-B(6)-B(10)	121.7(2)
B(5)-B(6)-B(10)	58.35(18)
B(11)-B(6)-B(10)	59.42(18)
B(1)-B(6)-B(10)	105.4(2)

B(7)-B(6)-B(10)	107.6(2)
Cl(6)-B(7)-B(2)	121.6(2)
Cl(6)-B(7)-B(1)	124.8(2)
B(2)-B(7)-B(1)	60.31(18)
Cl(6)-B(7)-B(11)	122.0(2)
B(2)-B(7)-B(11)	106.6(2)
B(1)-B(7)-B(11)	105.6(2)
Cl(6)-B(7)-B(8)	121.6(2)
B(2)-B(7)-B(8)	58.05(19)
B(1)-B(7)-B(8)	105.1(2)
B(11)-B(7)-B(8)	59.75(19)
Cl(6)-B(7)-B(6)	122.0(2)
B(2)-B(7)-B(6)	109.2(2)
B(1)-B(7)-B(6)	59.97(18)
B(11)-B(7)-B(6)	59.49(18)
B(8)-B(7)-B(6)	107.6(2)
B(2)-B(8)-Cl(7)	120.2(2)
B(2)-B(8)-B(9)	108.7(2)
Cl(7)-B(8)-B(9)	121.9(2)
B(2)-B(8)-B(3)	61.27(19)
Cl(7)-B(8)-B(3)	120.8(2)
B(9)-B(8)-B(3)	59.19(18)
B(2)-B(8)-B(11)	108.5(2)
Cl(7)-B(8)-B(11)	122.4(2)
B(9)-B(8)-B(11)	60.79(19)
B(3)-B(8)-B(11)	108.3(2)
B(2)-B(8)-B(7)	60.37(19)
Cl(7)-B(8)-B(7)	121.3(2)
B(9)-B(8)-B(7)	108.7(2)
B(3)-B(8)-B(7)	109.2(2)
B(11)-B(8)-B(7)	59.76(19)
B(3)-B(9)-B(4)	62.20(18)
B(3)-B(9)-Cl(8)	120.7(2)
B(4)-B(9)-Cl(8)	121.5(2)

B(3)-B(9)-B(8)	60.42(19)
B(4)-B(9)-B(8)	109.8(2)
Cl(8)-B(9)-B(8)	120.8(2)
B(3)-B(9)-B(10)	109.9(2)
B(4)-B(9)-B(10)	60.05(18)
Cl(8)-B(9)-B(10)	121.7(2)
B(8)-B(9)-B(10)	108.0(2)
B(3)-B(9)-B(11)	108.3(2)
B(4)-B(9)-B(11)	107.7(2)
Cl(8)-B(9)-B(11)	121.7(2)
B(8)-B(9)-B(11)	59.64(19)
B(10)-B(9)-B(11)	59.29(18)
B(5)-B(10)-Cl(9)	119.3(2)
B(5)-B(10)-B(11)	107.6(2)
Cl(9)-B(10)-B(11)	123.9(2)
B(5)-B(10)-B(4)	61.05(18)
Cl(9)-B(10)-B(4)	120.2(2)
B(11)-B(10)-B(4)	108.2(2)
B(5)-B(10)-B(9)	108.0(2)
Cl(9)-B(10)-B(9)	123.5(2)
B(11)-B(10)-B(9)	60.76(19)
B(4)-B(10)-B(9)	59.20(18)
B(5)-B(10)-B(6)	59.75(18)
Cl(9)-B(10)-B(6)	121.3(2)
B(11)-B(10)-B(6)	59.47(18)
B(4)-B(10)-B(6)	108.7(2)
B(9)-B(10)-B(6)	108.1(2)
Cl(10)-B(11)-B(10)	120.4(2)
Cl(10)-B(11)-B(6)	121.5(2)
B(10)-B(11)-B(6)	61.11(18)
Cl(10)-B(11)-B(8)	121.3(2)
B(10)-B(11)-B(8)	108.5(2)
B(6)-B(11)-B(8)	109.1(2)
Cl(10)-B(11)-B(7)	121.8(2)

B(10)-B(11)-B(7)	109.7(2)
B(6)-B(11)-B(7)	60.72(18)
B(8)-B(11)-B(7)	60.49(19)
Cl(10)-B(11)-B(9)	120.9(2)
B(10)-B(11)-B(9)	59.95(19)
B(6)-B(11)-B(9)	108.7(2)
B(8)-B(11)-B(9)	59.56(19)
B(7)-B(11)-B(9)	108.3(2)

Symmetry transformations used to generate equivalent atoms:

Appendix F 3 References:

1. *APEX 2,* version 2012.2-0, Bruker (2012), Bruker AXS Inc., Madison, Wisconsin, USA.
2. *SAINT,* version V8.18C, Bruker (2011), Bruker AXS Inc., Madison, Wisconsin, USA.
3. *SADABS,* version 2008/1, Bruker (2008), Bruker AXS Inc., Madison, Wisconsin, USA.
4. *SHELXTL,* version 2008/4, Bruker (2008), Bruker AXS Inc., Madison, Wisconsin, USA.

Appendix G

X-ray Determination of $C_{22}H_{26}B_{11}Cl_{10}CoN_3O$

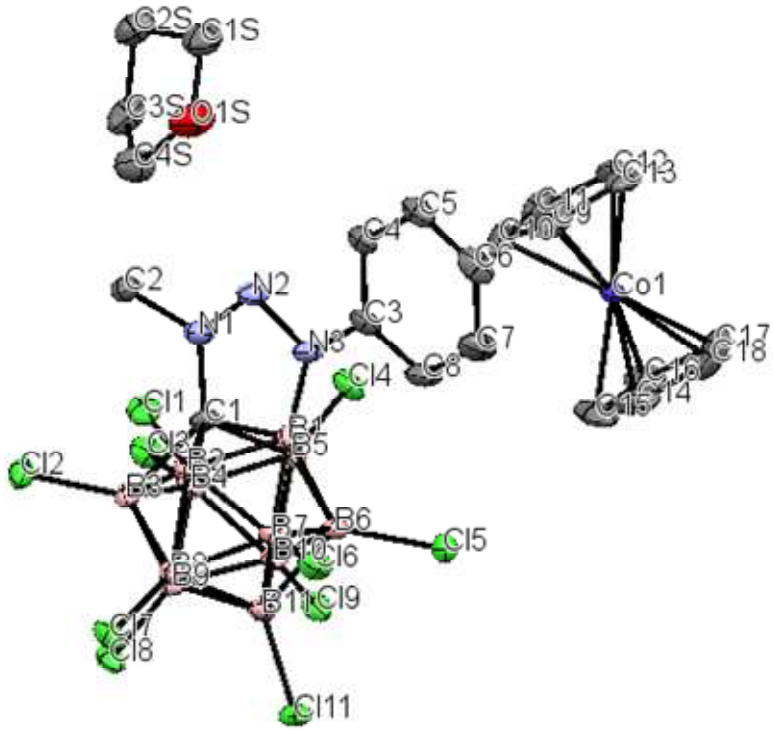

Table 1. Crystal data and structure refinement for $C_{22}H_{26}B_{11}Cl_{10}CoN_3O$.

Identification code	lavallo01	
Empirical formula	C22 H26 B11 Cl10 Co N3 O	
Molecular formula	C8 H8 B11 Cl10 N3, C10 H10 Co, C4 H8 O	
Formula weight	880.80	
Temperature	100 K	
Wavelength	0.71073 Å	
Crystal system	Triclinic	
Space group	P -1	
Unit cell dimensions	a = 12.1252(5) Å	α= 63.328(3)°.
	b = 17.5618(9) Å	β= 82.856(3)°.
	c = 18.6460(9) Å	γ = 88.571(3)°.
Volume	3518.3(3) $Å^3$	
Z	4	
Density (calculated)	1.663 Mg/m^3	

Absorption coefficient	1.276 mm^{-1}
F(000)	1756
Crystal size	0.317 x 0.211 x 0.135 mm3
Crystal color, habit	Dark Green Block
Theta range for data collection	1.298 to 26.386°.
Index ranges	-15<=h<=15, -19<=k<=21, 0<=l<=23
Reflections collected	14266
Independent reflections	14266 [R(int) = ?]
Completeness to theta = 25.000°	99.9 %
Absorption correction	Semi-empirical from equivalents
Max. and min. transmission	0.745373 and 0.637522
Refinement method	Full-matrix least-squares on F2
Data / restraints / parameters	14266 / 0 / 868
Goodness-of-fit on F2	1.035
Final R indices [I>2sigma(I)]	R1 = 0.0457, wR2 = 0.0961
R indices (all data)	R1 = 0.0738, wR2 = 0.1116
Extinction coefficient	n/a
Largest diff. peak and hole	0.742 and -0.820 e.Å-3

Table 2. Atomic coordinates (x 10^4) and equivalent isotropic displacement parameters ($Å^2$x 10^3)for $C_{22}H_{26}B_{11}Cl_{10}CoN_3O$. U(eq) is defined as one third of the trace of the orthogonalized U^{ij} tensor.

	x	y	z	U(eq)
Cl(1)	13358(1)	7714(1)	-2234(1)	26(1)
Cl(2)	11534(1)	8464(1)	-3774(1)	24(1)
Cl(3)	12256(1)	7446(1)	-5035(1)	26(1)
Cl(4)	14439(1)	5995(1)	-4257(1)	26(1)
Cl(5)	13375(1)	4305(1)	-2191(1)	26(1)
Cl(6)	12682(1)	5383(1)	-908(1)	27(1)
Cl(7)	10443(1)	6836(1)	-1714(1)	26(1)
Cl(8)	9762(1)	6689(1)	-3520(1)	24(1)
Cl(9)	11556(1)	5126(1)	-3817(1)	27(1)
Cl(11)	10509(1)	4763(1)	-1742(1)	28(1)
N(1)	14303(3)	7613(2)	-3921(2)	25(1)
N(2)	15201(3)	7346(2)	-3485(2)	24(1)
N(3)	14926(3)	6546(2)	-2841(2)	22(1)
C(1)	13318(3)	7110(3)	-3527(2)	18(1)
C(2)	14312(4)	8501(3)	-4468(3)	26(1)
C(3)	15741(3)	6201(3)	-2312(3)	22(1)
C(4)	16733(3)	6655(3)	-2458(3)	23(1)
C(5)	17522(4)	6307(3)	-1919(3)	27(1)
C(6)	17325(4)	5526(3)	-1250(3)	31(1)
C(7)	16337(4)	5083(3)	-1120(3)	35(1)
C(8)	15553(4)	5410(3)	-1650(3)	29(1)
B(1)	13753(4)	6280(3)	-2744(3)	16(1)
B(2)	12823(4)	7012(3)	-2558(3)	19(1)
B(3)	11962(4)	7405(3)	-3346(3)	18(1)
B(4)	12315(4)	6876(3)	-3986(3)	19(1)
B(5)	13383(4)	6139(3)	-3588(3)	20(1)
B(6)	12917(4)	5379(3)	-2602(3)	18(1)
B(7)	12578(4)	5908(3)	-1972(3)	17(1)
B(8)	11451(4)	6605(3)	-2357(3)	18(1)
B(9)	11126(4)	6534(3)	-3237(3)	17(1)
B(10)	12002(4)	5767(3)	-3387(3)	19(1)
B(11)	11502(4)	5606(3)	-2380(3)	19(1)

Co(1)	17330(1)	4136(1)	-3332(1)	17(1)
C(9)	17932(4)	5035(3)	-3062(3)	35(1)
C(10)	17271(4)	5421(3)	-3703(3)	34(1)
C(11)	17737(4)	5242(3)	-4349(3)	34(1)
C(12)	18688(4)	4764(3)	-4105(3)	35(1)
C(13)	18805(4)	4633(3)	-3313(3)	38(1)
C(14)	16296(4)	3356(3)	-2363(3)	40(1)
C(15)	15758(4)	3652(4)	-3063(4)	41(1)
C(16)	16368(4)	3395(3)	-3612(3)	32(1)
C(17)	17283(4)	2943(3)	-3244(3)	33(1)
C(18)	17232(5)	2909(3)	-2467(3)	40(1)
Cl(1')	10827(1)	9367(1)	-2307(1)	24(1)
Cl(2')	13087(1)	10182(1)	-3915(1)	23(1)
Cl(3')	12826(1)	12419(1)	-5019(1)	22(1)
Cl(4')	10399(1)	13021(1)	-4106(1)	24(1)
Cl(5')	10835(1)	12612(1)	-2028(1)	25(1)
Cl(6')	11156(1)	10270(1)	-869(1)	25(1)
Cl(7')	13627(1)	9690(1)	-1829(1)	25(1)
Cl(8')	14859(1)	11624(1)	-3570(1)	22(1)
Cl(9')	13216(1)	13408(1)	-3668(1)	23(1)
Cl(10)	13611(1)	11703(1)	-1687(1)	26(1)
N(1')	10401(3)	11089(2)	-3875(2)	26(1)
N(2')	9355(3)	11039(2)	-3466(2)	21(1)
N(3')	9461(3)	11106(2)	-2761(2)	18(1)
C(1')	11279(3)	11228(2)	-3512(2)	15(1)
C(2')	10476(5)	11096(5)	-4629(3)	57(2)
C(3')	8479(3)	10955(3)	-2220(3)	19(1)
C(4')	7470(3)	10796(3)	-2419(3)	22(1)
C(5')	6513(4)	10656(3)	-1875(3)	28(1)
C(6')	6551(4)	10653(3)	-1142(3)	30(1)
C(7')	7554(4)	10809(3)	-946(3)	32(1)
C(8')	8527(4)	10961(3)	-1487(3)	24(1)
B(1')	10627(4)	11252(3)	-2678(3)	16(1)
B(2')	11480(4)	10366(3)	-2581(3)	18(1)
B(3')	12572(4)	10772(3)	-3400(3)	17(1)
B(4')	12441(4)	11917(3)	-3964(3)	17(1)
B(5')	11257(4)	12234(3)	-3492(3)	18(1)
B(6')	11435(4)	11978(3)	-2502(3)	17(1)

B(7')	11572(4)	10831(3)	-1934(3)	18(1)
B(8')	12799(4)	10550(3)	-2396(3)	18(1)
B(9')	13402(4)	11490(3)	-3247(3)	16(1)
B(10')	12588(4)	12381(3)	-3300(3)	16(1)
B(11')	12786(4)	11536(3)	-2335(3)	17(1)
Co(1'	12996(1)	2270(1)	381(1)	22(1)
C(9')	14196(4)	2488(3)	927(3)	35(1)
C(10')	14290(4)	3092(3)	94(4)	49(2)
C(11')	14437(4)	2641(5)	-366(3)	52(2)
C(12')	14443(4)	1779(4)	167(3)	44(1)
C(13')	14306(4)	1682(3)	950(3)	33(1)
C(14')	11554(4)	2170(3)	1091(3)	25(1)
C(15')	11573(3)	2906(3)	341(3)	28(1)
C(16')	11706(4)	2648(3)	-280(3)	31(1)
C(17')	11752(4)	1757(3)	87(3)	35(1)
C(18')	11666(4)	1455(3)	931(3)	31(1)
O(1S)	17189(3)	8806(2)	-2704(2)	42(1)
C(1S)	18148(4)	9138(3)	-3301(3)	41(1)
C(2S)	17732(4)	9786(3)	-4063(3)	34(1)
C(3S)	16592(4)	9408(3)	-3994(3)	36(1)
C(4S)	16215(4)	9078(3)	-3102(3)	38(1)
O(2S)	12787(3)	7094(2)	686(2)	46(1)
C(5S)	12819(5)	7726(4)	-132(3)	46(2)
C(6S)	11650(4)	7734(4)	-355(3)	47(2)
C(7S)	11255(5)	6843(4)	185(3)	50(2)
C(8S)	11737(4)	6655(3)	938(3)	41(1)

Table 3. Bond lengths [Å] and angles [°] for $C_{22}H_{26}B_{11}Cl_{10}CoN_3O$.

Cl(1)-B(2)	1.764(5)
Cl(2)-B(3)	1.757(5)
Cl(3)-B(4)	1.763(5)
Cl(4)-B(5)	1.769(5)
Cl(5)-B(6)	1.792(5)
Cl(6)-B(7)	1.793(5)
Cl(7)-B(8)	1.772(5)
Cl(8)-B(9)	1.777(5)
Cl(9)-B(10)	1.775(5)

Cl(11)-B(11)	1.791(5)
N(1)-N(2)	1.386(5)
N(1)-C(1)	1.413(5)
N(1)-C(2)	1.429(5)
N(2)-N(3)	1.391(5)
N(3)-C(3)	1.413(5)
N(3)-B(1)	1.472(6)
C(1)-B(1)	1.666(6)
C(1)-B(2)	1.764(6)
C(1)-B(3)	1.750(6)
C(1)-B(4)	1.727(6)
C(1)-B(5)	1.758(7)
C(2)-H(2A)	0.9800
C(2)-H(2B)	0.9800
C(2)-H(2C)	0.9800
C(3)-C(4)	1.388(6)
C(3)-C(8)	1.382(6)
C(4)-H(4)	0.9500
C(4)-C(5)	1.400(6)
C(5)-H(5)	0.9500
C(5)-C(6)	1.378(7)
C(6)-H(6)	0.9500
C(6)-C(7)	1.380(6)
C(7)-H(7)	0.9500
C(7)-C(8)	1.381(6)
C(8)-H(8)	0.9500
B(1)-B(2)	1.809(7)
B(1)-B(5)	1.809(7)
B(1)-B(6)	1.799(7)
B(1)-B(7)	1.794(7)
B(2)-B(3)	1.778(7)
B(2)-B(7)	1.756(7)
B(2)-B(8)	1.755(7)
B(3)-B(4)	1.821(7)
B(3)-B(8)	1.787(7)
B(3)-B(9)	1.777(6)
B(4)-B(5)	1.787(7)
B(4)-B(9)	1.782(7)

B(4)-B(10)	1.778(7)
B(5)-B(6)	1.749(7)
B(5)-B(10)	1.747(7)
B(6)-B(7)	1.803(7)
B(6)-B(10)	1.819(7)
B(6)-B(11)	1.793(7)
B(7)-B(8)	1.803(7)
B(7)-B(11)	1.791(7)
B(8)-B(9)	1.792(7)
B(8)-B(11)	1.773(7)
B(9)-B(10)	1.793(7)
B(9)-B(11)	1.794(7)
B(10)-B(11)	1.795(7)
Co(1)-C(9)	2.036(5)
Co(1)-C(10)	2.044(4)
Co(1)-C(11)	2.029(5)
Co(1)-C(12)	2.019(5)
Co(1)-C(13)	2.021(4)
Co(1)-C(14)	2.004(5)
Co(1)-C(15)	2.017(5)
Co(1)-C(16)	2.041(4)
Co(1)-C(17)	2.029(4)
Co(1)-C(18)	2.025(5)
C(9)-H(9)	0.9500
C(9)-C(10)	1.420(7)
C(9)-C(13)	1.405(7)
C(10)-H(10)	0.9500
C(10)-C(11)	1.425(7)
C(11)-H(11)	0.9500
C(11)-C(12)	1.406(7)
C(12)-H(12)	0.9500
C(12)-C(13)	1.415(7)
C(13)-H(13)	0.9500
C(14)-H(14)	0.9500
C(14)-C(15)	1.410(7)
C(14)-C(18)	1.406(7)
C(15)-H(15)	0.9500
C(15)-C(16)	1.417(7)

C(16)-H(16)	0.9500
C(16)-C(17)	1.411(7)
C(17)-H(17)	0.9500
C(17)-C(18)	1.416(7)
C(18)-H(18)	0.9500
Cl(1')-B(2')	1.769(5)
Cl(2')-B(3')	1.761(5)
Cl(3')-B(4')	1.761(5)
Cl(4')-B(5')	1.762(5)
Cl(5')-B(6')	1.797(5)
Cl(6')-B(7')	1.786(5)
Cl(7')-B(8')	1.778(5)
Cl(8')-B(9')	1.780(5)
Cl(9')-B(10')	1.770(5)
Cl(10)-B(11')	1.784(5)
N(1')-N(2')	1.380(5)
N(1')-C(1')	1.411(5)
N(1')-C(2')	1.393(6)
N(2')-N(3')	1.393(5)
N(3')-C(3')	1.408(5)
N(3')-B(1')	1.481(6)
C(1')-B(1')	1.673(6)
C(1')-B(2')	1.758(6)
C(1')-B(3')	1.735(6)
C(1')-B(4')	1.741(6)
C(1')-B(5')	1.784(6)
C(2')-H(2'A)	0.9800
C(2')-H(2'B)	0.9800
C(2')-H(2'C)	0.9800
C(3')-C(4')	1.390(6)
C(3')-C(8')	1.380(6)
C(4')-H(4')	0.9500
C(4')-C(5')	1.391(6)
C(5')-H(5')	0.9500
C(5')-C(6')	1.370(7)
C(6')-H(6')	0.9500
C(6')-C(7')	1.379(6)
C(7')-H(7')	0.9500

C(7')-C(8')	1.400(6)
C(8')-H(8')	0.9500
B(1')-B(2')	1.799(7)
B(1')-B(5')	1.815(7)
B(1')-B(6')	1.793(7)
B(1')-B(7')	1.794(6)
B(2')-B(3')	1.778(7)
B(2')-B(7')	1.750(7)
B(2')-B(8')	1.746(6)
B(3')-B(4')	1.816(7)
B(3')-B(8')	1.788(7)
B(3')-B(9')	1.772(6)
B(4')-B(5')	1.798(7)
B(4')-B(9')	1.775(7)
B(4')-B(10')	1.789(7)
B(5')-B(6')	1.735(7)
B(5')-B(10')	1.746(7)
B(6')-B(7')	1.822(7)
B(6')-B(10')	1.805(7)
B(6')-B(11')	1.797(7)
B(7')-B(8')	1.796(7)
B(7')-B(11')	1.801(7)
B(8')-B(9')	1.788(7)
B(8')-B(11')	1.786(7)
B(9')-B(10')	1.799(6)
B(9')-B(11')	1.806(7)
B(10')-B(11')	1.785(7)
Co(1')-C(9')	2.012(5)
Co(1')-C(10')	2.011(5)
Co(1')-C(11')	2.014(5)
Co(1')-C(12')	2.010(5)
Co(1')-C(13')	2.017(4)
Co(1')-C(14')	2.017(4)
Co(1')-C(15')	2.022(4)
Co(1')-C(16')	2.024(5)
Co(1')-C(17')	2.026(5)
Co(1')-C(18')	2.021(4)
C(9')-H(9')	0.9500

C(9')-C(10')	1.426(8)
C(9')-C(13')	1.402(7)
C(10')-H(10')	0.9500
C(10')-C(11')	1.401(8)
C(11')-H(11')	0.9500
C(11')-C(12')	1.390(8)
C(12')-H(12')	0.9500
C(12')-C(13')	1.381(7)
C(13')-H(13')	0.9500
C(14')-H(14')	0.9500
C(14')-C(15')	1.413(6)
C(14')-C(18')	1.413(7)
C(15')-H(15')	0.9500
C(15')-C(16')	1.410(7)
C(16')-H(16')	0.9500
C(16')-C(17')	1.401(7)
C(17')-H(17')	0.9500
C(17')-C(18')	1.408(7)
C(18')-H(18')	0.9500
O(1S)-C(1S)	1.436(6)
O(1S)-C(4S)	1.430(6)
C(1S)-H(1SA)	0.9900
C(1S)-H(1SB)	0.9900
C(1S)-C(2S)	1.506(7)
C(2S)-H(2SA)	0.9900
C(2S)-H(2SB)	0.9900
C(2S)-C(3S)	1.515(6)
C(3S)-H(3SA)	0.9900
C(3S)-H(3SB)	0.9900
C(3S)-C(4S)	1.506(7)
C(4S)-H(4SA)	0.9900
C(4S)-H(4SB)	0.9900
O(2S)-C(5S)	1.423(6)
O(2S)-C(8S)	1.418(6)
C(5S)-H(5SA)	0.9900
C(5S)-H(5SB)	0.9900
C(5S)-C(6S)	1.524(7)
C(6S)-H(6SA)	0.9900

C(6S)-H(6SB)	0.9900
C(6S)-C(7S)	1.481(7)
C(7S)-H(7SA)	0.9900
C(7S)-H(7SB)	0.9900
C(7S)-C(8S)	1.483(7)
C(8S)-H(8SA)	0.9900
C(8S)-H(8SB)	0.9900

N(2)-N(1)-C(1)	114.0(3)
N(2)-N(1)-C(2)	115.7(3)
C(1)-N(1)-C(2)	123.5(4)
N(1)-N(2)-N(3)	108.1(3)
N(2)-N(3)-C(3)	115.1(3)
N(2)-N(3)-B(1)	113.5(3)
C(3)-N(3)-B(1)	130.2(4)
N(1)-C(1)-B(1)	103.1(3)
N(1)-C(1)-B(2)	116.7(3)
N(1)-C(1)-B(3)	130.6(3)
N(1)-C(1)-B(4)	126.3(4)
N(1)-C(1)-B(5)	110.8(3)
B(1)-C(1)-B(2)	63.6(3)
B(1)-C(1)-B(3)	114.7(3)
B(1)-C(1)-B(4)	115.5(3)
B(1)-C(1)-B(5)	63.7(3)
B(3)-C(1)-B(2)	60.8(3)
B(3)-C(1)-B(5)	113.7(3)
B(4)-C(1)-B(2)	113.4(3)
B(4)-C(1)-B(3)	63.2(3)
B(4)-C(1)-B(5)	61.7(3)
B(5)-C(1)-B(2)	114.4(3)
N(1)-C(2)-H(2A)	109.5
N(1)-C(2)-H(2B)	109.5
N(1)-C(2)-H(2C)	109.5
H(2A)-C(2)-H(2B)	109.5
H(2A)-C(2)-H(2C)	109.5
H(2B)-C(2)-H(2C)	109.5
C(4)-C(3)-N(3)	119.9(4)
C(8)-C(3)-N(3)	120.0(4)

C(8)-C(3)-C(4)	120.1(4)
C(3)-C(4)-H(4)	120.5
C(3)-C(4)-C(5)	119.0(4)
C(5)-C(4)-H(4)	120.5
C(4)-C(5)-H(5)	119.5
C(6)-C(5)-C(4)	120.9(4)
C(6)-C(5)-H(5)	119.5
C(5)-C(6)-H(6)	120.5
C(5)-C(6)-C(7)	119.1(4)
C(7)-C(6)-H(6)	120.5
C(6)-C(7)-H(7)	119.5
C(6)-C(7)-C(8)	120.9(5)
C(8)-C(7)-H(7)	119.5
C(3)-C(8)-H(8)	120.0
C(7)-C(8)-C(3)	120.0(4)
C(7)-C(8)-H(8)	120.0
N(3)-B(1)-C(1)	100.1(3)
N(3)-B(1)-B(2)	111.6(3)
N(3)-B(1)-B(5)	113.4(4)
N(3)-B(1)-B(6)	140.4(4)
N(3)-B(1)-B(7)	138.9(4)
C(1)-B(1)-B(2)	60.8(3)
C(1)-B(1)-B(5)	60.6(3)
C(1)-B(1)-B(6)	105.4(3)
C(1)-B(1)-B(7)	105.8(3)
B(5)-B(1)-B(2)	109.8(3)
B(6)-B(1)-B(2)	107.2(3)
B(6)-B(1)-B(5)	58.0(3)
B(7)-B(1)-B(2)	58.3(3)
B(7)-B(1)-B(5)	107.0(3)
B(7)-B(1)-B(6)	60.3(3)
Cl(1)-B(2)-B(1)	118.7(3)
Cl(1)-B(2)-B(3)	119.8(3)
C(1)-B(2)-Cl(1)	119.3(3)
C(1)-B(2)-B(1)	55.6(2)
C(1)-B(2)-B(3)	59.2(3)
B(3)-B(2)-B(1)	106.7(3)
B(7)-B(2)-Cl(1)	125.9(3)

B(7)-B(2)-C(1)	103.3(3)
B(7)-B(2)-B(1)	60.4(3)
B(7)-B(2)-B(3)	109.8(3)
B(8)-B(2)-Cl(1)	127.3(3)
B(8)-B(2)-C(1)	105.1(3)
B(8)-B(2)-B(1)	109.0(3)
B(8)-B(2)-B(3)	60.7(3)
B(8)-B(2)-B(7)	61.8(3)
Cl(2)-B(3)-B(2)	122.2(3)
Cl(2)-B(3)-B(4)	119.9(3)
Cl(2)-B(3)-B(8)	124.7(3)
Cl(2)-B(3)-B(9)	123.1(3)
C(1)-B(3)-Cl(2)	123.6(3)
C(1)-B(3)-B(2)	60.0(3)
C(1)-B(3)-B(4)	57.8(2)
C(1)-B(3)-B(8)	104.4(3)
C(1)-B(3)-B(9)	103.5(3)
B(2)-B(3)-B(4)	108.3(3)
B(2)-B(3)-B(8)	59.0(3)
B(8)-B(3)-B(4)	107.6(3)
B(9)-B(3)-B(2)	107.6(3)
B(9)-B(3)-B(4)	59.4(3)
B(9)-B(3)-B(8)	60.4(3)
Cl(3)-B(4)-B(3)	119.3(3)
Cl(3)-B(4)-B(5)	121.7(3)
Cl(3)-B(4)-B(9)	124.3(3)
Cl(3)-B(4)-B(10)	125.5(3)
C(1)-B(4)-Cl(3)	121.7(3)
C(1)-B(4)-B(3)	59.0(3)
C(1)-B(4)-B(5)	60.0(3)
C(1)-B(4)-B(9)	104.2(3)
C(1)-B(4)-B(10)	104.8(3)
B(5)-B(4)-B(3)	109.0(3)
B(9)-B(4)-B(3)	59.1(3)
B(9)-B(4)-B(5)	107.3(3)
B(10)-B(4)-B(3)	107.9(3)
B(10)-B(4)-B(5)	58.7(3)
B(10)-B(4)-B(9)	60.5(3)

Cl(4)-B(5)-B(1)	119.7(3)
Cl(4)-B(5)-B(4)	119.8(3)
C(1)-B(5)-Cl(4)	120.1(3)
C(1)-B(5)-B(1)	55.7(2)
C(1)-B(5)-B(4)	58.3(3)
B(4)-B(5)-B(1)	105.9(3)
B(6)-B(5)-Cl(4)	125.5(3)
B(6)-B(5)-C(1)	103.7(3)
B(6)-B(5)-B(1)	60.7(3)
B(6)-B(5)-B(4)	109.9(3)
B(10)-B(5)-Cl(4)	125.9(3)
B(10)-B(5)-C(1)	104.8(3)
B(10)-B(5)-B(1)	109.7(3)
B(10)-B(5)-B(4)	60.4(3)
B(10)-B(5)-B(6)	62.7(3)
Cl(5)-B(6)-B(1)	124.0(3)
Cl(5)-B(6)-B(7)	121.4(3)
Cl(5)-B(6)-B(10)	121.3(3)
Cl(5)-B(6)-B(11)	120.9(3)
B(1)-B(6)-B(7)	59.7(3)
B(1)-B(6)-B(10)	107.0(3)
B(5)-B(6)-Cl(5)	122.4(3)
B(5)-B(6)-B(1)	61.3(3)
B(5)-B(6)-B(7)	109.2(3)
B(5)-B(6)-B(10)	58.6(3)
B(5)-B(6)-B(11)	106.9(3)
B(7)-B(6)-B(10)	107.8(3)
B(11)-B(6)-B(1)	106.6(3)
B(11)-B(6)-B(7)	59.7(3)
B(11)-B(6)-B(10)	59.6(3)
Cl(6)-B(7)-B(1)	124.1(3)
Cl(6)-B(7)-B(6)	121.5(3)
Cl(6)-B(7)-B(8)	120.7(3)
B(1)-B(7)-B(6)	60.0(3)
B(1)-B(7)-B(8)	107.6(3)
B(2)-B(7)-Cl(6)	122.3(3)
B(2)-B(7)-B(1)	61.3(3)
B(2)-B(7)-B(6)	109.3(3)

B(2)-B(7)-B(8)	59.1(3)
B(2)-B(7)-B(11)	106.7(3)
B(6)-B(7)-B(8)	107.8(3)
B(11)-B(7)-Cl(6)	120.8(3)
B(11)-B(7)-B(1)	106.9(3)
B(11)-B(7)-B(6)	59.8(3)
B(11)-B(7)-B(8)	59.1(3)
Cl(7)-B(8)-B(3)	121.2(3)
Cl(7)-B(8)-B(7)	121.9(3)
Cl(7)-B(8)-B(9)	122.6(3)
Cl(7)-B(8)-B(11)	123.1(3)
B(2)-B(8)-Cl(7)	120.4(3)
B(2)-B(8)-B(3)	60.3(3)
B(2)-B(8)-B(7)	59.1(3)
B(2)-B(8)-B(9)	107.9(3)
B(2)-B(8)-B(11)	107.5(3)
B(3)-B(8)-B(7)	107.3(3)
B(3)-B(8)-B(9)	59.5(3)
B(9)-B(8)-B(7)	108.2(3)
B(11)-B(8)-B(3)	107.7(3)
B(11)-B(8)-B(7)	60.1(3)
B(11)-B(8)-B(9)	60.4(3)
Cl(8)-B(9)-B(4)	120.7(3)
Cl(8)-B(9)-B(8)	121.9(3)
Cl(8)-B(9)-B(10)	121.0(3)
Cl(8)-B(9)-B(11)	123.2(3)
B(3)-B(9)-Cl(8)	120.9(3)
B(3)-B(9)-B(4)	61.6(3)
B(3)-B(9)-B(8)	60.1(3)
B(3)-B(9)-B(10)	109.3(3)
B(3)-B(9)-B(11)	107.2(3)
B(4)-B(9)-B(8)	109.2(3)
B(4)-B(9)-B(10)	59.7(3)
B(4)-B(9)-B(11)	107.2(3)
B(8)-B(9)-B(10)	108.6(3)
B(8)-B(9)-B(11)	59.3(3)
B(10)-B(9)-B(11)	60.1(3)
Cl(9)-B(10)-B(4)	121.3(3)

Cl(9)-B(10)-B(6)	122.5(3)
Cl(9)-B(10)-B(9)	122.2(3)
Cl(9)-B(10)-B(11)	123.4(3)
B(4)-B(10)-B(6)	107.2(3)
B(4)-B(10)-B(9)	59.9(3)
B(4)-B(10)-B(11)	107.3(3)
B(5)-B(10)-Cl(9)	120.7(3)
B(5)-B(10)-B(4)	60.9(3)
B(5)-B(10)-B(6)	58.7(3)
B(5)-B(10)-B(9)	108.6(3)
B(5)-B(10)-B(11)	106.8(3)
B(9)-B(10)-B(6)	107.6(3)
B(9)-B(10)-B(11)	60.0(3)
B(11)-B(10)-B(6)	59.5(3)
Cl(11)-B(11)-B(6)	120.7(3)
Cl(11)-B(11)-B(7)	121.1(3)
Cl(11)-B(11)-B(9)	121.8(3)
Cl(11)-B(11)-B(10)	120.7(3)
B(6)-B(11)-B(9)	108.7(3)
B(6)-B(11)-B(10)	60.9(3)
B(7)-B(11)-B(6)	60.4(3)
B(7)-B(11)-B(9)	108.6(3)
B(7)-B(11)-B(10)	109.4(3)
B(8)-B(11)-Cl(11)	120.9(3)
B(8)-B(11)-B(6)	109.6(3)
B(8)-B(11)-B(7)	60.8(3)
B(8)-B(11)-B(9)	60.3(3)
B(8)-B(11)-B(10)	109.3(3)
B(9)-B(11)-B(10)	59.9(3)
C(9)-Co(1)-C(10)	40.73(19)
C(9)-Co(1)-C(16)	165.6(2)
C(11)-Co(1)-C(9)	69.0(2)
C(11)-Co(1)-C(10)	40.95(19)
C(11)-Co(1)-C(16)	108.2(2)
C(12)-Co(1)-C(9)	68.6(2)
C(12)-Co(1)-C(10)	68.3(2)
C(12)-Co(1)-C(11)	40.65(19)
C(12)-Co(1)-C(13)	41.0(2)

C(12)-Co(1)-C(16)	119.1(2)
C(12)-Co(1)-C(17)	107.8(2)
C(12)-Co(1)-C(18)	126.7(2)
C(13)-Co(1)-C(9)	40.5(2)
C(13)-Co(1)-C(10)	68.3(2)
C(13)-Co(1)-C(11)	68.9(2)
C(13)-Co(1)-C(16)	152.9(2)
C(13)-Co(1)-C(17)	118.5(2)
C(13)-Co(1)-C(18)	106.8(2)
C(14)-Co(1)-C(9)	106.9(2)
C(14)-Co(1)-C(10)	118.8(2)
C(14)-Co(1)-C(11)	153.4(2)
C(14)-Co(1)-C(12)	164.3(2)
C(14)-Co(1)-C(13)	126.0(2)
C(14)-Co(1)-C(15)	41.0(2)
C(14)-Co(1)-C(16)	69.0(2)
C(14)-Co(1)-C(17)	68.8(2)
C(14)-Co(1)-C(18)	40.8(2)
C(15)-Co(1)-C(9)	127.2(2)
C(15)-Co(1)-C(10)	108.4(2)
C(15)-Co(1)-C(11)	119.3(2)
C(15)-Co(1)-C(12)	153.5(2)
C(15)-Co(1)-C(13)	164.4(2)
C(15)-Co(1)-C(16)	40.88(19)
C(15)-Co(1)-C(17)	68.5(2)
C(15)-Co(1)-C(18)	68.7(2)
C(16)-Co(1)-C(10)	128.1(2)
C(17)-Co(1)-C(9)	152.2(2)
C(17)-Co(1)-C(10)	165.6(2)
C(17)-Co(1)-C(11)	127.2(2)
C(17)-Co(1)-C(16)	40.56(19)
C(18)-Co(1)-C(9)	117.8(2)
C(18)-Co(1)-C(10)	152.5(2)
C(18)-Co(1)-C(11)	164.8(2)
C(18)-Co(1)-C(16)	68.7(2)
C(18)-Co(1)-C(17)	40.9(2)
Co(1)-C(9)-H(9)	126.3
C(10)-C(9)-Co(1)	69.9(3)

C(10)-C(9)-H(9)	126.1
C(13)-C(9)-Co(1)	69.2(3)
C(13)-C(9)-H(9)	126.1
C(13)-C(9)-C(10)	107.8(5)
Co(1)-C(10)-H(10)	127.3
C(9)-C(10)-Co(1)	69.3(3)
C(9)-C(10)-H(10)	126.0
C(9)-C(10)-C(11)	108.1(4)
C(11)-C(10)-Co(1)	69.0(3)
C(11)-C(10)-H(10)	126.0
Co(1)-C(11)-H(11)	125.9
C(10)-C(11)-Co(1)	70.1(3)
C(10)-C(11)-H(11)	126.3
C(12)-C(11)-Co(1)	69.3(3)
C(12)-C(11)-C(10)	107.3(4)
C(12)-C(11)-H(11)	126.3
Co(1)-C(12)-H(12)	126.2
C(11)-C(12)-Co(1)	70.1(3)
C(11)-C(12)-H(12)	125.7
C(11)-C(12)-C(13)	108.6(5)
C(13)-C(12)-Co(1)	69.6(3)
C(13)-C(12)-H(12)	125.7
Co(1)-C(13)-H(13)	125.9
C(9)-C(13)-Co(1)	70.3(3)
C(9)-C(13)-C(12)	108.2(4)
C(9)-C(13)-H(13)	125.9
C(12)-C(13)-Co(1)	69.4(3)
C(12)-C(13)-H(13)	125.9
Co(1)-C(14)-H(14)	125.4
C(15)-C(14)-Co(1)	70.0(3)
C(15)-C(14)-H(14)	125.9
C(18)-C(14)-Co(1)	70.4(3)
C(18)-C(14)-H(14)	125.9
C(18)-C(14)-C(15)	108.3(5)
Co(1)-C(15)-H(15)	126.2
C(14)-C(15)-Co(1)	69.0(3)
C(14)-C(15)-H(15)	125.9
C(14)-C(15)-C(16)	108.2(5)

C(16)-C(15)-Co(1)	70.5(3)
C(16)-C(15)-H(15)	125.9
Co(1)-C(16)-H(16)	127.3
C(15)-C(16)-Co(1)	68.6(3)
C(15)-C(16)-H(16)	126.3
C(17)-C(16)-Co(1)	69.2(3)
C(17)-C(16)-C(15)	107.3(5)
C(17)-C(16)-H(16)	126.3
Co(1)-C(17)-H(17)	126.2
C(16)-C(17)-Co(1)	70.2(3)
C(16)-C(17)-H(17)	125.8
C(16)-C(17)-C(18)	108.5(5)
C(18)-C(17)-Co(1)	69.4(3)
C(18)-C(17)-H(17)	125.8
Co(1)-C(18)-H(18)	126.9
C(14)-C(18)-Co(1)	68.8(3)
C(14)-C(18)-C(17)	107.7(5)
C(14)-C(18)-H(18)	126.2
C(17)-C(18)-Co(1)	69.7(3)
C(17)-C(18)-H(18)	126.2
N(2')-N(1')-C(1')	114.8(3)
N(2')-N(1')-C(2')	117.9(4)
C(2')-N(1')-C(1')	126.9(4)
N(1')-N(2')-N(3')	108.8(3)
N(2')-N(3')-C(3')	115.8(3)
N(2')-N(3')-B(1')	113.2(3)
C(3')-N(3')-B(1')	130.7(4)
N(1')-C(1')-B(1')	103.2(3)
N(1')-C(1')-B(2')	113.9(3)
N(1')-C(1')-B(3')	129.1(3)
N(1')-C(1')-B(4')	129.0(3)
N(1')-C(1')-B(5')	113.8(3)
B(1')-C(1')-B(2')	63.2(3)
B(1')-C(1')-B(3')	114.5(3)
B(1')-C(1')-B(4')	114.6(3)
B(1')-C(1')-B(5')	63.2(3)
B(2')-C(1')-B(5')	113.7(3)
B(3')-C(1')-B(2')	61.2(3)

B(3')-C(1')-B(4')	63.0(3)
B(3')-C(1')-B(5')	113.2(3)
B(4')-C(1')-B(2')	113.2(3)
B(4')-C(1')-B(5')	61.3(3)
N(1')-C(2')-H(2'A)	109.5
N(1')-C(2')-H(2'B)	109.5
N(1')-C(2')-H(2'C)	109.5
H(2'A)-C(2')-H(2'B)	109.5
H(2'A)-C(2')-H(2'C)	109.5
H(2'B)-C(2')-H(2'C)	109.5
C(4')-C(3')-N(3')	120.5(4)
C(8')-C(3')-N(3')	119.3(4)
C(8')-C(3')-C(4')	120.2(4)
C(3')-C(4')-H(4')	120.4
C(3')-C(4')-C(5')	119.2(4)
C(5')-C(4')-H(4')	120.4
C(4')-C(5')-H(5')	119.4
C(6')-C(5')-C(4')	121.2(4)
C(6')-C(5')-H(5')	119.4
C(5')-C(6')-H(6')	120.2
C(5')-C(6')-C(7')	119.5(4)
C(7')-C(6')-H(6')	120.2
C(6')-C(7')-H(7')	119.8
C(6')-C(7')-C(8')	120.3(5)
C(8')-C(7')-H(7')	119.8
C(3')-C(8')-C(7')	119.6(4)
C(3')-C(8')-H(8')	120.2
C(7')-C(8')-H(8')	120.2
N(3')-B(1')-C(1')	100.0(3)
N(3')-B(1')-B(2')	112.2(3)
N(3')-B(1')-B(5')	112.9(3)
N(3')-B(1')-B(6')	139.4(4)
N(3')-B(1')-B(7')	138.9(4)
C(1')-B(1')-B(2')	60.7(3)
C(1')-B(1')-B(5')	61.4(3)
C(1')-B(1')-B(6')	105.8(3)
C(1')-B(1')-B(7')	106.0(3)
B(2')-B(1')-B(5')	110.3(3)

B(6')-B(1')-B(2')	107.7(3)
B(6')-B(1')-B(5')	57.5(3)
B(6')-B(1')-B(7')	61.1(3)
B(7')-B(1')-B(2')	58.3(3)
B(7')-B(1')-B(5')	107.5(3)
Cl(1')-B(2')-B(1')	118.9(3)
Cl(1')-B(2')-B(3')	119.6(3)
C(1')-B(2')-Cl(1')	118.8(3)
C(1')-B(2')-B(1')	56.1(2)
C(1')-B(2')-B(3')	58.8(2)
B(3')-B(2')-B(1')	106.5(3)
B(7')-B(2')-Cl(1')	125.6(3)
B(7')-B(2')-C(1')	104.4(3)
B(7')-B(2')-B(1')	60.7(3)
B(7')-B(2')-B(3')	110.2(3)
B(8')-B(2')-Cl(1')	127.1(3)
B(8')-B(2')-C(1')	105.3(3)
B(8')-B(2')-B(1')	109.0(3)
B(8')-B(2')-B(3')	61.0(3)
B(8')-B(2')-B(7')	61.8(3)
Cl(2')-B(3')-B(2')	121.9(3)
Cl(2')-B(3')-B(4')	119.6(3)
Cl(2')-B(3')-B(8')	125.4(3)
Cl(2')-B(3')-B(9')	123.7(3)
C(1')-B(3')-Cl(2')	122.3(3)
C(1')-B(3')-B(2')	60.0(2)
C(1')-B(3')-B(4')	58.7(2)
C(1')-B(3')-B(8')	104.5(3)
C(1')-B(3')-B(9')	104.2(3)
B(2')-B(3')-B(4')	108.7(3)
B(2')-B(3')-B(8')	58.6(3)
B(8')-B(3')-B(4')	107.6(3)
B(9')-B(3')-B(2')	107.4(3)
B(9')-B(3')-B(4')	59.3(3)
B(9')-B(3')-B(8')	60.3(3)
Cl(3')-B(4')-B(3')	119.5(3)
Cl(3')-B(4')-B(5')	122.0(3)
Cl(3')-B(4')-B(9')	123.9(3)

Cl(3')-B(4')-B(10')	125.4(3)
C(1')-B(4')-Cl(3')	122.2(3)
C(1')-B(4')-B(3')	58.3(2)
C(1')-B(4')-B(5')	60.5(2)
C(1')-B(4')-B(9')	103.8(3)
C(1')-B(4')-B(10')	104.7(3)
B(5')-B(4')-B(3')	108.8(3)
B(9')-B(4')-B(3')	59.1(3)
B(9')-B(4')-B(5')	107.2(3)
B(9')-B(4')-B(10')	60.7(3)
B(10')-B(4')-B(3')	107.9(3)
B(10')-B(4')-B(5')	58.3(3)
Cl(4')-B(5')-C(1')	118.4(3)
Cl(4')-B(5')-B(1')	119.4(3)
Cl(4')-B(5')-B(4')	119.1(3)
C(1')-B(5')-B(1')	55.4(2)
C(1')-B(5')-B(4')	58.2(2)
B(4')-B(5')-B(1')	105.4(3)
B(6')-B(5')-Cl(4')	126.9(3)
B(6')-B(5')-C(1')	103.6(3)
B(6')-B(5')-B(1')	60.6(3)
B(6')-B(5')-B(4')	109.9(3)
B(6')-B(5')-B(10')	62.5(3)
B(10')-B(5')-Cl(4')	127.5(3)
B(10')-B(5')-C(1')	104.7(3)
B(10')-B(5')-B(1')	109.1(3)
B(10')-B(5')-B(4')	60.6(3)
Cl(5')-B(6')-B(7')	122.0(3)
Cl(5')-B(6')-B(10')	121.5(3)
B(1')-B(6')-Cl(5')	122.9(3)
B(1')-B(6')-B(7')	59.5(3)
B(1')-B(6')-B(10')	107.5(3)
B(1')-B(6')-B(11')	106.6(3)
B(5')-B(6')-Cl(5')	120.6(3)
B(5')-B(6')-B(1')	61.9(3)
B(5')-B(6')-B(7')	109.7(3)
B(5')-B(6')-B(10')	59.1(3)
B(5')-B(6')-B(11')	107.4(3)

B(10')-B(6')-B(7')	107.7(3)
B(11')-B(6')-Cl(5')	122.2(3)
B(11')-B(6')-B(7')	59.7(3)
B(11')-B(6')-B(10')	59.4(3)
Cl(6')-B(7')-B(1')	124.3(3)
Cl(6')-B(7')-B(6')	122.2(3)
Cl(6')-B(7')-B(8')	120.8(3)
Cl(6')-B(7')-B(11')	121.0(3)
B(1')-B(7')-B(6')	59.4(3)
B(1')-B(7')-B(8')	107.1(3)
B(1')-B(7')-B(11')	106.4(3)
B(2')-B(7')-Cl(6')	122.2(3)
B(2')-B(7')-B(1')	61.0(3)
B(2')-B(7')-B(6')	108.6(3)
B(2')-B(7')-B(8')	59.0(3)
B(2')-B(7')-B(11')	106.9(3)
B(8')-B(7')-B(6')	107.4(3)
B(8')-B(7')-B(11')	59.6(3)
B(11')-B(7')-B(6')	59.5(3)
Cl(7')-B(8')-B(3')	121.1(3)
Cl(7')-B(8')-B(7')	122.1(3)
Cl(7')-B(8')-B(9')	121.6(3)
Cl(7')-B(8')-B(11')	122.6(3)
B(2')-B(8')-Cl(7')	121.1(3)
B(2')-B(8')-B(3')	60.4(3)
B(2')-B(8')-B(7')	59.2(3)
B(2')-B(8')-B(9')	108.1(3)
B(2')-B(8')-B(11')	107.7(3)
B(3')-B(8')-B(7')	107.7(3)
B(3')-B(8')-B(9')	59.4(3)
B(9')-B(8')-B(7')	108.7(3)
B(11')-B(8')-B(3')	107.9(3)
B(11')-B(8')-B(7')	60.4(3)
B(11')-B(8')-B(9')	60.7(3)
Cl(8')-B(9')-B(8')	122.2(3)
Cl(8')-B(9')-B(10')	120.7(3)
Cl(8')-B(9')-B(11')	122.7(3)
B(3')-B(9')-Cl(8')	121.4(3)

B(3')-B(9')-B(4')	61.6(3)
B(3')-B(9')-B(8')	60.3(3)
B(3')-B(9')-B(10')	109.4(3)
B(3')-B(9')-B(11')	107.7(3)
B(4')-B(9')-Cl(8')	120.5(3)
B(4')-B(9')-B(8')	109.4(3)
B(4')-B(9')-B(10')	60.0(3)
B(4')-B(9')-B(11')	107.4(3)
B(8')-B(9')-B(10')	108.2(3)
B(8')-B(9')-B(11')	59.6(3)
B(10')-B(9')-B(11')	59.3(3)
Cl(9')-B(10')-B(4')	121.0(3)
Cl(9')-B(10')-B(6')	123.3(3)
Cl(9')-B(10')-B(9')	120.9(3)
Cl(9')-B(10')-B(11')	122.2(3)
B(4')-B(10')-B(6')	107.2(3)
B(4')-B(10')-B(9')	59.3(3)
B(5')-B(10')-Cl(9')	121.8(3)
B(5')-B(10')-B(4')	61.1(3)
B(5')-B(10')-B(6')	58.5(3)
B(5')-B(10')-B(9')	108.4(3)
B(5')-B(10')-B(11')	107.4(3)
B(9')-B(10')-B(6')	108.0(3)
B(11')-B(10')-B(4')	107.7(3)
B(11')-B(10')-B(6')	60.1(3)
B(11')-B(10')-B(9')	60.5(3)
Cl(10)-B(11')-B(6')	121.7(3)
Cl(10)-B(11')-B(7')	121.4(3)
Cl(10)-B(11')-B(8')	121.0(3)
Cl(10)-B(11')-B(9')	121.8(3)
Cl(10)-B(11')-B(10')	120.9(3)
B(6')-B(11')-B(7')	60.8(3)
B(6')-B(11')-B(9')	108.0(3)
B(7')-B(11')-B(9')	107.7(3)
B(8')-B(11')-B(6')	108.9(3)
B(8')-B(11')-B(7')	60.1(3)
B(8')-B(11')-B(9')	59.7(3)
B(10')-B(11')-B(6')	60.5(3)

B(10')-B(11')-B(7')	109.5(3)
B(10')-B(11')-B(8')	108.9(3)
B(10')-B(11')-B(9')	60.1(3)
C(9')-Co(1')-C(11')	69.1(2)
C(9')-Co(1')-C(13')	40.7(2)
C(9')-Co(1')-C(14')	106.1(2)
C(9')-Co(1')-C(15')	117.3(2)
C(9')-Co(1')-C(16')	152.0(2)
C(9')-Co(1')-C(17')	165.3(2)
C(9')-Co(1')-C(18')	126.4(2)
C(10')-Co(1')-C(9')	41.5(2)
C(10')-Co(1')-C(11')	40.7(2)
C(10')-Co(1')-C(13')	68.5(2)
C(10')-Co(1')-C(14')	128.0(2)
C(10')-Co(1')-C(15')	108.4(2)
C(10')-Co(1')-C(16')	118.8(2)
C(10')-Co(1')-C(17')	152.3(2)
C(10')-Co(1')-C(18')	166.0(3)
C(11')-Co(1')-C(13')	68.1(2)
C(11')-Co(1')-C(14')	167.2(2)
C(11')-Co(1')-C(15')	129.6(2)
C(11')-Co(1')-C(16')	109.3(2)
C(11')-Co(1')-C(17')	119.0(2)
C(11')-Co(1')-C(18')	151.3(3)
C(12')-Co(1')-C(9')	68.4(2)
C(12')-Co(1')-C(10')	68.2(2)
C(12')-Co(1')-C(11')	40.4(2)
C(12')-Co(1')-C(13')	40.1(2)
C(12')-Co(1')-C(14')	150.3(2)
C(12')-Co(1')-C(15')	167.9(2)
C(12')-Co(1')-C(16')	129.6(2)
C(12')-Co(1')-C(17')	109.0(2)
C(12')-Co(1')-C(18')	117.4(2)
C(13')-Co(1')-C(14')	116.61(19)
C(13')-Co(1')-C(15')	150.8(2)
C(13')-Co(1')-C(16')	166.6(2)
C(13')-Co(1')-C(17')	128.2(2)
C(13')-Co(1')-C(18')	106.8(2)

C(14')-Co(1')-C(15')	40.95(18)
C(14')-Co(1')-C(16')	68.93(19)
C(14')-Co(1')-C(17')	68.56(19)
C(14')-Co(1')-C(18')	40.97(19)
C(15')-Co(1')-C(16')	40.79(19)
C(15')-Co(1')-C(17')	68.2(2)
C(16')-Co(1')-C(17')	40.49(19)
C(18')-Co(1')-C(15')	68.75(19)
C(18')-Co(1')-C(16')	68.8(2)
C(18')-Co(1')-C(17')	40.7(2)
Co(1')-C(9')-H(9')	125.8
C(10')-C(9')-Co(1')	69.2(3)
C(10')-C(9')-H(9')	126.7
C(13')-C(9')-Co(1')	69.8(3)
C(13')-C(9')-H(9')	126.7
C(13')-C(9')-C(10')	106.6(5)
Co(1')-C(10')-H(10')	126.5
C(9')-C(10')-Co(1')	69.3(3)
C(9')-C(10')-H(10')	126.1
C(11')-C(10')-Co(1')	69.8(3)
C(11')-C(10')-C(9')	107.9(5)
C(11')-C(10')-H(10')	126.1
Co(1')-C(11')-H(11')	126.3
C(10')-C(11')-Co(1')	69.5(3)
C(10')-C(11')-H(11')	126.1
C(12')-C(11')-Co(1')	69.6(3)
C(12')-C(11')-C(10')	107.7(5)
C(12')-C(11')-H(11')	126.1
Co(1')-C(12')-H(12')	125.9
C(11')-C(12')-Co(1')	70.0(3)
C(11')-C(12')-H(12')	125.5
C(13')-C(12')-Co(1')	70.2(3)
C(13')-C(12')-C(11')	109.1(5)
C(13')-C(12')-H(12')	125.5
Co(1')-C(13')-H(13')	126.8
C(9')-C(13')-Co(1')	69.4(3)
C(9')-C(13')-H(13')	125.6
C(12')-C(13')-Co(1')	69.7(3)

C(12')-C(13')-C(9')	108.7(5)
C(12')-C(13')-H(13')	125.6
Co(1')-C(14')-H(14')	126.1
C(15')-C(14')-Co(1')	69.7(3)
C(15')-C(14')-H(14')	126.1
C(15')-C(14')-C(18')	107.7(4)
C(18')-C(14')-Co(1')	69.7(3)
C(18')-C(14')-H(14')	126.1
Co(1')-C(15')-H(15')	126.7
C(14')-C(15')-Co(1')	69.3(2)
C(14')-C(15')-H(15')	125.9
C(16')-C(15')-Co(1')	69.7(3)
C(16')-C(15')-C(14')	108.2(4)
C(16')-C(15')-H(15')	125.9
Co(1')-C(16')-H(16')	126.1
C(15')-C(16')-Co(1')	69.5(3)
C(15')-C(16')-H(16')	126.2
C(17')-C(16')-Co(1')	69.8(3)
C(17')-C(16')-C(15')	107.7(4)
C(17')-C(16')-H(16')	126.2
Co(1')-C(17')-H(17')	126.8
C(16')-C(17')-Co(1')	69.7(3)
C(16')-C(17')-H(17')	125.6
C(16')-C(17')-C(18')	108.8(5)
C(18')-C(17')-Co(1')	69.5(3)
C(18')-C(17')-H(17')	125.6
Co(1')-C(18')-H(18')	126.2
C(14')-C(18')-Co(1')	69.4(3)
C(14')-C(18')-H(18')	126.2
C(17')-C(18')-Co(1')	69.8(3)
C(17')-C(18')-C(14')	107.6(4)
C(17')-C(18')-H(18')	126.2
C(4S)-O(1S)-C(1S)	108.4(4)
O(1S)-C(1S)-H(1SA)	110.5
O(1S)-C(1S)-H(1SB)	110.5
O(1S)-C(1S)-C(2S)	106.4(4)
H(1SA)-C(1S)-H(1SB)	108.6
C(2S)-C(1S)-H(1SA)	110.5

C(2S)-C(1S)-H(1SB)	110.5
C(1S)-C(2S)-H(2SA)	111.5
C(1S)-C(2S)-H(2SB)	111.5
C(1S)-C(2S)-C(3S)	101.4(4)
H(2SA)-C(2S)-H(2SB)	109.3
C(3S)-C(2S)-H(2SA)	111.5
C(3S)-C(2S)-H(2SB)	111.5
C(2S)-C(3S)-H(3SA)	111.6
C(2S)-C(3S)-H(3SB)	111.6
H(3SA)-C(3S)-H(3SB)	109.4
C(4S)-C(3S)-C(2S)	101.1(4)
C(4S)-C(3S)-H(3SA)	111.6
C(4S)-C(3S)-H(3SB)	111.6
O(1S)-C(4S)-C(3S)	106.5(4)
O(1S)-C(4S)-H(4SA)	110.4
O(1S)-C(4S)-H(4SB)	110.4
C(3S)-C(4S)-H(4SA)	110.4
C(3S)-C(4S)-H(4SB)	110.4
H(4SA)-C(4S)-H(4SB)	108.6
C(8S)-O(2S)-C(5S)	108.9(4)
O(2S)-C(5S)-H(5SA)	110.5
O(2S)-C(5S)-H(5SB)	110.5
O(2S)-C(5S)-C(6S)	106.2(4)
H(5SA)-C(5S)-H(5SB)	108.7
C(6S)-C(5S)-H(5SA)	110.5
C(6S)-C(5S)-H(5SB)	110.5
C(5S)-C(6S)-H(6SA)	111.5
C(5S)-C(6S)-H(6SB)	111.5
H(6SA)-C(6S)-H(6SB)	109.3
C(7S)-C(6S)-C(5S)	101.2(4)
C(7S)-C(6S)-H(6SA)	111.5
C(7S)-C(6S)-H(6SB)	111.5
C(6S)-C(7S)-H(7SA)	111.2
C(6S)-C(7S)-H(7SB)	111.2
C(6S)-C(7S)-C(8S)	102.8(4)
H(7SA)-C(7S)-H(7SB)	109.1
C(8S)-C(7S)-H(7SA)	111.2
C(8S)-C(7S)-H(7SB)	111.2

O(2S)-C(8S)-C(7S)	105.8(4)
O(2S)-C(8S)-H(8SA)	110.6
O(2S)-C(8S)-H(8SB)	110.6
C(7S)-C(8S)-H(8SA)	110.6
C(7S)-C(8S)-H(8SB)	110.6
H(8SA)-C(8S)-H(8SB)	108.7

Symmetry transformations used to generate equivalent atoms: